Human Estimation of Slope, Distance, and Height of Terrain in Simulated Lunar Conditions

by

Christopher Oravetz

B.S., Aeronautical Engineering
United States Air Force Academy, 2007

Submitted to the Department of Aeronautics and Astronautics in partial fulfillment of the requirements for the degree of

Master of Science in Aeronautics and Astronautics

at the

MASSACHUSETTS INSTITUTE OF TECHNOLOGY

February, 2009

Author .....
Department of Aeronautics and Astronautics
December 7, 2008

Certified by .....
Laurence R. Young
Apollo Program Professor of Astronautics
Professor of Health Sciences and Technology
Thesis Supervisor

Accepted by .....
Prof. David L. Darmofal
Associate Department Head
Chair, Committee on Graduate Students

Report Documentation Page

Form Approved
OMB No. 0704-0188

1. REPORT DATE	2. REPORT TYPE	3. DATES COVERED
01 FEB 2009	**N/A**	**-**

4. TITLE AND SUBTITLE	5a. CONTRACT NUMBER
Human Estimation of Slope, Distance, and Height of Terrain in Simulated Lunar Conditions	5b. GRANT NUMBER
	5c. PROGRAM ELEMENT NUMBER
6. AUTHOR(S)	5d. PROJECT NUMBER
	5e. TASK NUMBER
	5f. WORK UNIT NUMBER
7. PERFORMING ORGANIZATION NAME(S) AND ADDRESS(ES) **Massachusetts Institute of Technology**	8. PERFORMING ORGANIZATION REPORT NUMBER
9. SPONSORING/MONITORING AGENCY NAME(S) AND ADDRESS(ES) **AFIT/ENEL Bldg 16 Room 120 2275 D Street Wright-Patterson AFB, OH 45433-7221**	10. SPONSOR/MONITOR'S ACRONYM(S)
	11. SPONSOR/MONITOR'S REPORT NUMBER(S) **CI09-0036**

12. DISTRIBUTION/AVAILABILITY STATEMENT
Approved for public release, distribution unlimited

13. SUPPLEMENTARY NOTES
The original document contains color images.

14. ABSTRACT

15. SUBJECT TERMS

16. SECURITY CLASSIFICATION OF:			17. LIMITATION OF ABSTRACT	18. NUMBER OF PAGES	19a. NAME OF RESPONSIBLE PERSON
a. REPORT	b. ABSTRACT	c. THIS PAGE			
unclassified	**unclassified**	**unclassified**	**UU**	**260**	

To the families of the past, present, and future astronauts - together may we work to bring your husbands, wives, mothers, fathers, brothers, sisters, sons, and daughters home safely

Human Estimation of Slope, Distance, and Height of Terrain in Simulated Lunar Conditions

by

Christopher Oravetz

Submitted to the Department of Aeronautics and Astronautics on
December 12, 2008 in partial fulfillment of the requirements for the
Degree of Master of Science in Aeronautics and Astronautics

Abstract

As NASA's Vision for Space Exploration seeks to explore mountainous regions near the southern pole through frequent, long excursions, astronauts will require accurate navigational assistance. Current and future technology, including LIDAR data, laser rangefinders, and path planning programs will likely be available; however, the human's own perception of the terrain may affect their confidence in these instruments and be necessary during emergency situations. These unique lunar conditions are expected to affect human perception: the lack of an atmosphere (inhibiting the use of aerial perspective as a distance cue and causing the formation of deep cast shadows), the non-Lambertian regolith reflectance properties, the lack of familiar objects, and the physiological effects of reduced gravity. This project examines the inherent errors humans make when judging the slope, distance, and height of terrain, both on the Earth in a lunar-like environment and on the Moon using photographs from the Apollo missions.

Five experiments were conducted in field and Virtual Reality (VR) environments. The effects of true slope, true distance, and sun elevation on slope estimates were determined using visual and motor responses in a lunar-like Utah environment and reproduced in a VR environment using synoptically viewed images in two body positions, under normal and lunar G_z loading conditions. The effects of true slope, distance, and body position on slope, distance, and height estimates of synoptically viewed Apollo panoramic images were measured and compared to measurements obtained from topographical maps. Systematic and random errors were determined for all estimates. Slope estimate comparisons were made between lunar-like and lunar terrain and also between lunar hills and craters.

Slope was significantly overestimated in the field study by 13^o – 23^o with large between-subject errors. Lunar-like field and VR slope estimates were not significantly different from each other. Slope estimates were significantly greater at lower sun elevations and closer distances in the Lunar-like VR Study. Both slope and distance estimates were significantly greater from a lunar G_z supine position. Lunar distance estimates varied largely and slope estimation errors were significantly greater for craters than for hills. A new relationsihp between hill shape and perceived steepness was also discovered. The recommendations of this study include the development of a VR training tool to calibrate an astronaut's slope, distance, and height perception prior to lunar missions and future field studies at Devon Island to determine the effect of hill shape on estimates and to determine the regression coefficients of sun elevation and distance variables to be used in a model integrated with rangefinding devices in a Heads-Up-Display (HUD).

Thesis Advisor: Professor Laurence R. Young
Title: Apollo Program Professor of Astronautics
Professor of Health Sciences and Technology
This work was supported by the National Space Biomedical Research Institute through NASA NSC 9-58

ACKNOWLEDGEMENTS

First and Foremost, I thank God for the opportunity to come to MIT, for the funding He provided and the inspiration He gave to design these experiments, analyze the results, and the write this report. He never left my side during the late nights of writing computer code and testing subjects, He provided people to help and motivate me throughout this project, and He was present through all frustrations and triumphs.

I am grateful to Professor Laurence Young for the opportunity, funding, support, and expertise he provided throughout this project. He possessed confidence and patience in me and has allowed me to meet and collaborate with Apollo astronauts, NASA researchers, and attend several conferences.

Dr. Andy Lui and Dr. Alan Natapoff were great "offensive coordinators" throughout this project. Dr. Lui provided insightful direction on background references and the experimental design, reviewed papers, abstracts, and posters, and motivated me to ride my bike to the office during the summer. Dr. Natapoff taught me more about statistical analysis that I could have ever dreamed and always found ways to relate the analysis and our meetings to the Air Force.

Dr. Marcelo Vasquez deserves credit and tremendous gratitude for conducting a field study at Devon Island in August 2008. The days and hours he spent planning the trip, preparing for the experiment, training the subjects, and executing the experiment in below freezing conditions and 25 mph winds provided us with remarkable data that confirms several conclusions and proposes future questions. Thank you for the invitation and your time at Brookhaven this summer.

For the funding and request of this research, I am grateful to the National Space Biomedical Research Institute through NASA NCC 9-58 and Dr. Michael Gernhardt at the NASA Johnson Space Center.

The following people provided their time and resources to make this project a success:

- To the collaborative support of Prof. Heiko Hecht and Prof. Jan Koenderink during our winter and spring meetings and teleconferences and for offering your time and expertise. To the support and expertise from Dr. Jon Clark, Prof. Dava Newman, and Prof. Berthold Horn.

- To Katherine Ingle and all the abundant time and work she volunteered toward this project, including the pilot study at Waterville Valley.

- To my crewmembers on the MDRS Crew 65 Expedition – I appreciate the early wake-ups and long hours you put forth to this experiment…and for refueling the generator.

- To the crewmembers of the Mars Institute Haughton Mars Project Summer 2008 Expedition that volunteered and trained as subjects for this project.

- To Dr. Mark Robinson and his students at Arizona State University for providing high-resolution Apollo 17 digital images.

- To Astronaut Charles Duke, thank you for breakfast and for sharing your wonderful experiences from the Apollo 16 mission and your Air Force career!

- To the Mars Society for providing the opportunity to be a member of the Crew 65 Expedition

- To Dr. Eric Jones, David Harland, Ken Glover, and Syd Buxton for providing numerous resources from your *Apollo Lunar Surface Journal*, including panoramas and maps, and for your interest and support of this project.

"A faithful friend is beyond price, no sum can balance his worth." ~Sirach 6:15. The following friends and family were shining stars who offered their constant support and encouragement:

- Nathan Valle, Jeff Runyan, and JP Patino: You guys are my brothers for life, thank you for being at my side always when needed, hearing me out and helping me keep my identify when spending countless hours in the lab working on my wonderful computer.

- Brother Patrick Reilly: The impact you have made on me in Boston and the ways you have helped God to enter more deeply into my life goes beyond all words. Your wisdom has allowed me to achieve peace and hope throughout my journey through graduate school.

- Shaina Tanguay – Colucci: You have been a blessing in my life. I will forever be grateful for the impacts our friendship has made on me and the encouragement you gave me throughout the final months of research and thesis writing.

- Geoff Carrigan, Kyle Volpe, and Jared Krueger: I will miss the Hamburger Helper dinners and the Thursday community discussions. I couldn't have asked for better roommates!

- Mary Goldsmith: Your support and understanding during the difficult work days was a true gift. I will always be grateful for the things you have taught me and cherish all that we shared.

- Josh Kline: You were there when I needed someone the most. May God bless you and your future research – Go Steelers!

- MSgt Vince Meno: Even in the civilian environment of graduate school, your wonderful example of being considerate, professional, encouraging, selfless, and respectful has motivated me to be a better officer and pay forward these qualities to airmen throughout my career. I will tell them stories of the MSgt Meno who needed to hit the weights more often, but cooked great hamburgers. I will forever be grateful for the wisdom and advice you provided along the way.

- Kevin Marr: Thank you for keeping me up-to-date on the DCI and BCS rankings, inviting me to join you for Mass each week, and for the dinners at the Prudential – you friendship means a lot!

- Luis Zea: Mars wouldn't have been as interesting without you bro! Thanks for all the help with my experiment preparation, for all our great conversations while fixing broken water pipes, and for being a great role model to me and others. I have high hopes our paths will continue to cross in the future. But first, I have a question for you…

- MVL Students **–** You all were the greatest! Thank you for living the graduate school experience along with me, being examples, and making the lab a true family.

- And Most of All – To my Mom, Dad, and sister – I would not have made it without you. Your constant faith in me, encouragement, love, and forgiveness kept the fire within me alive. I will always cherish this time with you in Boston and be grateful for the blessing it was.

TABLE OF CONTENTS

LIST OF FIGURES

Chapter 1

Chapter 2

Chapter 3

Chapter 4

LIST OF TABLES

Chapter 3

Chapter 4

Chapter 5

LIST OF ACRONYMS

The following acronyms and abbreviations were used in this thesis:

°	degree
“	inch
2D	Two dimensional
3D	Three dimensional
ALSEP	Apollo Lunar Surface Experimental Package
ALSJ	Apollo Lunar Surface Journals
ANOVA	Analysis of variance
ASU	Arizona State University
BDRF	Bi-directional Reflection Distribution Function
cm	centimeter
COUHES	Committee On the Use of Humans as Experimental Subjects
deg	degree
DFS	Devon Island Lunar-like Field Study
et. al	et alia – “and others”
EVA	Extra-Vehicular Activity
ft	foot
FOV	Field-of-view
HMD	Head-mounted display
HMP	Mars Institute Haughton Mars Project
HUD	Heads-Up-Display
IPD	Inter-pupilary distance
km	kilometer
LANC	Local area network with a camera
LCD	Liquid crystal display
LM	Lunar Module
LIDAR	Light Detection and Ranging

LRF	Laser Rangefinder
LVS	Lunar VR Study
m	meter
MBA	Masters in Business Administration
MDRS	Mars Desert Research Station
MFS	MDRS Lunar-like Field Study
min	minute
MIT	Massachusetts Institute of Technology
mm	millimeter
ms	millisecond
MVL	Man Vehicle Lab
MVPS	MDRS Lunar-like VR Pilot Study
MVS	MDRS Lunar-like VR Study
NASA	National Aeronautics and Space Administration
NSBRI	National Space Biomedical Research Institute
PI	Principle Investigator
R^2	Coefficient of determination
RADAR	Radio Detection and Ranging
STA	Apollo EVA station
UROP	Undergraduate Research Opportunities Program
UT	Utah
VR	Virtual Reality
x	times

CHAPTER 1

INTRODUCTION

Apollo 14 Astronauts Shepard and Mitchell were 650 meters from the Lunar Module (LM) when they crossed onto the Cone ejecta blanket, and soon after encountered a 10^{o} slope. Their leisurely pace began to diminish, their time began to run short, and their breath began to quicken. The lunar surface was littered with fist-sized rocks causing Shepard to assist Mitchell with the EVA cart while counting a steady cadence: “Left…Right…Left…Right” [1]. One minute later, Shepard was forced to halt, with his heart racing at 140 beats/min within his stiff, cumbersome spacesuit. The two-man team continued to climb, pausing every minute, until Shepard evaluated their situation. They had already used a 30-minute extension and neither man had faith in their distance judgments. Without reaching the rim of Cone Crater, Shepard and Mitchell proceeded with sampling the terrain and continued the EVA without recognizing their position was only 30 meters from the rim of the crater! [1].

The Apollo 14 astronauts were never in a life-threatening situation during their climb, though they encountered spatial disorientation without familiar landmarks, an inability to accurately judge distance, and difficulty climbing up slopes. In a 1971 Technical Debrief, Astronaut Shepard stated:

> *"Until we really get a feel for navigation on the surface, there should be some strong (that is, well-defined) checkpoints to follow. First of all, it gives you a feeling of security to know where you are. You know where you are distancewise and what you have left to cover. Second, there's no question in my mind that it's easy to misjudge distances, not only high above the surface (that is, during the landing or from the LM windows) - that we discussed before - but also distances along the surface” ~Alan Shepard [44]*

Navigational challenges proved daunting during Apollo 14 and will remain challenging for future lunar missions. This study is the first step toward overcoming these challenges by collecting measures of the systematic and random errors humans make when judging slopes, distances, and heights in lunar and lunar-like environments, analyzing the effects of true slope, sun elevation, viewing distance, and gravity on these estimates, and proposing a future Virtual Reality training tool to refine their estimates, a measurement device to determine the slope of hills from any distance, and a Heads-Up-Display (HUD) design that integrates range-finding instruments and human perception.

1.1 Motivation

As the *Vision for Space Exploration*, initiated by George W. Bush in January 2004, continues to progress, lunar surface exploration remains at the top of the agenda, along with scientific research. Why does NASA desire to make exploration a fundamental goal when returning to the Moon? Exploration has always been present throughout human history, from Captain James Cook's sailing voyage to the South Pacific in 1770 [44] to Lewis and Clark's 1804 expedition across the unknown territories of North America [54]. Exploration enhances human knowledge and inspires youth. However, exploration also places humans in a harsh environment a vast distance away with unknown risks and limited time to respond to unpredictable situations. Reducing risks and preparing astronauts for overcoming the challenges they will face during exploration is **critical**.

NASA's Vision for Space Exploration calls for a return to the Moon for extended time periods, allowing astronauts to search for resources and teaching them how to safely work in a harsh environment [31]. Astronauts will make repeated excursions, with and without the use of a rover, and will be subject to uncertainties of the lunar surface and map limitations [83]. Planning and implementation of pre-defined routes with the aid of LIDAR/RADAR data, topographical maps, and laser ranging devices will likely be available, as well as path optimizing devices that considers locomotion risks and metabolic costs [83]. In addition to these sources of information, astronauts will use their own perception of terrain when making navigational decisions. However, just as aircraft pilots experience conflicts between their perceptual inputs and the aircraft instruments, astronauts may also experience conflicts between the appearance of slopes and distances on the lunar surface and the information provided by their navigational instruments. These conflicts may not only reduce their trust in these instruments, but may result in erroneous and even life-threatening decisions during emergencies without the availability of these instruments. Identifying the magnitude and variability of the perceptual errors humans make while judging lunar terrain is a critical step towards preparing astronauts for the challenges they will face, and integrating the factors affecting these errors with navigational instruments will enhance trust in their equipment.

Identifying the difficulties experienced by Apollo astronauts can further motivate the importance of this study. Following the Apollo 12 landing, Astronaut Al Bean recalled observing the side of the Surveyor crater and judging its slope as 40^{o} (See Figure 1.1). With part of its rim concealed by a shadow, Bean assumed from his experience in an Earth environment that "if something is sunny on one side and very dark on the other, it has to be a tremendous slope" [44]. After 20 hours passed and both astronauts descended into the crater, the shadowed areas were revealed illuminating the 11 degree slope. In a post-

mission interview, Bean commented: “Shows how the lighting can screw you up, because of those shadows being much darker because there isn’t that light [scattered by] the atmosphere filling in” [44]. Even with prior knowledge of the slopes, Apollo 16 Astronaut Charles Duke found the appearance of craters to be misleading. During his approach to the North Ray Crater on EVA 3, he passed the 10 – 12 degree slope of End Crater exclaiming: “Man, look at that slope!” [44]. While standing at the base of Turtle Mountain and observing the steepness of its 20 degree walls, Astronaut Duke concluded that the mountains on the lunar surface did not look like their training models.

Figure 1.1 Apollo 12 Surveyor Crater overestimated by 30^{o} because of the presence of deep shadows

Distance estimation suffered as well on the lunar surface, with errors in both directions. During the Apollo 14 hike to Cone Crater, Astronaut Mitchell recognized the crater “Old Nameless” and judged its distance as 200 – 300 meters away, which would place it on his traverse map. He was actually 2000 meters away from the crater. Future conflicts between maps and perception can cause astronauts to question their position or become spatially disoriented. Figure 1.2 illustrates Astronaut John Young sampling a light-colored boulder near the rim of North Ray Crater. Despite the apparent closeness of the surrounding objects, the boulder beyond his right shoulder is actually the size of a three-story house – 150 meters away and 12 meters tall [44]. Not all distances were underestimated, however. During the

deployment of the Apollo 12 ALSEP (Apollo Lunar Surface Experimental Package), Astronauts Bean and Conrad estimated the 450 ft distance from the Lunar Module (LM) to be at least 600 – 700 ft. With the presence of recognizable objects, however, Astronaut Conrad's 600 meter estimate to the Surveyor spacecraft 535 meters away was much more accurate. Without recognizable objects on the lunar surface, distance estimation becomes difficult, if not impossible. Astronaut Mitchell, recognizing this, stated in a post Apollo 14 interview: "We could put some work into a manual method of distance estimation better than your thumb up against the LM. We need a better manual method of estimating distance" [44].

Figure 1.2 House Rock, located beyond the right shoulder of Apollo 14 Astronaut Young, is 150 m away

Slope and distance estimation has clearly been a weakness for navigation during previous Apollo missions. This study offers the first step in quantifying these errors and suggesting training tools and integration of human perception with range-finding instruments to minimize these problems for tomorrow's lunar missions.

1.2 Contributions

The contributions from this study include providing astronauts and mission planners at NASA background information on the challenges of lunar navigation, identifying the need of a Virtual Reality

(VR) training program for astronauts to learn to appreciate their personal bias in slope estimation and to adapt to the specific slopes and distances they will experience around their landing site and lunar base, proposing a method to measure the slope of a hill from any distance and a design that integrates the factors likely to affect human perception of that terrain, and expanding the current research on slope and distance estimation of earth terrain.

The first contribution is to provide astronauts and mission planners with fundamental knowledge of the slope and distance errors that are likely to occur on the lunar surface. This will increase the importance of studying the terrain characteristics prior to the mission while developing training scenarios that require astronauts to make route decisions from their estimates. The knowledge of these errors will also increase awareness of the fallibility of human perception in a lunar environment, creating a stronger case for astronauts to trust their range-finding equipment and maps. A consistent error across all slopes may also allow astronauts to use simple mathematical operations to deduce a reasonable estimate.

The methods within the VR experiments of this thesis will contribute to the development of a VR training tool for astronauts to use prior to a lunar mission. The purpose of this tool would be to expose astronauts to the slopes and distances they will experience to prominent landmarks and allow them to refine their estimates with or without the use of range-finding instruments and maps. The VR experiments discussed in this thesis will aid in identifying the factors that should be considered during the design of this tool.

The third contribution of this thesis is to propose an on-site slope measurement device that determines the slope of terrain on the lunar surface and integrates the errors of human perception. The slope of terrain has traditionally been measured and calculated using an inclinometer while standing at the base of a hill or by identifying a hill on a topographic map. These methods may be impractical, inefficient, or obsolete on the lunar surface while standing at a distance from a hill that is unrecognizable. This thesis proposes the use of accurate range-finding equipment and mathematical relations to determine the slope of a distant hill while indicating to an astronaut the likelihood of their perceptive abilities to accurately estimate the slope with the present environment and lighting conditions.

The final contribution is to expand the current knowledge of slope and distance estimation studies of earth terrain within field and VR environments. Proffitt et. al determined slope estimate errors of “head-on” hills ranging from 2 – 34 degrees using verbal, visual, and haptic measures while having subjects stand at the base of each hill [60, 61]. Their results indicate a systematic overestimation of slope for the verbal and visual measures over the population of subjects; however, their experiment did not investigate the

within-subject differences of the same hill under different conditions. This study expands knowledge of human slope estimation by investigating the effects of viewing distance from the base of the hill and lighting conditions on estimates for each subject. Proffitt et. al also determined the consistency of results between field tests and VR tests that uses computer-graphics [60, 61]. This study also compares the results of field and VR tests, but uses stereo photographs of the actual hills seen within the field environment. Many VR distance estimation studies have been conducted at relatively short distances, where stereo vision, texture gradients, and angular declination provide useful cues to influence estimates. This study expands the knowledge of VR distance estimation for vaster distances without these cues.

1.3 Hypotheses

Although the thesis is divided into several experiments of both lunar-like and lunar terrain in field and VR environments, the hypotheses are consistent for each environment and listed below:

1. **Slope estimates from a distance are significantly greater than the true slope of a hill. Closer distances subtend a larger visual angle, increasing the perceived affordance and estimated slope. Low sun angles increase the contrast of a hill's texture, increasing the perceived affordance and estimated slope. The supine position is an unusual gravitational condition, increasing the estimated slope.**

2. **Distance estimates in a reduced-cue open field environment become more variable as the true distance increases. Low sun angles increase the contrast of the ground texture, increasing the estimated distance. The supine position is an unusual gravitational condition, increasing the estimated distance.**

3. **No significant difference exists between slope estimates of lunar-like terrain in a field study and a VR study that displays photographic images of the same terrain.**

4. **Slope estimates in a lunar environment are greater than a lunar-like earth environment without aerial perspective, familiar objects, and the formation of deep shadows.**

5. **Slope estimation errors are greater for craters than for hills in a lunar environment.**

1.4 Thesis Outline

The rest of this thesis is divided into four chapters, followed by references and appendices. Chapter 2 discusses the unique conditions of the lunar environment and previous studies on slope and distance estimation. Chapter 3 outlines the methods and procedures used for each experiment within this study. Chapter 4 presents and compares results of each experiment discussing whether they support the

hypotheses listed above. Chapter 5 states the conclusions that were developed from the results and lists recommendations for future studies and to prepare and aid astronauts for future lunar missions. The organization and specific information for each chapter is discussed below.

Chapter 2 – Background

Chapter 2 begins by relating the difficulties of slope and distance estimation to activities people encounter in daily life. After presenting a summary of these difficulties, the conditions of the lunar environment that increase these challenges are discussed in detail, including the lack of aerial perspective, non-Lambertian reflectance properties of the lunar regolith, the formation of deep shadows, the lack of familiar objects on the lunar surface, and the influence of lunar gravity. A literature review on previous slope estimation studies is described next by defining slant, explaining the equipment and protocol used in these studies, discussing slope overestimation trends, presenting the correspondence of field and VR tests, comparing the results of viewing hills from the side vs. head-on, and exploring the effect of affordance on estimates. A literature review on previous distance estimation studies follows by describing the factors affecting distance estimates, explaining various measurement protocols, discussing trends in errors, and presenting the potential limitation of testing in a VR environment.

Chapter 3 – Methods

Chapter 3 begins by explaining the order and purpose of all field and VR experiments in this study and discusses the environment for each. The characteristics of the subject population are next discussed for each study, followed by the equipment acquired and used throughout the entire study. The preparation and procedures for each experiment is discussed in detail, as well as the statistical methods used to analyze the data. This chapter contains all the information for an individual to reproduce this study.

Chapter 4 – Results and Discussion

Chapter 4 presents and discusses the results of this study. After providing an overview of the tables and graphs presented in this chapter, a regression model analysis with subject feedback and the estimation systematic and random errors are presented and discussed for each experiment. Additional comparisons are made between the lunar-like field and VR studies to confirm the consistency of results between the environments. Comparisons are also made between slope estimates of lunar hills and lunar-like hills, as well as between lunar hills and lunar craters.

Chapter 5 – Conclusions and Recommendations

Chapter 5 summarizes and presents the most significant results, including the overall systematic and random slope and distance errors for all the experiments conducted and the effects of slope, distance, sun elevation, and body position on estimates, while concluding whether a VR training tool for preparing astronauts for lunar missions can produce the same perceptual errors as the actual lunar environment. Recommendations will include areas of future slope and distance estimation research, a method to determine the slope of a hill from any distance using range-finding equipment, and the integration of navigational instruments and human perception to avoid conflicts and aid decisions.

CHAPTER 2

BACKGROUND

When was the last time you found your foot against the gas pedal of your car as you slowly "crept" up a steep canyon road to only find a sign indicating its slope to be 10 degrees? Have you ever experienced a bike race where the slightest change in the hill grade causes you to drop at least 5 gears to maintain your pedaling rhythm and breathing? Have you ever gone backpacking and felt apprehension while approaching an insurmountable "mountain" only to find it a leisurely hill? Are these illusions? Perhaps, though past research suggests that hills appear steeper than they really are. Distances can fool the eyes as well with or without salient cues. Many have experienced hiking toward a hill that appears to lie just beyond a ridge, only to find it miles beyond the ridge when more of the ground plane leading to the hill is revealed. If the hill possesses trees or buildings of a known size, distance perception may seem much easier; however, without these cues, the mind may be allowed to assume its own reference frame. If these cues can easily fool the most experienced hiker in a familiar earth environment, how would astronauts on their first lunar mission react in an unfamiliar, desolate lunar environment?

This chapter begins by explaining the previously identified challenges within the lunar environment and the effect each has on slope and distance estimation (Section 2.1). Section 2.2 reviews the methods used and results obtained from previous slope estimation studies, notably the magnitude of overestimation, the comparison between results obtained in field and Virtual Reality (VR) studies, the results obtained from viewing a hill from the side, and the effect of affordance to walk up an observed hill. Section 2.3 reviews the factors affecting distance estimates, the variety of measurements used to collect distance estimates, and the trends observed in both field and VR environments. This chapter will provide information that led to the formation of the hypotheses discussed in Chapter 1 and the Methods discussed in Chapter 3.

2.1 Challenges of the Lunar Environment

"Okay Houston. As I stand out here in the wonders of the unknown at Hadley, I sort of realize there's a fundamental truth to our nature. Man must explore. And this is exploration at its greatest." ~Astronaut Dave Scott [44]

Human exploration is challenging – it was challenging when Captain James Cook completed the first voyage to the South Pacific in 1770 and it was challenging for the human race to make its first landing upon the lunar surface in 1969 [44]. Despite the 20 months of preparation and 100,000 men and women

who helped prepare Apollo 15 for its launch in 1971, Astronauts Scott and Irwin could not fully prepare themselves for the environment they were about to encounter – an environment where a shadow would fully conceal the face of a mountain (Figure 2.6), an environment where mountains looked like foothills (Figure 2.8), and an environment where the combination of the sun position and lunar regolith reflectance could wash out textures and temporarily "erase" craters (Figure 2.4). The lunar environment provides numerous challenges to visual perception, impacting navigation and decision-making. The most critical challenges include the lack of aerial perspective and the formation of deep shadows without an atmosphere to reflect light, the non-Lambertian reflectance of the lunar regolith, the lack of familiar objects that are critical for using size-constancy to judge object size, and the influence of the $1/6^{th}$-G gravitational force. Each of these factors is further discussed in the following sections.

2.1.1 Lack of Aerial Perspective

"Because the Moon has no atmosphere – and therefore no atmospheric haze – objects in the distance look as clear and sharp as those nearby." ~ On the Moon [44]

The Earth's atmosphere affects the development of the visual perceptive cues that humans use when determining their position in space relative to their surroundings. When traveling to the lunar surface, astronauts will be forced to adapt to an environment where the lack of the typical cues created by an atmosphere can be misleading and even disorienting. The first challenge facing astronauts is the lack of aerial perspective, otherwise known as "haze", when judging the distance to far-away objects. Aerial perspective is caused by the absorption and scattering of particles of light, allowing an observer to notice the differences between the inherent contrast (the contrast at zero distance) and the effective contrast (contrast from the viewing distance) [67]. The distance between the near hills and far mountains in Figure 2.1 is apparent by the presence of aerial perspective.

Figure 2.1 Presence of aerial perspective within the Mars analog environment in Utah

Although there are only limited experiments showing the effects of aerial perspective on distance perception, Fry, Bridgman, and Ellebrock found that targets appeared to be twice as far when viewed in fog as opposed to clear weather [37]. Plenty of anecdotal evidence exists confirming this finding [67]. Bishop George Berkeley explains this phenomenon through his size-distance hypothesis, stating that visual angle alone is insufficient to judge the distance to an object and its size, while experience has taught that distant objects will appear fainter, causing an observer to judge its size as larger than its visual angle suggests [6]. Without this cue, astronauts are faced with readapting the interpretation of their sensory input on the Moon.

Figure 2.2 Lack of aerial perspective to discriminate the distance to the Mons Vitruvius (left) and the South Massif (right) in the Taurus-Littrow Valley from Apollo 17. (Notice the lunar rover to the right of the boulder)

Without aerial perspective, astronauts throughout the Apollo missions remarked on the clarity of objects in the distance. During an interview with Astronaut Jack Schmidt in November 2007, he compared the visibility on the moon to a clear day in Nevada [69]. This phenomenon was partly responsible for the navigational difficulties faced by Astronauts Shepard and Mitchell on EVA-2 of Apollo 14. During a Technical Debriefing in 1971, Shepard stated "There's no question in my mind that it's easy to misjudge distances, not only high above the surface…but also distances along the surface. It's crystal clear up there – there's no closeness that you try to associate with it in Earth terms – it just looks a lot closer than it is." [44]. Figure 2.2 illustrates this problem using an Apollo 17 panorama from STA-6. Although the distance to the base of the hills shown by the yellow arrows may seem similar, the Mons Vitruvius (left) is 14 km away, while the South Massif (right) is only 9.4 km away – the Mons Vitruvius is over 1.5 times further than the South Massif! Additionally, the panorama in Figure 2.2 was shot with only a 74 ft focus

and does not nearly possess the clarity of the actual hills as seen by the astronauts. This clarity confounded perceptual difficulties by increasing the contrast between luminous and shadowed regions, discussed in Section 2.1.3

2.1.2 Non-Lambertian Reflectance

> *"Man, I'll tell you, (driving) down-Sun is really grim. I was scared to go more than 4 or 5 kilometers an hour. Going out there (to Station 1), looking dead ahead, I couldn't see the craters, I could see the blocks all right and avoid them. But I couldn't see craters." ~Astronaut John Young [44]*

The Earth's atmosphere not only causes the unstructured diffusion of light through vapor and air molecules, it also allows the reflection of light off terrain into highly structured discontinuities and intensity gradients that depend on the properties of the reflecting surfaces [65]. The brightness and contrast information from these gradients can be analyzed to determine the orientation of the reflecting surface, a process known as "Shape from Shading."

The appearance of objects depends largely on its Bi-directional Reflection Distribution Function (BDRF). Many objects on Earth have varying degrees of Lambertian reflectance. The luminance of a Lambertian surface is directly proportional to the cosine of the incidence angle, thus, the incoming light is scattered equally in all directions, illustrated in Figure 2.3 (left). A person gazing upon a perfectly Lambertian surface would observe the same brightness, regardless of their orientation to the light source. Horn has elaborated on the methods that can be used to retrieve the surface relief of an object from its luminance, given its BDRF [46]. Ramachandran has identified shape assumptions humans are likely to make from shading information, with or without visible edges around an object [64]. For objects with varying degrees of Lambertian reflectance, Mingolla and Todd found that altering the illumination direction influenced the judged 3D shape [56]. The lunar regolith, however, possesses a unique BDRF, known as Non-Lambertian reflectance, where incoming light is reflected directly back to its source, illustrated in Figure 2.3 (right).

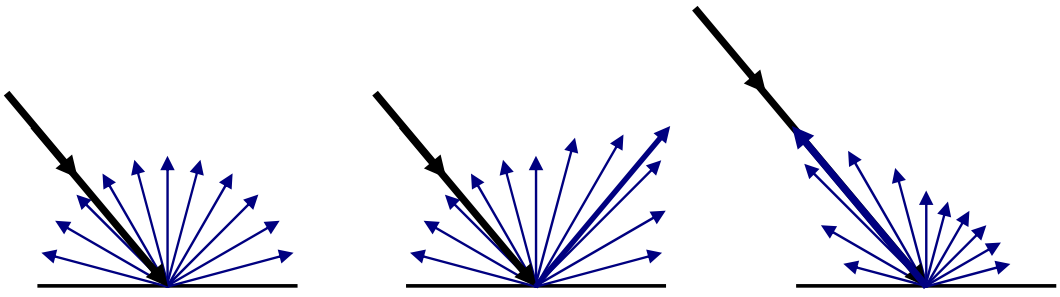

Figure 2.3 Brightness distribution models of Perfect Lambertian (left), Partial Lambertian (center) and Non-Lambertian (right) objects

The lunar regolith possesses non-Lambertian properties that preferentially reflect light back in the direction from which it came, known as backscatter. Backscatter becomes a serious problem when looking "down-sun" (away from the sun) on the lunar surface as the extreme brightness tends to wash away the surface features. Backscatter often occurs at angles less than six degrees from down-sun, increasing by 40% between 0 – 4 degrees [13], and with an extreme surge of brightness, by a factor of 2, occurring below 1 degree [12]. Looking "up-sun" (toward the sun) also causes problems creating glare and a loss of contrast through an astronaut's visor. "Cross-sun" appears to be the preferential viewing condition for Apollo astronauts, allowing them to observe surface texture, despite the deep cast shadows (discussed in the next section). Figure 2.4 illustrates the difficulties with each viewing conditions.

Figure 2.4 Changes in the brightness and contrast of the lunar surface when viewing "up-sun" (left), "down-sun" (center) and "cross-sun" (right) created perceptual difficulties.

Problems resulting from these viewing conditions are well-documented in research articles and mission reports. Prior to the Apollo 11 mission, Seminara and Kincaid predicted perceptual difficulties on the lunar surface due to its unique properties, including distortions in object geometry, disorientation with respect to sun position, and distorted depth/distance perceptions [71]. The Apollo 15 Mission Report stated "Looking up-sun, the surface features are obscured when direct sunlight is on the visor, although the sunshades on the lunar extravehicular visor assembly helped in reducing the Sun glare." [44]. Astronaut Eugene Cernan commented on looking up-sun: "We probably ran smack into a small crater – or maybe a boulder – that we couldn't see facing east and looking right into the sun." [44]. Astronaut John Young described his experience of driving down-sun as "grim" and couldn't see craters because of the abundance of light that was being reflected towards him. Additionally, viewing down-sun often hid shadows that revealed the size and appearance of objects. Although cross-sun viewing was preferred by astronauts, they faced dangers of misinterpreting the shadows, which will be discussed next.

2.1.3 Deep Shadows

> *"…on Earth, if something is sunny on one side and very dark on the other, it has to be a tremendous slope. We weren't getting [scattered] light in there like you do on Earth." ~Astronaut Al Bean [44]*

Shadows have been known to provide or conceal pictorial information necessary for spatial awareness of our surroundings. Some shadows exist on the object that creates them – half of a hill may be hidden from the light of a rising or setting sun. Additionally, large objects may project cast shadows upon smaller objects inhibiting its visibility entirely. Often, people will base their assumptions of the geometry of objects from the appearance of these shadows. Gibson refers to the objects that appear visible as reflecting light in an "ambient optic array", whose structure is invariantly related to the physical properties of the world [40]. One may likely conclude that a hill partially occluded by a shadow has different geometrical characteristics than the hill fully illuminated – see Figure 2.5.

Figure 2.5 Effect of shadows on the appearance and perception of a hill on Earth in different

The hill images in Figure 2.5, though the same from the same viewpoint, appear differently because of the greater textural contrast and the shadows shown in the right image. Although the right side of this hill is concealed by a shadow, the textural and shape information is still visible because of the light scattered in the atmosphere surrounding the hill and the light reflected from near objects. The lunar environment lacks the atmospheric scattering of light, causing shadows to appear much deeper with a starker contrast along the "terminator" line – the line separating the illuminated region from the shadowed region. This effect is illustrated in Figure 2.6.

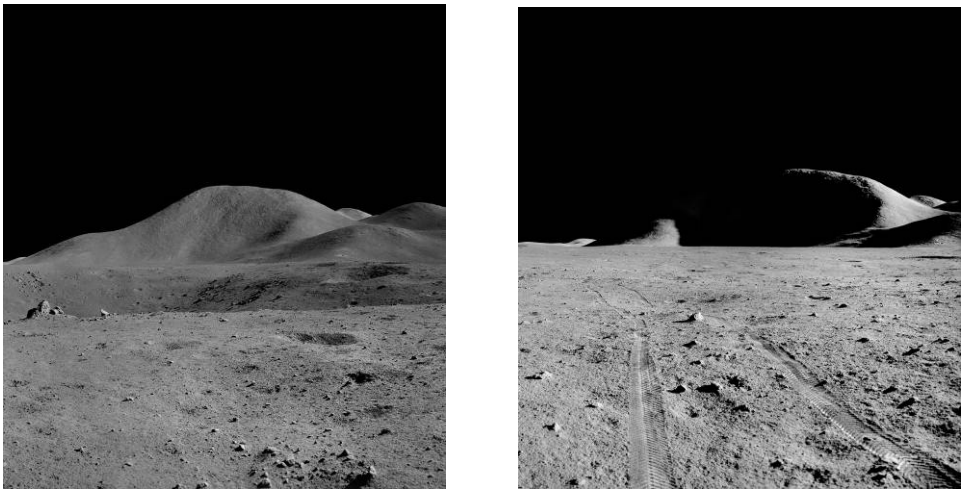

Figure 2.6 Effect of shadows on the appearance and perception of a hill on the Moon

The parallel sun rays and the lack of diffuse and ambient light cause one side of Mt. Hadley in Figure 2.6 to appear as a steep cliff. Beyond earthshine, H. Reynolds explains that "light from sources other than the sun is not available to "fill in" the shadowed areas" [65]. He comments that shadows are so dark that surfaces of a spacesuit are not even visible to the astronaut wearing it! Seminara and Kincaid's experiment determining the performance of control tasks in a lunar environment found that performance decreased when the astronaut's body obstructed the light to the task equipment [71]. Transcripts and interviews from the Apollo missions also indicate the difficulties created by shadows. During the exploration of the Surveyor Crater in Apollo 12, Astronaut Al Bean first thought the crater had a slope of 40 degrees and prepared to use ropes to descend into it, while 20 hours later, the shadows vanished revealing its 11 degree slope [44]. The sun elevation, a main driver for the appearance of these shadows, will be investigated in this study and may pose serious difficulties if the next lunar mission takes place around the South Pole.

2.1.4 Lack of Familiar References

"With no familiar objects to give a sense of scale, it is difficult to determine if a boulder on the horizon is small and nearby, or large and far away." ~On the Moon [44]

Generally speaking, humans are poor judges of absolute size and distance. Binocular disparity provides useful information for the brain to judge absolute distances of objects up to 15 meters away and humans can use the binocular disparity of the foreground to judge distances up to 100 meters away. Another useful cue that develops from one's awareness with the environment is the use of familiar objects to scale the size and distance to these objects. The traditional theory of size constancy holds that the brain accounts for the perceived distance and scales the size of the objects accordingly [11]. The process can

also be reversed and the distance can be deduced if the object has a known size. Contrary to Gibson's idea that textural gradients contain all the information necessary to know where an object lies in one's visual field, one's familiarity with the surrounding objects allows one to use size-constancy to judge distance when a textural gradient is non-existent. As the visual angle subtended by a familiar object increases in the field-of-view (FOV), the brain interprets the object as closer to the observer. This phenomenon is illustrated in Figure 2.7.

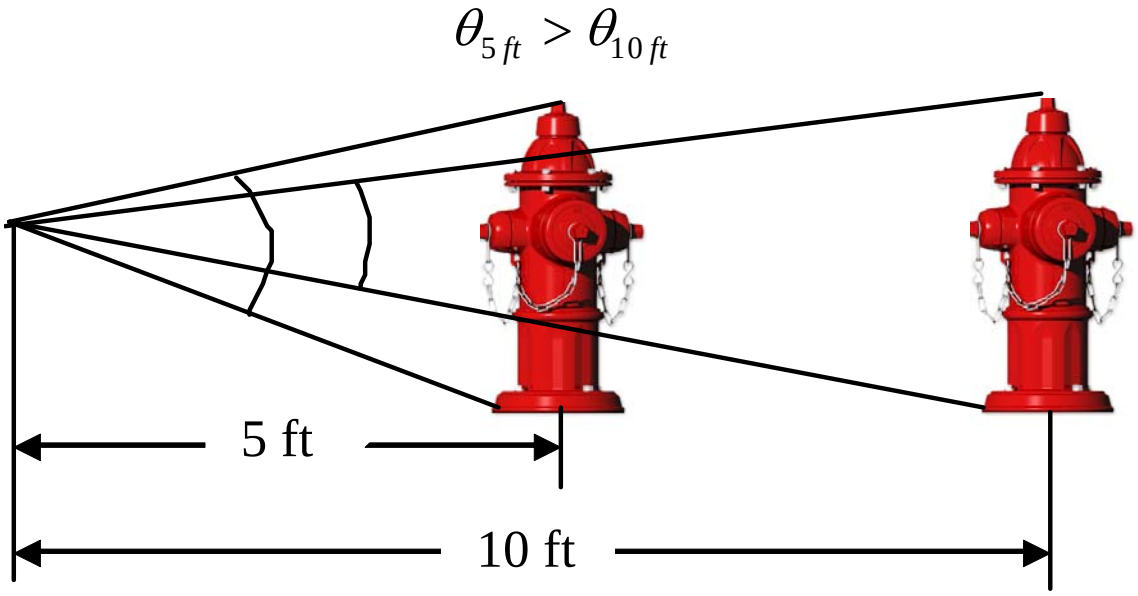

Figure 2.7 Distance determination using size-constancy with familiar objects

One danger when solely relying upon size-constancy to judge distance is that the brain enlarges distant objects so to compensate for a small retinal size, resulting in underestimation [67]. At vast distances, this phenomenon diminishes and errors increase with subjects equally likely to overestimate and underestimate distance. Without sufficient cues to base distance judgments at these vast distances, humans are likely to assume a frame of reference and base all future distance judgments off of that frame. The lunar environment is susceptible for committing this error. Figure 2.8 illustrates the potential of this problem.

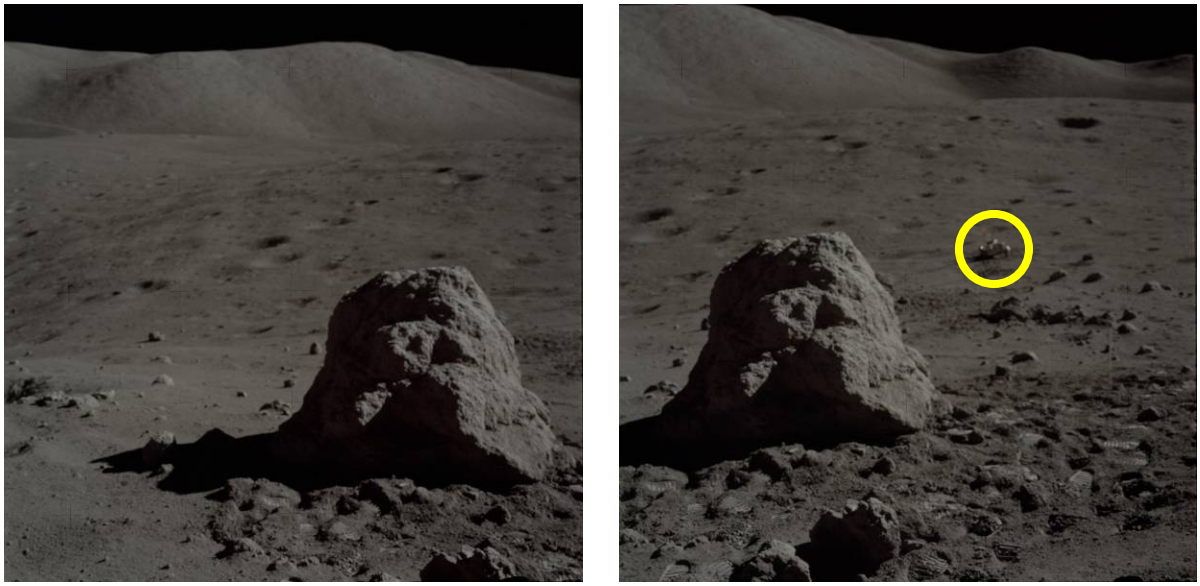

Figure 2.8 Human susceptibility of assuming one's own reference frame without familiar objects to correctly size this frame (left). The lunar rover provides clues to the vast distance (right)

The North Massif from the Apollo 17's Taurus-Littrow Valley is shown in both images of Figure 2.8. Without any familiar objects to correctly size the reference frame, an astronaut can easily assume the distance to the North Massif is several hundred meters or several thousand meters. When the lunar module appears in the image on the right, the astronaut will quickly refine his reference frame to several thousand meters (actual distance = 8,800 meters). The navigational difficulties during the Apollo missions from the lack of familiar objects are well documented in the *Apollo Lunar Surface Journals*. After Apollo 14, Astronaut Al Shepard commented "Until we really get a feel for navigation on the surface, there should be some strong [that is, well-defined] checkpoints to follow" [44]. Shepard's comments relate to their hike to Cone Crater, where they overestimated their progress by a factor of 2. Shepard later stated, "We could put some work into a manual method of distance estimation better than your thumb up against the LM [Lunar Module]. We need a better method of estimating distance" [44]. During Astronaut Pete Conrad's landing in Apollo 12, he saw a crater that appeared 300 meters southwest of his position with a diameter of 35 meters. The crater was actually 4500 meters west of his position with a diameter of 500 meters! [44] Without aerial perspective and familiar objects, the surrounding objects on the lunar surface appear much closer.

2.1.5 Influence of Reduced Gravity

"A simple distance perception test confirmed that the subjects underestimated the distance of objects in the depth plane in microgravity" ~ [19]

The brain can manipulate the appearance of objects, as evident with size-constancy, mentioned earlier. A large question that exists and should be addressed before returning to the Moon is whether the influence of the 1/6 gravitational environment can alter a human's perception and interpretation of distances and slopes, either at first or during prolonged stays. Astronaut Eugene Cernan, after the Apollo 17 mission, stated "you adapt very readily, very quickly, physiologically and psychologically…the human being is a very unique, very adaptable creature" [44].

Limited numbers of experiments have tested visual perception in microgravity. During visual perception, the brain integrates the 2D images from each retina, exaggerating and enhancing the perspective while generating a 3D image. Microgravity can alter this perspective enhancement because it obeys well-defined rules [19]. Perspective lines normally merge at a vanishing point on an imaginary horizontal line at eye-level. However, microgravity hinders the ability to define a horizontal line [36]. In microgravity, subjects have judged the vanishing point to be lower than in normal gravity, and have likewise judged a 3D cube with a larger width, smaller height, and longer depth, thus the distance in the depth plane was underestimated [19]. This microgravity experiment, however, was conducted during parabolic flight and no evidence yet exists whether these distance distortions would be present in a $1/6^{th}$ G environment and during long-term exposure to reduced gravity.

The present study was not able to be completed within reduced-g conditions; however, an alternative approach altered the magnitude of the gravitational force along the body's longitudinal axis. Previous studies have analyzed the effect of different body positions on visual perception, some indicating that geometric illusions are decreased with head-tilt relative to gravity [18]. The well known "Moon Illusion" is that the Moon appears larger when seen near the Earth's horizon. Many scientists, decades ago, sought to explain the Moon Illusion through a vestibular hypothesis, devised by Thor and Wood that suggested that the vestibular feedback from the head's location with respect to gravity can create an increase of perceived size of objects near the horizontal. This hypothesis has been tested and scrutinized by many researchers using a variety of experimental techniques. These techniques will be briefly discussed in the following paragraphs.

Berkley found that size-constancy was conditioned for horizontal viewing and that the horizontal enlargement of the Moon ceased when viewed inverted by bending over and viewing in between one's

legs [6]. Meili also discovered the perceived enlargement of distant hills was much less when viewed inverted between one's legs as well [55]. In 1992, Coren commented that the inverted position caused a reduction in the salience of depth cues [21]; however, *it is unclear whether the depth and size effects were caused by alternative otolith signals or rather from observing an unstructured scene* that would not allow the brain to use its adaptive abilities when viewing the Earth from an abnormal orientation.

Holway and Boring conducted an early experiment on the effect of viewing posture on the ratio of the diameter of the comparison stimuli (illuminated disc) near the horizon to the diameter at the zenith [45]. Their results indicated that the maximum ratios for the supine posture did not vary from the ratios obtained for the standing posture. They concluded that the apparent size of the Moon was independent of the orientation of the observer. Their experiment was conducted with only three subjects, two of which were Holway and Boring themselves. Thus, *their result by itself can't dismiss an effect of head-tilt.*

Various experiments on head-position were tested throughout the 1960's; however, most researchers found difficulties with separating the head-tilt and eye-elevation variables. Zinkus and Mountjoy attempted to isolate these variables in a 1969 experiment and had each of their 20 subjects view various discs at different elevations by only tilting their chair back and forth [84]. There were each tasked with adjusting both horizontal and upright discs to the same perceived distance as a disc located directly in front of them. Results indicated that the apparent distance to the vertical "upright" disc was typically about 27% larger than the horizontally located discs. They attributed these results to a change in the visual angle subtended by disc through stimulation of the vestibular system; however, *these results may only be applicable to objects viewed at relatively small distances, and should not be used to explain celestial distances.*

A 1962 experiment by King and Gruber utilized afterimages seen against the sky and asked their subjects to use monocular vision to estimate the ratios of the horizontal perceived length to the zenith perceived length [48]. Fourteen subjects participated and averaged a ratio of 1.63; however, King and Gruber were not able to separate the effects from head-tilt and illusions from atmospheric refraction of light. Experiments determining the combined effect of monocular vision with head-tilt were further conducted by Carter in 1977, who sought to expand the vestibular hypothesis of Thur and Wood to monocular conditions [16]. He used 24 students in a psychology class, equally distributed between genders, to estimate the distance of screwdriver heads placed in translucent plastic tubes. He mounted a comparison tube along the horizontal plane and adjusted a standard tube at either 45 degrees above or below the horizontal or along the horizontal. The visual field was consistent between different tube positions and

the subjects were forced to move their head in different orientations to look into the tube. The measurement method, though, was for the subjects to indicate if the comparison was "closer than" the standard at a number of distances. Although Carter found a significant difference between gender, with males averaging 19.75 errors out of 42 trials and females averaging 25.9 errors, *he found no significant effect of head position on the results.* He concluded that the head-tilt effect in this experiment could not alone be large enough to explain the Moon illusion, though the inclusion of terrain may have made the effect stronger.

Although scientists have not agreed on the effect of head position on size and distance perception, the potential perceptual difficulties astronauts may experience from the $1/6^{th}$ G gravitational environment necessitate testing for this condition. Parabolic flights were unavailable for the current study; however, effects of an altered head position were analyzed and reported to determine whether more advanced experiments should be conducted in future studies.

2.2 Previous Studies on Slope Estimation

"I think the trafficability is going to be excellent, though it looks like a steep slope climbing [to] that [North Ray] rim, doesn't it?" ~Astronaut Charles Duke [44]

Slope estimation is not only a problem in a lunar environment, but several studies have analyzed the effects and determined the errors of slope estimates on Earth, notably Dr. Dennis Proffitt [60, 61, 7, 22]. Proffitt's studies include slope estimates using visual, verbal, and haptic measures from the base or the sides of grassy hills or hills within a VR environment conducted at the University of Virginia. The present study seeks to extend the results obtained by Proffitt by collecting estimates in a reduced-cue environment from several distances and sun elevations. Many of the methods, hypotheses, and data analysis strategies used in the present study were obtained from Proffitt's experiments. This section explains techniques, results, and conclusions from these studies that can provide a baseline understanding of the estimation errors in a lunar environment.

2.2.1 Defining Slope

The slope of a hill, also known as its slant, can be classified as relative to the orientation of a surrounding surface (*relative slant*), relative to the line of sight of the observer (*optical slant*), or relative to a fixed environment reference frame, such as the horizontal ground plane (*geographical slant*) [60]. Several of Proffitt's previous studies [60, 7, 22] and the present study analyze the accuracy of slope perception from viewing each hill head-on. Figure 2.9 illustrates the orientation between the observer and the hill.

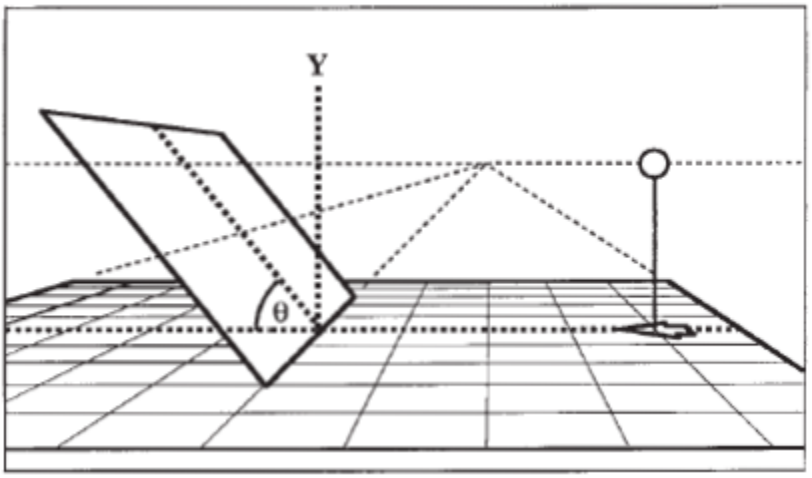

Figure 2.9 Orientation of observer and sloped surface for current/previous slope estimation studies

Prior to Proffitt, a few studies had been conducted on *geographical slant* estimation, including Kammann who found that a 34^{o} hill was estimated to be 48^{o} by males and 55^{o} by females [47]. Many researchers have investigated factors affecting *optical slant*, including the influence of textural gradients [45, 30, 33, 40, 42, 53], projective size [33, 35, 72], and motion parallax and binocular disparity [10, 17, 79]. A common trend from all these studies, including Proffitt's studies, is that the sloped surfaces appeared to lie closer to the frontal-parallel plane than its actual position, resulting in slope overestimations [60]. Both *geographical* and *optical slant* studies have proven slope overestimations, though few studies have combined the two types of slope perception. The current study merges both types of slope perception through its unique testing environment and similar test stimuli.

2.2.2 Equipment and Protocol

Much of the equipment used and procedures followed in the present study followed those used in Proffitt's slope perception studies [60, 7, 22]. Despite people's tendency to cognitively overestimate slope, the actions they make with their legs and feet do not follow the slope they visually perceive. Kinsella-Shaw, Shaw, and Turvey showed that people can accurately match the pitch of a distal surface using a motor response, such as a haptically perceived surface [49]. Proffitt et. al collected slope estimates using three different measures: verbally by characterizing the slope between 0 and 90 degrees, visually by matching the cross-section of the hill to a disc, shown in Figure 2.10 (left), and haptically, by adjusting the tilt-board with one's dominant hand without looking at the position of the board, shown in Figure 2.10 (right) [60].

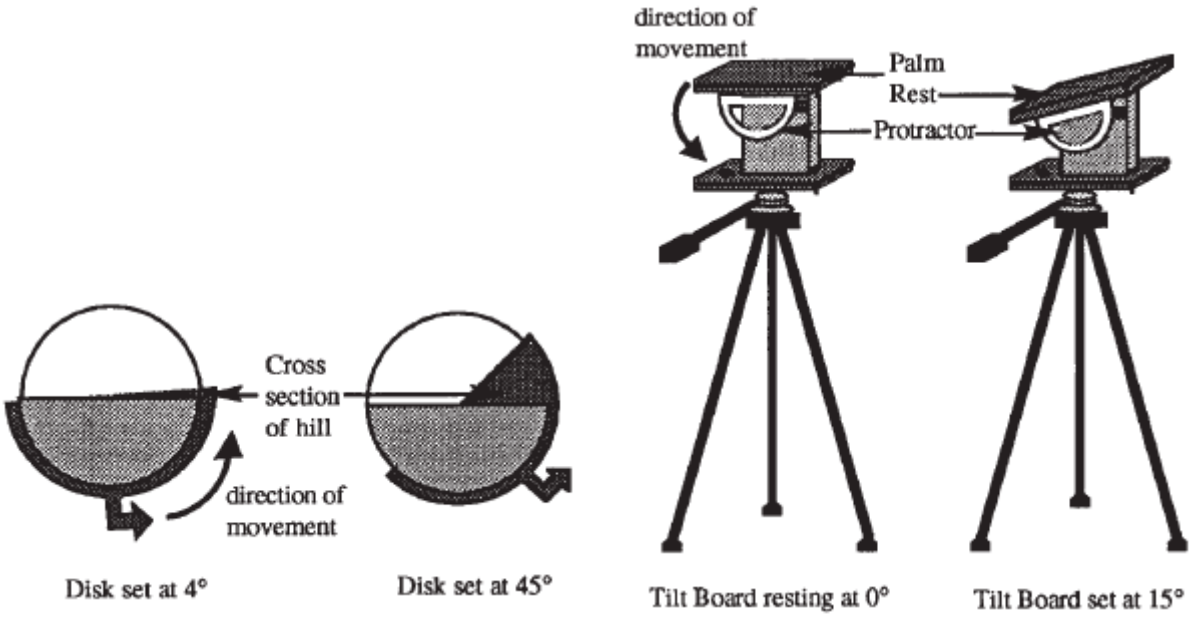

Figure 2.10 Visual (left) and haptic (right) measures used by Proffitt et. al [60] to estimate slope

Proffitt's field experiments were conducted in a high foot-traffic area at the University of Virginia. The magnitude of the "true" slope (actual slope) for the hills tested ranged between 2 and 34 degrees. Proffitt recruited 200-300 subjects for his experiments, though each subject only viewed one hill and the order of the measurements was counterbalanced. Proffitt collected 30 of each measurement for all of the hills tested, except for the 5^o hill where he collected 60 measurements [60]. The subjects viewed the hills with binocular vision while standing at their base and were instructed to directly face the hill without attempting to gain a side-view. All the subjects were naïve as to the purpose of the experiments and did not perform any training on how to make their estimates.

Proffitt's Virtual Reality experiments were conducted using a 185 x 139 pixel motion-sensing Head-Mounted Display (HMD) system with a total FOV of 90^o. He recruited 20 students with normal or corrected-to-normal vision that were naïve to the purpose of the study to view 12 "grassy" artificial hills in the VR display with slopes ranging from 5^o to 60^o. The distance along the sloped surface of the hill was held constant, while the height was varied as a function of the slope. All subjects viewed all 12 hills in a random order and provide a verbal measure, followed by a haptic measure [60]. The haptic device was initially set to zero before each measurement. The equipment and procedures used in the present study match well with Proffitt's experiments and will be discussed in detail in Chapter 3.

2.2.3 Slope Overestimation

Within the field study, Proffitt found that his subjects overall provided large overestimations of slope using the verbal and visual measures, while the haptic estimates were much more accurate (see Figure 2.11). He processed the data with statistical t-tests, comparing the estimates to the actual values. He showed linear trends using log transformations and produced power functions of estimated slope as a function of true slope with exponents of 0.564 (verbal), 0.543 (visual), and 0.650 (haptic). These exponents indicate a decelerating power function, meaning the amount of overestimation decreased as slope increased. Proffitt also found a significant effect of gender, with females producing a greater overestimation than males, a significant interaction between gender and measure, with the greatest gender difference occurring for the verbal estimates [60].

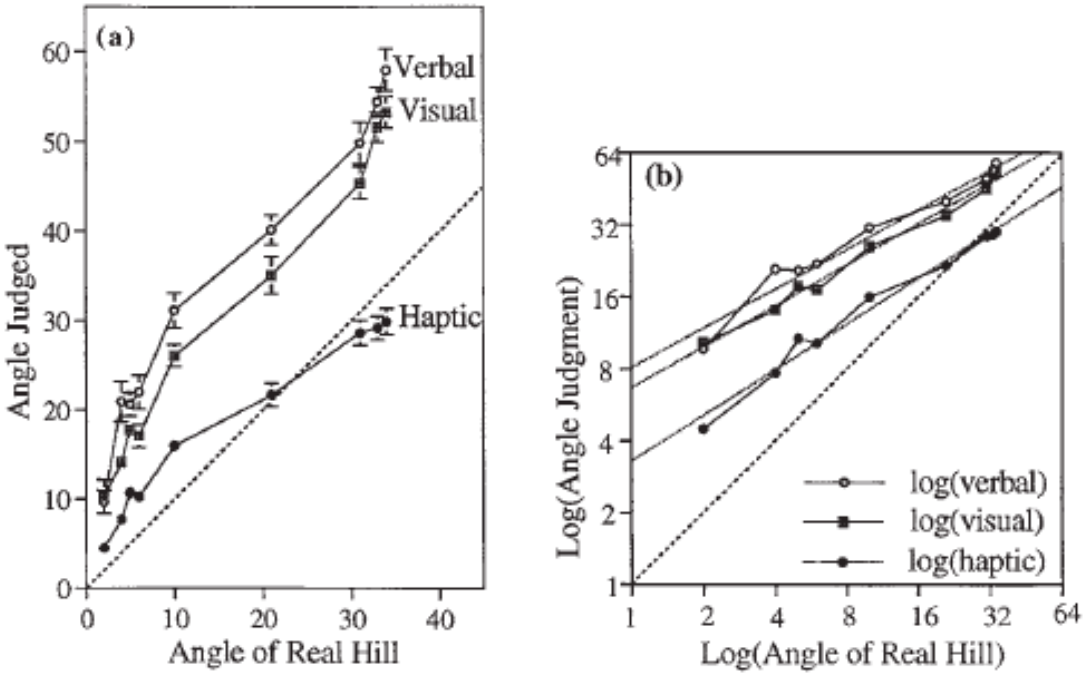

Figure 2.11 Proffitt's field study slope estimates as a function of actual slope for each measure in degrees (left) and as a log transformation (right)

Within the VR experiment, Proffitt found similar slope overestimations for the verbal measure and slope underestimations for the haptic measure (see Figure 2.12). He verified these results by using statistical t-tests comparing the mean estimate of each hill to the actual slope. The approximated power functions were well-fit with $R^2 = 0.99$ for the verbal response and $R^2 = 0.94$ for the haptic response, as well as decelerating exponents of 0.590 for the verbal estimates and the 0.740 for the haptic estimates [60]. In contrast to the field study, Proffitt *did not* find a significant effect of gender on the slope estimates for the VR study.

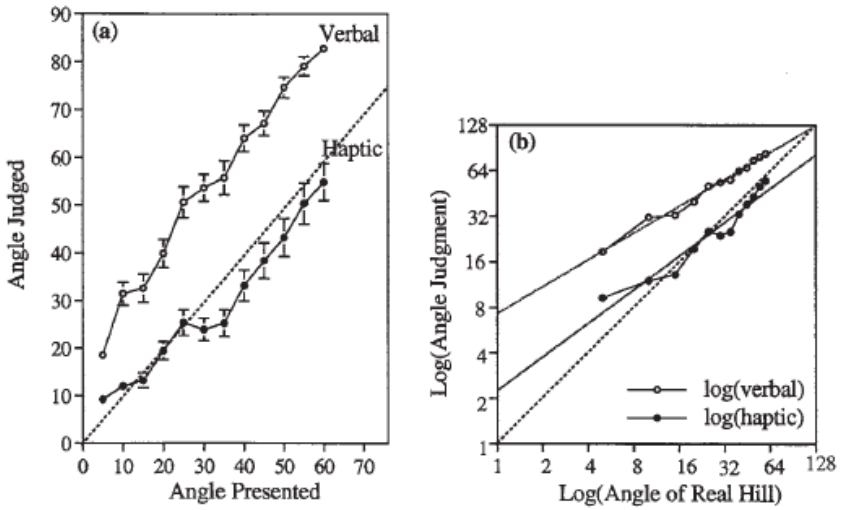

Figure 2.12 Proffitt's VR study slope estimates as a function of actual slope for each measure in degrees (left) and as a log transformation (right)

2.2.4 Correspondence of Field and VR Tests

Proffitt also found that across all angles, a close correspondence existed between the slope estimates made within field conditions and those made under VR conditions and verified this trend using a 2 x 2 ANOVA between gender and experiment type [60]. Figure 2.13 illustrates this correspondence for both verbal (left) and haptic (right) measures.

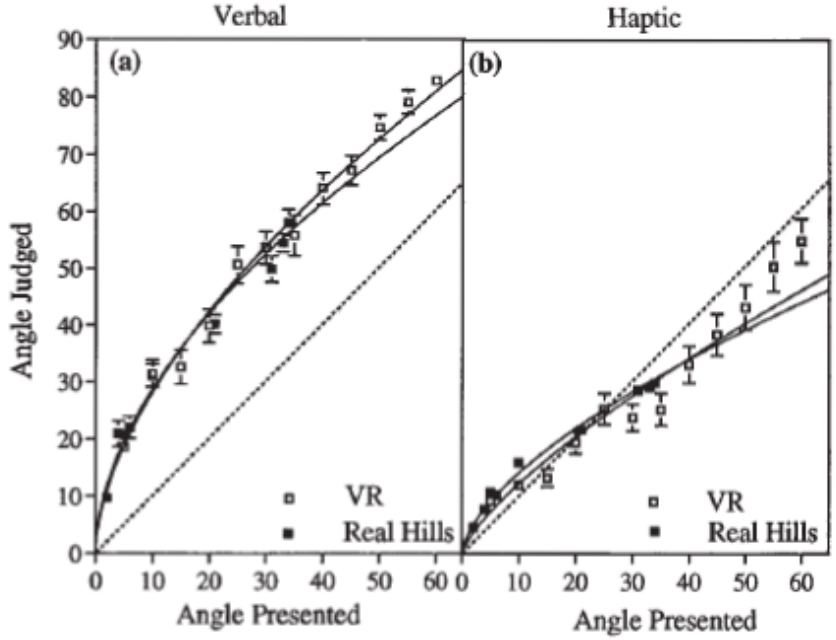

Figure 2.13 Comparison of Proffitt's field and VR results for verbal (left) and haptic (right) measures

2.2.5 Viewing Hills from the Side

Not only is the slope of hills overestimated when viewing them head-on, Proffitt, Creem, and Zosh replicated these conclusions while having observers view the cross-section of hills in real and VR environments [61]. They had 30 subjects view one of two hills (24^o and 34^o) from the side and provide the three measures mentioned previously. Proffitt, Creem, and Zosh found that slope estimations were similar, whether viewed from the front or from the side [61]. Using a 3 (hill) x 3 (measure) ANOVA, they found a significant effect of measure, with both verbal and visual measures being significantly greater than the haptic measure. Using a Scheffe post hoc comparison, the cross-section measurements of the 24^o and 34^o hills were not significantly different than the front-view judgment of the 31^o hill from the 1995 experiment previously discussed. These results are illustrated in Figure 2.14.

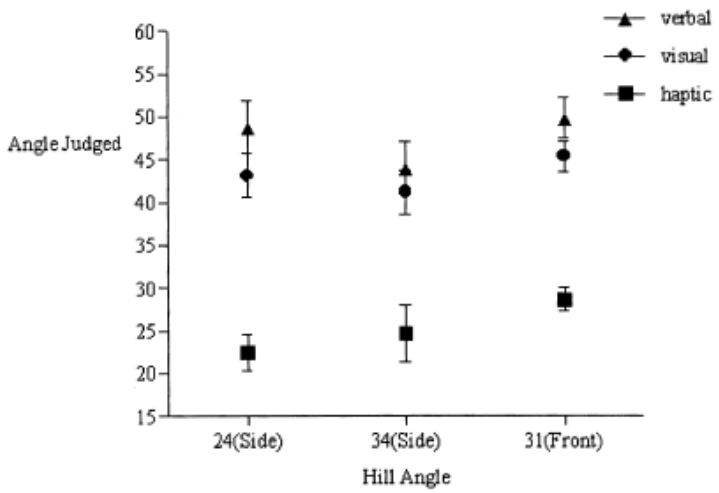

Figure 2.14 Mean verbal, visual, and haptic estimates of front-on hills [60] and side-view hills [61]

Proffitt, Creem, and Zosh also found that slope estimations from a side-view corresponded well with frontal-view estimations in a VR environment [61]. Using a 2(measure) x 12 (hill) x 2 (view) x 2 (sex) x 2 (order) ANOVA, they found no significant difference between the front and side views in the slope overestimation for the verbal measure and a somewhat greater estimation for views from the side when compared to the front. These results are further illustrated in Figure 2.15. This experiment verifies that the viewing position of a hill is independent of a subject's slope estimation. This was later used when selecting conical hills for the stimuli of the present study, described in detail in Chapter 3.

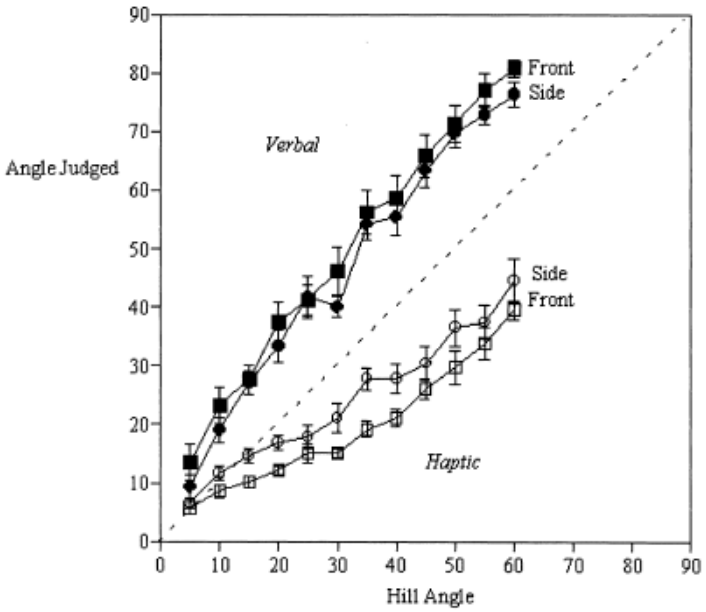

Figure 2.15 Mean verbal and haptic estimates of Proffitt's VR experiments [60], [61]

2.2.6 Effect of Affordance

Beyond visual information, slope estimation has been linked to one's physiological state. Gibson proposed that the perception of spatial layout can be described as the perception of affordances – the relationship of the physical properties of an object and the action potential one possesses for using the object [41]. The affordance one possesses when viewing and estimating a slope or a distance refers to the walk-ability by that person. Hills viewed from the top have been estimated as *steeper* than hills viewed from the bottom [60]. The explanation for this result concerns the biomechanical asymmetries that make descending a steep slope with stability more difficult that ascending it. Consistent with this notion, Proffitt et. al found that verbal and visual measures of slope estimation were significantly greater after reaching a state of fatigue [60]. This hypothesis was tested by having 60 subjects who frequently jogged at least 3 times a week for at least 3 miles estimate 2 hills (5^o and 31^o) – one before and one after a run that would put them in a state of fatigue. The results of this test are illustrated in Figure 2.16 and indicate the significant increase in mean verbal and visual estimates after the run. These results were expanded into distance estimation by Proffitt et. al by having 12 subjects verbally estimate the distance to a cone with and without a heavy backpack [62]. Although both conditions resulted in an underestimation of distance, those wearing a backpack made larger estimations.

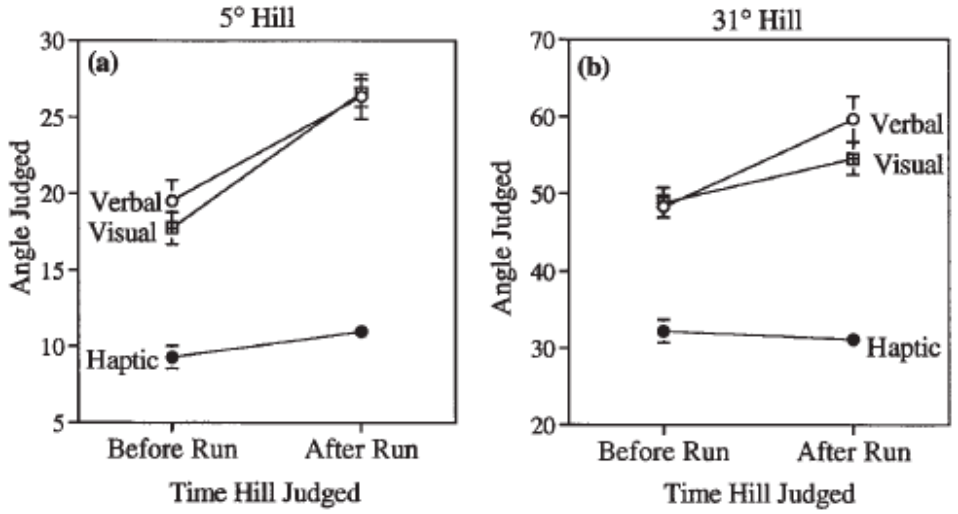

Figure 2.16 Significant increase in mean slope estimates after reaching fatigue by Proffitt et. al [60]

2.3 Previous Studies on Distance Estimation

"Distances on the lunar surface are deceiving. A large boulder field located north of the LM did not appear to be too far away when viewed from the LM cockpit. However, on the surface, we did not come close to this field, although we traversed about 100 feet toward it…Because distance judgment is related to the accuracy of size estimation, it is evident that these skills may require refinement in the lunar environment."
~ Astronauts Armstrong and Aldrin, Apollo 11[44]

Distance estimation presents a more widely researched topic than slope estimation, because of the larger number of factors affecting estimates and the variety of results obtained over the years from different experiments. Lunar distance estimation presents an even greater challenge without recognizable objects of known size, regular textures, and aerial perspective across terrain similar to a desert! This section will identify factors presenting salient distance cues from past research and determine whether they could be used within a lunar environment. This section also details various measurement protocols from previous experiments that were applied to the present study. It will present the results of previous studies and whether subjects more commonly overestimated or underestimated distances, and what limitations occur when testing in a VR environment.

2.3.1 Factors Affecting Distance Estimates

Estimating distance is unfortunately not as obvious as the colors of the rainbow. Rather, our cognitive abilities will consciously and subconsciously recognize and interpret the information available in the retinal images, through stereo fusion of these images or through other physiological factors unique to one's body. Beginning from a physiological perspective, Gibson studied an ecological approach to perception through affordances, stating that an environment will offer an observer some action potential

[41]. He specifies that our behavioral potential is a relation between the properties of the environment and an observer's body dimensions. This concept is consistent with the affordance defined in the previous section. Studies have shown that perceived egocentric distance increases when people wear a heavy backpack or when a visual-motor adaptation reduces the anticipated optic-flow that normally occurs when walking [62]. Because a greater effort is required to complete an action in these states, one's estimation of the action required (such as the distance) is affected.

One of the body dimensions affecting the affordance of traveling distances is eye height. Sedgwick first developed a theory, connected to the *horizon – ratio relation*, suggesting that the perceived object height is determined in relation to its position on the horizon [70]. This cue, however, relies on the interpretation of the horizon for comparison. The lunar environment not only possesses a different horizon than the earth, but an astronaut's ability to distinguish the horizontal may be altered by the reduced gravity. Therefore, the use of the horizon as an indicator for distance may develop with time, but only after adaptation to the environment. Another hypothesis, suggested by Ooi, Wu, and He, suggests the visual system uses angular declination below the horizon for distance judgments [59]. They had subjects binocularly view objects from distances of 1 – 8 meters and walk to the objects blindfolded to estimate the distance. When placing prism goggles upon the subjects to make the objects appear lower within their visual field, the subjects underestimated the distance, and after adapting to this viewing condition and removing the goggles, they overestimated the distance [59]. Their hypothesis is illustrated in Figure 2.17. They argue the errors were a result of a lower perceived eye-level, though this conclusion assumes that the vision system uses eye-level to determine angular declination, rather than only visual cues, such as the texture of the ground plane. The change in angular declination decreases exponentially as the distance to the objects increases much beyond the 8 meters used in this experiment. The use of angular declination would not be particularly useful for estimating distant objects in the lunar environment.

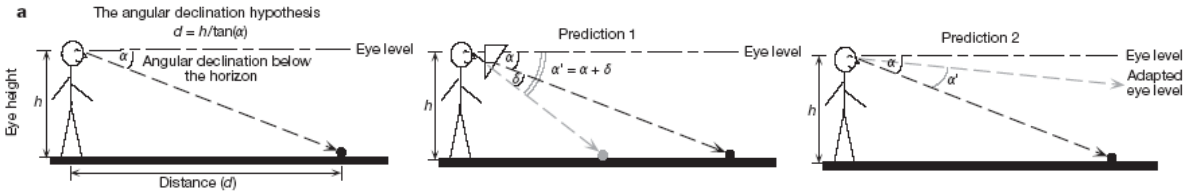

Figure 2.17 Ooi, Wu, and He's angular declination hypothesis [59]

Beyond physiological cues, the information within the retinal image has also been shown to provide cues that can be interpreted to determine the distance to an object. The use of binocular disparity and motion

parallax to judge absolute distance is a reliable indicator for distances within personal space, up to about 2 meters; however, these cues by themselves become less useful and more prone to error within action space, from 2 – 30 meters [4, 43]. Within this range, Wu, Ooi, and He argue that humans can accurately judge distance by integrating the local patches of the ground information from the point directly at the feet of the observer to the object [82]. The usefulness of this method, though, relies upon the availability of salient texture gradients throughout the distance being examined. Although the authors comment that distance judgments do improve with larger field sizes, because of more visual surface information, the lack of a systematic textural gradient upon the lunar surface may hinder the use of this method. Following the Apollo 14 landing, Astronauts Shepard and Mitchell commented on the resemblance of the lunar regolith to a fresh blanket of snow. The authors of On the Moon, a collection of the Apollo transcripts and interviews, suggested: "Because the lunar regolith completely blankets the surface, the subdued terrain makes it difficult to estimate distances" [44]. Without discrete texture in a lunar environment, surface integration becomes difficult, if not impossible.

2.3.2 Various Measurement Protocols

Experiments designed to measure distance estimation have all faced a common difficulty – how to measure a subject's cognitive state without biasing them with the measurement procedures. Perceived distance has been shown to increases as a power function of the actual distance [2]. The exponent of this power function reveals whether distance estimates are accelerating or decelerating, that is whether they are becoming more or less accurate as distance changes. Procedures used in previous experiments include verbal reports of physical units [38], magnitude estimation [3], fractionation and ratio estimation [24], magnitude production [75], and equal-appearing intervals or partition method [20]. To complicate matters, the exponents of the power functions have been shown to be sensitive to the experimental procedures used [23]. Additionally, the environment used to judge distance also affects the exponent of the power function – for example, R. Teghtsoonian & M. Teghtsoonian showed that distance estimates were an accelerating power function of actual distance indoors and a decelerating power function of actual distance outdoors [74]. Other researchers found that the more enclosed an environment appeared, the closer the exponent of the power function would approach 1.0 [57]. Even the subtle differences in the experiment instructions created large differences in the results [14]. Critical to magnitude estimation, the size of the standard or the value assigned to the standard may also influence the results [23].

Unfortunately, no single variable mentioned above can account for the differences found in a single experiment. Interactions are likely to occur between the instructions, the range of test distances, the

methods for obtaining the estimates, viewing conditions, and characteristics of the environment [23]. Despite the seemingly hopeless situation, Da Silva confirmed several trends important to constructing a distance estimation protocol. Using a large open field (300 meters long x 30 meters wide) with brush and trees on the edges, he marked several yellow triangles at distances from the baseline. He ensured all subjects had perfect 20/20 corrected vision, were naïve as to the nature of the experiment, and were not allowed to walk around the experimental area. He had all subjects view the distances binocularly.

During his first experiment, Da Silva used magnitude estimation for distances between 2 and 256 meters, with a standard reference of 32 meters. He divided his subject pool into three groups with different presentation of the standard reference. Group 1 was only presented the standard at the beginning of each series of judgments. Group 2 was presented the standard for 10 seconds preceding each distance judgment. Group 3 was presented the standard continuously throughout the experiment. Using Least Squares fits, the results indicated no effect of the presentation frequency of the standard [23]. The second experiment again analyzed the effect of the presentation of the standard; however, a modular distance was used rather than assigning it physical units. This modular distance consisted of a unitless range of values with a minimum and maximum (such as 0 to 10) with the standard assigned a number within that range. Again, the availability of the standard did not significantly affect the exponent of the power function [23]. During his third experiment, Da Silva divided each group into two sub-groups, which were told to estimate either the physical distance or the apparent distance between two stimuli presented one at a time. Da Silva found again that the presence of the standard and type of instruction were non-significant in affecting the exponent of the results [23]. Other experiments within the same study showed that magnitude estimation produced smaller exponents than both ratio estimation and fractionation and that increasing the range of distance decreased the mean exponent of the power function relating perceived distance and actual distance [23].

Given the results from the experiments discussed above, magnitude estimation was chosen due to its relation to the methods astronauts are likely to use on the lunar surface, and the procedures and results from Da Silva's study were critical in developing the test protocol outlined in Chapter 3.

2.3.3 Overestimations or Underestimations?

As Astronauts Shepard and Mitchell approached Station B2 during their climb of Cone Crater in Apollo 14, they approached a larger crater, thought to be "Old Nameless" [44]. During an interview following the mission, Mitchell commented about the identified crater: "It looks like that could be 200 or 300 yards

and yet 200 or 300 yards would put it on the traverse map." After recognizing the orientation of the crater with the Sun line, he realized "that's a lot more than 200 or 300 yards away. That's clear off of the map. That's a mile away" [44]. The astronauts during the Apollo missions were very susceptible to underestimating the distance to a crater or a hill within their visual frame. Without the presence of strong textural gradients and recognizable objects, the reference frame assumed by the astronauts was ambiguous and often left to self-interpretation. However, with the lack of aerial perspective, the clarity of distant objects often made them appear much closer. The combination of these cues is difficult to find within an environment on Earth. Additionally, researchers have found both distance underestimations and overestimations within an Earth environment.

Stefanucci, Proffitt, Banton, and Epstein found that distance estimates were larger when judged on steep uphill and downhill terrain than when judged upon flat terrain [73]. Proffitt's previous study indicated that people are likely to overestimate the slope of hills between 2 and 34 degrees [60]. Using geometry, it seems likely that subjects would also underestimate the distance to a point on that hill, as shown in Figure 2.18. However, Proffitt also found that the physiological effort associated with ascending a hill affected one's perception causing people to overestimate its slope. Using both physical and virtual hills, the authors found that distances on hills were overestimated and that one's perception of the spatial layout entails more than the geometry of the optical variables [73]. These results further support the effect of affordance on one's perception.

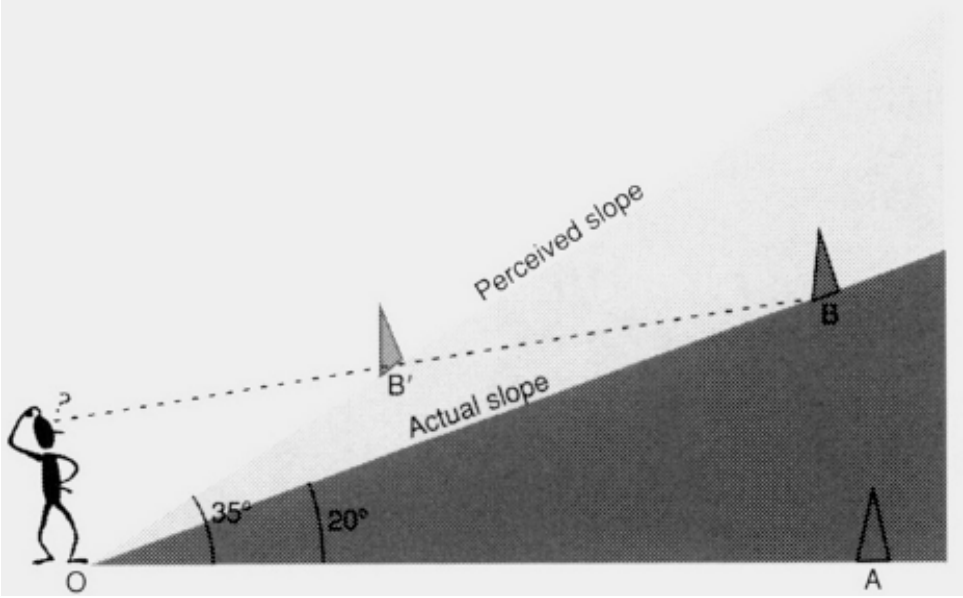

Figure 2.18 Geometrical hypothesis of distance underestimation when slope is overestimated

Without hills to influence one's affordance during distance estimation, other researchers have found different results in large, open environments. Daum and Hecht found both underestimations and overestimations, depending on the physical distance being estimated. They tested within both action space (up to 30 meters) and vista space (beyond 30 meters). They found subjects tended to underestimate distances up to 100 meters and overestimate distances beyond 100 meters [25]. They also found a significant effect of body position, with greater estimates from the prone position. Their results suggested a division between distance estimation in near vista space (below 100 meters) and far vista space (beyond 100 meters) [25].

Other researchers have also explored both near and far vista space. An early experiment by Gibson and Bergman in a large, open field found subjects more likely to underestimate distances between 48 and 361 meters, though, with a tendency to overestimate further distances [39]. These results were extended by Bee in a study where subjects estimated the distance to a Landrover between 500 and 2130 meters. Bee found the percentage error significantly increased with actual distance and the tendency to underestimate was found for only near distances [5]. Additionally, Fine and Kobrick, using a familiar military truck, found distance estimates were highly accurate up to 1100 meters, with a tendency to overestimate distance with high variability beyond this range [32].

Common trends for each of the open-field vista space studies were an increase in variability of estimates and the likelihood of overestimation at greater distances (These trends seem contrary to the astronauts' experiences of underestimating larger distances within the lunar environment; however, the lunar environment possesses several unique conditions not present in previous studies). Daum and Hecht developed a model outlining the interaction of these effects, shown in Figure 2.19

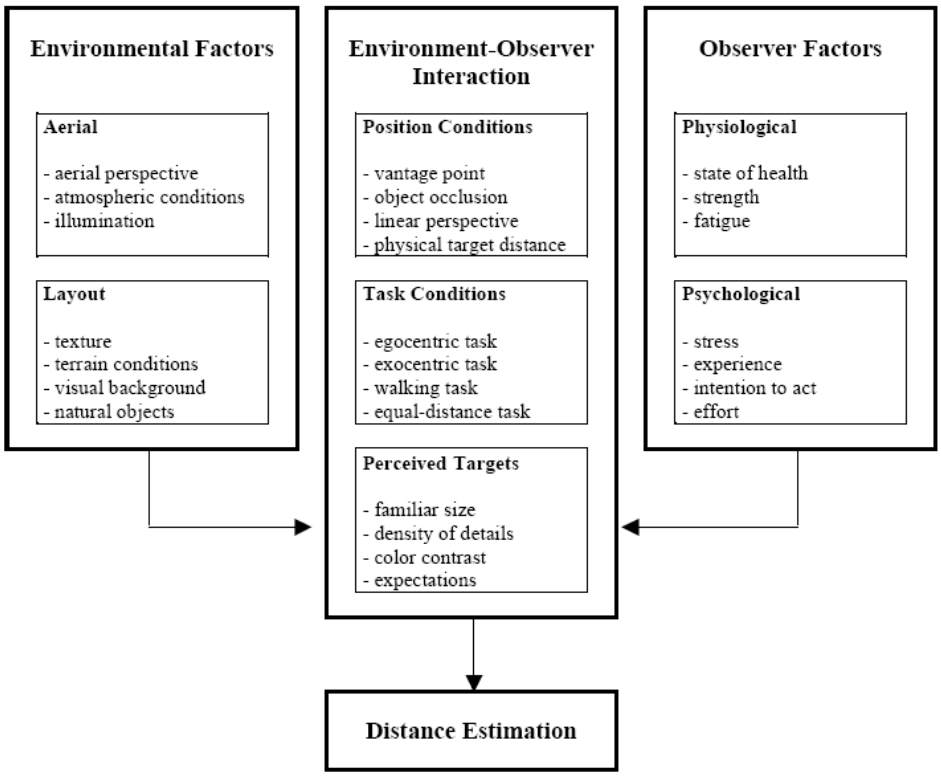

Figure 2.19 Daum and Hecht's model of interactions affecting distance estimation [25]

Using the model in Figure 2.19, the lunar environment fails to have targets of familiar size and possesses a large amount of clarity without aerial perspective. The targets may or may not be obstructed by other ridges or hills and the physiological and psychological states may vary with the type of excursion they are undertaking and the resistance they face moving within their spacesuits. Therefore, the errors expected in the present study are expected to be highly variable. Daum and Hecht did find a correlation between texture compression and distance, universal across a variety of distances and likely to influence the visual system [25]. Since the sun elevation has a direct effect on the appearance of texture across the ground plane, the present study will determine the effect of sun elevation on distance estimates.

2.3.4 Testing Limitations in a Virtual Environment

Virtual Reality environments offer a unique testing arena for distance estimation. Identifying the challenges of this environment is critical for future training simulations that will prepare astronauts for the visual conditions and illusions they will face on the lunar surface. Several of these challenges include a systematic underestimation of distance, the limitations on the FOV, and the effect of stereo viewing conditions.

Many previous researchers have found that egocentric distances are significantly underestimated in a VR environment [80, 81, 51, 28]. The reason for these conclusions may be connected to several factors present in a HMD environment, such as the inconsistency between accommodative and simulated distance [8], the spatial resolution of the HMD display, the fidelity of the cues available in the environment, limited FOV, and knowledge that a person is within a VR environment [52]. However, no significant effects of graphical fidelity on distance perception was found by Thompson et. al in photorealistic and wireframe VR environments with a high–resolution HMD [76].

Conflicting results were produced concerning whether the FOV affected distance estimation. Knapp and Loomis found no significant effect of FOV on verbal report and blind-walking responses for distances between 2 and 15 meters [52]. The two FOV conditions used in this study were an unrestricted (180^o horizontal x 120^o vertical) FOV and a reduced (58^o horizontal x 43^o vertical) FOV restricted by a rectangular box. Two other teams of researchers, however, found a similar reduced FOV provided small, though significant, underestimations of distance [9, 77]. Additionally, Kline and Witmer showed that a limited vertical FOV produced significant underestimations of distance for a range consistent with the Knapp and Loomis study [50]. These results express the importance of viewing the ground plane from the feet of the observer to the target, whether or not a strong textural gradient exists.

Another potential explanation for the compression of distance found in many VR studies relates to the properties that affect the binocular presentation of the scene. Although accommodation and eye convergence are closely linked under normal viewing conditions [43], binocular disparity is subject to distortions within HMD's, such as the difficulty in matching the inter-pupilary distance (IPD) at near distances [66]. Additionally, calibrated measurement of the accommodative distance in a particular HMD is not easily obtained [78]. As previously mentioned, stereo information is helpful at near distances, but deteriorates in vista space. Willemsen et. al hypothesized that the combination of stereo information from near locations and relative information of farther points would improve a person's ability to scale their frame of reference within a VR environment. Their tests, however, failed to show that compression of distance judgments were affected by stereo manipulations, suggesting binocular presentation in not a source of distance compression found in VR environments [78].

Distance estimation within a VR environment remains an issue to be faced within the current experiment and future lunar navigation training tools for astronauts. Although the use of stereo vision may not play a significant role in the potential distance compression, high-resolution graphics and virtual displays with a larger vertical FOV would provide the most optimal and realistic conditions.

CHAPTER 3

METHODS

Current and future Virtual Reality (VR) technology provides an ideal environment to train astronauts for the perceptual difficulties they will face while navigating the lunar environment. Before such protocols are developed, confidence must be obtained with the accuracy of a VR environment in providing a realistic setting that causes that same magnitude of errors that will be experienced on the actual lunar surface. Although incorporating the effect of $1/6^{th}$ gravity during a training protocol will be a challenge to be faced in future years, the current study provides a foundational analysis of the errors and factors affecting slope, distance, and height estimation.

This chapter first outlines the experimental approach toward validating a VR environment as a training tool for astronauts preparing for a lunar mission (Section 3.1). Section 3.2 discusses the number and characteristics of the subjects within each experiment and the external conditions of the environment that may have impacted their judgments. Section 3.3 provides an overview of each piece of experimental equipment used with the field and VR studies. Section 3.4 outlines the instructions and protocol for each experiment and Section 3.5 overviews the statistical tests used to analyze the errors and factors affecting each measure. The content of this chapter will allow future researchers to reproduce the results of this study and further develop a training tool for lunar missions.

3.1 Experiment Design

Any VR training tool for astronauts would be useless unless it can accurately portray the same environment and difficulties they will face on the lunar surface. Although previous studies have determined the estimation errors in both field and VR environments [60, 61], neither study has recreated the exact field scene within the VR environment, but used artificial objects and graphics instead. Lunar regolith properties, terrain topography, and lighting conditions of the lunar surface are not currently available in a VR environment without the use of panoramic images obtained from the Apollo missions. Although future studies and the VR training tool will likely incorporate a computer generated environment from the high-quality LIDAR and RADAR data now available, the current study seeks to evaluate the perceptual errors using photographic images.

To validate the consistency of slope and distance errors of photographic images between field and VR environments, an environment with lunar-like terrain was selected in Hanksville, UT and an initial field study was conducted in January 2008 as part of the Mars Society, Mars Desert Research Station (MDRS) Crew 65 expedition. The terrain within this environment includes vast, flat distances (Figure 3.1 – upper left) with abundant hills (Figure 3.1 – upper right) and irregular shaped rocks (Figure 3.1 – lower left). The soil possesses a reddish tint that contains little or no vegetation and the shadows created at low sun angles provide a large degree of contrast within the surface texture (Figure 3.1 – lower right).

Figure 3.1 Mars Society Mars Desert Research Station (MDRS) field environment, Hanksville, UT (clear, dry and high altitude location)

Beyond the collection of slope measurements, the MDRS Field Study (MFS) sought to obtain stereo photographs of all the estimated hills using digital cameras and a LANC controller described in Section 3.2. These images were placed within a VR environment using WorldViz Vizard 3.0. The Lunar-like VR Pilot Study (MVPS) was first conducted in May 2008 to determine the effect of stereo vs. synoptic viewing of the images to decide if manipulations were needed to the panoramic lunar images for stereo

presentation. The results of the MVPS were implemented into the viewing conditions of the Lunar-like VR Study (MVS), conducted in June 2008, where synoptic images from the MFS were presented and slope and distance estimates were collected and compared to the MFS for validation of the VR training environment. The Lunar VR Study (LVS), conducted in September 2008, evaluated the slope, distance, and height errors of subject estimates for lunar terrain. The lunar terrain consisted of Apollo images acquired from Arizona State University (ASU) and the *Apollo Lunar Surface Journals*.

The final field study, Lunar-like Field Study #2 (DFS), was conducted at the Mars Institute Haughton Mars Project (HMP), located on a large impact crater on Devon Island in August 2008. This project, funded and conducted by our sponsoring organization, the National Space Biomedical Research Institute (NSBRI), sought to further evaluate the slope and distance errors of hills in a different lunar-like environment. The Devon Island environment provides a similar rocky, desert terrain to that found in Utah and on the lunar surface with a great sense of relative isolation and remoteness [26] (Figure 3.2). Table 3.1 summarizes the experiments in this study.

Figure 3.2 Mars Institute Haughton Mars Project (HMP) field environment, Devon Island, Canada

Table 3.1 Overview of all experiments

Experment	Designation	Environment	Location	Date
Lunar-like Field Study #1	MFS	Field	Mars Desert Research Station, Hanksville, UT	January-08
Lunar-like VR Pilot Study	MVPS	Virtual Reality	Man Vehicle Lab, MIT	May-08
Lunar-like VR Study	MVS	Virtual Reality	Man Vehicle Lab, MIT	June-08
Lunar VR Study	LVS	Virtual Reality	Man Vehicle Lab, MIT	September-08
Lunar-like Field Study #2	DFS	Field	Mars Institute Haughton Mars Project, Devon Island	August-08

3.2 Subjects

Ideally, the subjects participating in this study should complete all experiments to determine the amount of inter-subject differences and whether these differences were consistent. Due to test site limitations and financial costs of transporting subjects to a lunar-like environment for the field studies, it was determined

most effective to utilize the subjects available at each field study test location site and to recruit a separate pool of subjects to complete both VR experiments at MIT. Additionally, since the MFS and the MVS contained the same hills as test stimuli, including the same pool of subjects in both experiments may have introduced previous knowledge of the actual field environment, something that the astronauts will be unable to obtain before traveling to the Moon. Therefore, the number of subjects included within the VR studies was large enough to obtain a normal distribution of estimates for each hill so systematic and random errors could accurately be calculated.

All crew members on the Mars Society MDRS Crew 65 Expedition, excluding the author of this study, were subjects within the MFS and completed a Subject Consent Form (see Appendix A) and a Subject Information Form (see Appendix B). Gender was disproportional (4 males, 1 female) and was not analyzed as a factor. Age ranged from 24 – 52 years old and all subjects had obtained at least a Bachelor's degree. One subject had prior knowledge of previous slope estimation studies from Proffitt et. al [60] and was advised to estimate the slope as it appeared without compensating for the trends discussed in the study. All subjects wore the Mar Society MDRS spacesuit, shown in Figure 3.3, which weighed 15-20 kg and possessed a spherical helmet. Although the helmet possessed an unrestricted FOV, the ventilation system was inadequate at times and allowed water vapor from the subjects' breath to collect and disrupt the clarity of their view. Additionally, post-experiment feedback indicated that "suits were tiresome," potentially impacting their affordance of walking up each hill. The results from all subjects were included in the analysis in Chapter 4.

Figure 3.3 Mars Society spacesuits worn by all subjects in MFS

Seven subjects were recruited and completed the MVPS at MIT. All subjects were students and faculty affiliated with the Man Vehicle Lab and completed a Subject Consent Form and a Subject Information Form. Two of the seven subjects were excluded from the results analysis due to their roles as the Principle Investigator (PI) and Undergraduate Research Opportunities Program (UROP) assistant possessing knowledge of the actual slope and distance of the hills within the study. Of the remaining five subjects (three male, two female), age ranged from 22 – 31 years and all subjects possessed normal or corrected-to-normal vision. All subjects completed the experiment in its entirety.

Twenty-five subjects were recruited for the MVS at MIT through a COUHES approved advertisement (see Appendix C) that was posted in buildings and sent via email. All subjects completed the Subject Consent Form and Subject Information Form. Five subjects were excluded from the results analysis due to prior knowledge of the experiment and failure to follow the instructions of the experiment. Three of these subjects were the PI, UROP assistant, and a project engineer who possessed knowledge of the actual slopes and distances within the study. Of the 20 remaining subjects used within the analysis, gender was disproportional (16 males, 4 females) and excluded from the analysis and age ranged from 20 – 40 years. All subjects possessed normal or corrected-to-normal vision with the exception of one subject whose corrected vision was 20/50. One subject possessed prior scientific knowledge of slope estimation studies, as well as extensive VR experience. This subject was included without any evidence or indication that his naivety of the stimuli was compromised by prior knowledge.

Thirty-one subjects were recruited for the LVS using the advertisement in Appendix C and through contacting the subjects from the MVS. All subjects completed the Subject Consent form and Subject Information Form; however, six subjects were excluded from the analysis for the following reasons: completing a pilot study version of the experiment (2), not completing the experiment (2), and failure to follow the instructions (2). Of the 25 subjects whose data was analyzed, 11 had previously participated in the MVS and one had previously participated in the MPVS. Gender was again disproportional (20 males, 5 females) and was not analyzed as a factor affecting estimates. Age ranged from 20 – 40 years and all subjects possessed normal or corrected-to-normal vision. No subjects possessed prior knowledge of slope estimation beyond occasional recreational hiking.

Six subjects were recruited for the DFS and completed the Subject Consent Form and the Subject Information Form; however, due to deteriorating weather conditions during the expedition, only two subjects participated in the experiment. Both subjects were male with vision correctable to at least 20/25. One subject was 46 years old with an MBA in mechanical engineering and the other subject was 52 years

old with a Masters degree in geology. Neither subject possessed difficulties with depth perception nor were required to wear a spacesuit. The subject characteristics for all experiments are summarized in Table 3.2.

Table 3.2 Subject information for each experiment

Experment	Designation	Total Subjects	Subjects Analyzed	Male/Female
Lunar-like Field Study #1	MFS	5	5	4/1
Lunar-like VR Pilot Study	MVPS	7	5	3/2
Lunar-like VR Study	MVS	25	20	16/4
Lunar VR Study	LVS	31	25	20/5
Lunar-like Field Study #2	DFS	2	2	2/0

3.3 Equipment

The following equipment was used to perform the field and VR experiments within the present study. Characteristics of the equipment and the procedures for their use are described in this section.

3.3.1 Laser Range Finder

The actual slope and distance of the hills in the MFS and DFS were determined using a *Bushnell Pinseeker 1500 w/Slope* Laser Rangefinder (LRF). This rangefinder possesses a distance range between 5 and 1500 yards with an accuracy of +/- 1 yard and a slope range between 0 and 20 degrees with an accuracy of +/- 1 degree. The maximum range is 1500 yards for reflective objects and 1000 yards for trees. Its magnification is 7x and its objective lens is 26 mm. The units of its distance output may be either yards or meter, though meters were used in this study. The slope output is the angle between the horizontal and the straight line distance between the LRF and the target object. The actual slope of each hill in the field studies was calculated using the output of the LRF and the Law of Sines/Cosines and will be further discussed in Section 3.4.1. The LRF is illustrated in Figure 3.4

Figure 3.4 Bushnell Pinseeker w/Slope Laser Rangefinder

3.3.2 Stereo Cameras/LANC Controller

Two *Sony V3* digital cameras were used to collect stereo images of each hill within the MFS to be later presented in the MVS. The maximum effective pixel size is 7.1 Megapixels and the maximum image resolution is 3072 x 2304. The cameras possess a 2.5 inch LCD screen and allow manual control of aperture, shutter speed, and focus settings. This control was necessary to ensure consistent lighting conditions for each stereo pair of photographs. The synchronization between the stereo cameras was accomplished with a Shepherd LANC (Local Area Network within a camera) controller, which coordinates the power-up, power-down, focus lock, shutter, and zoom functions. It also coordinates a single flash and displays the synchronization (time between the shutter of each camera) in both fraction and decimal form. Figure 3.5 illustrates both pieces of equipment.

Figure 3.5 Sony V3 digital camera (left) and Shepherd LANC controller (right)

3.3.3 Tripod

The camera tripod was acquired through a personal friend and held both the stereo cameras/LANC controller and the palm board for haptic measurements. The two digital cameras were secured side-by-side on a twin camera-bar that possessed a bubble level. The IPD between the two cameras was 13.1 cm. The typical IPD between humans is much less, though stereo fusion was verified by the authors, using a polarized lens during the field study and under VR conditions following the field study. Although IPD has been known to cause distortions within VR [66], the objects being viewed by subjects were at least 25 meters away, beyond action space, where stereo information is much less useful. The twin bar was placed on top of the tripod (shown in Figure 3.6) and adjusted using pitch, roll, and yaw movements until the cameras were pointed directly at the hill of interest and the bubble was centered on the bubble level.

Figure 3.6 MFS and DFS camera tripod

3.3.4 Visual Estimation Device

Visual slope estimation within the MFS and the DFS was accomplished by a matching task using a set of 61 flashcards displaying a black semi-circular wedge rotated at angles ranging from 0 to 60 degrees with respect to a green horizontal plane in increasing order. Figure 3.7 illustrates the set of cards with the "zero degree wedge" shown on top. Although subjects viewed the slope head-on, the cards were from a side-view of the hill, requiring subjects to mentally make a 90^{o} yaw transformation. This matching task was very similar to the continuous adjustment of the circular wedge visual task used by Proffitt et. al [60].

The subjects were given the flashcards with a random card on top and asked to look at the hill they were judging and envision the view of the hill from the side. They next flipped through all the cards and selected the card with a slope that matched the slope of the hill envisioned from the side view. There was unlimited time to select a card. The back of the cards possessed an alphabetized code that was recorded when a subject selected a card, and subjects were instructed to avoid looking at the back of the cards. After the subject has selected a card, they gave the stack of cards back to the investigator with the selected card on top.

Figure 3.7 MFS visual estimation device

3.3.5 Haptic Estimation Device

Haptic slope estimation in the MFS and DFS was accomplished using a palmboard device constructed within the MVL at MIT, similar to the palm-board used by Proffitt et. al [60]. The dimensions of the palm-board are 9.5" x 5.5" and the hinge of the palmboard is located 5.25 inches behind its front edge. A digital slope gauge is attached to the right side of the palm-board, shown in Figure 3.8. The device was located at waist-level in front and to the right of the subject's body, allowing them to make a 90^{o} angle between their upper and lower arm. Height adjustments were made using the legs of the tripod. All subjects in the field studies used their right hand to make haptic estimations by placing it on the surface of the palmboard. Without looking at the board, they were instructed to match the angle of the board to the slope of the hill they are judging. They had unlimited time and could move the board up and down before stopping at their final position. After reaching their final position, they notified the investigator who recorded their measurement from the digital slope gauge.

Figure 3.8 MFS haptic estimation device

3.3.6 Virtual Reality Head-Mounted Display

The images within the VR experiments (MPVS, MVS, LVS) were displayed using an nVis nVisor SX binocular Head-Mounted Display (HMD) with a 1280 x 1024 pixel resolution and a 60^{o} diagonal FOV. The resolution of the HMD was much greater than the resolution used in the 1995 slope estimation study by Proffitt et. al [60]. To preserve the vertical FOV of the stereo photographs from the field study, the images were scaled and cropped horizontally to fit within the HMD display. Head tracking was not used in this study due to the size of the photographs, but is available within the MVL for future studies with larger panoramic images. The HMD was well-fitted to the head of each subject using two adjustable knobs and was large enough to allow subjects to wear glasses during the experiment. An illustration of the HMD is shown in Figure 3.9.

Figure 3.9 nVis nVisor SX binocular Head-Mounted Display for MVS and LVS

3.3.7 Supine Support Structure

The supine support structure is a wooden structure, constructed within the MVL at MIT, allowing the subjects to wear the HMD while positioning their body so $1/6^{th}$ G acted along their longitudinal body axis. The dimensions of this structure are shown in Figure 3.10 and it was designed for a maximum subject standing height of 6 ft. 6 inches (78 inches). The top of the board is covered with padded material to alleviate any subject discomfort with a 12” x 12” gap in the head region, allowing the subject to wear the HMD without it interfering with the structure. The neck of each subject was supported by a foam material. The keyboard and mouse were positioned on a stand using Velcro, allowing them to easily manipulate the visual estimation devices.

TOP VIEW

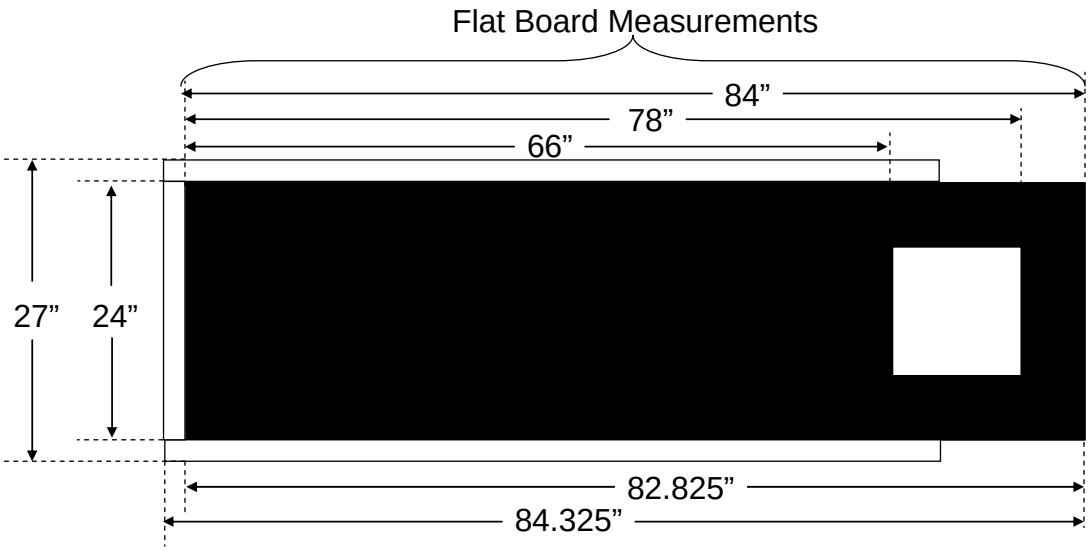

FRONT VIEW

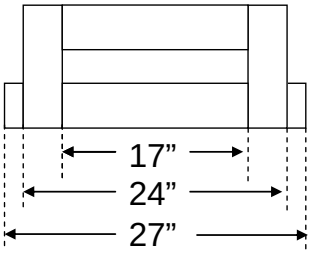

SIDE VIEW

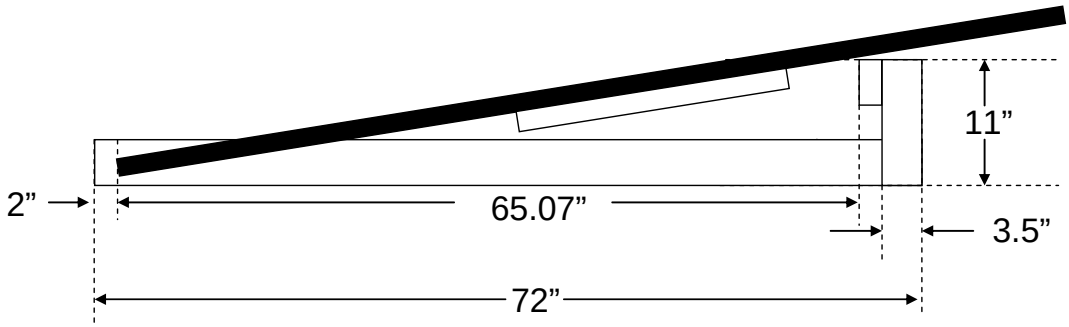

Figure 3.10 Supine support structure for MVS and LVS

3.4 Experimental Design and Procedures

This section describes the design and procedures of each experiment to independently isolate the design factors and collect unbiased slope, distance, and height estimates.

3.4.1 MDRS Field Study

The first lunar-like field study, the MDRS Field Study (MFS), was conducted in Hanksville, UT from January 26, 2008 to February 1, 2008. The experimental design factorially analyzed the effects of true slope, true distance, and sun angle for similarly shaped hills. The range of slopes selected was 10 – 25 degrees to align with the upper boundary of slopes that Proffitt stated as walk-able without slipping [60]. The distance conditions ranged from 25 meters – 75 meters to the base of each hill to explore the region beyond action space where stereo vision becomes of less use. Finally, sun elevation and sun azimuths were varied by testing at three different times during the day, including 8:00 a.m., 12:00 p.m., and 4:00 p.m. Figure 3.11 illustrates the sun data for one of the test days in Hanksville, UT.

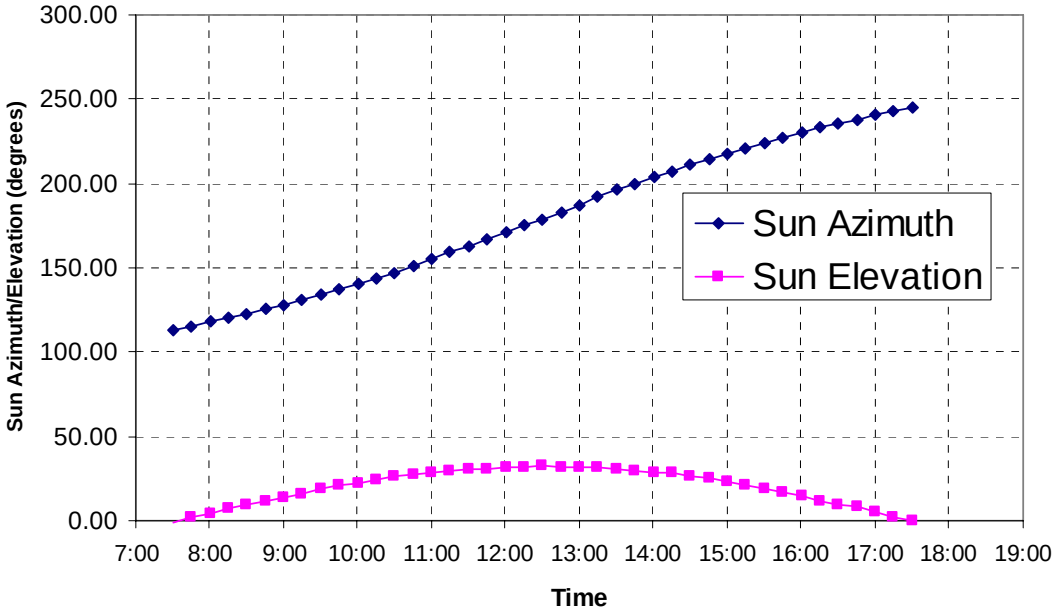

Figure 3.11 Sun Position Data in Hanksville, UT on January 26, 2008

The maximum sun elevation only increased slightly from 32 to 34 degrees from the first to the last testing day, while the sun azimuth at any particular time only varied by 1 degree across the range of test days. The final test matrix for the MFS is shown in Table 3.3.

Table 3.3 Factorial design matrix for MFS

Time-of-day	Distance (m)	Slopes (deg)
8:00 AM	**25**	14.3, 18.1, 19.2, 22.8, 23.3
Sun Elevation	**50**	
10°	**75**	
12:00 PM	**25**	
Sun Elevation	**50**	
33°	**75**	
4:00 PM	**25**	
Sun Elevation	**50**	
11°	**75**	

3.4.1.1 Pre-Experimental Preparation

After arriving on site, the environment was explored to find the optimal test area that provided hills with the desired range of 10 – 25 degrees that were in proximity to each other to avoid long transit times and was surrounded by flat terrain to test the range of distance conditions. The chosen hills are illustrated in Appendix D.1. The distance to the base of each hill was measured using the distance output on the LRF. The slope of each hill was measured using the distance and slope outputs of the LRF and the Law of Sines/Cosines. The investigator first stood 10 – 15 meters from the base of each hill and aimed the LRF at the base of the hill. After recording the distance and slope output from the LRF, he aimed the LRF at the top of the hill and again recorded the distance and slope. He repeated this procedure 10 – 15 times and calculated an average distance and an average slope to both the bottom and top of each hill. Figure 3.12 illustrate the relationship of these averages and the actual slope of the hill.

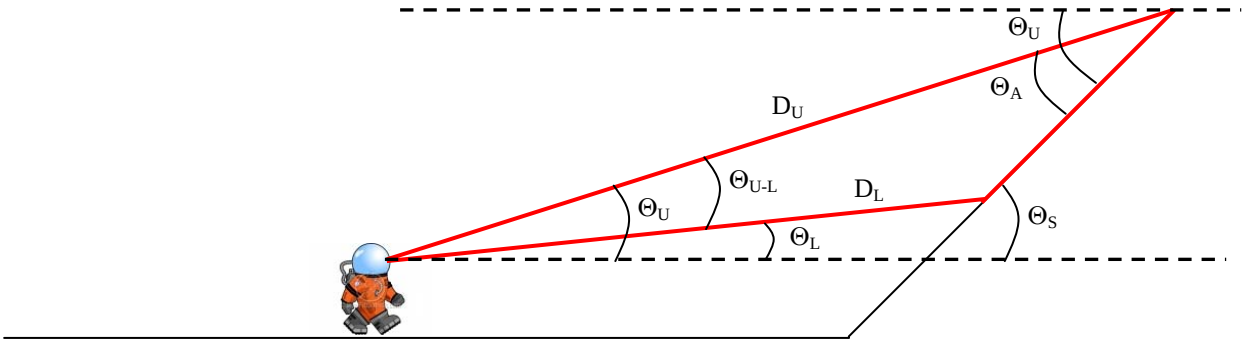

Figure 3.12 Geometric relationship between the output of the LRF and the true slope

The geometric relationship between the output of the LRF and the actual slope of the hill relies on the lengths and angles of the isosceles triangle outlined in red. The distance between the investigator and the

bottom of the region being estimated (D_L) and the distance between the investigator and the top of the region being estimated (D_U) make up the lower leg and hypotenuse of the triangle, respectively. The angle between these sides (Θ_{U-L}) was calculated by subtracting the LRF slope output to the bottom of the hill (Θ_L) from the slope output to the top of the hill (Θ_U). Using the Law of Sines/Cosines, Eqn. 3.1 explains how the angle Θ_A was calculated from the LRF information.

$$\theta_A = \sin^{-1}\left(\frac{D_L}{D_L{}^2 + D_U{}^2 - 2D_L D_U \cos(\theta_{U-L})}\sin(\theta_{U-L})\right) \qquad \text{Eqn. 3.1}$$

After Θ_A was determined, the slope of each hill (Θ_S) was calculated by subtracting the angle Θ_A from the angle Θ_U. Table 3.3 lists the calculated slope for each hill in the MFS. Pre-experimental preparations included preparing the testing environment for quick identification of each location for estimation by placing small flags in the ground. These flags did not interfere with slope estimation and distance estimation was not conducted in this field study since subjects frequently walked throughout the testing area during the tests, providing additional knowledge and cues of the actual distance. The presentation of the hills was also randomized and adjusted to maximize the number of hills presented between subsequent estimations of any one particular hill. Prior to the experiment, subjects were briefed on the use of both visual and haptic estimation devices and were instructed to avoid looking at the test hills during their transit to and from the testing area. They were asked to complete three separate sessions, one at each time-of-day (8:00 a.m., 12:00 p.m., and 4:00 p.m.) and estimate 15 hills (5 hills x 3 distances) per session.

3.4.1.2 Experimental Procedures

At the start of each session, subjects put on their MDRS spacesuits and followed the investigator to the test site. After arriving at the first test location, the investigator spread the legs of the tripod and leveled the camera mount, using the bubble level on the camera mount as verification. The time was recorded on the experiment datasheet and the LANC controller was powered on to see the initial synchronization time displayed on the LANC device. If the synchronization time was not less than 0.5 ms, the cameras were powered off and powered back on using the LANC controller (this process was repeated until the synchronization time was below 0.5 ms). The zoom option was not used and both cameras were placed on the "automatic" setting. The cameras were aimed at the hill being estimated, placing the hill in the center of the camera LCD. The investigator verified the flash was turned off by observing a "lightning bolt with a slash through it" near the battery level indicator in the upper left corner of the LCD screen for each camera. The large button on the LANC was then pressed halfway down and the bottom of the

camera viewfinders were observed to see the shutter speed and aperture values for each camera. If the shutter speed and aperture values corresponded between cameras, the large button on the LANC was pressed the full way down until the picture was taken. If the values did not correspond, the large button was released and then pressed halfway again. If after several tries without shutter speed and aperture consistency between cameras, the investigator would set one or both camera dials to "M" to manually set the aperture and shutter speed values before pressing the large button on the LANC to take the picture.

After each picture was taken, the cameras were powered off to preserve the batteries. The shutter speed, aperture, and synchronization values were recorded on the experiment datasheet. The investigator next asked each subject to visually estimate the slope of the hill using the procedure in 3.3.4. While the subjects selected a flashcard, the investigator ensured the digital slope gauge on the palmboard read 0 +/- 0.5 deg (See Figure 3.13 – left). After selecting a flashcard, each subject haptically estimated the slope using the procedure in 3.3.5 and the investigator recorded the estimated slope from the digital slope gauge. Once all subjects completed both estimates, the investigator led the subjects to the next test location and began setting up the camera tripod. After all test locations were completed, the investigator led the subjects back to the habitat and collected feedback about the methods used and difficulties experienced during the experiment. Figure 3.13 shows a subject during visual estimation.

Figure 3.13 Visual slope estimation during the MFS

3.4.2 MDRS Virtual Reality Study

The MDRS VR Study, MVS, was factorially designed to analyze the same factors controlled in the MFS. To avoid the effects of boredom and fatigue in the experiment, the number of hills, distances, and time-of-day conditions were reduced from the MFS to three, two, and two, respectively. All 12 possible combinations of slope, distance, and time-of-day conditions were viewed for each of 4 sessions in a random order, without presenting any one hill consecutively. Sessions 3 and 4 were a repetition of sessions 1 and 2. A training session, containing five images of the 18.1° and 23.3° hills from the MFS preceded the four main sessions. Additionally, all conditions were viewed in two body positions: standing with 1 G acting along the body axis (session 1 and 4) and inclined 10° above the horizontal supine position with 1/6th G acting along the body axis (sessions 2 and 3). The test matrix for the MVS is shown in Table 3.4 and the conditions for each session are shown in Table 3.5

Table 3.4 Factorial design matrix for MVS

Body Position	Time-of-day	Distance (m)	Slopes (deg)
Standing 1 g along body axis	**8:00 AM**	**25**	14.3 19.2 22.8
	Sun Elevation (10°)	**75**	
	12:00 PM	**25**	
	Sun Elevation (33°)	**75**	
Inclined 10° above Supine 1/6th g along body axis	**8:00 AM**	**25**	
	Sun Elevation (10°)	**75**	
	12:00 PM	**25**	
	Sun Elevation (33°)	**75**	

Table 3.5 Testing conditions for each session in the MVS (left) and the MPVS (right)

Session	Body Position	Repetition
Training	Standing	1
1	Standing	1
2	Supine	1
3	Suping	2
4	Standing	2

Session	Body Position	Presentation
Training	Standing	Stereo
1	Standing	Synoptic
2	Supine	Stereo
3	Supine	Synoptic
4	Standing	Stereo

Prior to the MVS, the MPVS was completed to determine the effect of stereo when viewing the images of the lunar-like terrain. Without using a repetition of test conditions in this study, the first and third sessions were under synoptic viewing conditions, while the second and fourth sessions were under stereo viewing conditions. None of the subjects indicated a noticeable difference between the different presentations in a post-experiment survey and the results, discussed in detail in Chapter 4, also indicated

no consistent significant difference between the estimates for the two viewing conditions. Since the LVS would be conducted under synoptic viewing conditions, this condition was also chosen for the MVS.

WorldViz Vizard 3.0 was the VR programming software used to develop the MPVS and the MVS. The code was originally created by the author of this study and is located in Appendix E. Since the MFS indicated little difference between the visual and haptic estimates, only visual estimations were collected. Without a subject's familiarity of the testing environment, distance estimates were collected for each hill using magnitude estimation with lower and upper limits set to 0 and 100 meters, respectively. The distance estimation device consisted of a scroll bar that was adjusted between the lower and upper limits without a quantitative output of the slider's current position. One of the two hills from the MFS that were not included in the design of the MVS was used as the standard reference from a location 50 meters from the base of the hill. Since Da Silva found that the availability of the standard reference during a distance magnitude experiment had no effect on results [23], the 50 meter reference in the MVS was displayed only at the start of the training session. Illustrations of the estimation devices are shown in Figure 3.14.

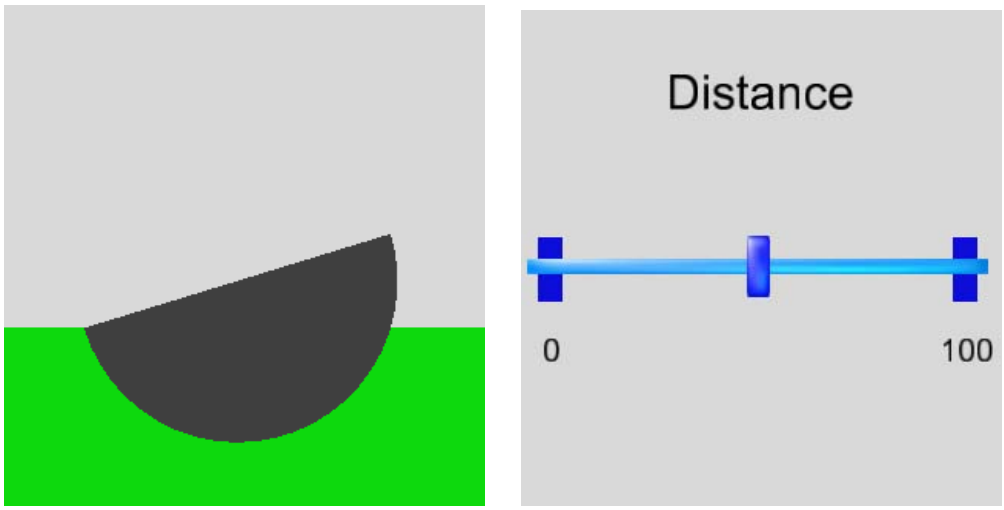

Figure 3.14 Slope (left) and distance (right) visual estimation devices for the MVS

After each subject completed the forms at the beginning of the experiment, a presentation was shown training them on the experimental design and the use of the estimation devices (See Appendix F.1). The subjects had the opportunity to ask questions following the presentation, and once satisfied, donned the HMD and adjusted it to fit comfortably on their head. Prior to beginning the training session, a white screen with words introducing the training session was shown at different depths and the subjects were asked which words appeared closest to them, verifying their ability to perceive depth under VR conditions. After pressing the spacebar to begin, the subjects viewed the standard reference hill at 50

meters. No estimates were collected for the reference hill, though a red box appeared over the region of the hill and remained until the subject pressed the spacebar to advance to the next hill.

The remaining four hills in the training session and all other hills in the experiment followed the same protocol. A red box appeared over the region of the hill to be estimated and remained visible for 3.0 seconds (See Figure 3.15). After the red box disappeared, the visual estimation device appeared with an initial slope of 0 degrees and the subjects then adjusted the slope of the device by scrolling the mouse wheel away from them (increasing slope) or toward them (decreasing slope). At any point during their estimation, the subjects were allowed to re-highlight the region to be estimated by pressing the left mouse button. After they were satisfied with their slope estimate, the subjects pressed the spacebar and advanced to the distance estimation device. This device had an initial distance of 50 meters, which subjects adjusted by scrolling the mouse wheel away from them (increasing distance) or toward them (decreasing distance). Once satisfied with their distance estimate, the space bar was pressed and the scene was advanced to the next image. At the end of each session, a white screen with the words "END OF SESSION" was displayed.

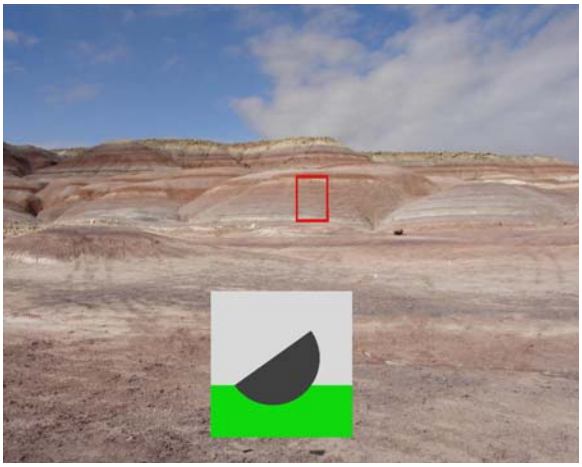

Figure 3.15 Red box indicating region to be estimated and location of estimation device in MVS

The subjects were given an optional 5 minute break following the second session and any hills that were mistakenly skipped were estimated at the end of each session. Following the completion of the fourth session, subjects were given a post-experiment feedback form, found in Appendix G.1. No feedback on performance was given during/after the experiment with the expectation of their participation in the LVS.

3.4.3 Lunar Virtual Reality Study

The Lunar VR study, LVS, evaluated slope, distance, and height estimation on the lunar surface using Apollo lunar surface imagery. Unlike the MFS and the MVS, the ability to create a factorial design of test conditions was limited by the location and time each Apollo photograph was taken. Additionally, feedback from the MVS indicated that subjects recognized previously viewed hills under new lighting or distance conditions, suggesting the potential that later estimates had dependence on earlier estimates. To maximize the independence between estimates, the number of hills included in the LVS was maximized. Therefore, the objective of the experimental design was to collect at least two distance conditions for six hills on the lunar surface, though the distances between hills were different. An additional obstacle in the experimental design was collinearity between distance and sun elevation effects, which will later be discussed in the results of the LVS in Chapter 4. A personal interview with Astronaut Charles Duke suggested the lunar craters appeared steeper than lunar hills because misjudging a crater and getting stuck inside presents a greater safety concern than misjudging the slope of a hill and walking back down [27]. Therefore, six lunar craters were also analyzed.

The acquisition of lunar photographs included the *Apollo Lunar Surface Journals* (ALSJ) and Arizona State University. Dr. Eric Jones, David Harland, Sydney Buxton, and Ken Glover assisted in providing high-resolution panoramas of the craters and training hills for the experiment from the Apollo 12, 15, 16, and 17 missions. Dr. Mark Robinson and his team at Arizona State University provided individual high-resolution scans of the original photographs from the Apollo 17 mission in the Taurus-Littrow Valley from the station (STA) 1, 2, and 7 locations. These images served as the stimuli for the lunar hills in the experiment. Tables 3.6 and 3.7 summarize the experimental design matrix for the LVS and Appendix D.2 contains the photographs shown in these tables.

Table 3.6 Experimental design matrix of hills within LVS

Hill	Mission	Name	STA	Image #	Slope (deg)	Distance (m)	Height (m)	Sun Elevation (deg)
1	17	Wessex Cleft	1	AS17-134-20431	14.7	5200	700	16
1	17	Wessex Cleft	2	AS17-137-20955	14.7	11400	700	26
2	17	Bear Mountain	1	AS17-134-20418	15.1	4000	276	16
2	17	Bear Mountain	7	AS17-146-22349	15.1	8400	276	37
3	17	Sculptured Hill	1	AS17-134-20431	22.2	5000	1110	16
3	17	Sculptured Hill	2	AS17-137-20955	22.2	11500	1110	26
4	17	Mons Vitruvius	1	AS17-134-20414	24.1	10900	2091	16
4	17	Mons Vitruvius	7	AS17-146-22347	24.1	13900	2091	37
5	17	North Massif	1	AS17-134-20429	25.6	4300	1551	16
5	17	North Massif	2	AS17-137-20953	25.6	8800	1551	26
6	17	South Massif	1	AS17-134-20421	25.6	6500	2341	16
6	17	South Massif	7	AS17-146-22352	25.6	9800	2341	37

Table 3.7 Experimental design matrix of craters within LVS

Crater	Mission	Name	STA	Slope (deg)	Diameter (m)	Sun Elevation (deg)
7	12	Surveyor	LM	7	180	8
8	17	Camelot	5	16	550	28
9	16	Spook	2	17	250	25
10	17	Shorty	4	20	123	27
11	16	Flag	1	30	209	24
12	16	North Ray	11	30	877	46

To further maximize the independence between estimates of the same hill, the experiment was divided into a training session and 5 main sessions. The training session contained two hills and two craters. The first and third sessions contained the 12 lunar hill slope/distance combinations in a pseudo-random order so hills presented early in a session were presented toward the end to balance any session effects of fatigue or improved performance. The second and fourth sessions contained the six lunar craters in a random order. The fifth session was a repetition of the six lunar hills (each hill at one distance condition), followed by the six lunar craters. The first, second, and fifth sessions were conducted from the standing position, and the third and fourth sessions were conducted from the supine support structure. Table 3.8 summarizes the session order.

Table 3.8 Testing conditions for each session in the LVS

Session	Stimuli	Body Position	Repetition
Training	Hills/Craters	Standing	1
1	Hills	Standing	1
2	Craters	Standing	1
3	Hills	Supine	1
4	Craters	Supine	1
5	Hills/Craters	Standing	2

The actual slopes, distances, and heights were calculated using a plot digitizer software program and Pythagorean's Theorem on lunar topographic maps from the *Apollo Lunar Surface Journals*. The topographic maps for the Apollo 15 and 17 missions contained both coordinate information and elevation contours, while coordinate information for the Apollo 16 mission was obtained from photographic maps that were complimentary to the topographic maps that possessed elevation contours. A topographic map with coordinate information of the Apollo 12 Surveyor Crater was also used. All maps are found in Appendix H. The distance between the elevation contours of the chosen hills and craters were mostly consistent, thus, the slope along these hills and craters had little variance. After the axes were calibrated on each topographic map within the digitizer, the distance between each STA and the base of the hill was

calculated by digitizing the position of each and using Pythagorean's Theorem. This distance is illustrated In Figure 3.16 by the solid red line from STA 1 to the base of the South Massif. The distance across a crater was calculated by digitizing the points at the near and far lips, with respect to the orientation of the photographer. The slope of each hill and crater was calculated by digitizing the position of each contour along a straight line, calculating the distance between these points using Pythagorean's Theorem, and calculating the slope between the contours using the inverse tangent. The average slope of the entire hill was calculated using only the points at the lowest and highest contour lines on the hill. The points that were digitized along the contours for the Apollo 17 South Massif are shown in Figure 3.16 by small red circles. The heights of the hills were calculated by subtracting the elevation marking at the top of each hill by the elevation at its base.

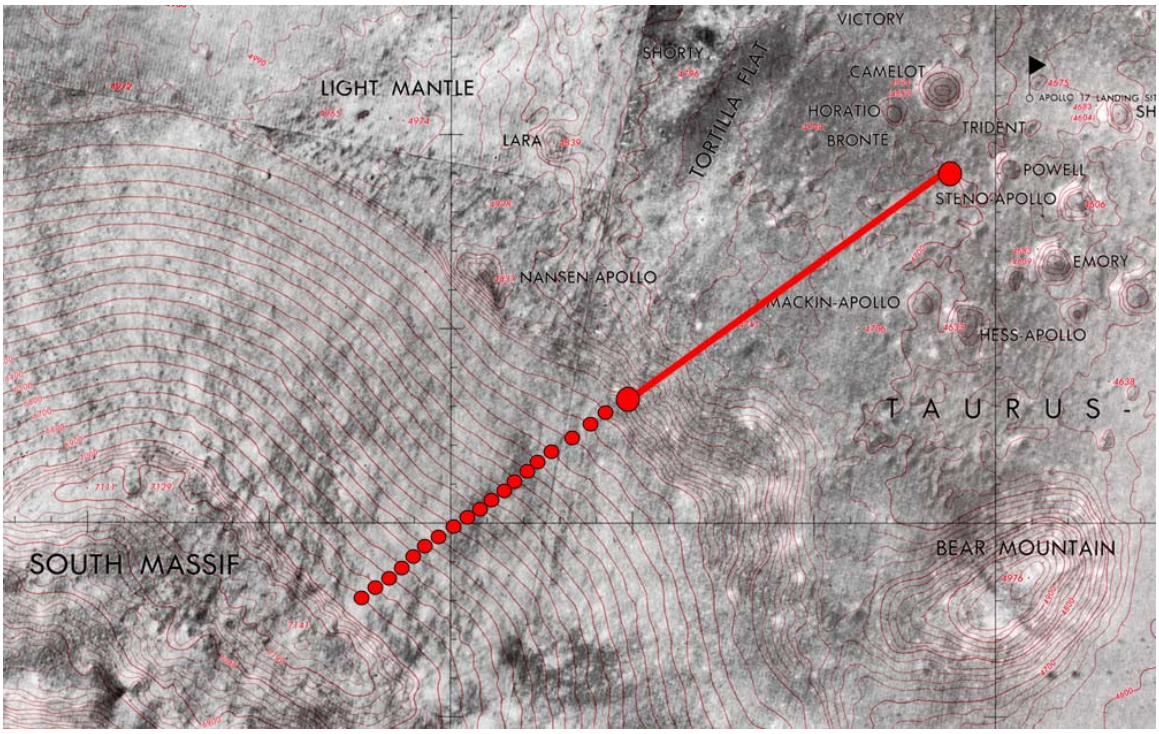

Figure 3.16 Digitized points for determining the distance and slope of the South Massif from STA 1

WorldViz Vizard 3.0 software was used to develop the LVS. The code was originally created by the author of this study and is located in Appendix E.3. The experimental measures within the LVS were slope, distance to the base, and height estimates of each hill and slope and distance across each crater. Slope estimates were measured using the visual matching task from the MFS and the MVS and the estimation device began at zero degrees for each hill. Distance estimation to the lunar hills was measured using magnitude estimation with lower and upper limits set to 0 and 20.0 km, respectively. The

estimation device consisted of a horizontal scroll bar (Figure 3.17 – center) that was incremented by 0.1 km by scrolling the mouse wheel away from (increasing distance) or toward (decreasing distance) the subject. The device was initially set to 10.0 km for each hill. Distance estimation across the lunar craters was measured using magnitude estimation with lower and upper limits set to 0 and 1500 m, respectively. The estimation device consisted of a horizontal scroll bar that was incremented by 10 m by scrolling the mouse wheel away from (increasing distance) or toward (decreasing distance) the subject. The device was initially set to 750 m for each crater. Height estimation was measured using magnitude estimation with lower and upper limits set to 0 and 4000 m, respectively. The estimation device consisted of a vertical scroll bar (Figure 3.17 – right) that was incremented by 25 m by scrolling the mouse wheel away from (increasing height) or toward (decreasing height) the subject. The device was initially set to 2000 m for each hill. Figure 3.17 illustrates the estimation devices used for the lunar hills.

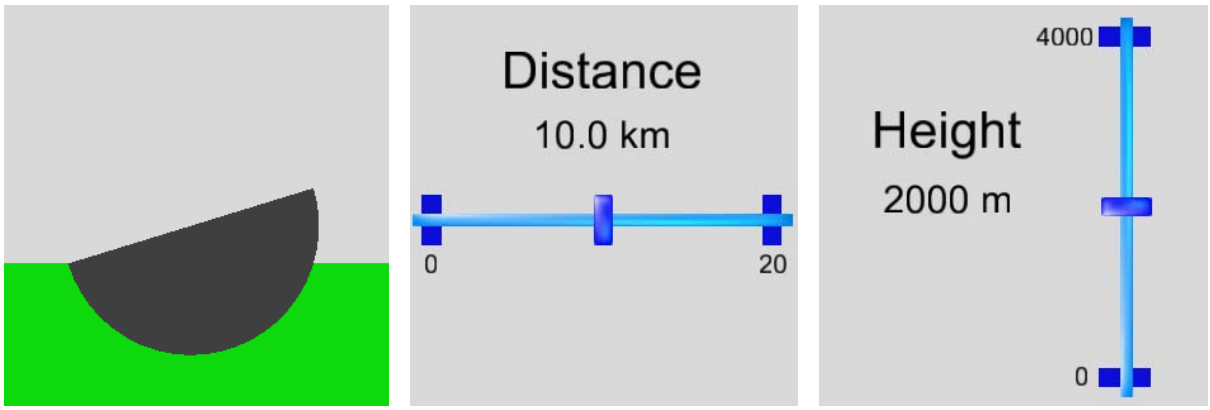

Figure 3.17 Slope (left), distance (center), and height (right) estimation devices for hills in the LVS

The training session included two hills followed by two craters, not included in Tables 3.6 and 3.7. The first hill served as a standard reference for the distance and height magnitude estimation with an actual distance of 7.1 km and actual height of 1200 m. The second hill did not provide distance or height information and served only for practice. The first crater served as a standard reference for the distance magnitude estimation with an actual distance of 440 m and the second crater only served as practice.

Consistent with the MVS, the subjects pressed the spacebar to advance to each new image or estimation device. Rather than using a red box to indicate the region of the hill for estimation, the LVS used two arrows, at the top and bottom of each hill or the near and far lip of each crater, to identify the region of the hill or crater for estimation (See Figure 3.18). After a new image was displayed, the arrows were visible for three seconds until the estimation devices appeared. The subjects were able to re-display the arrows by pressing the left mouse button and hide the estimation device by pressing the right mouse button.

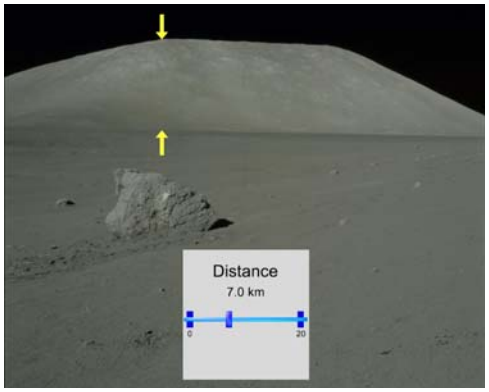

Figure 3.18 Placement of estimation devices and arrows within the LVS

After each subject completed the forms at the beginning of the experiment, a presentation was shown training them on the experimental design and the use of the estimation devices (See Appendix F.2). The subjects had the opportunity to ask questions following the presentation, and once satisfied, donned the HMD and adjusted it to fit comfortably on their head. Prior to beginning the training session, a white screen with words introducing the training session was shown at different depths and the subjects were asked which words appeared closest to them, verifying their ability to perceive depth under VR conditions. After all images in a session were displayed, an "End of Session" screen was shown. Subjects were permitted a five minute break between the second and third sessions. Following the experiment, subjects were asked to complete a post-experiment feedback form, found in Appendix G.2. Subjects were also debriefed on their performance in the MVS and the overall results of the study.

3.4.4 Devon Island Field Study

The second lunar-like field study at Devon Island, DFS, was factorially designed to test the same range of hills from the MFS at a larger range of distances (0 – 200 meters). The investigator of this study was different than all previous studies, but received thorough training to ensure the testing procedures were consistent with the MFS. A document of the instructions for the new investigator is located in Appendix I. The sun elevation and sun azimuth were not studied due to time constraints on the study. Although five hills were selected ranging from 10 – 40 degrees, poor weather conditions throughout the expedition only allowed two hills to be tested at four distances, shown in Table 3.9.

Table 3.9 Factorial design matrix for DFS

Slopes (deg)	Distance (m)
20.0	25
	50
	100
	200
39.6	25
	50
	100
	200

After arriving, the environment was surveyed until five hills were found within close proximity and the actual slope was determined by placing the digital slope gauge on the hill. The distance to each hill was determined using the LRF and marked. See Appendix D.3 for images of the two hills that were tested during the experiment.

The procedures followed during the DFS were consistent with the procedures for the MFS and will not be restated in its entirety in this section. Both visual and haptic slope estimates were collected for each hill, as well as stereo photographs using the Sony V3 digital cameras. Several differences between the MFS and the DFS include the absence of spacesuits worn by the subjects and the incorporation of distance estimation for each test location. Distance estimation was conducted by collecting a verbal estimate (in meters) of the distance between the observer and the base of the hill. Prior to the start of the experiment, a distance calibration session was completed by all subjects. Each subject was given a distance reference guide (See Appendix J) that stated the distance of familiar athletic courts. Additionally, red and green distance reference cards were placed on the ground at the distances indicated on the reference guide allowing the subjects to mentally correlate each familiar athletic court distance to the same distance in a featureless, lunar-like environment. Distance estimates were always collected after the haptic slope estimates. Figure 3.19 illustrates the placement of the distance reference cards.

Figure 3.19 Distance reference card placement during distance calibration in the DFS

All other procedures for the DFS were consistent with the MFS in Section 3.4.1. Following the experiment, subjects were given a feedback form (See Appendix G.3) to indicate the methods they used for estimating the slopes and distances. Limited data was collected because of weather conditions; however, results will still be discussed in Chapter 4.

3.5 Data Analysis and Statistics

The objectives of the data analysis for each study was to determine the slope, distance, and height systematic and random errors, and to determine the factors that significantly affect the slope, distance, and height estimates. A log or square root transformation of each estimate was regressed using a categorical hierarchical regression with subject as the identifier to determine what factors had a significant effect on the estimates. The residuals of each model were analyzed and tested for normality and homoscedasticity. All factors were listed as fixed effects. Individual paired t-tests with a Bonferroni Adjustment compared the estimates between different conditions of each factor in the regression. The systematic biases of all combinations of significant factors are displayed in the results sections in both physical units (degrees or meters) and as a percent of the actual measure and are compared to zero in a one-sample t-test. Standard

deviations are listed for each bias to represent the between-subject error, as well as standard errors to represent within-subject error. Two-sample t-tests compared the estimation errors between the MFS and MVS experiments and a one-sample t-test with a Bonferroni Adjustment compared the within subject differences between the MVS and LVS, as well as between the lunar hills and craters of the LVS. Paired t-tests, correlations coefficients, and Least Squares regressions were used to compare the slope and distance estimates of each subject with the DVS. The results of the statistical analysis and the post-experiment feedback were used to evaluate the hypotheses in Chapter 1 and suggest recommendations for future studies.

CHAPTER 4

RESULTS AND DISCUSSION

This chapter presents the results and analysis from each of the field and VR studies. Section 4.1 provides a brief overview of the type of results presented in each experiment. Section 4.2 presents the significant factors affecting slope estimates and the systematic and random errors found in the MDRS Field Study (MFS). Section 4.3 presents the effect of stereo presentation from the MDRS Pilot VR Study (MPVS), as well as the significant factors affecting slope and distance estimates and the systematic and random errors found in the MDRS VR Study (MVS). This section also compares the results from the MFS and the MVS and determines whether a VR environment can produce the same magnitude and variability of slope estimates as the actual environment. Section 4.4 presents the significant factors affecting slope, distance, and height estimates of lunar hills and craters and the systematic and random errors found in the Lunar VR Study (LVS), as well as comparisons between the MVS and LVS terrain and between the craters and hills in the LVS. Section 4.5 presents the slope and distance estimates from the Devon Island Field Study (DFS). This chapter will provide an understanding of the expected performance of slope, distance, and height judgment of lunar and lunar-like terrain in both field and VR environments.

4.1 Presentation

The following sections in this chapter present the results from each of the experiments in this study. Color-coded tables are incorporated to facilitate the understanding of each set of results. The analysis of each experiment consists of a mixed hierarchical regression using categories with fixed effects for each of the design variables. The coefficients and significance of each variable are shown in color-coded tables with yellow indicating hill/crater categories, green indicating distance categories, red indicating sun elevation categories, blue indicating measurement type categories, turquoise indicating body position categories, and purple indicating the continuous test session variable. The residuals and tests of normality and homoscedasticity are shown and discussed. Line graphs with standard errors visually display the trends for each design variable. The results of paired t-tests for each variable are also shown in blue and red color-coded tables, which will be explained in detail for each case. The presentation of systematic and random errors for each experiment includes bar graphs displaying the mean systematic biases, with one standard error shown for both physical units and as a percent of the actual measure (i.e. slope,

distance, or height), as well as color-coded tables that display the mean bias, standard deviation (between-subject variation), standard error (within-subject variation), and one-sample t-test results comparing the mean bias to zero. The mean bias, standard deviation, and standard error columns are color-coded yellow for physical units (degrees or meters) and green for unitless measures (percent of actual slope, distance, or height). Insufficient data was collected from the DFS to conduct a regression analysis. The results from this study consist of line graphs displaying the raw data for each subject and color-coded tables displaying the results of paired t-tests, correlation coefficients, and Least Square regression coefficients.

4.2 MDRS Field Study Results

The MFS analyzed the systematic and random errors of slope estimation in a lunar-like field environment within different combinations of the following factors: hill slope, distance from the base of the hill, sun elevation, and measurement type. This section presents the significant factors affecting slope estimates, graphs illustrating the trends of these factors, and tables summarizing the effects of each factor for individual combinations of the other factors in the experiment. This section also presents both systematic and random errors of slope estimates from this study and draws comparisons to past studies and experiences of Apollo astronauts on the lunar surface.

4.2.1 Slope Estimation Analysis

A mixed hierarchical regression with subject as the identifier and a square root transformation (to increase the model fit) of the estimated slope as the dependent variable was used to analyze the effects of the slope, distance, sun elevation, measurement, and session factors in the MFS. Table 4.1 shows the main effects of the regression. The residuals, shown in Figure 4.1, were analyzed for normality and homoscedasticity. Lilliefors test confirmed that the distribution of residuals was not significantly different than a normal distribution ($N = 450$, $p = 0.781$). The residuals were sliced into groups, shown in Table 4.2, and tested for homoscedasticity by hypothesis testing of the equality of several variances. Group 5 was excluded from the test with only 5 data points and the variances of the remaining groups were not found to be significantly different by Levene's Test ($F = 1.991$, $p = 0.095$).

Table 4.1 Mixed regression of estimated slope with categorized variables in MFS

Mixed Linear Regression on Square Root of Estimated Slope				
Variable	**Estimate**	**Standard Error**	**Z**	**p-value**
INTERCEPT	0.746	0.041	18.399	0.000
Hill #1 (14.3°)	-0.064	0.017	-3.857	0.000
Hill #2 (18.1°)	-0.010	0.017	-0.589	0.556
Hill #3 (19.2°)	-0.046	0.017	-2.767	0.006
Hill #4 (22.8°)	0.053	0.017	3.161	0.002
Hill #5 (23.3°)	0.067	0.017	4.052	0.000
Distance #1 (25 m)	0.002	0.004	0.475	0.635
Distance #2 (50 m)	0.003	0.004	0.603	0.547
Distance #3 (75 m)	-0.005	0.004	-1.078	0.281
Sun Elevation #1 (10°, 11°)	-0.002	0.003	-0.641	0.521
Sun Elevation #2 (33°)	0.002	0.003	0.641	0.521
Visual Measure	0.010	0.003	3.223	0.001
Haptic Measure	-0.010	0.003	-3.223	0.001
Session	0.024	0.004	6.078	0.000

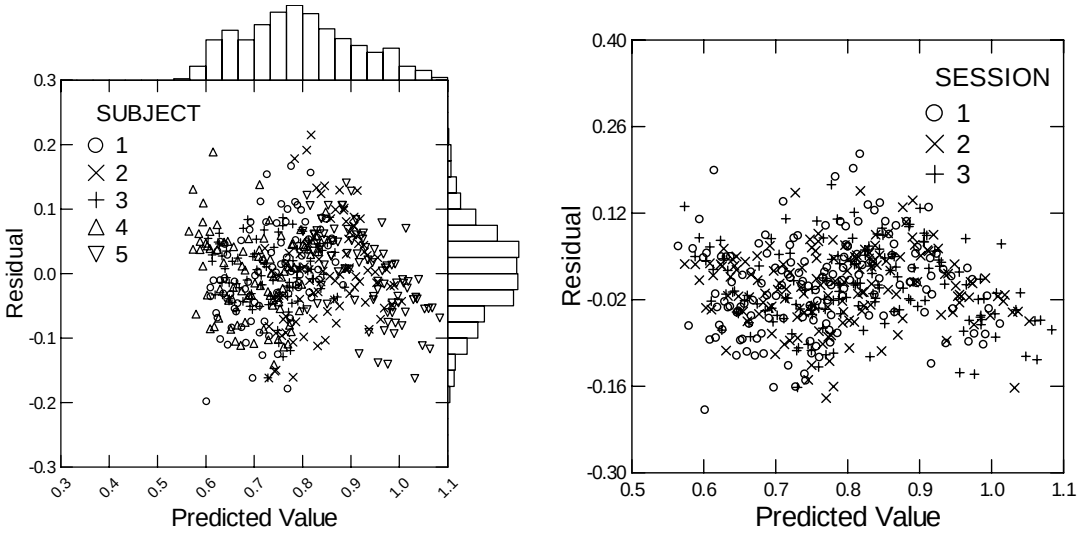

Figure 4.1 Residuals labeled by subject (left) and session (right) for the slope regression in the MFS

Table 4.2 Variance of residual groups for the slope regression in MFS

GROUP	N	Mean	Variance	Median
0	58	0.007	0.004	0.018
1	109	-0.023	0.004	-0.025
2	150	0.012	0.005	0.010
3	81	0.028	0.003	0.031
4	47	-0.034	0.002	-0.025
5	5	-0.070	0.001	-0.055

The results of this regression indicate a significant coefficient ($p < 0.05$) for 4 out of the 5 hills. With exception to Hill #2, the coefficients of the hills increase linearly, indicating the estimated slope increases with true slope for each subject, corresponding with Proffitt et. al's results [60]. This trend is further illustrated in Figure 4.2 (left) for both visual and haptic estimates. Surprisingly, Hill #2 (18.1^o) was on average estimated to be greater than Hill #3 (19.2^o) and the mean estimated slope for Hill #5 (23.3^o) is at least 2-3 degrees greater than Hill #4 (22.8^o), despite the true slope only increasing by 0.5 degrees. These peculiarities can be explained by the difference characteristics of each hill, such as the smaller heights of Hills #2 and #5 (< 3 meters) compared to the heights of the other three hills (> 6 meters). Height was not factorially designed in this experiment but should in future experiments to understand its effect on slope estimates.

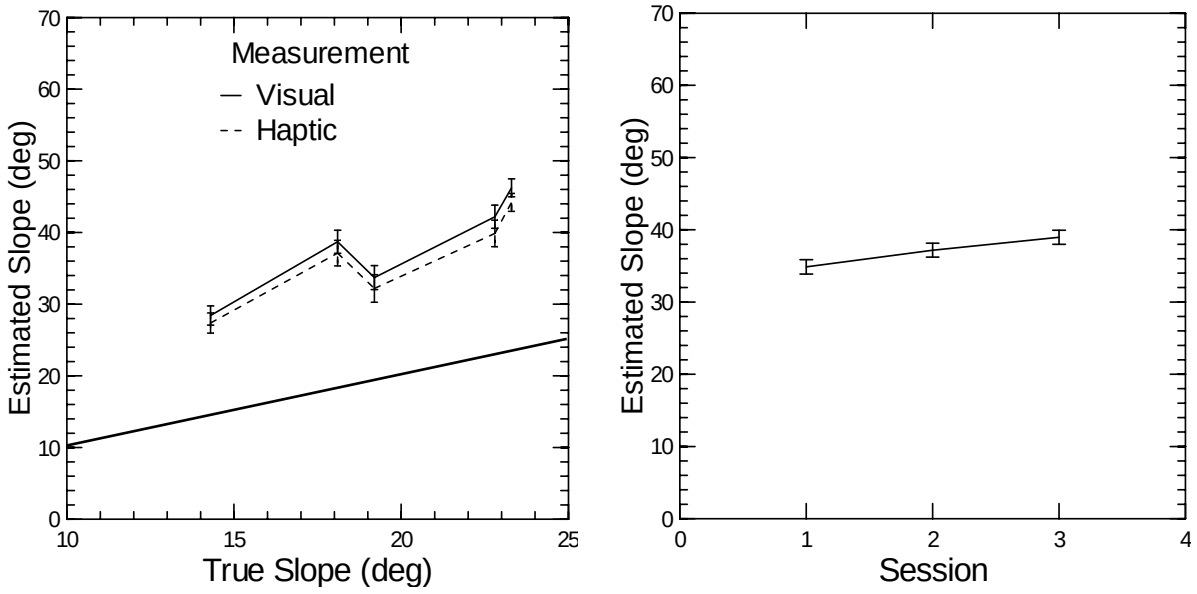

Figure 4.2 Effect of measurement method (left) and session (right) on slope estimates in MFS

None of the distances or sun elevations in Table 4.1 were significantly different from each other with coefficients within one standard error of the mean. However, the coefficients of the 25 m and 50 m distances were *greater* than the coefficient for the 75 m distance, suggesting that slope estimates were slightly *greater* at closer distances. Following the experiment, subjects commented that closer distances made a hill appear steeper because it filled up more of the FOV, and farther distances increased the difficult of observing the slope. The coefficient of the $10^o/11^o$ sun elevations was *less* than the coefficient of the 33^o sun elevation, suggesting that slope estimates were slightly *less* at lower sun elevations. The lack of significance for both factors could potentially be caused by the familiarity the subjects had with the test environment for repeated estimates of the same hills and the psychological effect that the true

slope of the hill does not change as distance from the base of the hill increases. This explanation was confirmed by the subjects in the post-experiment feedback.

Table 4.1 also shows a significant effect of measurement method, with the visual method producing a larger estimate than the haptic method, supporting Proffitt et. al's results [60]. Individual paired t-tests with a Bonferroni Adjustment for each hill were conducted with the null hypothesis that the visual and haptic estimates were equal for each subject. Table 4.3 illustrates the mean of the visual/haptic difference for each combination of factors with a positive mean (shaded blue in the table) indicating a greater visual estimate. The results revealed that overall visual estimates were greater than haptic estimates for all five hills and significantly greater for the steepest two.

Table 4.3 Paired t-tests between visual and haptic estimates for each subject in MFS

Hill	Slope (deg)	Mean of Difference (deg)	t Statistic	p-value
1	14.3	1.046	1.324	0.192
2	18.1	1.587	1.862	0.069
3	19.2	1.513	1.754	0.086
4	22.8	2.329	2.435	**0.019**
5	23.3	2.036	2.547	**0.014**

The continuous variable test session also had a significant effect on results with slope estimates increasing with session, shown in Figure 4.2 (right). Post-experiment feedback indicates that the number of hills per session and the spacesuits were tiresome. Since the experiment was conducted over several consecutive days, the cumulative fatigue may have affected the physical potential of the subjects, therefore, explaining the increase in slope estimates. The increase of slope estimates across session may also be attributed to boredom, which several subjects expressed following the experiment. Interestingly, many of the outlier residuals in Figure 4.1 (right) occurred in the first session, possibly due to their inexperience with estimating slopes before the study and the process of refining the methods they chose to employ. This result suggests the need for slope estimation training prior to lunar missions to allow astronauts to refine their estimates of the terrain they will encounter, making their errors more predictable.

4.2.2 Slope Estimation Systematic and Random Errors

Due to the lack of significance of the distance and sun elevation factors on slope estimates, these subpopulations were combined to present the total systematic (bias) and random errors of the slope estimates. Figure 4.3 illustrates the mean overestimation bias with one standard error for each of the five

hills using visual and haptic measures. Tables 4.4 and 4.5 summarize these results and highlight the minimum and maximum biases found in this study.

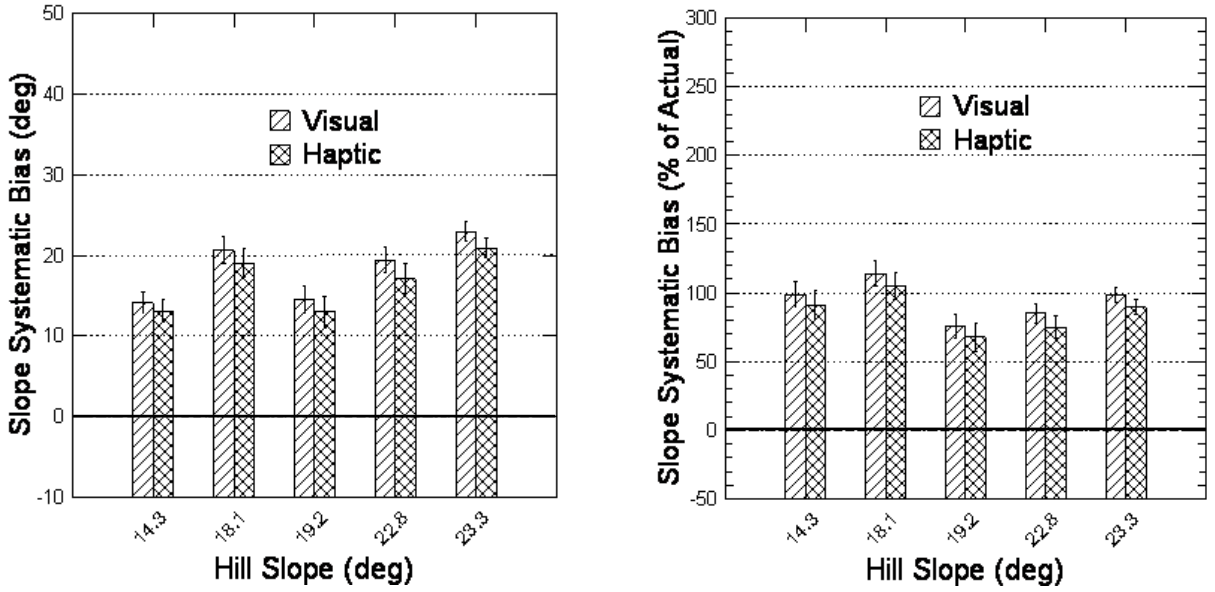

Figure 4.3 Bar graphs of slope estimation error (bias and one standard error), in degrees (left) and percent of actual slope (right), for each hill in MFS (positive error indicates overestimation)

Table 4.4 Mean systematic bias of slope estimates with standard deviations, standard errors, and 1-sample t-tests for each hill in the MFS

Measure	Hill	Slope (deg)	Mean Bias (deg)	Stand. Dev (deg)	Stand. Err (deg)	t Statistic	p-value
Visual	1	14.3	14.1	8.9	1.3	10.669	0.000
	2	18.1	20.6	10.7	1.6	12.871	0.000
	3	19.2	14.5	11.0	1.7	8.812	0.000
	4	22.8	19.4	10.7	1.6	12.136	0.000
	5	23.3	22.9	8.3	1.2	18.559	0.000
Haptic	1	14.3	13.1	9.3	1.4	9.434	0.000
	2	18.1	19.0	11.8	1.8	10.802	0.000
	3	19.2	13.0	12.8	1.9	6.831	0.000
	4	22.8	17.1	12.3	1.8	9.324	0.000
	5	23.3	20.9	8.3	1.2	16.951	0.000

Table 4.5 Mean systematic bias of slope estimates (in percent of actual slope) with standard deviations and standard errors for each hill in MFS

Measure	Hill	Slope (deg)	Mean Bias (%)	Stand. Dev (%)	Stand. Err (%)
Visual	1	14.3	98.8	62.1	9.3
	2	18.1	113.9	59.3	8.9
	3	19.2	75.6	57.5	8.6
	4	22.8	85.1	47.0	7.1
	5	23.3	98.5	35.6	5.3
Haptic	1	14.3	91.4	65.0	9.8
	2	18.1	105.1	65.3	9.8
	3	19.2	67.7	66.5	10.0
	4	22.8	74.9	53.9	8.1
	5	23.3	89.7	35.5	5.3

With the exception of the 18.1^{o} slope, the mean overestimation bias increases as the true slope increases between 14 and 24 degrees. Table 4.4 shows the bias ranges between 13.0 and 22.9 degrees, depending on the type of measurement and the true slope of the hill. One-sample t-tests comparing the mean to zero were significant in all cases. Interestingly, the mean bias and the true slope have a correlation coefficient of 0.717 and Table 4.5 shows the mean bias of the smallest and largest slopes are within one standard error of 100%. These results suggest the tendency to estimate a slope in the field within the distance of 25 – 75 meters to be *twice* its actual slope! Although other slopes had mean biases less than 100%, these results help explain how Astronaut Al Bean in Apollo 12 could overestimate the slope of the Surveyor Crater by over a factor of two. Additionally, the between-subject variation of slope biases, expressed by the standard deviation, ranges between 8 and 11 degrees, suggesting that subjects may have large differences in their bias and confirming the need to calibrate and model each astronaut's bias using a VR training tool prior to future lunar missions.

4.3 MDRS Virtual Reality Results

This section presents and discusses the results of the MPVS and the MVS. Both studies used the same stimuli, but with different subjects. The MPVS analyzed the effect of stereo viewing of the MDRS hills in a VR environment. The MVS analyzed the systematic and random errors of slope and distance estimates in a lunar-like VR environment with different combinations of the following factors: hill slope, distance from the base of the hill, sun elevation, and body position. This section presents the significant factors affecting slope and distance estimates, graphs illustrating the trends of these factors, and tables summarizing the effects of each factor for individual combinations of the other factors in this experiment. This section also presents both systematic and random errors of slope and distance estimates from this

study and draws comparisons to the MFS to determine whether a VR environment can provide the same magnitude and variance of estimates as the actual terrain, therefore supporting the case to develop a VR training tool for future lunar missions.

4.3.1 Comparison of Stereo and Synoptic Viewing Conditions

Since the minimum distance to the base of the MDRS hills in the MFS and the MVS was 25 meters, beyond personal space and at the end of action space where stereo vision normally provides useful distance cues, it was questionable whether stereo presentation of the MFS photographs would affect slope estimates. The MPVS collected slope estimates of all distance/sun elevation/body position conditions from five subjects under stereo and synoptic presentations and Figure 4.4 shows the distribution of the differences between the estimates (synoptic estimate – stereo estimate) for each subject.

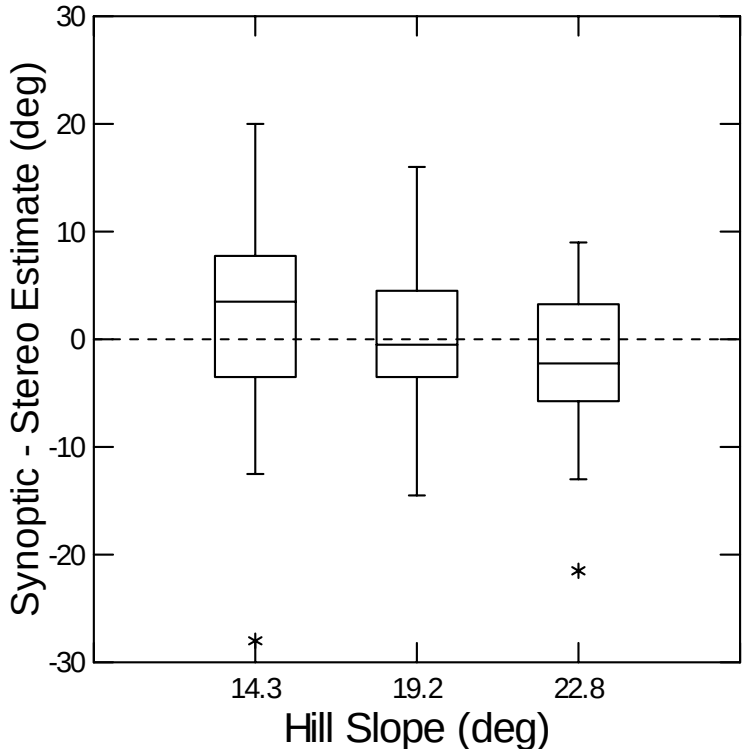

Figure 4.4 Box-plot of the difference between stereo and synoptic estimates of each subject for each hill

The box-plot in Figure 4.4 shows that zero lies within the inter-quartile range for each hill tested. These differences were compared to zero using a one-sample t-test for each hill and the results, located in Table 4.6, show that the slope estimates from the stereo and synoptically viewed images are *not* significantly different from each other. One-sample t-tests were further conducted for each of the 24 hill/distance/sun

elevation/body position combinations and 23 of the tests produced non-significant results. The only significant result was for the 22.8^{o} hill at a distance of 25 meters, 10^{o} sun elevation, while in the supine position ($t(4) = -3.281$, $p = 0.03$). This hill contained the greatest amount of texture, which would be the most visible at the closest distance (25 m) and lowest sun elevation (10^{o}). The stereo viewing of this condition further enhanced the texture, possibly causing the hill to stand out and appear steeper. All five subjects, however, were consistent in stating no noticeable difference in between the stereo and synoptic viewing conditions in the post-experiment feedback. Based off of the t-test results, the feedback from subjects, and the lack of stereo photographs for the LVS, it was decided to synoptically present all photographs in the MVS.

Table 4.6 One-sample t-test results of the difference of slope estimates between stereo and synoptic viewing conditions

Hill	Slope (deg)	Mean Difference (deg)	Stand. Dev (deg)	Stand. Err (deg)	t Statistic	p-value
1	14.3	2.213	8.721	2.79	1.605	0.117
3	19.2	0.000	6.446	2.062	0.000	1.000
4	22.8	-2.025	6.969	2.229	-1.838	0.074

4.3.2 Slope Estimation Analysis

A mixed hierarchical regression with subject as the identifier and a log transformation (to increase the model fit) of the estimated slope as the dependent variable was used to analyze the effects of the slope, distance, sun elevation, body position, and session factors in the MVS. Table 4.7 shows the main effects of the regression. The residuals, shown in Figure 4.5 were analyzed for normality and homoscedasticity. One extreme residual was found with a value of -1.472 and corresponded to the 22.8^{o} hill at a 75 m distance, a 33^{o} sun elevation from the standing position. This photograph was the last one presented in the second session, and the subject's estimate was much less than their previous estimates, suggesting they may have been rushed to finish. This point was excluded from further analysis. A One-sample Kolmogorov-Smirnov test confirmed the distribution of residuals was *not significantly* different than a normal distribution with a mean of zero and 0.20 standard deviation ($N = 947$, $p = 0.722$). The residuals were sliced into groups, shown in Table 4.8, and tested for homoscedasticity by hypothesis testing of the equality of several variances. Levene's Test found the differences between the variances to be *non-significant* ($F = 1.489$, $p = 0.191$). The hills in Table 4.7, labeled as 1, 3, and 4, correspond with Hills 1, 3, and 4 in the MFS, respectively.

Table 4.7 Mixed regression of estimated slope with categorized variables in MVS

Mixed Linear Regression on Natural Log of Estimated Slope				
Variable	**Estimate**	**Standard Error**	**Z**	**p-value**
INTERCEPT	-0.847	0.083	-10.180	0.000
Hill #1 (14.3°)	-0.051	0.010	-5.120	0.000
Hill #3 (19.2°)	-0.054	0.010	-5.346	0.000
Hill #4 (22.8°)	0.105	0.010	10.466	0.000
Distance #1 (25m)	0.049	0.007	6.920	0.000
Distance #2 (75m)	-0.049	0.007	-6.920	0.000
Sun Elevation #1 (10°)	0.019	0.007	2.631	0.009
Sun Elevation #2 (33°)	-0.019	0.007	-2.631	0.009
Standing Estimate	-0.025	0.007	-3.508	0.000
Supine Estimate	0.025	0.007	3.508	0.000
Session	0.033	0.006	5.236	0.000

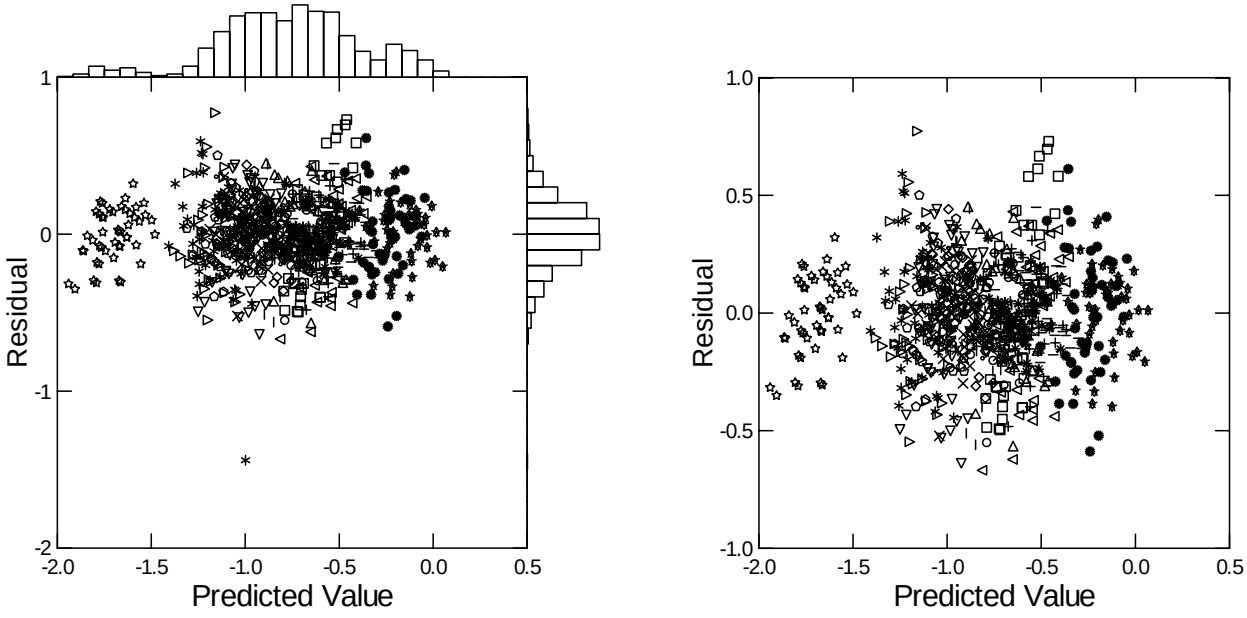

Figure 4.5 Residuals labeled by subject with (left) and without (right) extreme residual (-1.472) for the slope regression in the MVS

Table 4.8 Variance of residual groups for the slope regression in MVS

GROUP	N	Mean	Variance	Median
0	38	-0.031	0.028	-0.020
1	52	0.032	0.066	0.014
2	334	0.009	0.045	0.015
3	369	-0.008	0.045	-0.015
4	146	0.009	0.041	0.034
5	8	-0.087	0.011	-0.077

The results of this regression indicate a significant coefficient for all three hills ($p < 0.001$). The coefficient of Hill #4 is much greater than the coefficients of Hill #1 and Hill #3, supporting Hypothesis #1 that slope estimates increase with the true slope of the hill. This trend is illustrated in Figure 4.6. The coefficients of the regression, though, indicate little effect between the estimates of Hills #1 and #3. These hills consisted of similar shapes, color, and texture, and their total heights were within 0.25 m of each other. These similarities can explain the consistencies between their estimates and provide further evidence that height and hill shape and texture should be analyzed in future studies.

The regression in Table 4.7 also indicates a significant effect of distance on slope estimates ($p < 0.001$) with closer distances producing larger estimates. This result is illustrated in Figure 4.6 (left), and Table 4.9 shows individual paired t-tests with a Bonferroni Adjustment for each set of conditions finding that 8/12 sets produced a larger slope estimate at 25 m (shown in blue), five of which were significant ($p < 0.05$). Interestingly, the 19.2^{o} slope at a 10^{o} sun elevation produced a significantly greater slope estimate at 75 meters. Post-experiment feedback found that 60% of subjects agreed that hills appeared steeper at near distances vs. 25% who felt they appeared steeper at far distances. Subjects commented that closer distances offered more visual cues, made the textural gradient more obvious, occupied a greater FOV, and seemed taller. One subject commented that farther hills seemed steeper because they "looked more like walls." Although distant hills may look more like walls without accurate depth perception across the surface of the hill, the smaller FOV they occupy (about 9 degrees less for the average MVS hill) may negate the judgment of their steepness when compared to closer distances. The results of the regression, t-tests, and the consensus of subject feedback together support Hypothesis #1 that closer distances increase the perceived slope.

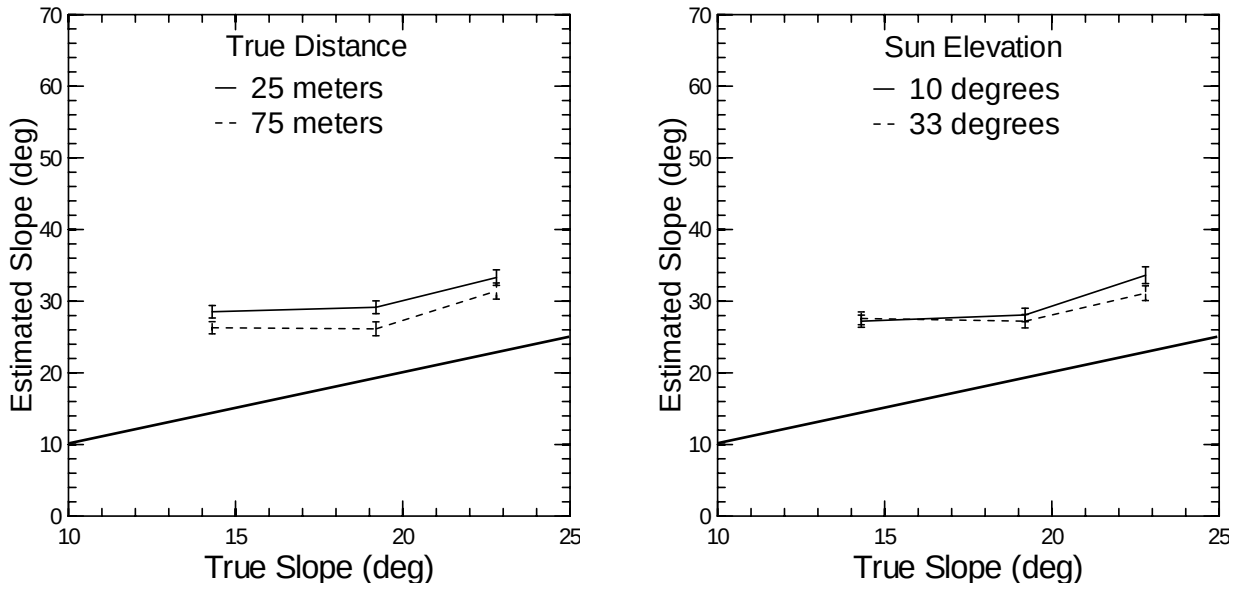

Figure 4.6 Effects of distance (left) and sun elevation (right) on slope estimates in MVS

Table 4.9 Paired t-tests between 25m and 75m (distance) slope estimates for each subject in MVS

Hill	Slope (deg)	Sun Elevation (deg)	Position	Mean of Differences (deg)	t Statistic	p-value
1	14.3	10	Standing	2.225	1.393	0.171
			Supine	11.526	6.365	**0.000**
		33	Standing	3.050	2.537	**0.015**
			Supine	2.205	1.798	0.080
3	19.2	10	Standing	-2.550	-2.275	**0.028**
			Supine	-3.208	-2.408	**0.021**
		33	Standing	3.175	3.192	**0.003**
			Supine	2.256	1.714	0.095
4	22.8	10	Standing	7.150	3.653	**0.001**
			Supine	5.528	2.910	**0.006**
		33	Standing	-1.400	-1.004	0.322
			Supine	-1.923	-1.130	0.265

The regression in Table 4.7 also indicates a significant effect of sun elevation on slope estimates with a lower sun elevation producing larger estimates ($p < 0.01$). Figure 4.6 (right) illustrates that this trend is evident for the 22.8^o slope, but little effect seems to occur for the 14.3^o and 19.2^o slope. Individual paired t-tests with a Bonferroni Adjustment for each set of conditions, shown in Table 4.10, found that 7/12 sets produced a larger slope estimate at 10^o (shown in blue), four of which were significant ($p < 0.05$). No sets showed a significantly larger slope at a 33^o sun elevation. Three of the significant sets of conditions were for the 22.8^o slope and a close inspection of the photographs, located in Appendix D.1, reveal a more obvious presence of texture along this slope. Post-experiment feedback indicated that 35% of the subjects reported using texture and 25% of the subjects reported using shadows when judging slope. Together,

these results support Hypothesis #1 that lower sun elevations increase the contrast of the hill's texture, therefore, increasing the perceived affordance and estimated slope.

Table 4.10 Paired t-tests between 10^o and 33^o (sun elevation) slope estimates for each subject in MVS

Hill	Slope (deg)	Distance (m)	Position	Mean of Differences (deg)	t Statistic	p-value
1	14.3	25	Standing	0.550	0.456	0.651
			Supine	1.641	1.549	0.130
		75	Standing	-1.275	-1.035	0.307
			Supine	-2.487	-1.920	0.062
3	19.2	25	Standing	-0.125	-0.101	0.920
			Supine	-0.667	-0.784	0.438
		75	Standing	1.075	1.167	0.250
			Supine	2.026	2.636	**0.012**
4	22.8	25	Standing	4.200	3.254	**0.002**
			Supine	2.846	1.765	0.086
		75	Standing	1.050	0.842	0.405
			Supine	4.974	2.734	**0.009**

The regression in Table 4.7 indicates a significant effect of body position on slope estimates with the supine position producing larger estimates ($p < 0.001$). Figure 4.7 (left) illustrates this trend for all three hills. Individual paired t-tests with a Bonferroni Adjustment for each set of conditions, shown in Table 4.11, found that 11/12 sets produced a larger slope estimate from the supine position (shown in red), three of which were significant ($p < 0.05$). No sets showed a significantly larger slope from the standing position. All three significant sets of conditions were for the 19.2^o slope. The order of standing and supine session were balanced (see Figure 3.5), thus eliminating the influence of fatigue on this effect. Post-experiment feedback indicated that 68% of subjects agreed that their body position *did not* affect their estimates vs. 24% who believed their estimates may have been influenced. Several subjects who believed their estimates were influenced commented that hills appeared slightly steeper when lying and that they felt in more control from the standing position. The results of the regression, t-tests, and subject comments together support Hypothesis #1 that a subject's ability to climb a hill decreases from the supine position, increasing slope estimates.

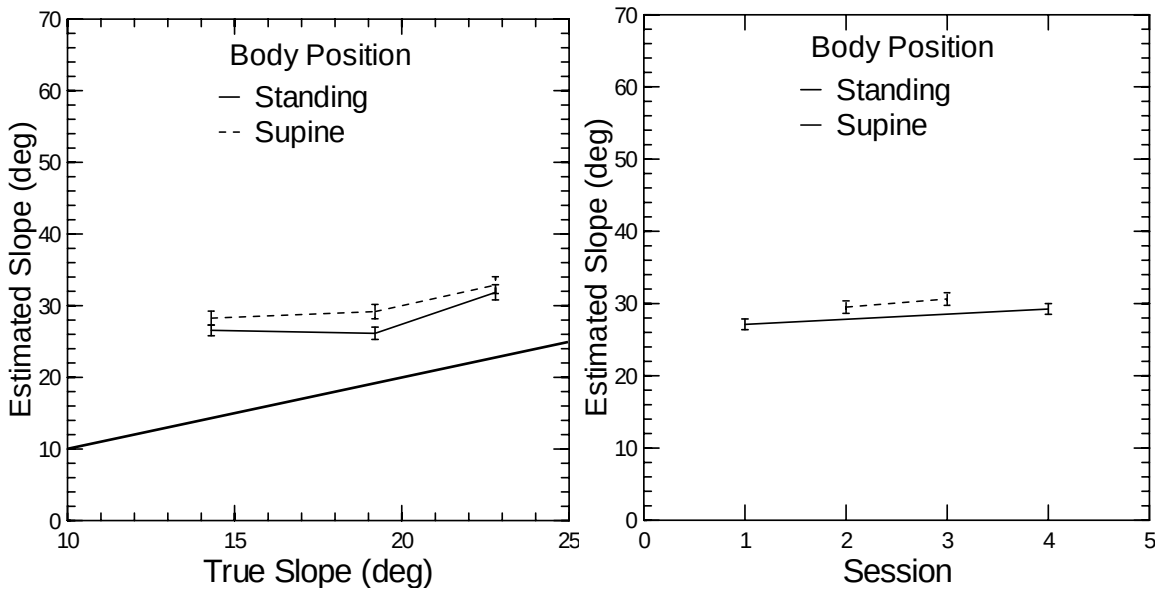

Figure 4.7 Effect of body position (left) and session (right) on slope estimates in MVS

Table 4.11 Paired t-tests between standing and supine slope estimates for each subject in MVS

Hill	Slope (deg)	Distance (m)	Sun Elevation (deg)	Mean of Differences (deg)	t Statistic	p-value
1	14.3	25	10	-1.795	-1.123	0.269
			33	-0.487	-0.413	0.682
		75	10	-1.308	-1.124	0.268
			33	-2.59	-1.971	0.056
3	19.2	25	10	-1.974	-1.865	0.07
			33	-2.436	-2.287	**0.028**
		75	10	-3.359	-3.152	**0.003**
			33	-2.667	-2.97	**0.005**
4	22.8	25	10	-0.872	-0.553	0.583
			33	-2.282	-1.894	0.066
		75	10	-2.641	-1.442	0.157
			33	1.179	0.692	0.493

The regression in Table 4.7 also shows a significant effect of session on the estimated slope with a positive coefficient indicating an increase of estimates during later sessions ($p < 0.001$). This trend is evident in Figure 4.7 (right) for both standing and supine cases. Although this effect could be attributed to learning, it seems likely that subjects suffered from slight fatigue throughout the study. Future VR training tool designs for astronauts should be aware of this effect.

Prior to the experiment, subjects were not instructed on any methods to use for estimating slope. Post-experiment feedback asked each subject to list the methods they used to estimate the slopes. The frequency of each method is shown below in Figure 4.8.

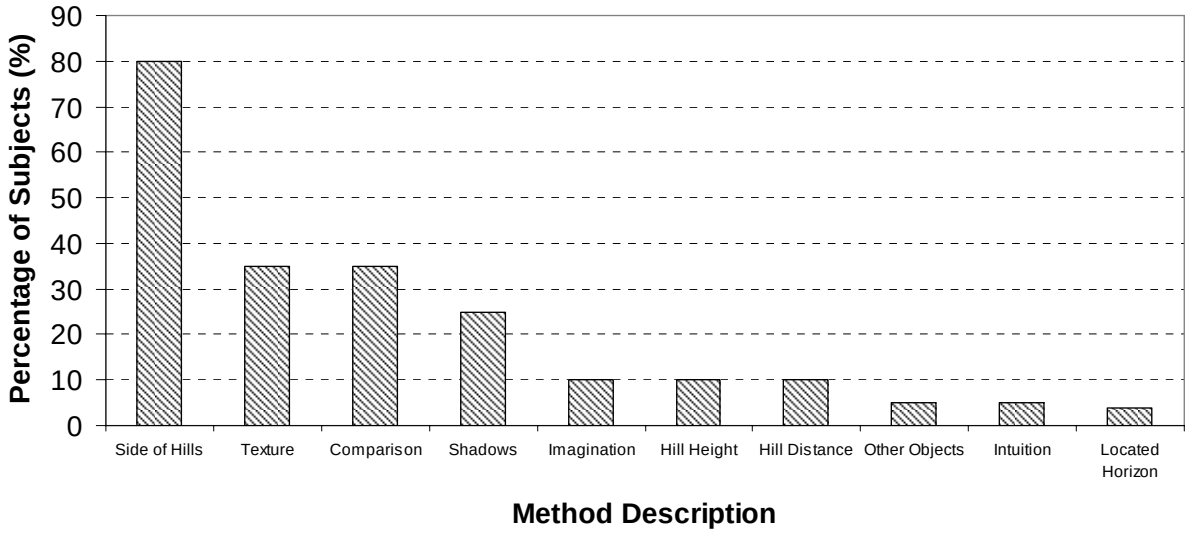

Figure 4.8 Frequency of methods used to estimate slope in MVS

The most frequent method that influenced estimates was the use of the side of the hills to interpolate the slope they viewed "head-on." A total of 80% of subjects indicated using this method, suggesting that the shape of the hill is often the most salient cue when available. The hills in the MVS all possessed a conical shape, allowing the use of this method. The effect of this method could not be independently analyzed in this experiment due to collinearity with the true slope. The use of texture and shadows were enhanced by the different sun elevation conditions, though none of the hills possessed the deep illusionary shadows that would be present on the lunar surface. Future studies should independently analyze the effect of shadow size and darkness. Thirty-five percent of subjects also indicated using comparisons of hills to judge slope, suggesting that humans are more capable of judging geometrical quantities relatively vs. absolutely. All other methods in Figure 4.8 were used by 10% or less of the subjects.

4.3.3 Slope Estimation Systematic and Random Errors

Since each design factor produced a significant effect on the slope estimates, none of the subpopulations for each set of conditions were combined. The mean overestimation bias with one standard error for each of the 24 slope/distance/sun elevation/body position sets of conditions are displayed in Figure 4.9 and Figure 4.10. Tables 4.12 and 4.13 summarize these results and highlight the minimum and maximum biases found in this study.

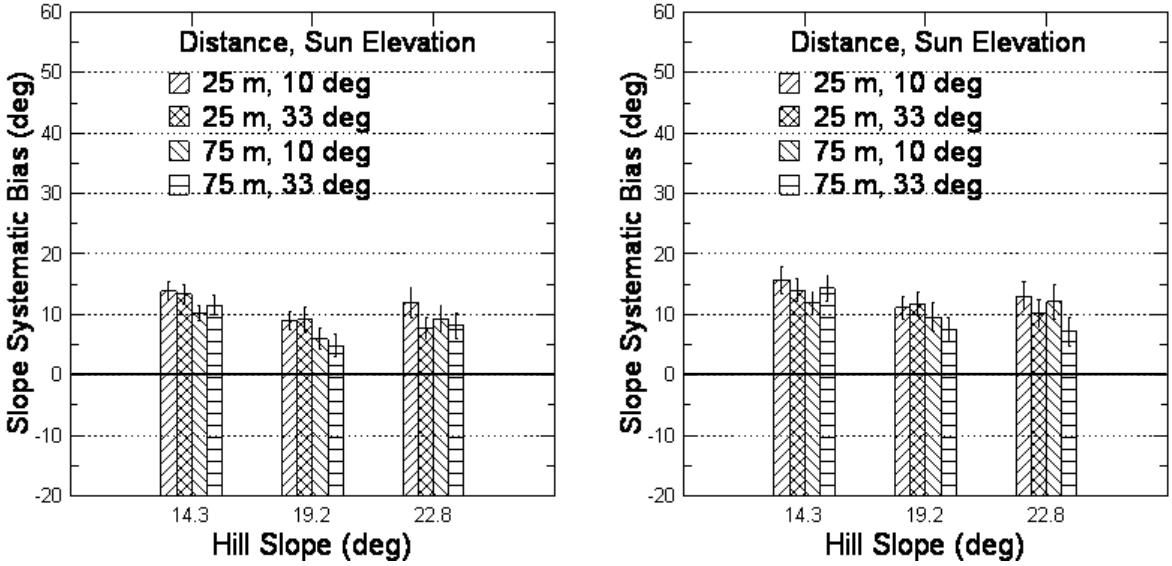

Figure 4.9 Bar graphs of slope estimation error (in degrees, bias and one standard error) from standing (left) and supine (right) positions, for each hill in MVS (positive error indicates overestimation)

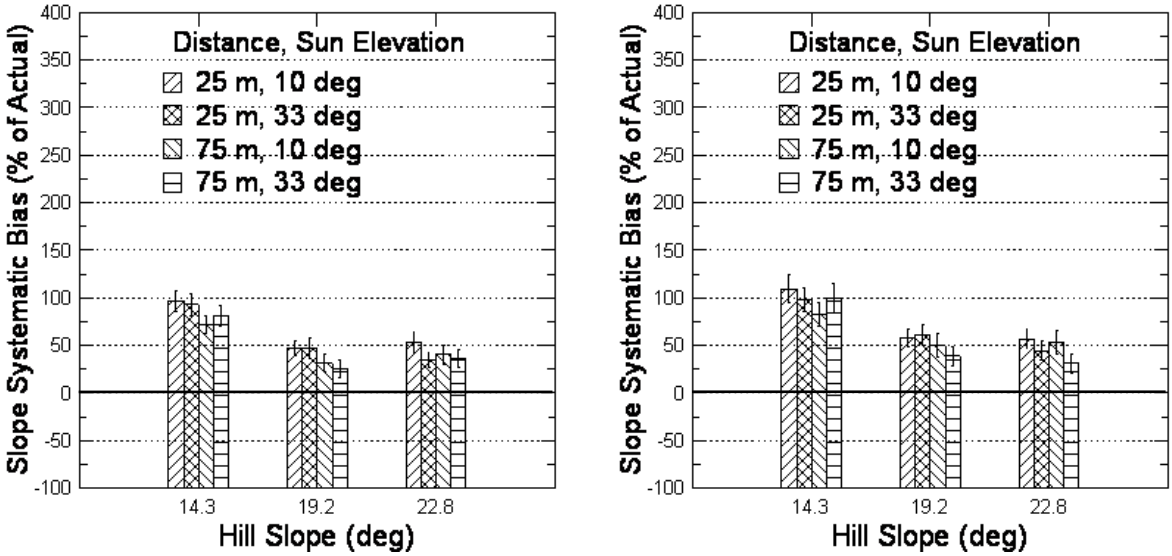

Figure 4.10 Bar graphs of slope estimation error (in percent of actual, bias and one standard error) from standing (left) and supine (right) positions, for each hill in MVS (positive error indicates overestimation)

Table 4.12 Mean systematic bias of slope estimates with standard deviations, standard errors, and 1-sample t-tests for each hill in the MVS

Position	Distance (m)	Sun Elevation (deg)	Hill	Slope (deg)	Mean Bias (deg)	Stand. Dev (deg)	Stand. Err (deg)	t Statistic	p-value
Standing	25	10	1	14.3	13.9	9.4	1.5	9.295	0.000
			3	19.2	9.0	9.3	1.5	6.136	0.000
			4	22.8	12.0	15.7	2.5	4.842	0.000
		33	1	14.3	13.3	10.4	1.7	8.108	0.000
			3	19.2	9.1	13.3	2.1	4.352	0.000
			4	22.8	7.8	10.7	1.7	4.622	0.000
	75	10	1	14.3	10.3	7.7	1.2	8.481	0.000
			3	19.2	6.0	11.1	1.8	3.395	0.002
			4	22.8	9.2	14.6	2.3	4.003	0.000
		33	1	14.3	11.6	9.7	1.5	7.513	0.000
			3	19.2	**4.9**	**11.3**	**1.8**	2.724	0.010
			4	22.8	8.2	13.0	2.1	3.981	0.000
Supine	25	10	1	14.3	**15.7**	**13.1**	**2.1**	7.464	0.000
			3	19.2	11.1	11.3	1.8	6.115	0.000
			4	22.8	13.0	14.8	2.4	5.511	0.000
		33	1	14.3	14.0	10.8	1.7	8.092	0.000
			3	19.2	11.8	12.4	2.0	5.909	0.000
			4	22.8	10.2	14.0	2.3	4.527	0.000
	75	10	1	14.3	11.8	10.7	1.7	6.899	0.000
			3	19.2	9.5	14.4	2.3	4.127	0.000
			4	22.8	12.1	17.3	2.8	4.367	0.000
		33	1	14.3	14.3	13.6	2.2	6.560	0.000
			3	19.2	7.5	12.1	2.0	3.869	0.000
			4	22.8	7.1	14.0	2.3	3.185	0.003

Table 4.13 Mean systematic bias of slope estimates (in percent of actual slope) with standard deviations and standard errors for each hill in MVS

Position	Distance (m)	Sun Elevation (deg)	Hill	Slope (deg)	Mean Bias (%)	Stand. Dev (%)	Stand. Err (%)
Standing	25	10	1	14.3	97.0	66.0	10.5
			3	19.2	46.9	48.3	7.7
			4	22.8	52.7	68.9	11.0
		33	1	14.3	93.2	72.7	11.6
			3	19.2	47.5	69.1	11.0
			4	22.8	34.3	47.0	7.5
	75	10	1	14.3	71.9	53.6	8.5
			3	19.2	31.0	57.7	9.2
			4	22.8	40.5	63.9	10.2
		33	1	14.3	80.8	68.0	10.8
			3	19.2	**25.4**	**58.9**	**9.4**
			4	22.8	35.9	57.0	9.1
Supine	25	10	1	14.3	**109.6**	**91.7**	**14.8**
			3	19.2	57.1	64.7	10.4
			4	22.8	57.9	59.1	9.5
		33	1	14.3	98.1	75.7	12.2
			3	19.2	61.3	64.8	10.5
			4	22.8	44.6	61.6	9.9
	75	10	1	14.3	82.7	74.9	12.1
			3	19.2	49.6	75.0	12.1
			4	22.8	53.1	75.9	12.2
		33	1	14.3	100.1	95.3	15.4
			3	19.2	39.0	63.0	10.2
			4	22.8	31.2	61.3	9.9

From both standing and supine positions, the overestimation bias is greatest for the 14.3^{o} slope. Figure 4.10 shows that at 25 meters from the base of this hill, the mean estimate was within one standard error of

twice the true slope of the hill. Figure 4.10 also shows that the mean biases for the remaining two hills were about half of the true slope. Table 4.12 shows the bias ranges between 4.9 and 15.7 degrees. One-sample t-tests comparing the mean bias for each set of conditions to zero were found to be significant in all cases. Table 4.12 also shows a large range of the between-subject variation of slope biases, expressed by the standard deviation, from 7.7 to 17.3 degrees. The size of these random errors further confirms the need to calibrate and model each astronaut's bias using a VR training tool prior to future lunar missions.

4.3.4 Distance Estimation Analysis

A mixed hierarchical regression with subject as the identifier and a square root transformation (to increase the model fit) of the estimated distance as the dependent variable was used to analyze the effects of the slope, distance, sun elevation, body position, and session factors in the MVS. Table 4.14 shows the main effects of the regression. The residuals, shown in Figure 4.11 were analyzed for normality and homoscedasticity. Lilliefors test confirmed the distribution of residuals was *not significantly* different than a normal distribution (N = 871, p = 0.359). The residuals were sliced into groups, shown in Table 4.15, and tested for homoscedasticity by hypothesis testing of the equality of several variances. Including all points, Levene's test was *significant* (F = 6.502, p = 0.000). Interestingly, the six most extreme residuals were of the same hill (#1 – 14.3^{o} slope). These residuals, as well as Groups 0 and 6 were excluded from the analysis, yet Levene's test again was *significant* (F = 3.437, p = 0.008). A log transformation of the estimated distance was further applied and also failed to provide a constant variance fit. Excluding the residuals in Groups 0 and 1 in Table 4.15, a conical shape of residuals is noticeable in Figure 4.11 and suggests that subjects with higher predicted values made more consistent estimates.

Table 4.14 Mixed regression of estimated distance with categorized variables in MVS

Mixed Linear Regression on Square Root of Estimated Distance				
Variable	**Estimate**	**Standard Error**	**Z**	**p-value**
INTERCEPT	6.612	0.234	28.286	0.000
Hill #1 (14.3°)	0.227	0.040	5.654	0.000
Hill #3 (19.2°)	-0.179	0.040	-4.454	0.000
Hill #4 (22.8°)	-0.048	0.040	-1.200	0.230
Distance #1 (25m)	-0.871	0.028	-30.630	0.000
Distance #2 (75m)	0.871	0.028	-30.630	0.000
Sun Elevation #1 (10°)	0.106	0.029	3.727	0.000
Sun Elevation #2 (33°)	-0.106	0.029	3.727	0.000
Standing Estimate	-0.075	0.029	-2.638	0.008
Supine Estimate	0.075	0.029	-2.638	0.008
Session	0.141	0.025	5.575	0.000

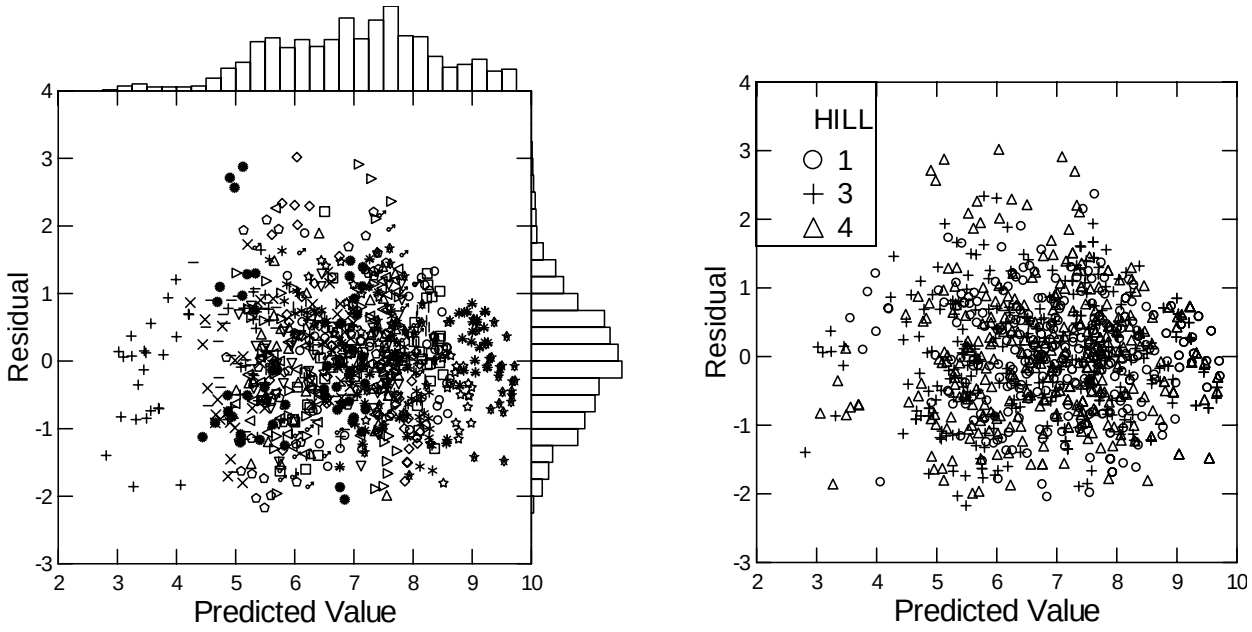

Figure 4.11 Residuals labeled by subject (left) and hill (right) for the distance regression in the MVS

Table 4.15 Variance of residual groups for distance regression in MVS

GROUP	N	Mean	Variance	Median
0	15	-0.369	0.479	-0.130
1	23	0.036	0.790	0.245
2	173	-0.067	1.068	-0.093
3	216	0.000	0.801	0.015
4	306	0.091	0.765	0.059
5	159	-0.035	0.501	0.030
6	56	-0.108	0.243	-0.085

The regression results in Table 4.14 show a significant effect of hill on distance estimates across the three hills tested ($p < 0.05$). Figure 4.12 (left) illustrates this effect, though shows a difference at only the 25 m location. The 14.3° hill produced the largest distance estimates at this location, on average 5 – 10 m greater than the other two hills. This hill also possessed the smallest height, suggesting that subjects may have allowed the visual angle subtended by the hill in their FOV to influence their judgments. However, the height of the 19.2° hill was only 0.25 m taller, yet prompted subjects to make distance estimates that were on average 10 m less. Appendix D.1 shows, though, a metal barrel lying near the base of the 19.2° hill, providing an additional cue to the closeness of the hill and explaining why distance estimates were less. The distance estimates of all three hills were on average the same at the 75 m location. The visual angles subtended by the hills in these images were only within 1.7 deg of each other and Appendix D.1 reveals that in every image at this distance, at least one of the other test hills were visible. Furthermore,

Figure 4.13 shows that the use of surrounding objects, such as other hills and metal barrels, was the most common distance estimation method, used by 55% of the subjects. Since all three hills sat next to each other, it seems plausible that the distance estimates to the hills at the 75 m location would be similar.

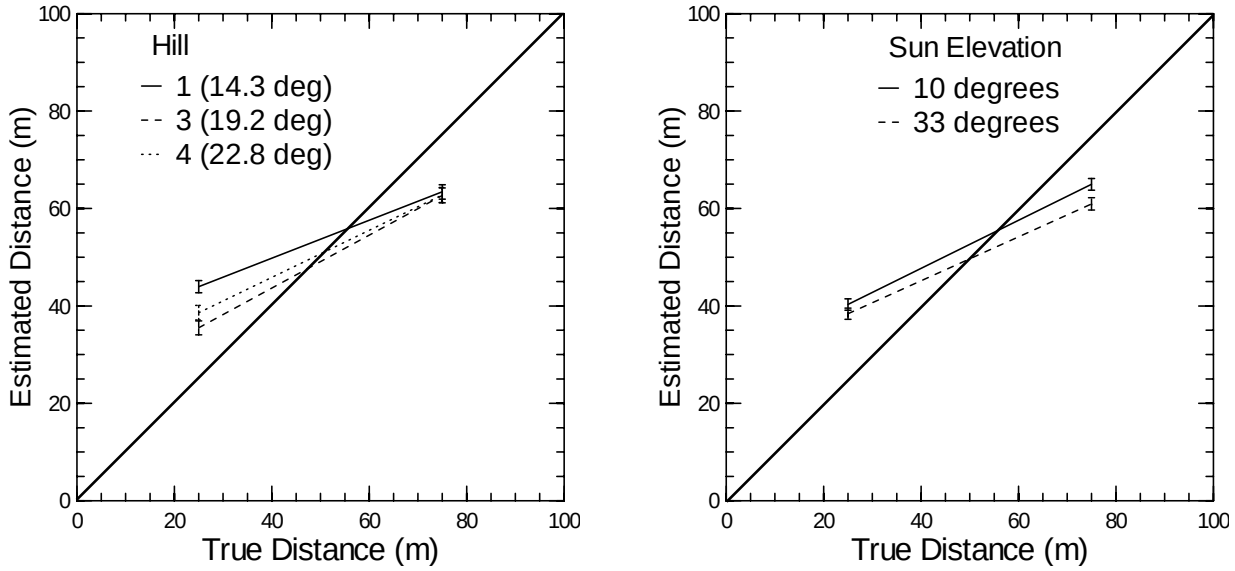

Figure 4.12 Effects of hill (left) and sun elevation (right) on distance estimates in MVS

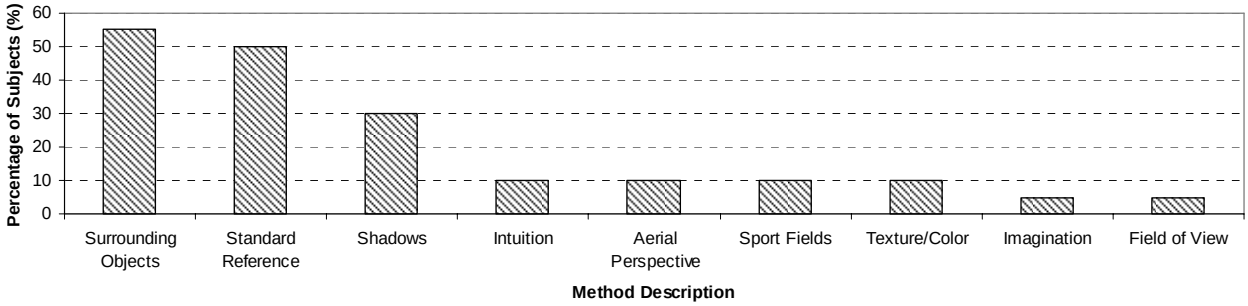

Figure 4.13 Frequency of methods used to estimate distance in MVS

The true distance had a significant effect on the distance estimates, shown in Table 4.14 ($p < 0.001$). As expected, the estimates at the 25 m location were on average less than the estimates at 75 m. The visual angle subtended by the hills at the 25 m location was at least 9 degrees greater than at the 75 m location and the area of the visible ground plane lying between the subjects and the base of the hill was also greater at the 75 m location. Interestingly, the distance was overestimated at the 25 m location and underestimated at the 75 m location. The likely cause for this occurrence was the subject's ability to judge distance relatively, rather than absolutely. Fifty percent of subjects indicated using the 50 m standard reference hill at the beginning of the experiment to estimate each distance. It is likely that

subjects knew the 75 m distances were farther than the reference and the 25 m distances were closer than the reference, though the cues indicating the exact distance were ambiguous. Since the initial position of the distance estimation device was also 50 m, subjects may have likely been influenced to make estimates closer to this position.

The regression in Table 4.14 also indicates a significant effect of sun elevation on distance estimates ($p < 0.001$). Figure 4.12 (right) shows that for both true distance locations, the estimated distance was on average greater at the lower 10^o sun elevation. Individual paired t-tests with a Bonferroni Adjustment for each set of conditions, shown in Table 4.16, found that 9/12 sets produced a larger distance estimate at the 10^o sun elevation (shown in blue), six of which were significant ($p < 0.05$). No sets showed a significantly larger distance estimate at a 33^o sun elevation. Four of the significant sets of conditions were from the 75 m locations, which revealed a larger ground plane leading to the base of the hills. It seems likely that the lower sun elevation increased the contrast of the ground texture, making the distance appear farther. The regression and t-test results, therefore, support Hypothesis #2 that a lower sun elevation increases the estimated distance.

Table 4.16 Paired t-tests between 10^o and 33^o (sun elevation) distance estimates for each subject in MVS

Hill	Slope (deg)	Distance (m)	Position	Mean of Differences (m)	t Statistic	p-value
1	14.3	25	Standing	-1.25	-0.561	0.578
			Supine	-1.03	-0.715	0.479
		75	Standing	3.85	2.250	**0.030**
			Supine	8.00	3.279	**0.002**
3	19.2	25	Standing	-1.70	-1.188	0.242
			Supine	1.00	0.461	0.648
		75	Standing	5.50	2.937	**0.006**
			Supine	2.44	1.381	0.175
4	22.8	25	Standing	7.00	3.372	**0.002**
			Supine	7.49	2.577	**0.014**
		75	Standing	4.03	2.629	**0.012**
			Supine	0.15	0.066	0.948

Table 4.14 also indicates that body position had a significant effect on distance estimates with the supine position producing greater estimates than the standing position ($p < 0.001$). This effect is illustrated in Figure 4.14 (left) for both true distance conditions. Individual paired t-tests with a Bonferroni Adjustment for each set of conditions, shown in Table 4.17, found that 9/12 sets caused a larger distance estimate from the supine position (shown in red), three of which were significant ($p < 0.05$). No sets caused a significantly larger distance estimate from the standing position. Although 68% of subjects felt

their position did not affect their estimates, we attribute this effect to the change of affordance a subject experiences from the supine position. Figure 4.14 (right) shows an average increase in distance estimates with session for both standing and supine conditions. The effect of session was found significant in the regression in Table 4.14. A likely explanation for this effect is the increase potential for fatigue and boredom at later test sessions. These results again support that a VR training tool for astronauts should consider that duration of training can affect estimates.

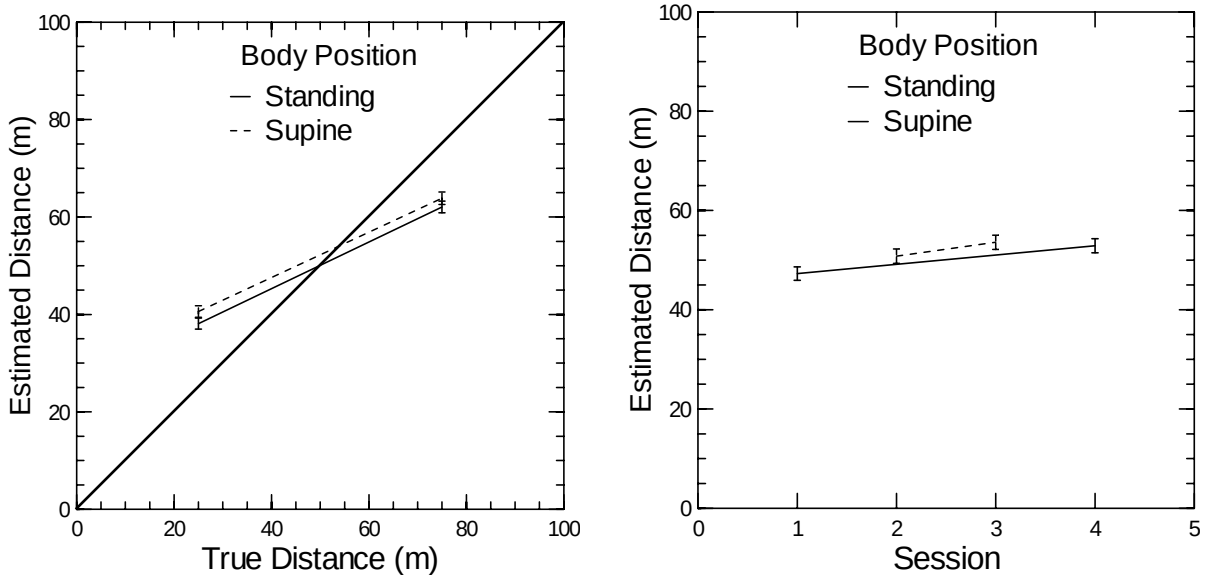

Figure 4.14 Effect of body position (left) and session (right) on distance estimates in MVS

Table 4.17 Paired t-tests between standing and supine distance estimates for each subject in MVS

Hill	Slope (deg)	Distance (m)	Sun Elevation (deg)	Mean of Differences (m)	t Statistic	p-value
1	14.3	25	10	-3.56	-2.078	**0.045**
			33	-3.64	-3.000	**0.005**
		75	10	-2.62	-1.489	-1.489
			33	0.62	0.352	0.727
3	19.2	25	10	-1.72	-0.982	0.332
			33	0.54	0.280	0.781
		75	10	0.36	0.181	0.858
			33	-2.44	-1.056	0.298
4	22.8	25	10	-3.51	-1.485	0.146
			33	-3.08	-1.376	0.177
		75	10	-1.87	-0.710	0.482
			33	-5.74	-2.402	**0.021**

Other methods that subjects employed to determine distance estimates are shown in Figure 4.13. Only 10% of subjects indicated using aerial perspective, though with test distances less than 100 meters on a clear day, it was expected that aerial perspective would not provide a salient cue in this experiment. Future studies with distances beyond 100 meters with varying conditions of aerial perspective would be

beneficial for lunar missions. Ten percent of subjects indicated using sport fields to influence their judgments and post-experiment feedback indicated that 50% of subjects used other mental references to judge distance in this experiment. Since many mental references, such as sport fields, are within 100 meters, their use in this experiment did not seem to increase the errors in the results. The use of such references across vast lunar distances could likely cause distance underestimations and should be used cautiously in a lunar environment. Post-experiment feedback also indicated that 80% of subjects felt that the limits of the distance estimation device influenced their judgment, providing them with a reference frame to base their estimates. Had the upper limit of the device been increased to 200 m, it seems likely that the distance estimates would have increased as well. This feedback supports that distance judgments in a reduced-cue environment are made relatively, rather than absolutely. Astronauts traveling to an unfamiliar environment should possess previous knowledge of the distance frame of that environment using recognizable landmarks to aid their navigation.

4.3.5 Distance Estimation Systematic and Random Errors

Each design factor produced a significant effect on the distance estimates; therefore, none of the subpopulations for each set of conditions were combined. The mean bias with one standard error for each of the 24 slope/distance/sun elevation/body position sets of conditions are displayed in Figure 4.15 in meters, and in Figure 4.16 as a percentage of the actual distance. Tables 4.18 and 4.19 summarize these results and highlight the maximum underestimation and overestimation biases found in this study.

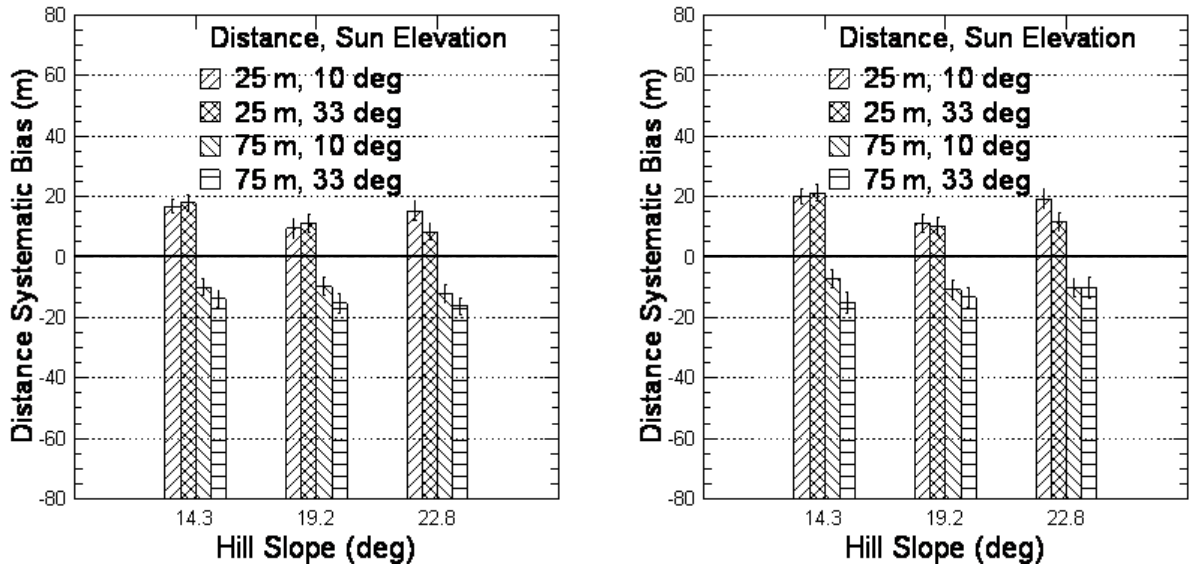

Figure 4.15 Bar graphs of distance estimation error (meters, bias and one standard error) from standing (left) and supine (right) positions, for each hill in MVS (positive error indicates overestimation)

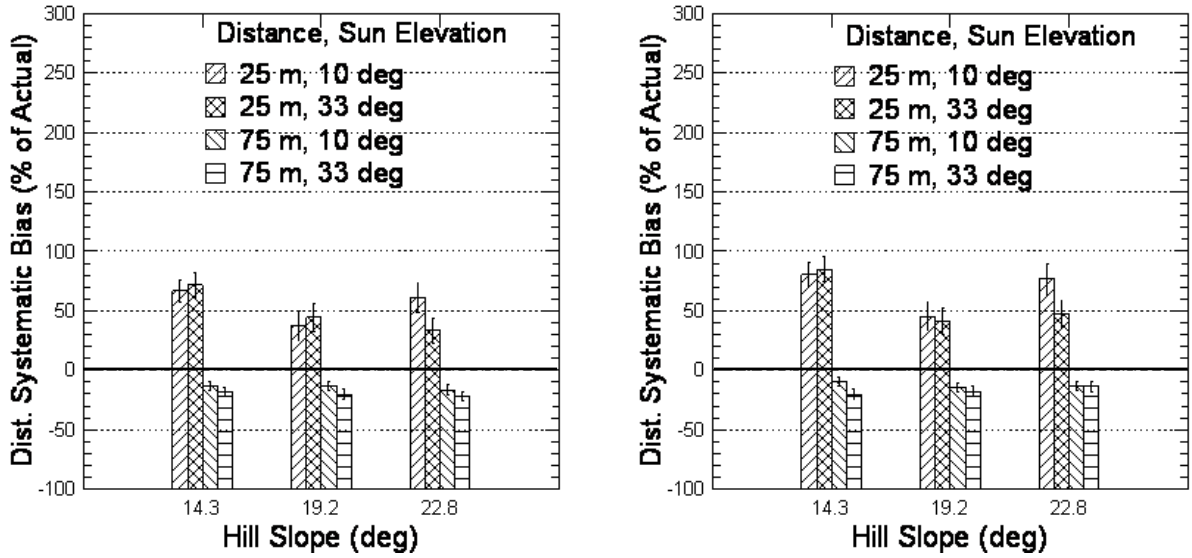

Figure 4.16 Bar graphs of distance estimation error (percent of actual, bias and one standard error) from standing (left) and supine (right) positions, for each hill in MVS (positive error indicates overestimation)

Table 4.18 Mean systematic bias of distance estimates with standard deviations, standard errors, and 1-sample t-tests for each hill in the MVS

Position	Distance (m)	Sun Elevation (deg)	Hill	Slope (deg)	Mean Bias (m)	Stand. Dev (m)	Stand. Err (m)	t Statistic	p-value
Standing	25	10	1	14.3	16.7	14.0	2.2	7.534	0.000
			3	19.2	9.4	18.7	3.0	3.185	0.003
			4	22.8	15.3	19.6	3.1	4.946	0.000
		33	1	14.3	17.9	16.8	2.7	6.759	0.000
			3	19.2	11.1	18.2	2.9	3.859	0.000
			4	22.8	8.3	16.7	2.7	3.135	0.003
	75	10	1	14.3	-10.0	17.0	2.7	-3.717	0.001
			3	19.2	-9.8	18.4	2.9	-3.378	0.002
			4	22.8	-12.3	19.0	3.0	-4.085	0.000
		33	1	14.3	-13.9	18.2	2.9	-4.825	0.000
			3	19.2	-15.3	19.6	3.1	-4.937	0.000
			4	22.8	**-16.3**	**18.0**	**2.9**	-5.727	0.000
Supine	25	10	1	14.3	20.1	15.7	2.5	8.026	0.000
			3	19.2	11.2	18.1	2.9	3.865	0.000
			4	22.8	19.2	19.9	3.2	6.024	0.000
		33	1	14.3	**21.2**	**16.4**	**2.6**	8.072	0.000
			3	19.2	10.2	17.7	2.9	3.618	0.001
			4	22.8	11.7	17.4	2.8	4.190	0.000
	75	10	1	14.3	-7.3	17.5	2.8	-2.590	0.014
			3	19.2	-10.8	19.2	3.1	-3.528	0.001
			4	22.8	-10.0	19.0	3.1	-3.298	0.002
		33	1	14.3	-15.3	21.3	3.4	-4.471	0.000
			3	19.2	-13.3	19.5	3.1	-4.262	0.000
			4	22.8	-10.2	20.5	3.3	-3.106	0.004

Table 4.19 Mean systematic bias of distance estimates (in percent of actual distance) with standard deviations and standard errors for each hill in MVS

Position	Distance (m)	Sun Elevation (deg)	Hill	Slope (deg)	Mean Bias (%)	Stand. Dev (%)	Stand. Err (%)
Standing	25	10	1	14.3	66.7	56.0	8.9
			3	19.2	37.6	74.7	11.9
			4	22.8	61.2	78.3	12.5
		33	1	14.3	71.7	67.1	10.7
			3	19.2	44.4	72.8	11.6
			4	22.8	33.2	67.0	10.7
	75	10	1	14.3	-13.3	22.7	3.6
			3	19.2	-13.1	24.5	3.9
			4	22.8	-16.4	25.4	4.0
		33	1	14.3	-18.5	24.2	3.9
			3	19.2	-20.4	26.2	4.2
			4	22.8	**-21.8**	**24.0**	**3.8**
Supine	25	10	1	14.3	80.5	62.6	10.1
			3	19.2	44.9	72.6	11.7
			4	22.8	76.7	79.5	12.8
		33	1	14.3	**84.6**	**65.5**	**10.6**
			3	19.2	40.9	70.6	11.4
			4	22.8	46.8	69.7	11.2
	75	10	1	14.3	-9.7	23.3	3.8
			3	19.2	-14.5	25.6	4.1
			4	22.8	-13.4	25.3	4.1
		33	1	14.3	-20.3	28.4	4.6
			3	19.2	-17.7	25.9	4.2
			4	22.8	-13.6	27.3	4.4

From both standing and supine positions, subjects on average overestimated all 25 m distances and underestimated all 75 m distances. The largest overestimation bias was 21.2 m (84.6% of the actual distance) and the largest underestimation bias was 16.3 m (21.8% of the actual distance). This result contradicts the conclusions of Daum and Hecht [25] that distances less than 100 meters are always underestimated. The reason for this disparity is believed to be the lack of absolute distance cues in this experiment and the combination of the standard reference and estimation device. The initial position of the estimation device was 50 m. Subjects may have avoided adjusting the device to either extreme, thus causing the overestimation and underestimation biases observed in the tables above. One-sample t-tests with a Bonferroni Adjustment comparing the mean bias for each set of conditions to zero were found to be significant in all cases. Table 4.18 also shows a large range of the between-subject variation of distance biases, expressed by the standard deviation, from 14.0 to 21.3 meters (23.3% to 79.5%). The size of these random errors confirms the need to calibrate each astronaut with the distances they will encounter upon the lunar surface.

4.3.6 Comparison of Field and Virtual Reality Results

A critical question concerning the development of a VR training tool to prepare astronauts for future lunar missions is whether a VR environment can accurately produce the same magnitude of errors as the actual field environment. This study was ideal for making such a comparison with the same hills being presented in both environments; however, the number of subjects and subjects themselves were different between experiments. Figures 4.17 and 4.18 show that the average field slope estimation biases were at least one standard error greater than the average VR biases for 7/12 combinations of slope/distance/sun elevation conditions. The reason for this difference is likely the affordance one experiences from being in the actual environment, the unlimited resolution and FOV available to observe the texture of the environment, and the fatiguing effect the spacesuits had on the subjects in the field study. Interestingly, the difference in biases between the environments is the greatest for the steepest slope, 22.8^{o}. This hill possessed the greatest amount of texture and the tallest height. Two-sample t-tests comparing the mean slope biases between the populations surprisingly showed a non-significant difference for 11/12 combination of conditions. The only significant results occurred for the 22.8^{o} hill at a 25 m distance and a 33^{o} sun elevation. The size of the standard errors in Tables 4.20 and 4.21 are the likely cause of the non-significant t-test results, and future studies should contain a larger subject pool that participate in both field and VR experiments to determine within-subject differences of estimates.

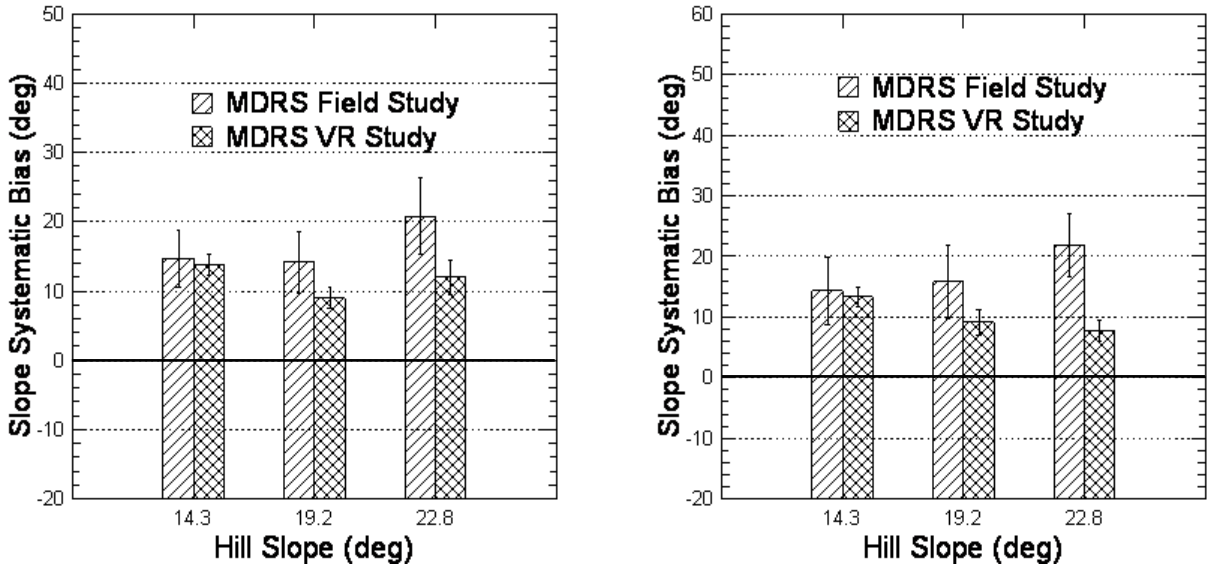

Figure 4.17 Comparison of MDRS field and VR overestimation biases (with one standard error) at 25 meter distance for 10^{o} (left) and 33^{o} (right) sun elevations

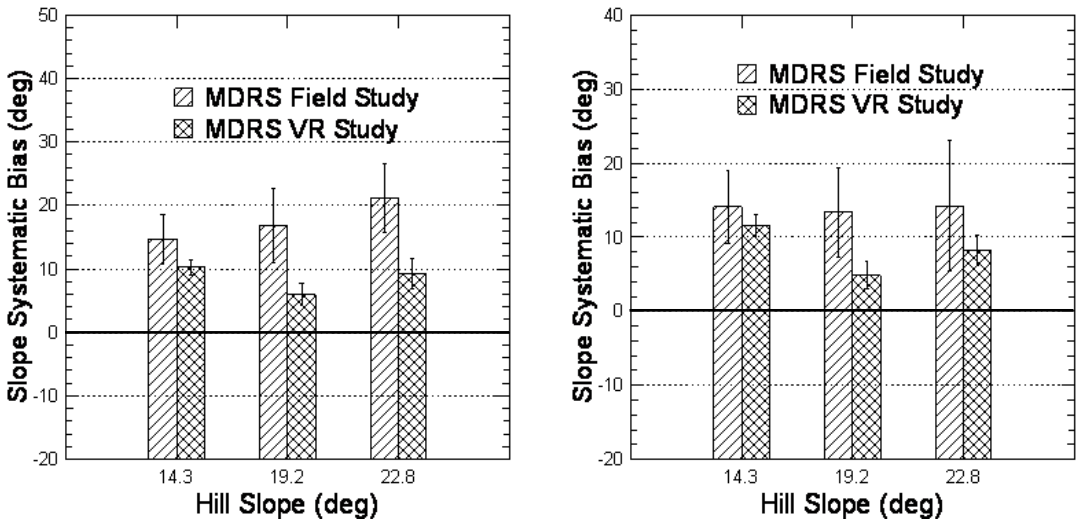

Figure 4.18 Comparison of MDRS field and VR overestimation biases (with one standard error) at 75 meter distance for 10° (left) and 33° (right) sun elevations

Table 4.20 Comparison and two-sample t-tests between MDRS field and VR study populations for each distance/sun elevation/slope combination (in meters)

Distance (m)	Sun Elevation (deg)	Hill	Slope (deg)	Mean Difference (deg)	Stand. Err (deg)	t Statistic	p-value
25	10	1	14.3	0.8	5.0	0.209	0.842
		3	19.2	5.2	5.3	1.246	0.266
		4	22.8	8.8	6.6	1.609	0.156
	33	1	14.3	1.0	6.6	0.190	0.857
		3	19.2	6.7	7.3	1.155	0.298
		4	22.8	14.0	6.2	2.887	0.033
75	10	1	14.3	4.4	4.6	1.238	0.270
		3	19.2	10.9	7.0	1.995	0.103
		4	22.8	12.0	6.5	2.259	0.064
	33	1	14.3	2.6	5.9	0.554	0.603
		3	19.2	8.5	7.2	1.530	0.187
		4	22.8	6.0	10.5	0.756	0.487

Table 4.21 Comparison between MDRS field and VR study populations for each distance/sun elevation/slope combination (in percent)

Distance (m)	Sun Elevation (deg)	Hill	Slope (deg)	Mean Difference (%)	Stand. Err (%)
25	10	1	14.3	5.8	34.7
		3	19.2	27.1	27.6
		4	22.8	38.5	28.9
	33	1	14.3	6.8	46.4
		3	19.2	34.8	38.1
		4	22.8	61.3	27.0
75	10	1	14.3	30.9	31.9
		3	19.2	56.5	36.5
		4	22.8	52.5	28.4
	33	1	14.3	17.8	41.3
		3	19.2	44.4	37.4
		4	22.8	26.4	46.2

4.4 Lunar VR Results

The LVS analyzed the systematic and random errors of slope, distance, and height estimation in a lunar VR environment with different combinations of the following factors: hill slope, distance from the base of the hill and body position. Although sun elevation is suspected to significantly affect these estimates, it was not possible to independently analyze the effects of distance and sun elevation in this study due to the limited amount of lunar photographs taken from the Apollo missions. The distance and sun elevation variables presented collinearity in the photographs used for the LVS. Table 3.6 in Chapter 3 shows a positive correlation between distance and sun elevation. Since the MVS concludes that both near distance and low sun elevation produced larger slope estimates, we are unable to determine whether the effects of different distances are caused solely by distance or also by sun elevation. This ambiguity will remain a problem to be solved by future studies. This section also presents the significant factors affecting slope, distance, and height estimates, graphs illustrating the trends of these factors, and tables summarizing the effects of each factor for individual combinations of the other factors in the experiment. This section presents both systematic and random errors of slope, distance, and height estimates from this study and compares these errors to those found in the MVS. The section concludes with a comparison of slope estimates between lunar hills and craters.

4.4.1 Lunar Hill Slope Estimation Analysis

A mixed hierarchical regression with subject as the identifier and a square root transformation (to increase the model fit) of the estimated slope as the dependent variable was used to analyze the effects of slope, distance, and body position of lunar hills in the LVS. Table 4.22 shows the main effects of the regression. The residuals, shown in Figure 4.19 were analyzed for normality and homoscedasticity. Lilliefors test confirmed the distribution of residuals was *not significantly* different than a normal distribution ($N = 742$, $p = 0.265$). The residuals were sliced into groups, shown in Table 4.23, and tested for homoscedasticity by hypothesis testing of the equality of several variances. Levene's test was *not significant* ($F = 1.946$, $p = 0.101$). Interestingly, Figure 4.19 (right) shows the most extreme residuals were for the same distance condition (1 = far), but for different subjects and different hills.

Table 4.22 Mixed regression of estimated slope for lunar hills with categorized variables in LVS

Mixed Linear Regression on Square Root of Estimated Slope				
Variable	**Estimate**	**Standard Error**	**Z**	**p-value**
INTERCEPT	0.683	0.024	28.494	0.000
Hill #1 (14.7°)	-0.077	0.006	-11.938	0.000
Hill #2 (15.1°)	-0.114	0.006	-17.661	0.000
Hill #3 (22.2°)	0.054	0.007	8.318	0.000
Hill #4 (24.1°)	0.02	0.006	3.175	0.002
Hill #5 (25.6°)	0.07	0.007	10.772	0.000
Hill #6 (25.6°)	0.047	0.006	7.334	0.000
Distance #1 (Near)	0.009	0.003	3.217	0.001
Distance #2 (Far)	-0.009	0.003	-3.217	0.001
Standing Estimate	-0.006	0.003	-1.977	0.048
Supine Estimate	0.006	0.003	1.977	0.048

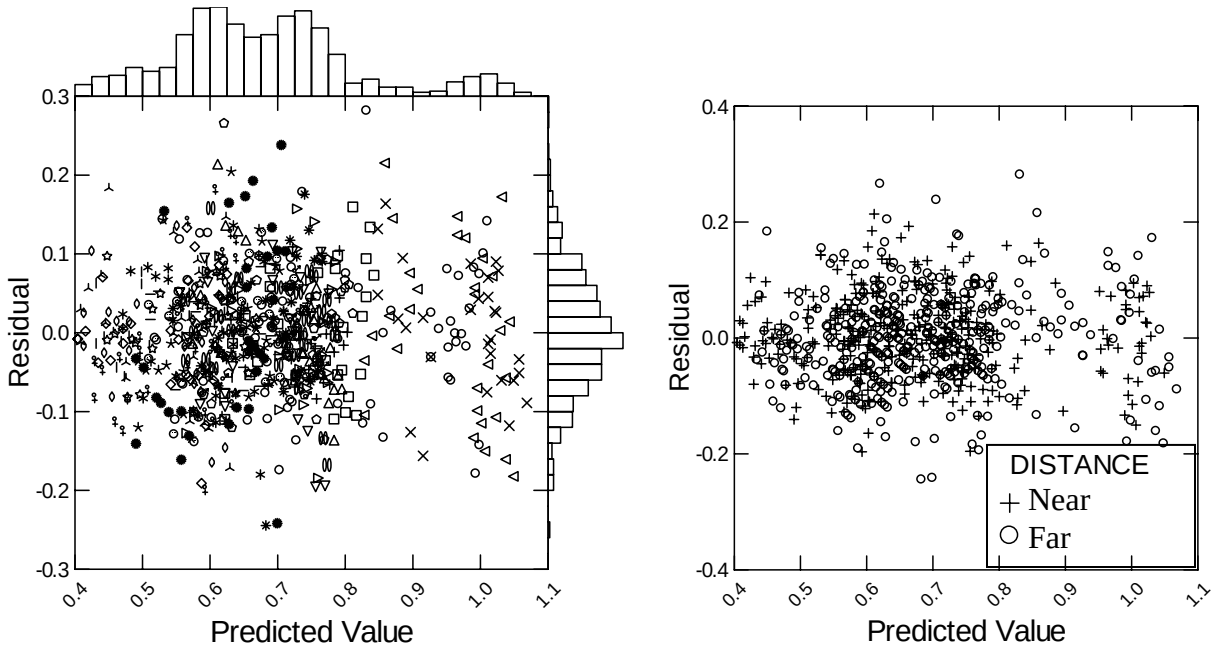

Figure 4.19 Residuals grouped by subject (left) and distance (right) for lunar hill estimated slope regression in LVS

Table 4.23 Variance of residual slices for the lunar hill estimated slope regression in LVS

GROUP	N	Mean	Variance	Median
0	120	-0.003	0.004	-0.007
1	363	0.001	0.006	-0.001
2	191	0.001	0.006	-0.002
3	61	0.005	0.007	0.014
4	7	-0.074	0.004	-0.061

The regression in Table 4.22 indicates a significant coefficient ($p < 0.01$) for all 6 hills. The sign and magnitude of the coefficients indicate a larger slope estimate as the true slope increases. This overall trend is illustrated in both graphs in Figure 4.20. The average slope estimate for the 22.2° slope appears greater than the 24.1° slope; though this result may have been caused by the hill shape or the presence of a large shadow covering the left side of the 22.2° hill. The top three methods for estimating slopes found during the post-experiment feedback included interpolating the sides of the hills (80% subjects agreed), the use of shadows (48% subjects agreed) and the use of texture (28% subjects agreed). Both 22.2° and 24.1° hills possessed similar shapes and contained shadows (see Appendix D.2), though the 22.2° possessed a more observable texture gradient, potentially increasing its perceived slope.

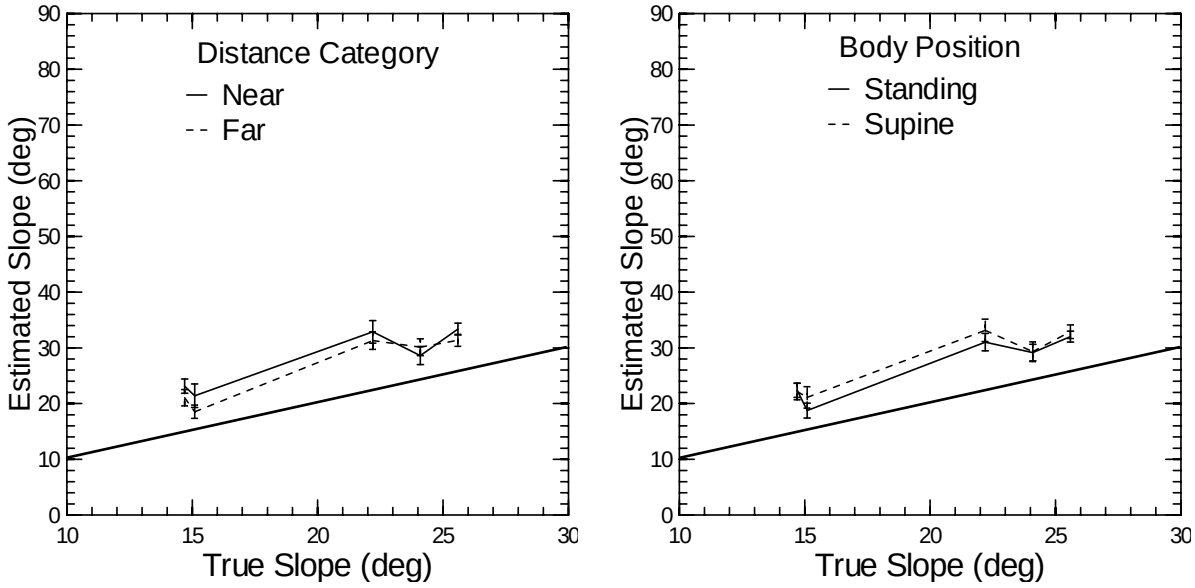

Figure 4.20 Effects of distance category (left) and body position (right) on hill slope estimates in LVS

The true distances had a significant effect on the slope estimates, shown in Table 4.22 ($p < 0.01$). The coefficients in the table and Figure 4.20 illustrate that subjects on average made greater slope estimates at nearer distances for the same hill. Individual paired t-tests with a Bonferroni Adjustment for each set of conditions, shown in Table 4.24, found that exactly one-half (6/12) caused a larger slope estimate from a near versus far location (shown in blue), two of which were significant ($p < 0.05$). One set showed a significantly greater estimate at the far location. This result illustrates competing effects that near and far distances have on slope estimates. Subject feedback indicated that 64% of subjects felt hills appeared steeper at a close distance vs. 12% who felt hills appeared steeper at a far distance. Comments concerning why hills appeared steeper from a near distance included a larger apparent height, more textural definition, a larger FOV, and adjectives such as “impressive”, “intimidating”, and “imposing.”

Those subjects suggesting that hills appeared steeper from a far distance commented that hills appeared "shear." Subject #820 explains well the competing effect of distance: "Far away looked like walls sometimes, but it was more how much of the screen was filled." Therefore, although subjects experienced a greater difficulty observing the depth across the surface of distant hills, their estimates often were more influenced by the FOV the hill occupied. However, as previously stated, the sun elevation and true distance were collinear in this experiment; therefore, we are unable to state which of these variables caused the greater slope estimates. The photographs in Appendix D.2 show large shadows on several of the hills at the near distance condition and 48% of subjects indicated using shadows to influence their estimates. Separating the effects of distance and sun elevation on slope estimation in a lunar environment is critical and should be further investigated in future studies.

Table 4.24 Paired t-tests between near and far (distance) hill slope estimates for each subject in LVS

Hill	Slope (deg)	Position	Mean of Differences (deg)	t Statistic	p-value
1	14.7	Standing	0.200	0.118	0.907
		Supine	3.680	3.443	**0.002**
2	15.1	Standing	3.280	1.763	0.091
		Supine	2.200	1.201	0.241
3	22.2	Standing	-2.240	-1.352	0.189
		Supine	-5.917	-3.661	**0.001**
4	24.1	Standing	-0.920	-0.403	0.690
		Supine	-3.040	-1.772	0.089
5	25.6	Standing	-0.375	-0.184	0.856
		Supine	1.583	0.890	0.383
6	25.6	Standing	3.240	2.741	**0.011**
		Supine	-1.200	-0.779	0.444

The regression in Table 4.22 and Figure 4.20 (right) indicate a significant effect of body position with the supine position causing a greater slope estimate ($p < 0.05$). Individual paired t-tests with a Bonferroni Adjustment for each set of conditions, shown in Table 4.25, found that 9/12 sets caused a larger slope estimate from the supine position (shown in red); however, only one condition was significant ($p < 0.05$). These results suggest that although subjects tended to make greater estimates under the supine condition, the variability of the estimates and the conditions of the LVS inhibited this effect from standing out. If the effect of position is in fact due to a change of affordance to walk up the hill, the vast distances in the LVS may have diminished the effect of body position. The majority of the subjects (68%) in the LVS post-experiment feedback indicated no noticeable difference between the body position conditions. Subjects indicating a difference commented that the hills looked steeper from the supine position, an increase effort would be required to climb a hill/crater, and the supine position offered a greater amount

of comfort, reducing one's physical potential. The regression results and these comments together support Hypothesis #1.

Table 4.25 Paired t-tests between standing and supine lunar hill slope estimates for each subject in LVS

Hill	Slope (deg)	Distance (m)	Mean of Differences (deg)	t Statistic	p-value
1	14.7	5200	-2.000	-1.806	0.084
		11400	1.480	1.187	0.247
2	15.1	4000	-1.600	-0.827	0.416
		8400	-2.680	-2.629	**0.015**
3	22.2	5000	-0.269	-0.201	0.842
		11500	-3.667	-1.701	0.102
4	24.1	10900	0.680	0.441	0.663
		13900	-1.440	-1.291	0.209
5	25.6	4300	-3.560	-1.641	0.114
		8800	-1.522	-0.769	0.450
6	25.6	6500	3.160	2.046	0.052
		9800	-1.280	-0.950	0.352

The most common methods used by subjects to estimate slope in the LVS is shown in Figure 4.21. Consistent with the MVS, subjects used the sides of the hills to interpolate the slope of the hill when available. Many of the lunar hills in his study were also conical in shape allowing this method to be used. Future studies should isolate this effect to determine the effect and reliability of this method for hills with irregular shapes. Shadows and texture were identified by 48% and 28%, respectively, and discussed previously. The only other method used by over 10% of subjects was imagining being present in the actual lunar environment.

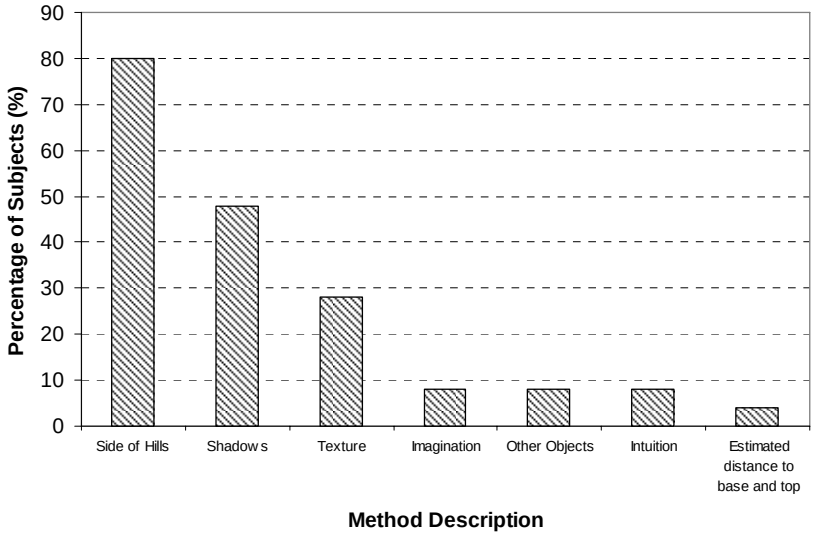

Figure 4.21 Frequency of methods used to estimate slope in LVS

4.4.2 Lunar Hill Slope Estimation Systematic and Random Errors

Each factor produced a significant effect on the hill slope estimates; therefore, none of the subpopulations for each set of conditions were combined. The mean bias with one standard error for each of the 24 slope, distance, and body position sets of conditions are displayed in Figure 4.22 in degrees, and in Figure 4.23 as a percentage of the actual slope. Tables 4.26 and 4.27 summarize these results and highlight the minimum and maximum overestimation biases found in this study.

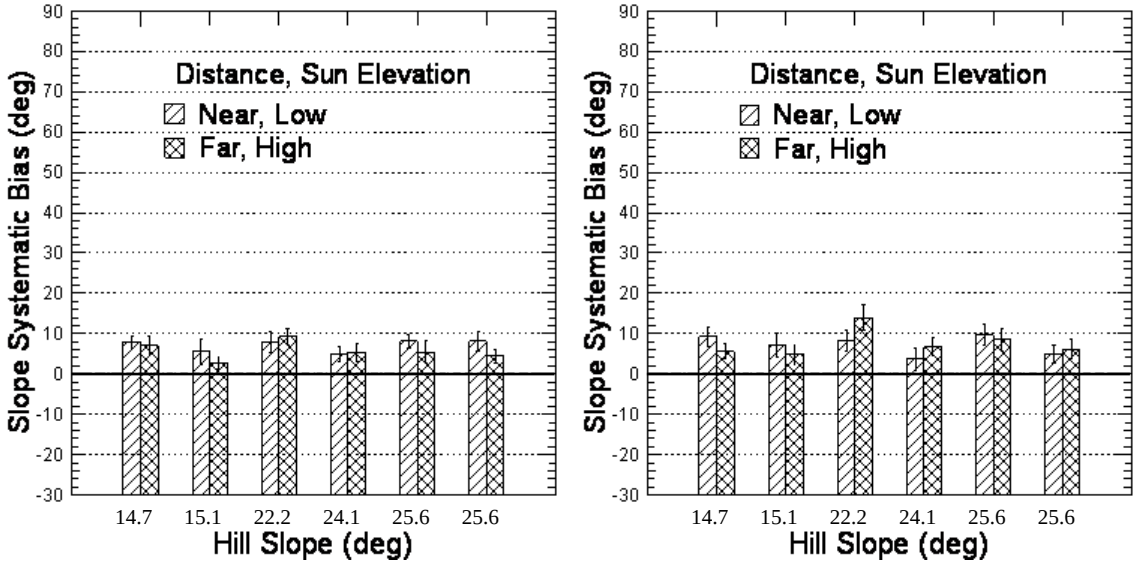

Figure 4.22 Bar graphs of slope estimation error (in degrees, bias and one standard error) from standing (left) and supine (right) positions, for each hill in LVS (positive error indicates overestimation)

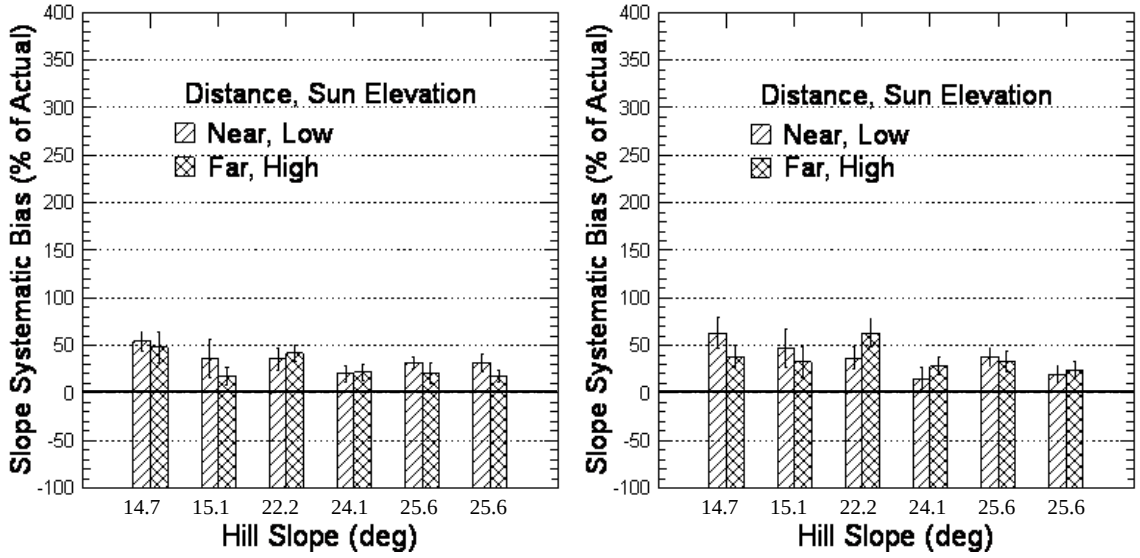

Figure 4.23 Bar graphs of slope estimation error (in percent of actual, bias and one standard error) from standing (left) and supine (right) positions, for each hill in LVS (positive error indicates overestimation)

The mean overestimation bias varies across the true slopes used in this study, though no trend appears between the true slope and the bias in Figure 4.22 or Figure 2.23. Table 4.26 shows the bias ranges between 2.7 and 14.0 degrees, depending on the body position, distance, and the true slope of the hill. One-sample t-tests comparing the mean systematic bias for each condition to zero were found to be significant for 20/24 cases. Additionally, the between-subject variation of slope biases, expressed by the standard deviation, ranges between 8.7 and 15.2 degrees, showing that within the lunar environment, subjects have large difference in their bias, further confirming the need to calibrate and model each astronaut's bias using a VR training tool prior to future lunar missions.

Table 4.26 Mean systematic bias of slope estimates with standard deviations, standard errors, and 1-sample t-tests for each hill in the LVS

Position	Distance	Hill	Slope (deg)	Mean Bias (deg)	Stand. Dev (deg)	Stand. Err (deg)	t Statistic	p-value
Standing	Near	1	14.7	8.0	10.6	1.5	5.263	0.000
		2	15.1	5.5	14.7	3.0	1.872	0.074
		3	22.2	7.9	12.3	2.5	3.215	0.004
		4	24.1	4.9	14.0	2.0	2.461	0.017
		5	25.6	8.1	11.8	1.7	4.798	0.000
		6	25.6	8.1	12.0	2.4	3.375	0.003
	Far	1	14.7	7.1	11.6	2.4	3.061	0.005
		2	15.1	**2.7**	**9.4**	**1.4**	1.997	0.051
		3	22.2	9.3	14.0	2.0	4.657	0.000
		4	24.1	5.3	10.3	2.1	2.582	0.016
		5	25.6	5.4	13.6	2.8	1.943	0.064
		6	25.6	4.4	10.9	1.6	2.815	0.007
Supine	Near	1	14.7	9.3	11.7	2.4	3.984	0.001
		2	15.1	7.1	15.1	3.1	2.343	0.028
		3	22.2	8.1	12.9	2.6	3.214	0.004
		4	24.1	3.7	13.7	2.8	1.354	0.188
		5	25.6	9.7	12.5	2.5	3.86	0.001
		6	25.6	5.0	10.9	2.2	2.284	0.032
	Far	1	14.7	5.6	8.7	1.8	3.242	0.003
		2	15.1	4.9	11.8	2.4	2.081	0.048
		3	22.2	**14.0**	**15.2**	**3.2**	4.511	0.000
		4	24.1	6.7	10.9	2.2	3.099	0.005
		5	25.6	8.4	12.6	2.6	3.288	0.003
		6	25.6	6.2	12.3	2.5	2.512	0.019

Table 4.27 Mean systematic bias of slope estimates (in percent of actual slope) with standard deviations and standard errors for each hill in LVS

Position	Distance	Hill	Slope (deg)	Mean Bias (%)	Stand. Dev (%)	Stand. Err (%)
Standing	Near	1	14.7	54.4	72.3	10.4
		2	15.1	36.4	97.3	19.8
		3	22.2	35.7	55.5	11.3
		4	24.1	20.4	58.1	8.3
		5	25.6	31.6	46.1	6.6
		6	25.6	31.7	47.0	9.5
	Far	1	14.7	48.3	78.9	16.0
		2	15.1	17.9	62.6	9.0
		3	22.2	41.8	62.9	9.0
		4	24.1	22.0	42.6	8.6
		5	25.6	21.1	53.2	11.0
		6	25.6	17.1	42.5	6.1
Supine	Near	1	14.7	**63.3**	**79.4**	**16.1**
		2	15.1	47.0	100.3	20.4
		3	22.2	36.5	57.9	11.5
		4	24.1	**15.4**	**56.7**	**11.5**
		5	25.6	37.8	49.0	9.9
		6	25.6	19.4	42.4	8.6
	Far	1	14.7	38.2	59.0	12.0
		2	15.1	32.5	78.0	15.8
		3	22.2	63.1	68.5	14.2
		4	24.1	28.0	45.1	9.2
		5	25.6	33.0	49.1	10.2
		6	25.6	24.1	47.9	9.7

4.4.3 Lunar Crater Slope Estimation Analysis

A mixed hierarchical regression with subject as the identifier and a square root transformation (to increase the model fit) of the estimated slope as the dependent variable was used to analyze the effects of slope and body position of lunar craters in the LVS. Table 4.28 shows the main effects of the regression. The residuals, shown in Figure 4.24, were analyzed for normality and homoscedasticity. One extreme residual (-0.303) was identified for the 20^{o} crater and supine position, but was included in the analysis. Lilliefors test confirmed the distribution of residuals was *not significantly* different than a normal distribution (N = 435, p = 0.253). The residuals were sliced into groups, shown in Table 4.29, and tested for homoscedasticity by hypothesis testing of the equality of several variances. Levene's test was *not significant* (F = 1.755, p = 0.107). The lunar craters were numbered 7 – 12 to avoid confusion with the lunar hills.

Table 4.28 Mixed regression of estimated slope for lunar craters with categorized variables in LVS

Mixed Linear Regression on Square Root of Estimated Slope				
Variable	**Estimate**	**Standard Error**	**Z**	**p-value**
INTERCEPT	0.735	0.022	33.565	0.000
Crater #7 (7°)	-0.070	0.008	-8.599	0.000
Crater #8 (16°)	-0.083	0.008	-10.217	0.000
Crater #9 (17°)	-0.028	0.008	-3.413	0.001
Crater #10 (20°)	0.062	0.008	7.432	0.000
Crater #11 (30°)	-0.004	0.008	-0.447	0.655
Crater #12 (30°)	0.123	0.008	15.244	0.000
Standing Estimate	-0.007	0.004	-1.714	0.086
Supine Estimate	0.007	0.004	1.714	0.086

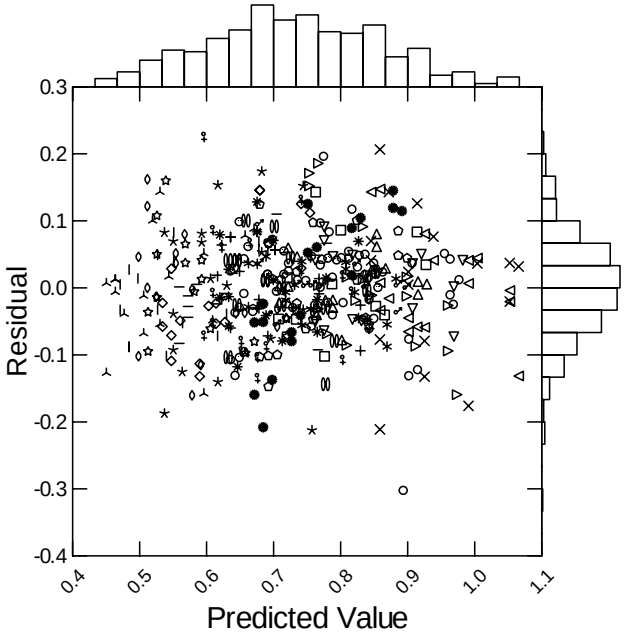

Figure 4.24 Residuals grouped by subject for lunar crater estimated slope regression in LVS

Table 4.29 Variance of residual slices for lunar crater estimated slope regression in LVS

GROUP	N	Mean	Variance	Median
0	14	-0.026	0.003	0.000
1	59	-0.003	0.008	-0.006
2	112	-0.005	0.006	-0.009
3	116	0.006	0.005	0.001
4	87	0.012	0.006	0.016
5	39	-0.017	0.005	0.002
6	8	-0.003	0.003	0.014

The regression in Table 4.28 indicates that 5/6 craters possess a coefficient significantly different from zero ($p < 0.05$) and Figure 4.25 shows an overall increase in estimated slope as the true slope of the craters increase. The trend lines for both standing and supine positions in Figure 4.25 are not linear; however, the likely cause of this result is the amount of the crater visible in the photographs used for this experiment. The peculiarities of each crater affecting its appearance are discussed in the next section. The regression in Table 4.28 also shows a non-significant effect of body position on the estimated slope of the lunar craters ($p = 0.086$). The coefficients of the regression suggest the supine estimates may be slightly larger than the standing estimates, illustrated below in Figure 4.25. Individual paired t-tests with a Bonferroni Adjustment for each set of conditions, shown in Table 4.30, found that 5/6 caused a larger slope estimate from the supine position (shown in red); however, only one condition was significant ($p < 0.05$). These results, consistent with the lunar hill analysis, show a tendency to judge slopes as steeper from the supine position, but the overall effect is likely diminished by the vast distances and the unfamiliarity of the lunar environment.

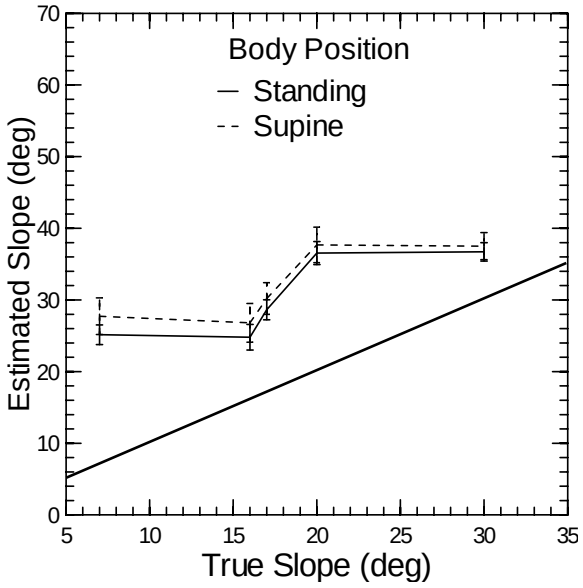

Figure 4.25 Effect of body position on crater slope estimates in LVS

Table 4.30 Paired t-tests between standing and supine crater slope estimates for each subject in LVS

Crater	Slope (deg)	Mean of Differences (deg)	t Statistic	p-value
7	7	-2.167	-1.045	0.307
8	16	-2.542	-2.106	**0.046**
9	17	-2.125	-1.619	0.119
10	20	-2.130	-0.988	0.334
11	30	0.042	0.030	0.976
12	30	-0.125	-0.070	0.945

4.4.4 Lunar Crater Slope Estimation Systematic and Random Errors

Due to the significant t-test result between standing and supine conditions in Table 4.30, these subpopulations were not combined. The mean bias with one standard error for each of the 12 slope and body position sets of conditions are displayed in Figure 4.26. Tables 4.31 and 4.32 summarize these results and highlight the minimum and maximum overestimation biases found in this study.

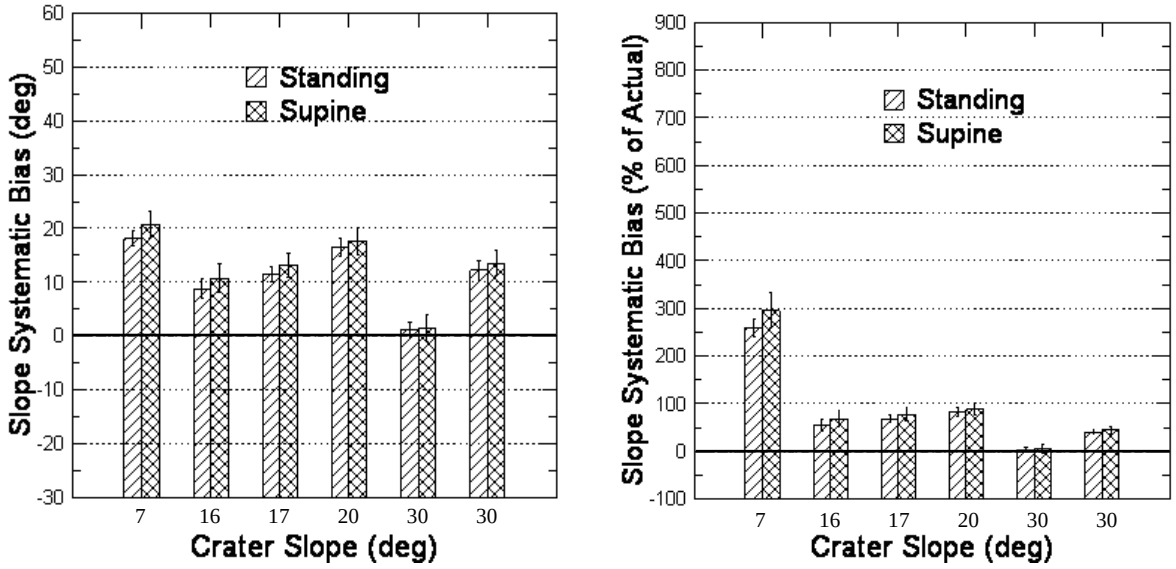

Figure 4.26 Bar graphs of slope estimation error (bias and one standard error) in degrees (left) and percent of actual slope (right) for each crater in LVS (positive error indicates overestimation)

Figure 4.26 shows a large range of systematic biases with the 7°, 20°, and second 30° slope producing the largest biases. A close inspection of each photograph shows several interesting trends. Appendix D.2 reveals that the bottom of the 7° crater was visible and half of its area was immersed in a dark shadow, potentially causing its estimates to be much greater than the true slope. Astronaut Al Bean faced similar conditions with a different side of this crater during Apollo 12 and overestimated its slope by about 30 degrees. Appendix D.2 also shows that the bottom of the 20° is visible and the rocks and debris along its side and at its bottom may have caused it to appear steeper than the other hills. Rockslide and debris of similar nature was also visible along the sides of the second 30° crater in Figure 4.26, the North Ray Crater from Apollo 16. One subject stated his estimation method included judging "whether rocks looked like they were sitting precariously." Appendix D.2 also illustrates the smoothness of the other three craters, potentially explaining their lower systematic biases. Table 4.31 shows the bias ranges between 1.1 and 20.7 degrees. One-sample t-tests comparing the mean systematic bias for each condition in Table 4.31 to zero were significant for 10/12 cases. The non-significant cases were both for the smooth 30°

Flag Crater from Apollo 16. Additionally, the between-subject variation of slope biases, expressed by the standard deviation, ranges between 9.5 and 13.3 degrees, showing again that subjects have large differences in their slope systematic biases within the lunar environment.

Table 4.31 Mean systematic bias of slope estimates with standard deviations, standard errors, and 1-sample t-tests for each crater in the LVS

Position	Crater	Slope (deg)	Mean Bias (deg)	Stand. Dev (deg)	Stand. Err (deg)	t Statistic	p-value
Standing	7	7	18.1	9.5	1.4	13.274	0.000
	8	16	8.8	12.2	1.8	4.992	0.000
	9	17	11.6	9.6	1.4	8.423	0.000
	10	20	16.5	10.7	1.6	10.390	0.000
	11	30	**1.1**	**10.1**	**1.5**	0.789	0.434
	12	30	12.3	12.2	1.8	6.966	0.000
Supine	7	7	**20.7**	**12.5**	**2.5**	8.258	0.000
	8	16	10.8	13.3	2.7	4.068	0.000
	9	17	13.2	10.8	2.2	6.110	0.000
	10	20	17.7	12.2	2.5	7.269	0.000
	11	30	1.5	12.1	2.5	0.613	0.546
	12	30	13.5	11.7	2.4	5.782	0.000

Table 4.32 Mean systematic bias of slope estimates (in percent of actual slope) with standard deviations and standard errors for each crater in LVS

Position	Crater	Slope (deg)	Mean Bias (%)	Stand. Dev (%)	Stand. Err (%)
Standing	7	7	259.2	135.3	19.6
	8	16	54.9	76.3	11.1
	9	17	68.4	56.2	8.2
	10	20	82.7	53.4	8.0
	11	30	**3.8**	**33.5**	**4.9**
	12	30	40.9	40.7	5.9
Supine	7	7	**296.0**	**179.2**	**36.4**
	8	16	67.5	83.0	16.9
	9	17	77.6	63.5	12.9
	10	20	88.4	60.8	12.4
	11	30	4.9	40.3	8.2
	12	30	45.1	39.0	7.9

4.4.5 Lunar Hill Distance Estimation Analysis

A mixed hierarchical regression with subject as the identifier and a square root transformation (to increase the model fit) of the estimated distance as the dependent variable was used to analyze the effects of slope, distance, and body position of lunar hills in the LVS. Table 4.33 shows the main effects of the regression and their significance. The residuals, shown in Figure 4.27 were analyzed for normality and homoscedasticity. The subject with the symbol "x" in Figure 4.27 (left) possesses residuals with higher

predicted values and a lower variance than the rest of the subject pool. This subject was at least 10 years older than all remaining subjects and did not possess the characteristics of a current or recent college/graduate student. He was excluded from further analysis. Lilliefors test confirmed the distribution of residuals was *not significantly* different than a normal distribution (N = 714, p = 0.347). The residuals were sliced into groups, shown in Table 4.34, and tested for homoscedasticity by hypothesis testing of the equality of several variances. Levene's test was *not significant* (F = 1.491, p = 0.178).

Table 4.33 Mixed regression of estimated distance for lunar hills with categorized variables in LVS

Mixed Linear Regression on Square Root of Estimated Distance				
Variable	**Estimate**	**Standard Error**	**Z**	**p-value**
INTERCEPT	88.526	2.546	34.775	0.000
Hill #1 (5200 - 11400 m)	-3.214	1.392	-2.31	0.021
Hill #2 (4000 - 8400 m)	4.518	1.392	3.247	0.001
Hill #3 (5000 - 11500 m)	0.463	1.409	0.329	0.742
Hill #4 (10900 - 13900 m)	1.752	1.392	1.259	0.208
Hill #5 (4300 - 8800 m)	-7.32	1.399	-5.234	0.000
Hill #6 (6500 - 9800 m)	3.801	1.392	2.709	0.007
Distance #1 (Near)	-10.688	0.624	-17.114	0.000
Distance #2 (Far)	10.688	0.624	17.114	0.000
Standing Estimate	-0.055	0.631	-0.086	0.931
Supine Estimate	0.055	0.631	0.086	0.931

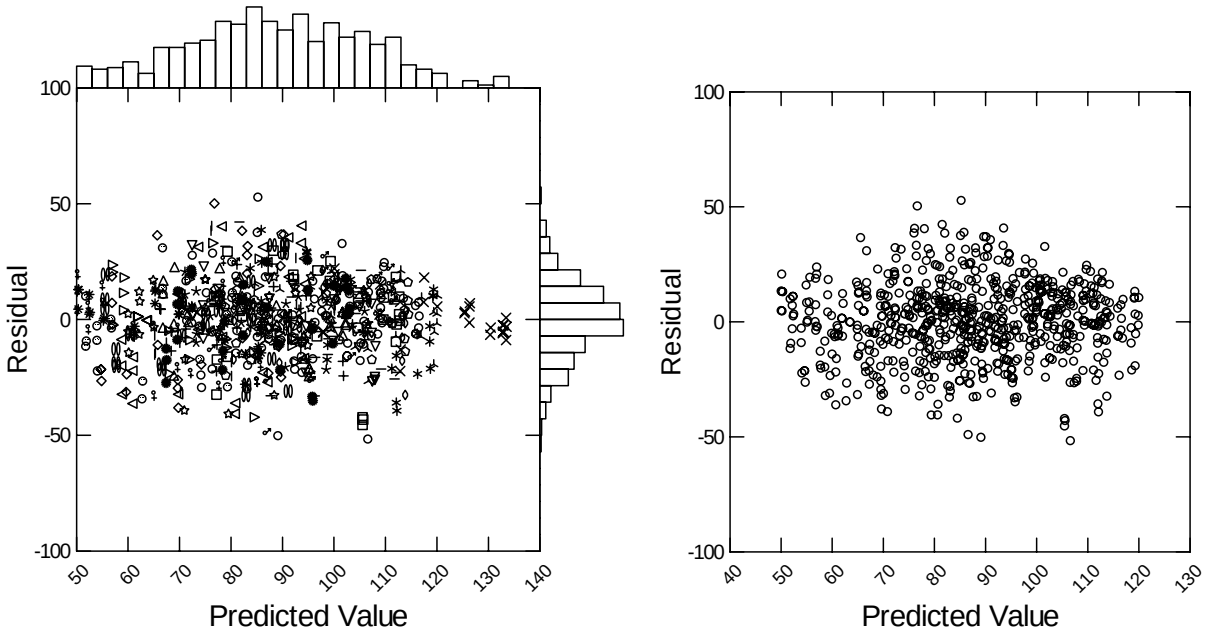

Figure 4.27 Residuals grouped by subject with (left) and without (right) subject #804 (symbol "X" in left graph) for lunar hill estimated distance regression in LVS

Table 4.34 Variance of residual slices for lunar hill estimated distance regression in LVS

GROUP	N	Mean	Variance	Median
0	55	-2.549	231.766	-0.433
1	81	-3.73	253.342	-2.658
2	144	2.019	308.742	2.552
3	176	0.145	334.672	-0.675
4	133	1.968	211.653	3.24
5	105	-1.406	266.56	-0.033
6	20	-2.032	116.705	-2.265

The regression results in Table 4.33 indicate a significant effect of hill on distance estimates ($p < 0.05$). The actual distances of each hill (each hill was presented from two distances) is located in the parentheses next to the hill number in the table. Based on the signs of the coefficients, we can conclude that neither the slope of the hills (Hills 1- 6 have increasing slope) nor the true distance alone can explain the nature of the estimates. Each hill was analyzed separately.

Hill #1 has true distances of 5200 and 11400 meters, near the middle of the range of all true distances, yet has a negative regression coefficient, indicating its estimates were significantly less than the mean distance estimate. This result could be attributed to the nature of the slope. Hill #1 was not a hill, but rather a rising valley between two hills. The ambiguous base may have caused subjects to underestimate its distance. A significant interaction between hill and distance ($p < 0.001$) showed that the 5200 m distance estimate was less than its prediction with the main effect alone, and the 11400 m distance was greater than its prediction with only the main effect. This result is not surprising upon inspection of the photographs in Appendix D.2, where the size of the lunar rover for the 11400 m distance provides cues of the vastness between the observer and the base of Hill #1.

Hill #2 has true distances of 4000 and 8400 meters, at the low range of all true distances, though its significant positive coefficient in Table 4.33 implies that its estimates were greater than the mean estimate across all hills. The height of Hill #2 is only 276 m, much less than all other hills; therefore, subjects may likely have assumed the small angle it subtended indicated a distance further than its true distance. A significant interaction between hill and distance ($p < 0.001$) showed the 4000 m mean distance estimate was greater than its prediction with the main effect alone, and the 8400 mean distance estimate was less than its prediction with the main effect alone. The cause of this interaction is likely due to the lack of a noticeable change in the visual angle subtended by the hill between the 4000 m and 8400 m photographs, because the base of the 4000 m hill seems to be slightly occluded from the rising terrain leading to the hill. This trend is shown in Figure 4.28 by the blue line and the images are located in Appendix D.2.

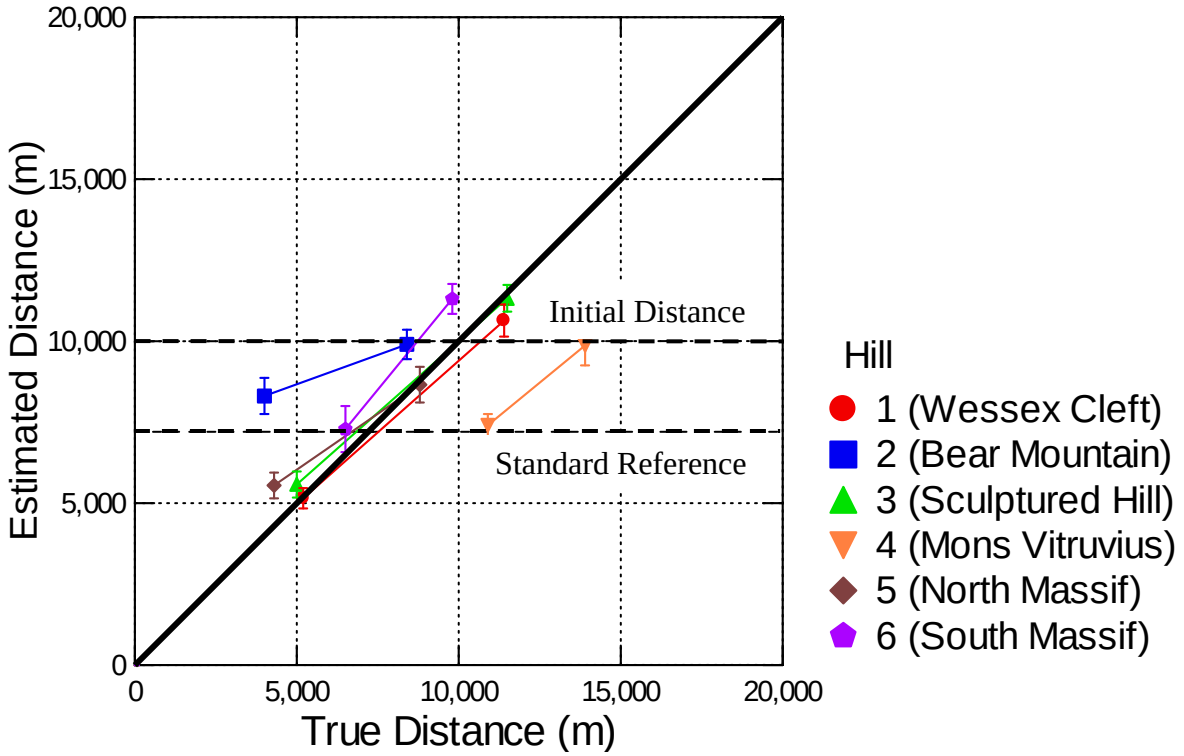

Figure 4.28 Mean estimated distance with one standard error for each hill in the LVS

Hill #3 has true distances of 5000 and 11500 meters, near the middle of the range of all true distances, and consequently has a non-significant regression coefficient in Table 4.33. The photographs used to display Hill #3 were the same images used to display Hill #1. As expected, a significant interaction between hill and distance ($p < 0.01$) showed that the 5000 m distance estimate was less than its prediction with the main effect alone, and the 11500 m distance was greater than its prediction with only the main effect. The reason for this interaction is again likely to be the appearance of the lunar rover within the middle of the image, revealing the vast distance between the observer and the base of the hill.

Hill #4 has true distances of 10900 and 13900 meters, at the top of the range of all true distances, and possesses a positive, though non-significant regression coefficient in Table 4.33. Interestingly, Figure 4.28 (orange line) reveals that the mean estimates were much less than the true distance (black line). This hill possesses a larger than average hill height of 2091 meters, which may have misled subjects to believe it was closer. Additionally, the standard reference hill presented at the beginning of the experiment was 1200 meters tall and only 7200 meters away, potentially biasing judgments of other hills with similar features and visual angles to be near these quantities as well. A significant interaction between hill and distance was found ($p < 0.01$) and showed that the 10900 m distance estimate was greater than its

prediction with the main effect alone, and the 13900 m distance was less than its prediction with only the main effect. The 13900 m photograph in Appendix D.2 contains a lunar rover only meters in front of the photographer, potentially causing the subjects to compress the size of the reference frame between them and the Hill #4.

Hill #5 has true distances of 4300 and 8800 meters, near the bottom of the range of all distances, and consequently possesses a significant negative regression coefficient in Table 4.33. The large visual angle subtended by this hill at 4300 m and its location at the top of the screen may have provided cues to the subjects indicating its distance relative to the standard reference. Despite how close the 4300 m image may seem in Appendix D.2, insufficient absolute distance cues are present, informing the subject that its base is over 2.5 miles away. No significant interactions were found for this hill.

Hill #6 has true distances of 6500 and 9800 meters, near the middle of the range of all true distances; however, it possesses a significantly positive regression coefficient in Table 4.33 indicating its distance estimates were greater than average across all hills. Surprisingly, Hill #6 possesses the greatest height, 2341 m, and Appendix D.2 reveals that a lunar rover in the 6500 m image could have influenced subjects to believe the hill appeared nearer. However, the images in Appendix D.2 also reveal a number of similar sized rocks that lie within the ground plane between the photographer and the hill that were likely to cause the subjects to believe the hill lied further than its true distance. Post-experiment feedback found that 64% of subjects used surrounding objects to base their distance estimates, such as rocks, other hills, or lunar rovers. It seems plausible that the perspective created by the receding rocks caused subjects to overestimate the distance to this hill. No significant interactions were found for this hill.

The distance category coefficient for the regression in Table 4.33 was very highly significant ($p < 0.001$) with the near distance for each hill producing a lower distance estimate than the far distance. The most visible difference between the hills at near and far distances in Appendix D.2 is the visual angle subtended by each and could provide a useful cue for astronauts during lunar excursions. With previous knowledge of the heights of each hill, the visual angle it subtends would be proportional to the distance to its base. Dangers of using this method alone include illusions when the base of the hill is occluded by rising terrain in one's foreground or the lack of noticeable changes of the FOV for objects across vast distances. Distance estimation methods will be further discussed in Chapter 5.

The effect of body position was non-significant in the regression in Table 4.33 ($p = 0.931$). This result is illustrated in Figure 4.29. Individual paired t-tests with a Bonferroni Adjustment for each set of

conditions, shown in Table 4.35, found that 7/12 sets caused a larger slope estimate from the supine position (shown in red); however, only one condition was significant ($p < 0.05$). These results do not fully support our hypothesis that the supine position hinders size-constancy and increases distance estimates, though the vast distance and lack of familiar objects in the LVS were likely to hinder the use of size-constancy from even the standing position.

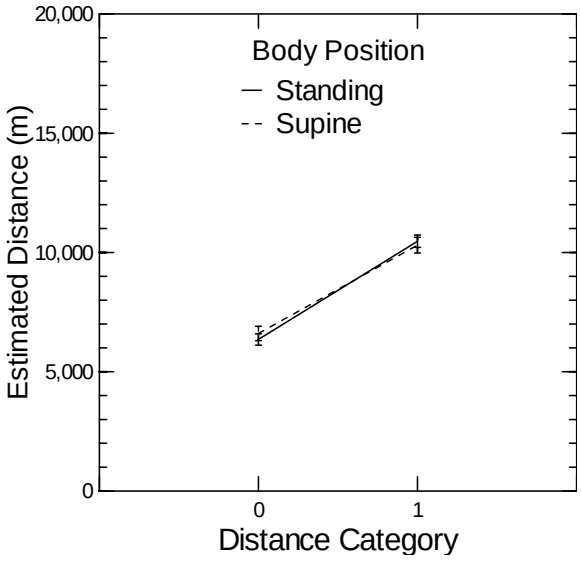

Figure 4.29 Effect of body position on hill distance estimates in LVS

Table 4.35 Paired t-tests between standing and supine hill distance estimates for each subject in LVS

Hill	Slope (deg)	Distance (m)	Mean of Differences (m)	t Statistic	p-value
1	14.7	5200	276	0.589	0.562
		11400	-1676	-2.332	**0.028**
2	15.1	4000	-316	-0.471	0.642
		8400	-8	-0.014	0.989
3	22.2	5000	-369	-0.535	0.597
		11500	525	1.100	0.283
4	24.1	10900	-620	-1.036	0.311
		13900	964	1.163	0.256
5	25.6	4300	-1260	-2.042	0.052
		8800	429	0.667	0.511
6	25.6	6500	-192	-0.307	0.761
		9800	224	0.344	0.734

The most commonly used distance estimation methods in the LVS are shown in Figure 4.30. The availability of surrounding objects aided at least 64% of subjects, helping them to refine the size of their reference frame in each image. Twenty-eight percent of subjects indicated using the standard reference to estimate distance. This reference is influential in a reduced-cue environment; however, it may have been

responsible for misleading some estimates, discussed earlier in this section. Texture was an important cue for 12% of subjects; however, this experiment was not able to isolate the sun elevation's effect on surface texture and distance estimates. Future experiments should determine this effect before planning missions to the South Pole where low sun elevation angles may cast long shadows and cause large textural contrast.

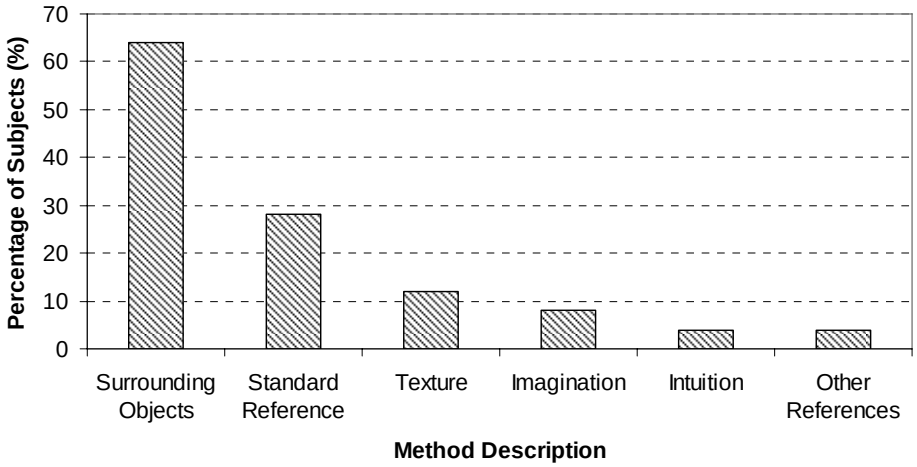

Figure 4.30 Frequency of methods used to estimation distance in LVS

4.4.6 Lunar Hill Distance Estimation Systematic and Random Errors

Due to the significant t-test result between standing and supine conditions, these subpopulations were not combined. The mean biases with one standard error for each of the 24 hill/distance/body position sets of conditions are displayed in Figure 4.31. Tables 4.36 and 4.37 summarize these results and highlight the maximum underestimation and overestimation biases found in this study.

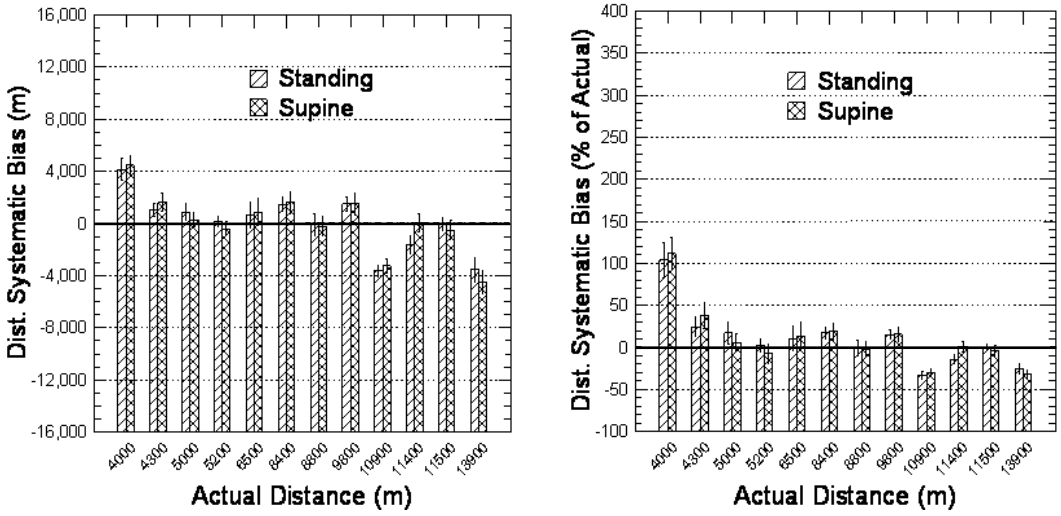

Figure 4.31 Bar graphs of distance estimation error (bias and one standard error), in meters (left) and percent of actual distance (right) for each hill in LVS (positive error indicates overestimation)

Both graphs in Figure 4.31 indicate that three of the distances have systematic biases of at least 3000 meters. The likely cause of the 4148 m overestimation bias to the base of Hill #2 4000 m away was the small hill height and the occlusion of the base of the hill, reducing its visual angle. The likely causes of the 3618 m and 3548 m underestimation biases to the base of Hill #4 were the large hill height and influence the standard reference had on estimates. One-sample t-tests with a Bonferroni Adjustment comparing the mean bias to zero in Table 4.36 revealed that 13/24 conditions produced a mean bias that was not significantly different than zero. Despite this favorable result, the standard deviation of estimates was often as large as or larger than the mean bias. Even the within-subject variation, expressed by the standard error, was at times greater than 1000 meters. These results confirm Hypothesis #2 that accurate distance judgments unaided by range-finding instruments in a reduced-cue environment, such as the lunar surface, becomes difficult and dangerous and can vary largely with local cues, such as surrounding objects, texture gradients, or rising terrain. Table 4.37 shows these biases and errors as a percent of the true distance, though future experiments should be conducted at smaller distances to determine whether biases and errors are consistent with the results of this study. A detailed discussion on the distance estimation methods that astronauts may use on the lunar surface can be found in Chapter 5.

Table 4.36 Mean systematic bias of distance estimates with standard deviations, standard errors, and 1-sample t-tests for each hill in the LVS

Position	Hill	Slope (deg)	Distance (m)	Mean Bias (m)	Stand. Dev (m)	Stand. Err (m)	t Statistic	p-value
Standing	2	15.1	4000	4148	4140	841	5.010	0.000
	5	25.6	4300	1045	3443	494	2.124	0.039
	3	22.2	5000	852	3024	642	1.352	0.190
	1	14.7	5200	124	2638	379	0.330	0.743
	6	25.6	6500	688	4817	978	0.714	0.482
	2	15.1	8400	1443	3768	541	2.681	0.010
	5	25.6	8800	-79	3962	822	-0.098	0.923
	6	25.6	9800	1494	3835	551	2.727	0.009
	4	24.1	10900	-3618	3058	439	-8.283	0.000
	1	14.7	11400	-1604	3381	687	-2.372	0.000
	3	22.2	11500	-10	3510	494	-0.020	0.984
	4	24.1	13900	-3548	4479	910	-3.961	0.001
Supine	2	15.1	4000	4696	3867	769	6.193	0.000
	5	25.6	4300	1636	3361	683	2.434	0.023
	3	22.2	5000	300	2372	503	0.607	0.550
	1	14.7	5200	-400	2777	564	-0.720	0.478
	6	25.6	6500	880	5217	1060	0.843	0.407
	2	15.1	8400	1608	4175	848	1.926	0.066
	5	25.6	8800	-208	3760	764	-0.277	0.784
	6	25.6	9800	1520	4198	853	1.811	0.083
	4	24.1	10900	-3256	2693	547	-6.046	0.000
	1	14.7	11400	72	3411	693	0.106	0.917
	3	22.2	11500	-500	3898	761	-0.667	0.511
	4	24.1	13900	-4512	4186	850	-5.390	0.000

Table 4.37 Mean systematic bias of distance estimates (in percent of actual distance) with standard deviations and standard errors for each hill in LVS

Position	Hill	Slope (deg)	Distance (m)	Mean Bias (%)	Stand. Dev (%)	Stand. Err (%)
Standing	2	15.1	4000	103.7	103.5	21.0
	5	25.6	4300	24.3	80.1	11.5
	3	22.2	5000	17.0	60.5	12.8
	1	14.7	5200	2.4	50.7	7.3
	6	25.6	6500	10.6	74.1	15.1
	2	15.1	8400	17.2	44.9	6.4
	5	25.6	8800	-0.9	45.0	9.3
	6	25.6	9800	15.2	39.1	5.6
	4	24.1	10900	-33.2	28.1	4.0
	1	14.7	11400	-14.1	29.7	6.0
	3	22.2	11500	-0.1	30.5	4.3
	4	24.1	13900	-25.5	32.2	6.5
Supine	2	15.1	4000	117.4	96.7	19.2
	5	25.6	4300	38.0	78.2	15.9
	3	22.2	5000	6.0	47.4	10.1
	1	14.7	5200	-7.7	53.4	10.8
	6	25.6	6500	13.5	80.3	16.3
	2	15.1	8400	19.1	49.7	10.1
	5	25.6	8800	-2.4	42.7	8.7
	6	25.6	9800	15.5	42.8	8.7
	4	24.1	10900	-29.9	24.7	5.0
	1	14.7	11400	0.6	29.9	6.1
	3	22.2	11500	-4.3	33.9	6.6
	4	24.1	13900	-32.5	30.1	6.1

4.4.7 Lunar Crater Distance Estimation Analysis

A mixed hierarchical regression with subject as the identifier and a square root transformation (to increase the model fit) of the estimated distance as the dependent variable was used to analyze the effects of slope, body position, and session of lunar craters in the LVS. Table 4.38 shows the main effects of the regression. The residuals, shown in Figure 4.32 were analyzed for normality and homoscedasticity. The subject with the symbol "x" (same subject "x" from the lunar hill distance analysis) in Figure 4.32 (left) again possessed residuals with higher predicted values and a lower variance than the rest of the subject pool and was excluded from further analysis. Lilliefors test confirmed the distribution of residuals was *not significantly* different than a normal distribution ($N = 419$, $p = 0.253$). The residuals were sliced into groups, shown in Table 4.39, and tested for homoscedasticity by hypothesis testing of the equality of several variances. Levene's test was *not significant* ($F = 1.468$, $p = 0.211$).

Table 4.38 Mixed regression of estimated distance for lunar craters with categorized variables in LVS

Mixed Linear Regression on Square Root of Estimated Distance				
Variable	**Estimate**	**Standard Error**	**Z**	**p-value**
INTERCEPT	23.497	1.092	21.527	0.000
Crater #7 (180 m)	0.982	1.551	0.633	0.527
Crater #8 (550 m)	-4.146	1.551	-2.673	0.008
Crater #9 (250 m)	-1.937	1.551	-1.249	0.212
Crater #10 (123 m)	1.398	1.579	0.885	0.376
Crater #11 (209 m)	2.471	1.551	1.593	0.111
Crater #12 (877 m)	1.232	1.551	0.811	0.417
Standing Estimate	0.220	0.241	0.915	0.360
Supine Estimate	-0.220	0.241	-0.915	0.360
Session	0.462	0.186	2.487	0.013

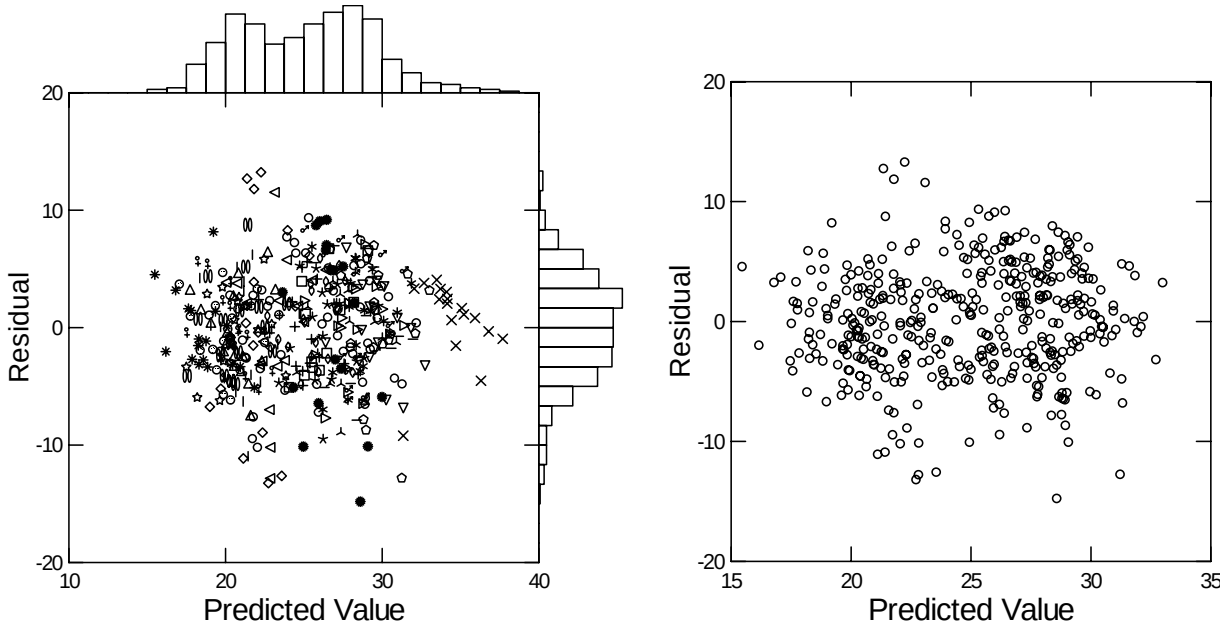

Figure 4.32 Residuals grouped by subject with (left) and without (right) subject #804 (symbol "X" in left graph) for lunar crater estimated distance mixed regression in LVS

Table 4.39 Variance of residual slices for lunar crater estimated distance regression in LVS

GROUP	N	Mean	Variance	Median
0	29	0.158	11.851	0.678
1	127	-0.844	21.675	-0.767
2	115	0.785	23.512	1.049
3	134	0.101	18.594	0.664
4	14	-0.947	23.236	-0.275

The regression in Table 4.38 indicates that the mean distance estimate for 5/6 craters was *not* significantly different than that mean estimates across all the craters. The distance estimates of Crater #8 (550 m) were on average significantly less than the estimates of the other craters ($p < 0.05$). This result came as a surprise, since its true distance was the second largest of all the craters in this experiment; however, the visual angle subtended between the near and far lips of the crater in the photograph in Appendix D.2 was the smallest of all the craters and may have influenced subjects to believe its distance was less than on average. This cue is misleading because the visual angle increases as the distance to the near lip of the crater increases; however, subjects may have used this cue without any other salient cues to influence their judgment. Figure 4.33 shows that the mean distance estimate and one standard error for 5/6 craters were within the initial distance on the estimation device (750 m) and the reference distance from the beginning of the experiment (440 m). This result leads us to conclude that subjects lacked strong distance cues and tended to decrease the initial estimate on the device toward the standard reference distance.

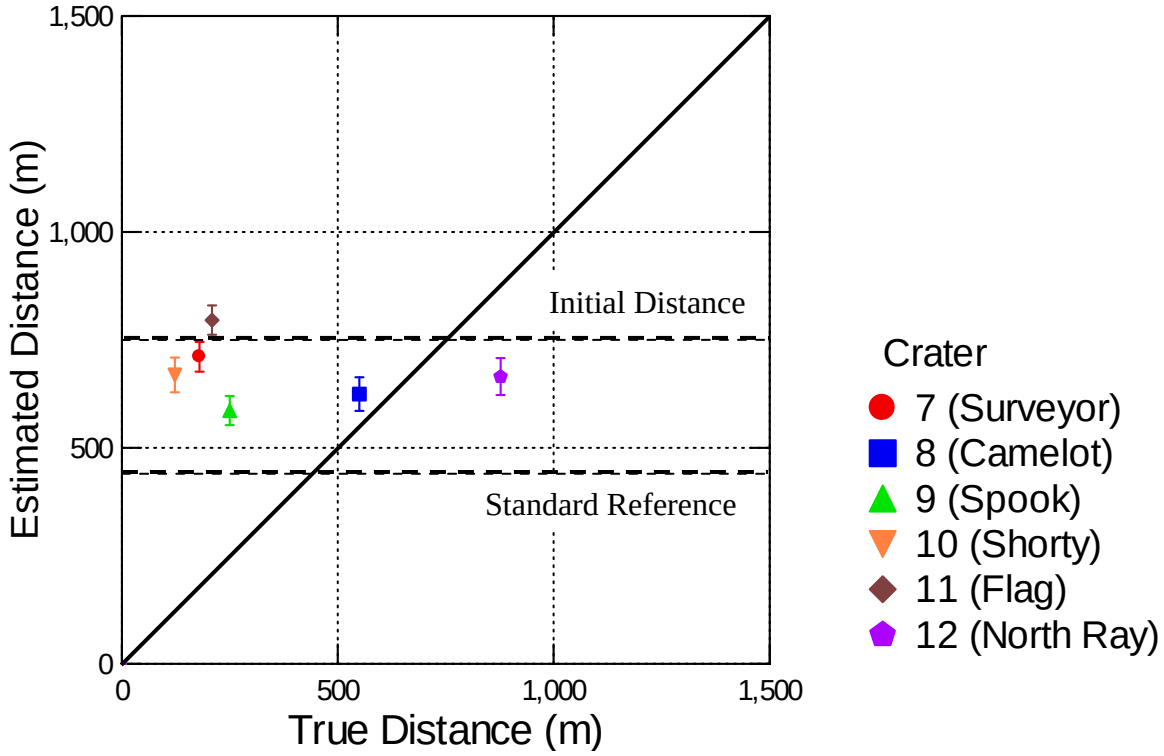

Figure 4.33 Mean estimated distance with one standard error for each crater in the LVS

The regression in Table 4.38 also indicates no significant effect of body position on the distance estimates of the lunar craters ($p = 0.360$). Figure 4.34 (left) shows the lack of consistency of this effect across all craters. Individual paired t-tests with a Bonferroni Adjustment for each crater, shown in Table 4.40,

found that 4/5 craters caused a larger distance estimate from the supine position (shown in red); however, only one condition was significant ($p < 0.05$). These results do not fully support our hypothesis that the supine position hinders size-constancy and increases distance estimates, though the lack of familiar objects in the LVS were likely to hinder the use of size-constancy in all cases. The test session also produced a significant effect in the regression in Table 4.38 ($p < 0.05$) causing distance estimates of the lunar craters to increase throughout the duration of the experiment, shown in Figure 4.34 (left). The cause of this effect is likely fatigue or boredom and further complicates the determination of the effect of body position. Designers of a VR training tool that calibrates slope and distance estimation on a future lunar mission should be aware of this effect and avoid long training sessions

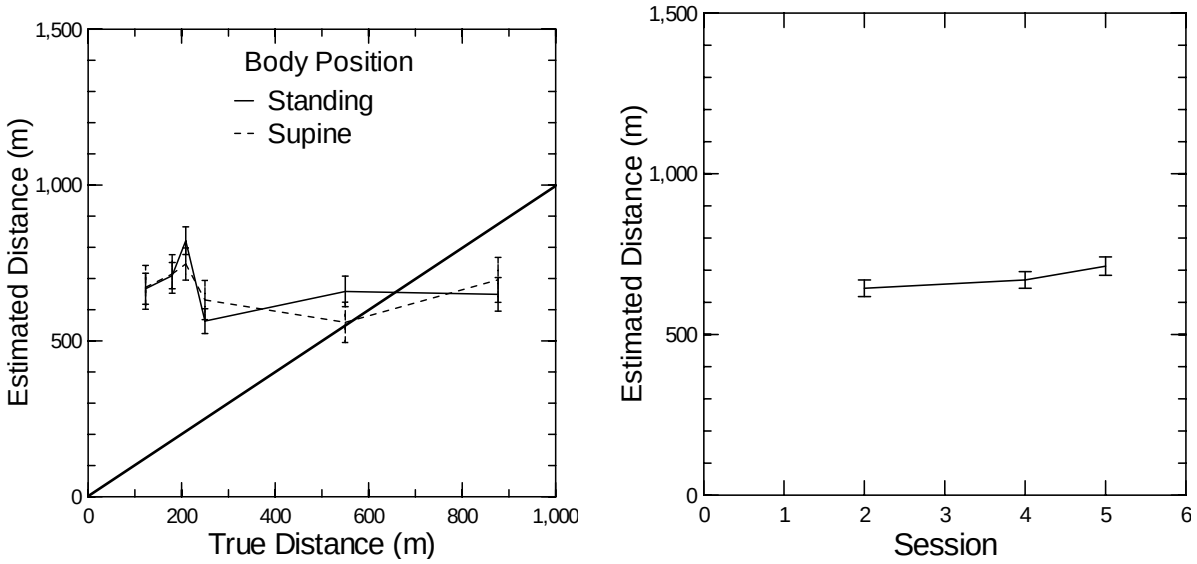

Figure 4.34 Effect of body position (left) and session (right) on crater distance estimates in LVS

Table 4.40 Paired t-tests between standing and supine crater distance estimates for each subject in LVS

Crater	Slope (deg)	Distance (m)	Mean of Differences (m)	t Statistic	p-value
10	20	123	-13.913	-0.207	0.838
7	7	180	-47.5	-1.067	0.297
11	30	209	35.417	0.771	0.448
9	17	250	-105.417	-2.247	**0.035**
8	16	550	-1.667	-0.027	0.979
12	30	877	-38.333	-0.81	0.426

4.4.8 Lunar Crater Distance Estimation Systematic and Random Errors

Due to the significant t-test result between standing and supine conditions, these subpopulations were not combined. The mean biases with one standard error for each of the 24 hill/distance/body position sets of conditions are displayed in Figure 4.35. Tables 4.41 and 4.42 summarize these results and highlight the maximum underestimation and overestimation biases found in this study.

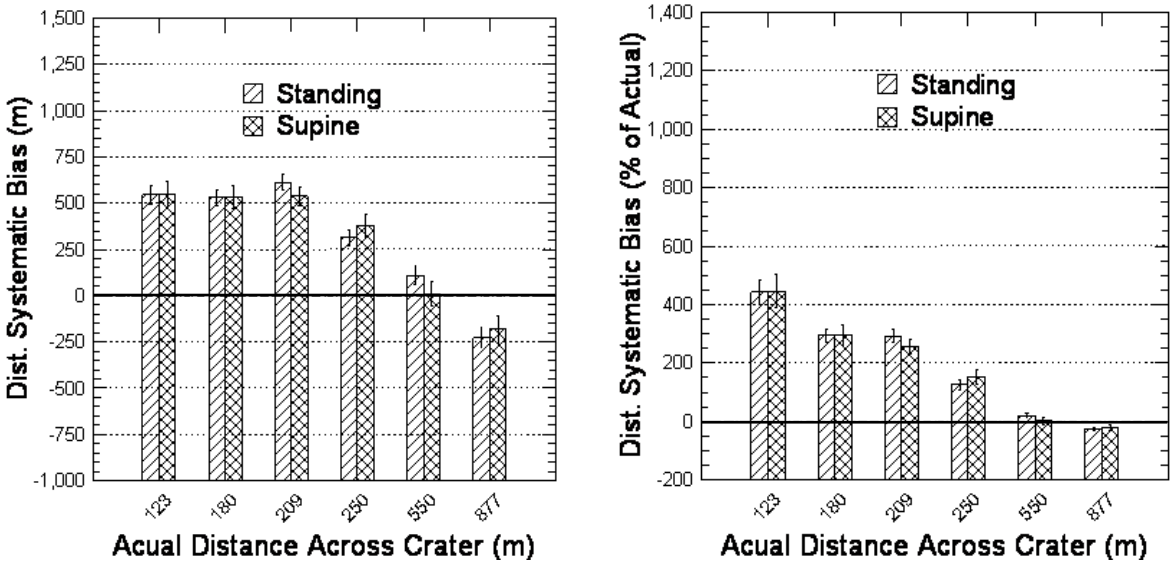

Figure 4.35 Bar graphs of distance estimation error (bias and one standard error), in meters (left) and percent of actual distance (right) for each crater in LVS (positive error indicates overestimation)

Figure 4.35 shows a distance overestimation systematic bias that decreases as the true distance increases until the 550 m crater. The 877 m crater produced a large underestimation systematic bias. Interestingly, the standard reference for the experiment was a 440 meter crater, and likely influenced the distance estimates of all other craters without any salient visual distance cues. One-sample t-tests with a Bonferroni Adjustment comparing the mean bias to zero in Table 4.41 revealed that the four craters with a true distance less than the reference distance had a mean estimate that was significantly greater than zero ($p < 0.001$) and the 877 meter crater, possessing a true distance greater than the reference had a mean estimate that was significantly less than zero ($p < 0.05$). The standard deviation ranged between 252 and 368 meters (or up to 281% of the true distance) indicating that distance estimates varied largely across subjects. Providing astronauts with knowledge of the distances across craters they may encounter on future lunar missions would be a critical asset allowing them to maintain their spatial awareness.

Table 4.41 Mean systematic bias of distance estimates with standard deviations, standard errors, and 1-sample t-tests for each crater in the LVS

Position	Crater	Slope (deg)	Distance (m)	Mean Bias (m)	Stand. Dev (m)	Stand. Err (m)	t Statistic	p-value
Standing	10	20	123	544	335	50	11.024	0.000
	7	7	180	529	290	42	12.631	0.000
	11	30	209	612	304	44	13.970	0.000
	9	17	250	313	273	40	7.934	0.000
	8	16	550	109	335	49	2.247	0.029
	12	30	877	-228	368	53	-4.292	0.000
Supine	10	20	123	549	345	70	7.943	0.000
	7	7	180	534	304	62	8.796	0.000
	11	30	209	537	252	51	10.654	0.000
	9	17	250	381	307	62	6.200	0.000
	8	16	550	9	316	64	0.145	0.886
	12	30	877	-181	354	72	-2.560	0.017

Table 4.42 Mean systematic bias of distance estimates (in percent of actual distance) with standard deviations and standard errors for each crater in LVS

Position	Crater	Slope (deg)	Distance (m)	Mean Bias (%)	Stand. Dev (%)	Stand. Err (%)
Standing	10	20	123	442.4	272.2	40.4
	7	7	180	294.0	161.2	23.4
	11	30	209	292.9	145.3	21.1
	9	17	250	125.3	109.4	15.9
	8	16	550	19.7	60.8	8.8
	12	30	877	-26.0	42.0	6.1
Supine	10	20	123	446.0	280.8	57.0
	7	7	180	296.9	168.8	34.3
	11	30	209	257.1	120.7	24.5
	9	17	250	152.3	122.8	24.9
	8	16	550	1.7	57.5	11.7
	12	30	877	-20.7	40.4	8.2

4.4.9 Lunar Hill Height Estimation Analysis

A mixed hierarchical regression with subject as the identifier and a square root transformation (to increase the model fit) of the estimated height as the dependent variable was used to analyze the effects of slope, distance, and body position of lunar hills in the LVS. Table 4.43 shows the main effects of the regression and their significance. The residuals, shown in Figure 4.36 were analyzed for normality and homoscedasticity. Subject "x" in Figure 4.36 (left) again possessed residuals with higher predicted values and a lower variance than other subjects and was excluded from analysis. Lilliefors test confirmed the distribution of residuals was *not significantly* different than a normal distribution ($N = 714$, $p = 0.216$). The residuals were sliced into groups, shown in Table 4.44, and tested for homoscedasticity by hypothesis testing of the equality of several variances. Levene's test was *not significant* ($F = 0.816$, $p = 0.588$).

Table 4.43 Mixed regression of estimated height for lunar hills with categorized variables in LVS

Mixed Linear Regression on Square Root of Estimated Height				
Variable	**Estimate**	**Standard Error**	**Z**	**p-value**
INTERCEPT	37.742	1.258	29.994	0.000
Hill #1 (700 m)	-7.867	0.508	-15.480	0.000
Hill #2 (276 m)	-9.596	0.508	-18.883	0.000
Hill #3 (1110 m)	0.221	0.515	0.430	0.668
Hill #4 (2091 m)	2.857	0.508	5.621	0.000
Hill #5 (1551 m)	4.321	0.511	8.461	0.000
Hill #6 (2341 m)	10.065	0.508	19.805	0.000
Distance #1	0.298	0.228	1.308	0.191
Distance #2	-0.298	0.228	-1.308	0.191
Standing Estimate	-0.113	0.230	-0.489	0.625
Supine Estimate	0.113	0.230	0.489	0.625

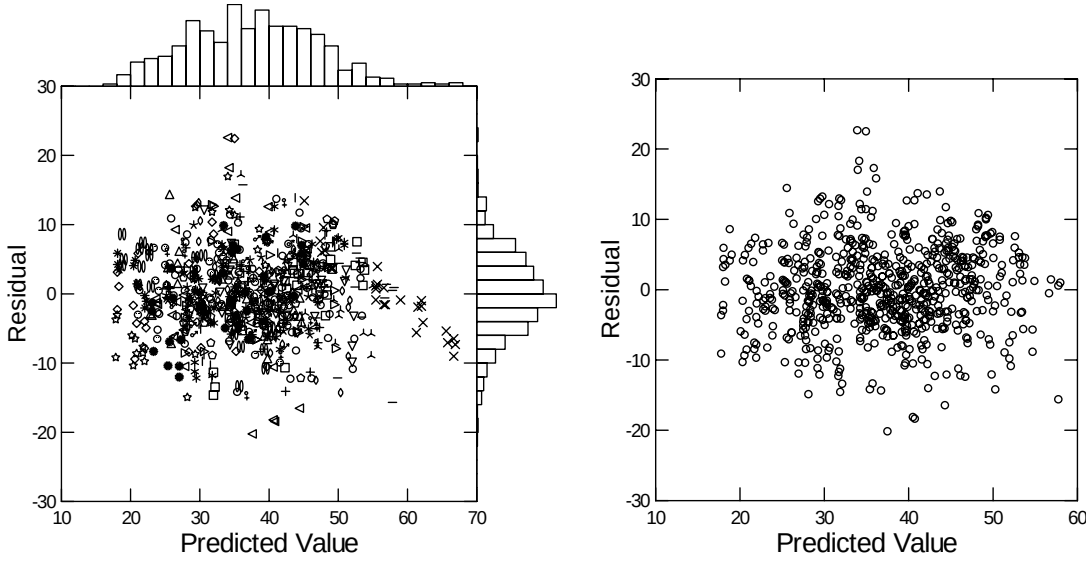

Figure 4.36 Residuals grouped by subject with (left) and without (right) subject #804 (symbol "X" in left graph) for lunar hill estimated height mixed regression in LVS

Table 4.44 Variance of residual slices for lunar hill estimated height regression in LVS

GROUP	N	Mean	Variance	Median
0	12	1.412	25.157	3.290
1	47	-1.652	23.556	-1.639
2	116	-0.281	32.838	-0.305
3	118	1.076	44.563	0.099
4	155	-0.752	35.924	-1.323
5	132	-0.270	38.095	-0.308
6	92	1.407	30.671	1.578
7	37	-0.410	33.601	1.142
8	5	-2.705	53.219	0.488

The regression in Table 4.43 indicates the mean height estimate for 5/6 hills was significantly different than the mean estimate across all hills ($p < 0.001$). Interestingly, the regression coefficients in Table 4.43 increase as the true height increases. The only exception to this trend is Hill #4 (2091 m), possessing a larger height than Hill #5 (1551 m), yet the regression indicates its height estimates were on average less than the estimates of Hill #5. This trend is also illustrated in Figure 4.37, and likely caused by the higher range of true distances to Hill #4 (10900 – 1399 m) when compared to Hill #5 (4300 – 8800 m), which reduced the visual angle subtended by the hill, making its height appear less. This conclusion suggests that distance and height estimates on the lunar surface are inter-related through the visual angle subtended by the hill and could be used to determine each other. Figure 4.38 illustrates the relationship between the distance and height errors for each data point in the LVS and the Pearson Correlation Coefficient was determine to be 0.590. This result suggests that given previous knowledge of the height of the hills that astronauts will encounter on their lunar excursions, their distance estimates may become more reliable.

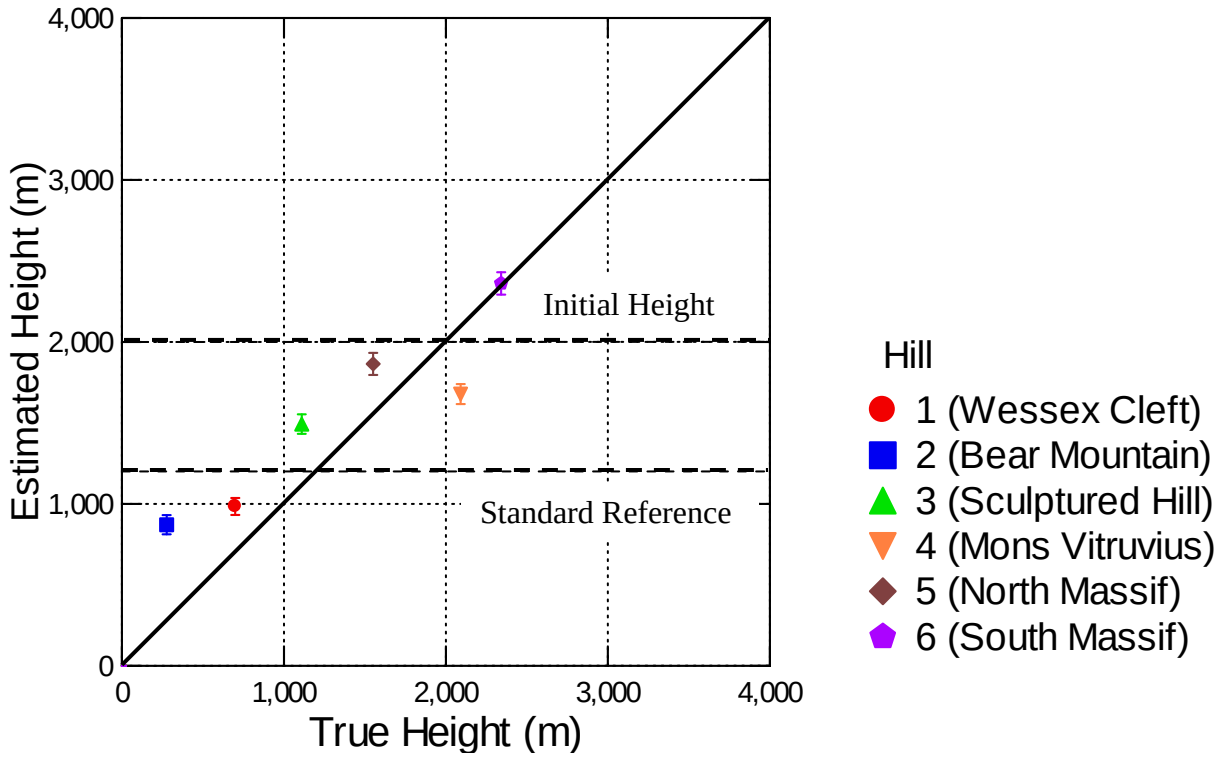

Figure 4.37 Mean estimated height with one standard error for each hill in the LVS

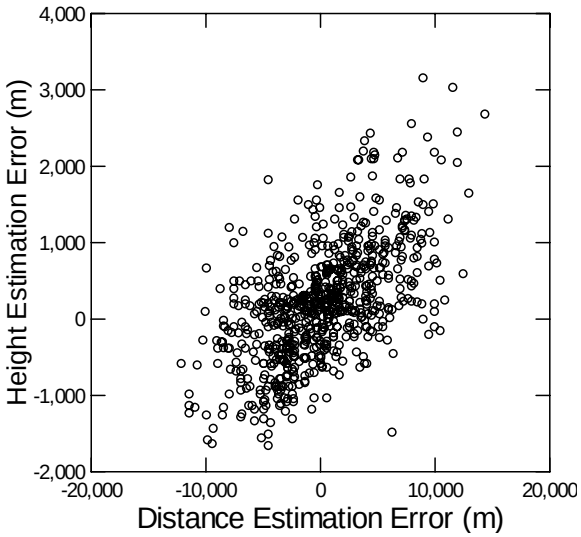

Figure 4.38 Positive correlation between distance and height hill estimates in LVS

The distances for each hill did not cause a significant effect on the height estimate regression in Table 4.43 ($p = 0.191$). This effect is illustrated in Figure 4.39 (left). Individual paired t-tests with a Bonferroni Adjustment for each hill/body position condition, shown in Table 4.45, found that 6/12 sets of conditions caused a larger height estimate from the near distance (shown in blue), only one of which was significant ($p < 0.05$). Although we expected the height estimates to be greater from the near distance due to the increase in the visual angle subtended by the hill, half of the t-tests did not support this hypothesis, three of which suggested that the far distance caused a significantly greater height estimate. Two of these three significant t-test results were from Hill #4 (Mons Vitruvius) and Appendix D.2 reveals the lunar rover within the far distance photograph of this hill, suggesting its presence affected estimates.

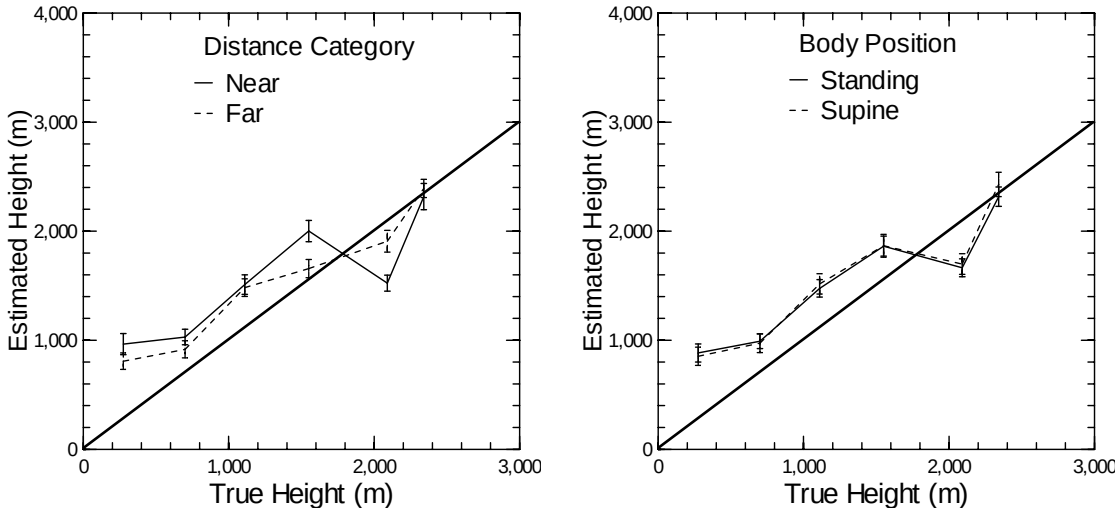

Figure 4.39 Effect of distance category (left) and body position (right) on hill height estimates in LVS

Table 4.45 Paired t-tests between near and far (distance) hill height estimates for each subject in LVS

Hill	Height (m)	Position	Mean of Differences (m)	t Statistic	p-value
2	276	Standing	172	1.604	0.122
		Supine	123	1.352	0.189
1	700	Standing	63	0.858	0.400
		Supine	115	1.345	0.191
3	1110	Standing	-229	-2.174	**0.040**
		Supine	-99	-0.940	0.357
5	1551	Standing	232	1.396	0.176
		Supine	369	3.121	**0.005**
4	2091	Standing	-397	-3.155	**0.004**
		Supine	-383	-3.320	**0.003**
6	2341	Standing	-90	-0.655	0.519
		Supine	-39	-0.356	0.725

Body position also did not cause a significant effect within the height estimate regression in Table 4.43 ($p = 0.625$). Figure 4.39 (right) illustrates this result, showing little or no difference between the average estimates for each position. Individual paired t-tests with a Bonferroni Adjustment for each hill/body position condition, shown in Table 4.45, found that 6/12 sets of conditions caused a larger height estimate from the supine position (shown in red), none of which were significant ($p < 0.05$). None of sets causing a greater height estimate from the standing position (shown in blue) were significant as well. The lack of an effect is not surprising, considering little or no body position effects were observed in the LVS slope and distance regressions. This could again be attributed to the lack of familiar objects and vastness within lunar images used for this experiment.

Table 4.46 Paired t-tests between standing and supine hill height estimates for each subject in LVS

Hill	Height (m)	Distance (m)	Sun Elevation (deg)	Mean of Differences (m)	t Statistic	p-value
2	276	4000	16	100	0.922	0.365
		8400	37	51	0.671	0.509
1	700	5200	16	-49	-0.712	0.484
		11400	26	3	0.070	0.944
3	1110	5000	16	-139	-1.621	0.118
		11500	26	-9	-0.087	0.932
5	1551	4300	16	-113	-0.630	0.534
		8800	26	20	0.162	0.872
4	2091	10900	16	22	0.162	0.872
		13900	37	36	0.443	0.661
6	2341	6500	16	-185	-1.595	0.124
		9800	37	-134	-1.238	0.228

Post-experiment feedback indicated that the most common reported method for estimating height was the use of the standard reference from the beginning of the experiment (40% response). Figure 4.37 indicates

the mean height estimate for the four smallest hills was greater than the true height, suggesting that subjects were likely biased by both the 1200 m reference and the 2000 m initial position of the estimation device, causing their estimates to be greater than the true height. Surrounding objects was the next most commonly used method (32% response), though the lunar rover in Hill #4 likely caused subjects to assume the hill was much closer and underestimated its height. Twenty-eight percent of subjects reported using their distance estimates to judge height, and the correlation between the errors of both estimates in Figure 4.38 verify the use of this method. This method could potentially cause accurate height estimates, though only if the distance was known or accurately estimated and the bottom of the hill was not occluded by terrain. Interestingly, 12% of subjects indicated using slope estimates to derive their height estimate. Slope and height were also collinear in the design of this experiment (shallowest slopes possessed the smallest heights), though it seems plausible that the slope of a hill can dramatically change the visual angle subtended by the hill at close distances, affecting the height estimates. Future studies should analyze slope and height changes independently from both close and far range, determining if any effect or interactions exist. Only 8% of subjects reported using the percent of the FOV covered by the hill to estimate height, though we suspect this was a method used commonly among other subjects. All other methods shown in Figure 4.40 were used by less than 5% of subjects.

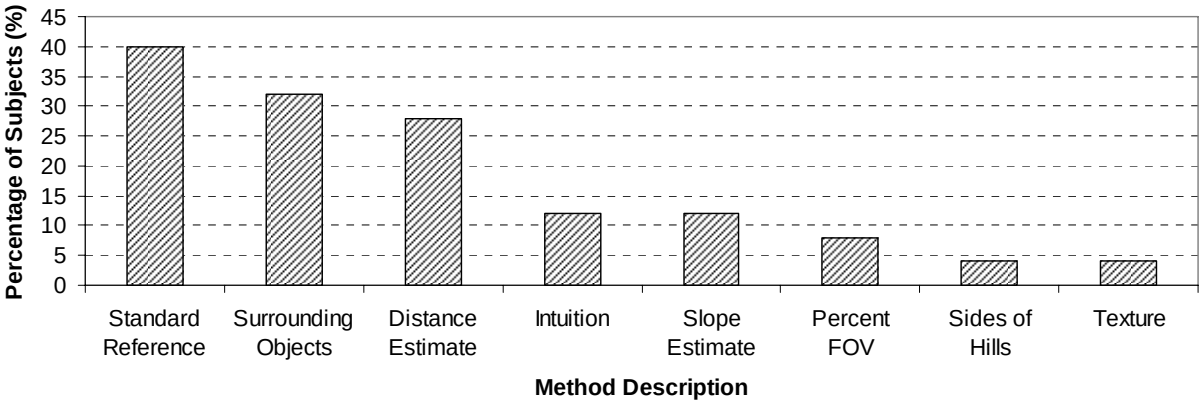

Figure 4.40 Frequency of methods used to estimate height in LVS

4.4.10 Lunar Hill Height Estimation Systematic and Random Errors

Due to the lack of significant t-test results between standing and supine positions, these subpopulations were combined. The mean biases with one standard error for each of the 12 hill/distance sets of conditions are displayed in Figure 4.41. Tables 4.47 and 4.48 summarize these results and highlight the maximum underestimation and overestimation biases found in this study.

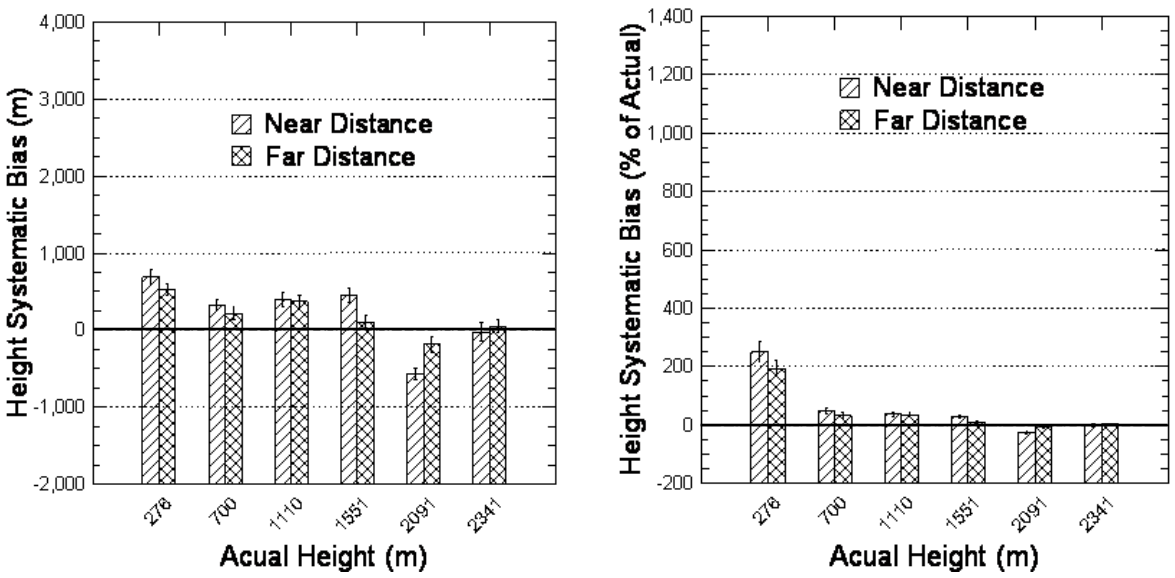

Figure 4.41 Bar graphs of height estimation error (bias and one standard error), in meters (left) and percent of actual height (right) for each hill in LVS (positive error indicates overestimation)

Figure 4.41 shows a decreasing overestimation bias as the actual hill height increases toward 2000 m, the initial position of the visual device. One-sample t-tests with a Bonferroni Adjustment comparing the mean bias to zero in Table 4.48 revealed that the four hills with a true height less than the reference had a mean estimate that was significantly greater than zero ($p < 0.001$). As mentioned previously, the device and the 1200 m reference height likely affected subject estimates without the presence of absolute distance or height cues. The height of the 2091 m hill (Mons Vitruvius) was likely underestimated because of the presence of the lunar rover within the photograph. The standard deviation ranged between 548 and 844 m (up to 246% of true height) indicating that height estimates varied largely across subjects.

Table 4.47 Mean systematic bias of height estimates with standard deviations, standard errors, and 1-sample t-tests for each hill in the LVS

Hill	Height (m)	Distance (m)	Mean Bias (m)	Stand. Dev (m)	Stand. Err (m)	t Statistic	p-value
2	276	4000	688	678	96	7.173	0.000
		8400	532	645	75	7.092	0.000
1	700	5200	329	607	71	4.663	0.000
		11400	217	548	78	2.795	0.007
3	1110	5000	400	596	88	4.555	0.000
		11500	371	707	80	4.641	0.000
5	1551	4300	450	830	97	4.662	0.000
		8800	106	580	83	1.282	0.206
4	2091	10900	-568	625	73	-7.818	0.000
		13900	-183	701	100	-1.847	0.071
6	2341	6500	-25	844	120	-0.205	0.838
		9800	50	712	83	0.607	0.546

Table 4.48 Mean systematic bias of height estimates (in percent of actual height) with standard deviations and standard errors for each hill in LVS

Hill	Height (m)	Distance (m)	Mean Bias (%)	Stand. Dev (%)	Stand. Err (%)
2	276	4000	249.3	245.7	34.9
		8400	192.8	233.9	27.2
1	700	5200	47.0	86.7	10.1
		11400	30.9	78.3	11.1
3	1110	5000	36.1	53.7	8.0
		11500	33.5	63.7	7.2
5	1551	4300	29.0	53.5	6.2
		8800	6.8	37.4	5.4
4	2091	10900	-27.2	29.9	3.5
		13900	-8.8	33.5	4.8
6	2341	6500	-1.0	36.0	5.1
		9800	2.1	30.4	3.5

4.4.11 Comparison of Lunar-like and Lunar Hills in Virtual Reality

Training and calibrating the slope and distance estimation tendencies of astronauts prior to future lunar missions must use a realistic VR environment that can simulate the errors and illusions humans are likely to face in the actual environment. The analysis in Section 4.3.6 concluded that the slope estimation errors were not significantly different between the lunar-like field and VR environments. Although we believe that a field study with a larger subject pool would show that field estimates are significantly greater and VR estimates, it was also necessary to compare the systematic and random errors committed by the same subjects between the lunar-like study (MVS) and the lunar study (LVS).

Figure 4.42 shows a similar range of test slopes between the two studies with all systematic biases within one standard deviation of each other. These large errors made it impractical to compare the studies as two separate populations; therefore, the within-subject differences between the two studies were analyzed by determining a mean lunar-like slope bias and lunar slope bias for each of the eleven subjects that completed both experiments. The variance of the lunar-like slope biases and lunar slope biases were also calculated for each subject and Figure 4.43 shows a rather interesting positive correlation between the mean and variances for each subject. As the mean overestimation bias increases for any particular subject, the variance of their estimates also increases. The outlier subject in Figure 4.43 (left) with a variance of over 200 deg was excluded and a Least Squares regression was fit for the remaining 10 subjects. The lunar-like bias/variance relationship has a correlation of 0.633 and a significant regression coefficient of 1.662 ($p < 0.05$). The lunar bias/variance relationship has a correlation of 0.650 and a significant regression coefficient of 0.893 ($p < 0.05$). The intercept for both regressions was 23 degrees.

These regressions show that under both lunar and lunar-like conditions, a subject's variance is likely to increase around one degree for every one degree increase in their systematic bias. Future studies comparing lunar and lunar-like environments should use a larger subject pool to confirm these results.

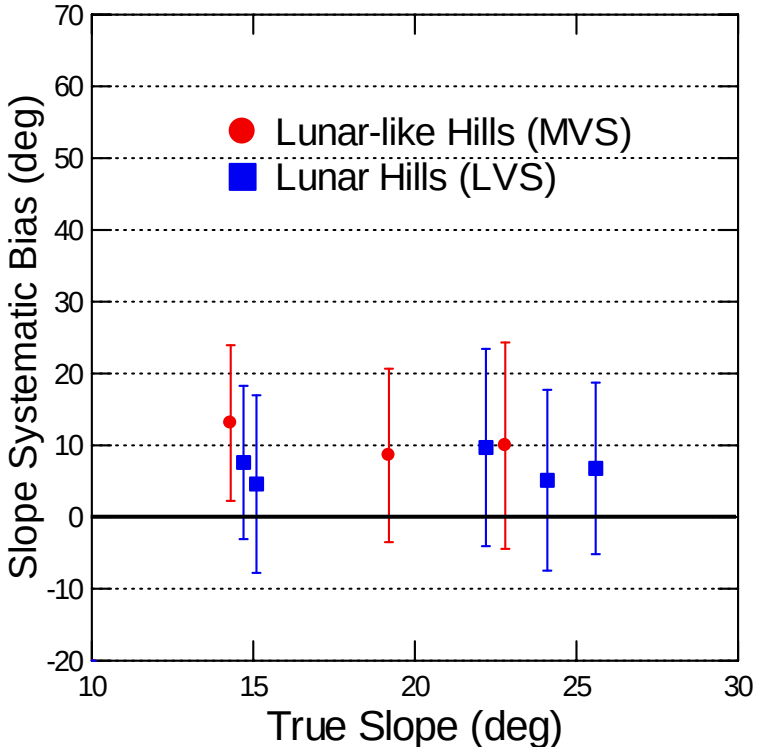

Figure 4.42 Comparison of slope systematic biases between lunar-like and lunar VR studies

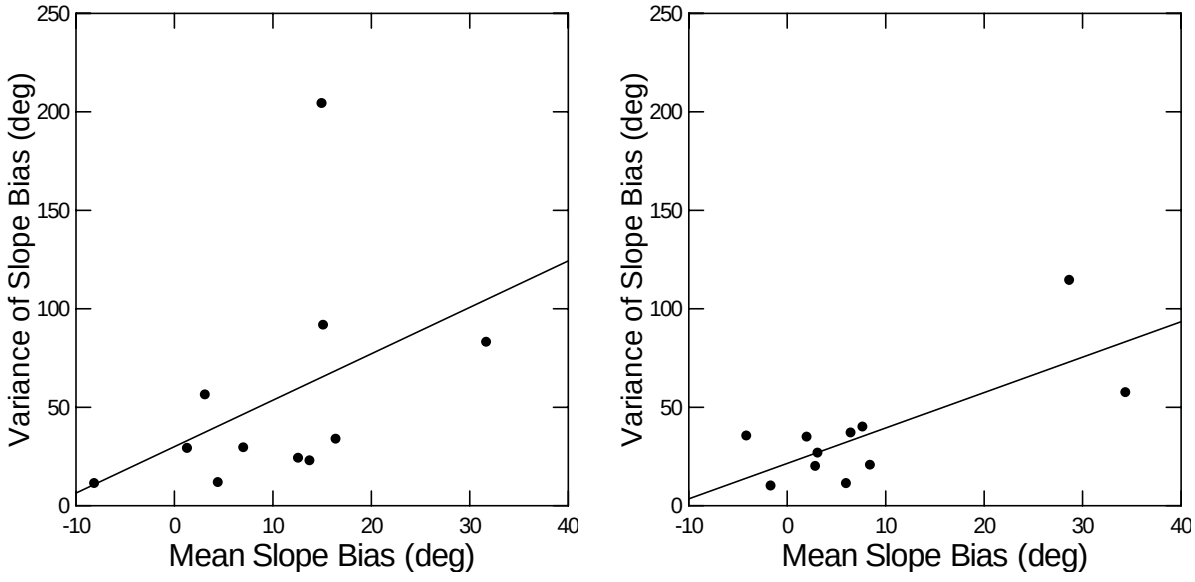

Figure 4.43 Mean and variance of slope systematic biases for each subject in MVS (left) and LVS (right)

The difference of the mean slope biases between the lunar-like (MVS) and lunar (LVS) VR studies were calculated, along with the difference of their variances, and shown below in Table 4.49. Only two subjects (shown in blue) possess a greater mean slope bias for the lunar VR study, though Subject #5 in Table 4.49 was excluded from the analysis because of his outlier variance in Figure 4.43 (left). One-sample t-tests with a Bonferroni Adjustment found the mean biases between the environments *significantly* different with a larger lunar-like bias on average of 3.2 degrees ($p = 0.048$). These results suggest that the slope overestimation bias would be less in a lunar environment than a lunar-like environment; however, the size, distance, and texture of the hills were extremely different between the two studies, thus this conclusion should not be accepted without future testing with similar hills between the two studies. One-sample t-tests with a Bonferroni Adjustment also show *no significant* difference between the within-subject variances of the two studies, indicating that the precision of slope estimates of any particular subject was not be affected under lunar conditions.

Table 4.49 Difference of mean slope biases between lunar-like (MVS) and lunar (LVS) VR studies

Subject	N (MVS)	N (LVS)	Difference of Mean Slope Biases (deg)	Difference of Variance of Slope Biases (deg)
1	48	30	-5.02	5.39
2	48	30	-5.31	-2.21
3	48	30	-0.02	-29.54
4	48	30	-8.65	-54.75
5	48	30	13.69	-89.82
6	48	30	4.00	24.12
7	48	29	-2.98	-19.10
8	48	30	-8.73	6.15
9	48	29	2.68	-25.57
10	48	30	-6.58	-12.91
11	36	30	-1.57	8.26

4.4.12 Differences in Slope Estimation between Lunar Hills and Craters

A personal interview with Astronaut Charles Duke in May 2008 [27] caused us to suspect a difference in slope estimates between lunar hills and craters. Not only did craters present a greater personal risk of being trapped within, but the rock slide along the side of the craters and the lack of side references that subjects used to estimate hill slopes would likely cause them to appear steeper than hills. The range of true slopes for the hills and craters used in the Lunar VR Study coincided between 5 and 30 degrees and Figure 4.44 shows the mean slope estimates with standard deviations across all subjects for each. The large errors for each slope made it impractical to analyze the difference between hills and craters as two separate populations over all subjects; therefore, the within-subject differences between the two types of

slopes were analyzed by determining a mean lunar hill slope bias and lunar crater slope bias for each of the 25 subjects that successfully completed the experiment.

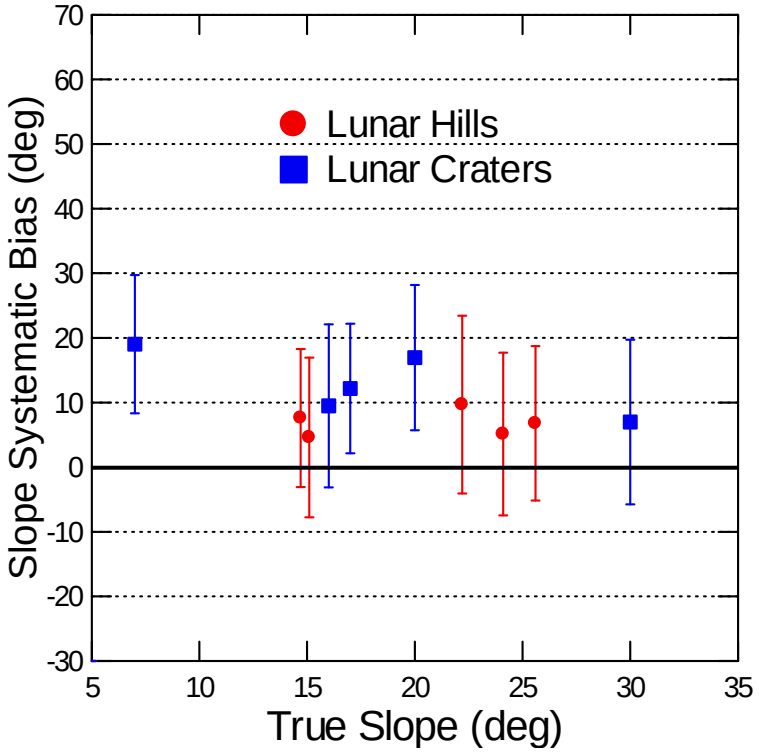

Figure 4.44 Comparison of slope systematic biases between lunar hills and craters

The mean and variance of the lunar hill slope biases and crater slope biases were also calculated for each subject and Figure 4.45 shows a positive correlation, similar to the correlation in Section 4.4.11. As the mean overestimation bias increases for any particular subject, the variance of their estimates also increases. A Least Squares regression was fit for all 25 subjects for both hills and craters. The lunar hill bias/variance relationship has a correlation of 0.721, a *significant* regression coefficient of 2.253 ($p < 0.001$), and an intercept of 29.8 deg. The lunar crater bias/variance relationship has a correlation of 0.357, though a *non-significant* regression coefficient of 1.209 ($p = 0.08$), and an intercept of 62.3 deg. These results indicate that the variance of lunar hill slope estimates across the 25 test subjects increased by a factor of 2.3 degrees for every degree increase in their overestimation bias, thus those subjects with a large overestimation bias also tended to lack precision in their estimates. The variance, and thus precision, of crater slope estimates were high, regardless of a subject's mean overestimation bias. The difference of the mean slope biases between the lunar hills and craters were calculated, along with the difference of their variances, and shown below in Table 4.50.

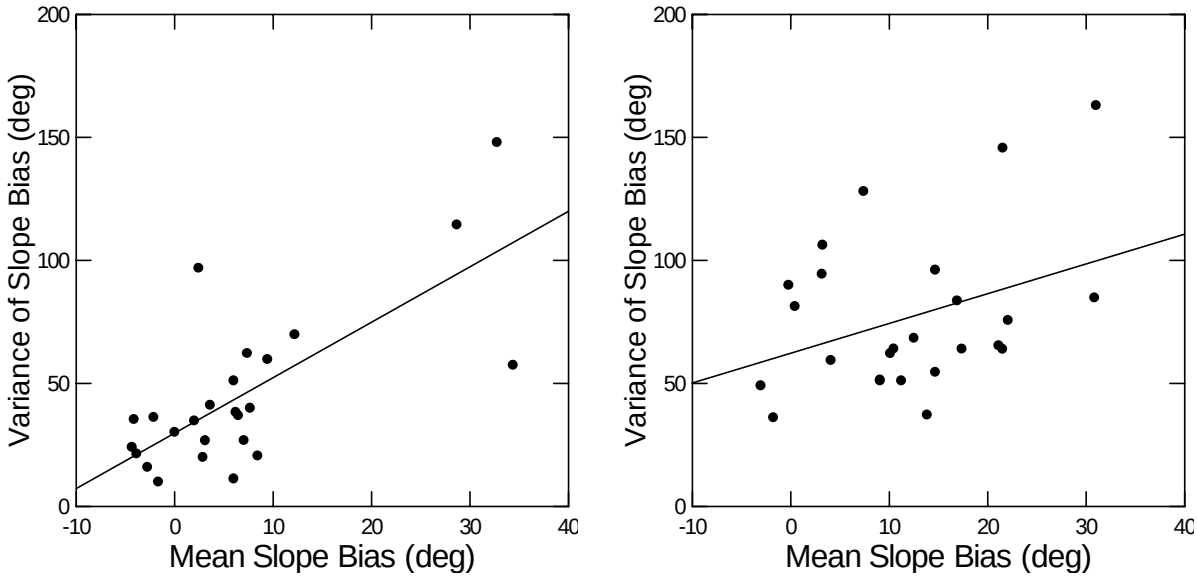

Figure 4.45 Mean and variance of slope biases of each subject for lunar hills (left) and craters (right)

Table 4.50 Difference of mean slope biases and variances between lunar hill and crater estimates

Subject	N (MVS)	N (LVS)	Difference of Mean Slope Biases (deg)	Difference of Variance of Slope Biases (deg)
803	30	18	5.03	12.77
804	29	17	-3.36	105.51
805	30	18	0.63	30.84
806	30	18	9.23	43.66
807	30	18	15.59	38.71
808	30	18	-1.89	-63.11
809	30	18	13.75	3.13
810	30	12	5.17	-5.78
811	30	18	7.51	70.34
812	29	17	2.09	71.28
813	30	18	5.24	-5.17
814	30	18	0.99	20.19
815	30	17	1.20	39.39
817	30	18	3.65	68.51
819	30	18	1.08	13.70
820	30	18	1.23	71.41
821	30	18	12.51	38.20
822	30	18	3.06	-0.02
823	30	18	12.24	-0.75
824	30	18	7.84	25.95
825	30	18	9.53	91.81
827	30	18	3.08	35.31
828	30	18	7.35	37.30
829	24	12	17.93	104.49
830	30	18	-7.16	-50.53

Table 4.50 indicates that 22/25 subjects (shown in blue) possess a greater mean slope bias for the lunar craters. A one-sample t-test with a Bonferroni Adjustment found the mean biases between the slope types *significantly* different with a larger crater bias on average of 5.3 degrees ($p < 0.001$). This result was confirmed by post-experiment feedback, where 60% of subjects responded that craters overall appeared steeper than hills, while only 16% of subjects believed hills appeared steeper than craters. Subjects perceiving craters as steeper commented that they possessed more texture, lacked a horizon for making comparisons, and possessed more rocks with greater indications of rock slide. Other subjects who agreed that craters appeared steeper imagined going into the crater and looking up or felt it would be more difficult to climb out. Numerous subjects agreed the lighting and shadows made the crater slope more pronounced. Subjects who agreed that hills appeared steeper commented that hills were exposed to light and looking up at them made them appear steeper. A one-sample t-test with a Bonferroni Adjustment also shows a *significant* difference between the within-subject variances of the crater and hill slope biases, with the lunar craters causing greater variance ($p < 0.01$). This result implies that the precision of slope estimates of craters would be more deteriorated than hills. The consensus of the feedback and the t-test results together support the hypothesis that both systematic and random slope estimation errors are greater for craters than for hills in a lunar environment.

4.5 Devon Island Field Study Results

The Devon Island Field Study (DFS) successfully provided additionally slope and distance estimate data to test the hypothesis in Chapter 1. Due to deteriorating weather conditions throughout the duration of the experiment, only two subjects were tested using two hills. The limited amount of total data points (32) prevented the use of a mixed hierarchical regression to model the effects of the study; however, t-tests and correlation coefficients were used to make inferences on the observed trends. The slope estimation errors (estimated slope – true slope) for each subject using visual and haptic measures for each hill are shown in Figure 4.46 and Figure 4.47. Contrary to our hypothesis, both subjects seemed to provide both slope overestimations and underestimations. Subject #1 provided constant visual and haptic overestimations at all distances for the 20.0^o slope, but constant visual and haptic underestimations at all distances for the 39.6^o slope. His feedback, though, indicated his estimation method consisted of "eyeballing" the slope. The feedback also stated the temperature was 0^o Celsius with 25 mph winds, causing the subject to move quickly through his estimates. Subject #2 provided haptic overestimations at the nearest two distances (25 and 50 m) for both hills, though also provided consistent visual underestimations for both hills. Individual paired t-tests with a Bonferroni Adjustment compared the slope estimates between the 39.6^o and 20.0^o hills for each subject/body position condition, shown in Table 4.51, and found only Subject #2's

estimates between the two hills to be significantly different ($p < 0.05$). Appendix D.3 reveals that the slope of the sides of the two hills seem surprisingly similar, explaining how the "eyeball" method used by Subject #1 may have caused such similar estimates. Post-experiment feedback from Subject #2 indicated an extensive use of other visual cues such as the rock debris along the front and base of the hill, knowledge of the angle of repose, and knowledge of other slopes in addition to using the slope of the sides of the hill to influence his estimates. This result leads us to believe that the sides of a hill can be misleading in informing a subject of the slope "head-on" and should be further investigated in future studies within both field and VR environments.

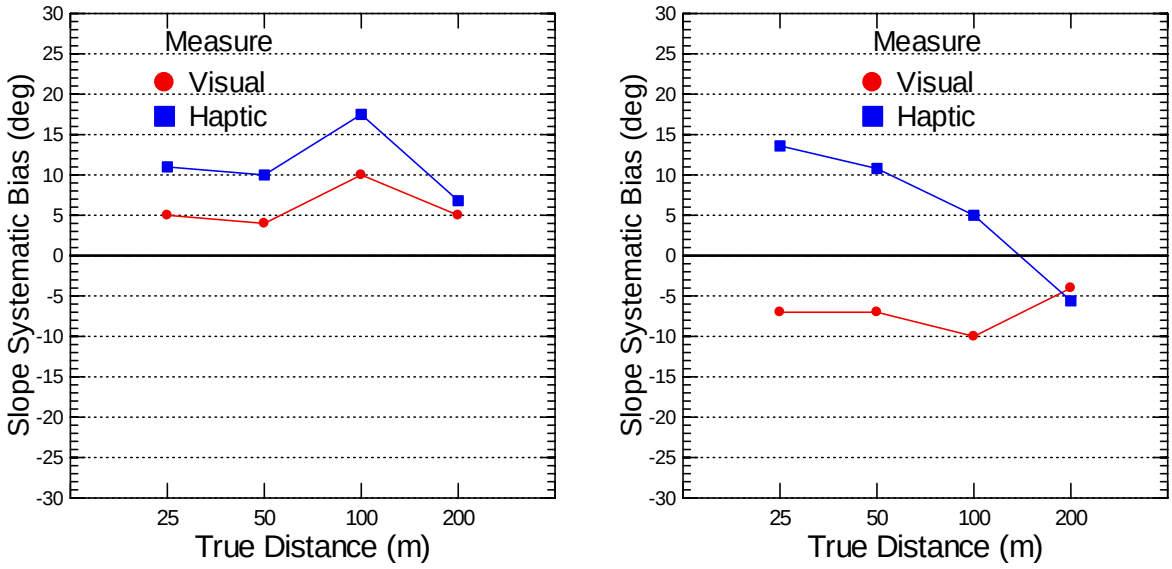

Figure 4.46 Slope errors of the 20.0° hill for Subjects #1 (left) and #2 (right) in DFS

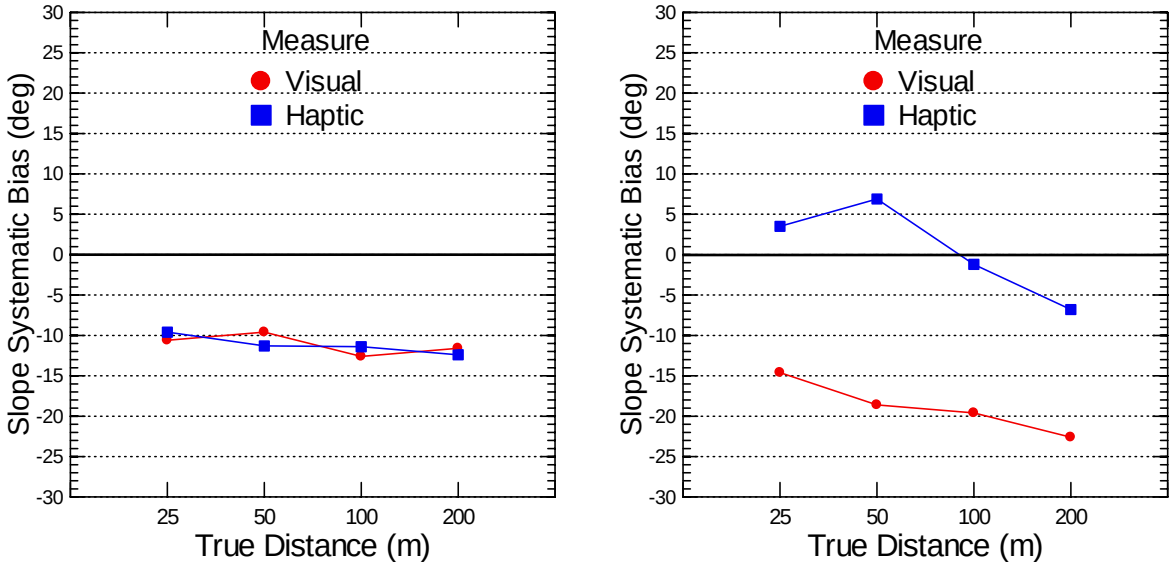

Figure 4.47 Slope errors of the 39.6° hill for Subjects #1 (left) and #2 (right) in DFS

Table 4.51 Paired t-tests between 39.6° and 20.0° hill estimates for each subject in DFS

Subject	Measure	N	Mean of Differences (deg)	t Statistic	p-value
1	Visual	4	2.50	1.291	0.287
	Haptic	4	-2.90	-1.332	0.275
2	Visual	4	7.75	3.238	**0.048**
	Haptic	4	14.25	7.562	**0.005**

Slope estimates were collected at four distances between 25 and 200 meters for each method and each hill. Figure 4.46 and Figure 4.47 indicate that Subject #1 did not show any consistent trend between different distances, which was confirmed by his post-experiment feedback stating neither close nor far away hills seemed steeper and it was "simply difficult" to estimate slopes head-on. However, Subject #2 showed a decreasing systematic bias for his haptic estimates on the 20° hill and for both his visual and haptic estimates on the 39.6° hill. This subject also indicated during post-experiment feedback that close hills often appear steeper "with better resolution/details of what sticks to them and what rolls down." Correlation coefficients were also determined for each subject/measure/hill condition, shown in Table 4.52, and 6/8 conditions possessed negative correlations, four of which were between -0.8 and -1.0. Least Squares regressions were determined for each condition and Subject #2's haptic measure of the 20° hill had a significant regression slope of -0.11 ($p < 0.001$), stating that their slope estimate decreased on average by 1.1 degrees for every additional 10 meter distance between them and the base of the hill. All other non-significant regressions had a smaller (more positive) slope. The subject feedback, correlation results, and regressions together support the hypothesis that slope estimates are greater as the distance to the base of the hill decreases and future studies with more subjects should attempt to determine the regression slopes for each subject.

Table 4.52 Correlation and regression results of estimated slope and true distance for each subject in DFS

Subject	Measure	Hill	Slope (deg)	Correlation	Regression Slope	p-value
1	Visual	1	20.0	0.119	0.004	0.881
		2	39.6	-0.542	-0.009	0.458
	Haptic	1	20.0	-0.347	-0.020	0.653
		2	39.6	**-0.869**	-0.013	0.131
2	Visual	1	20.0	0.528	0.017	0.472
		2	39.6	**-0.921**	-0.039	0.079
	Haptic	1	20.0	**-1.000**	**-0.110**	**0.000**
		2	39.6	**-0.922**	-0.071	0.078

Slope estimates were also collected using visual and haptic measurement devices. Figure 4.46 shows that both subjects made greater slope estimates using the haptic device on the 20° hill and Figure 4.47 shows

that Subject #2 made greater slope estimates using the haptic device on the 39.6° hill. Paired t-tests using a Bonferroni Adjustment, shown in Table 4.53, compared the visual and haptic estimates for each subject and hill and found that 3/4 combinations possessed a greater haptic slope on average, two of which were significant ($p < 0.05$). These results are contrary to both Proffitt et. al's conclusions that visual estimates were significantly greater than haptic estimates [60] and the results we obtained from the MFS that confirmed this conclusion. We suspect that due to the harsh weather conditions, the subjects in this experiment may not have observed the full range of visual flashcards and were quick to choose a card. This explanation does not fully explain why visual underestimations of slope were consistent; however, future testing in the Devon Island environment with more subjects during the upcoming years can help explain these abnormal results.

Table 4.53 Paired t-tests between visual and haptic slope estimates for each subject in DFS

Subject	Hill	Slope (deg)	N	Mean of Differences (deg)	t Statistic	p-value
1	1	20.0	4	-5.33	-4.340	**0.023**
	2	39.6	4	0.08	0.107	0.922
2	1	20.0	4	-12.95	-2.599	0.080
	2	39.6	4	-19.45	-9.268	**0.003**

Distance estimation errors (estimated distance – true distance) for each subject using visual and haptic measures for each hill are shown below in Figure 4.48.

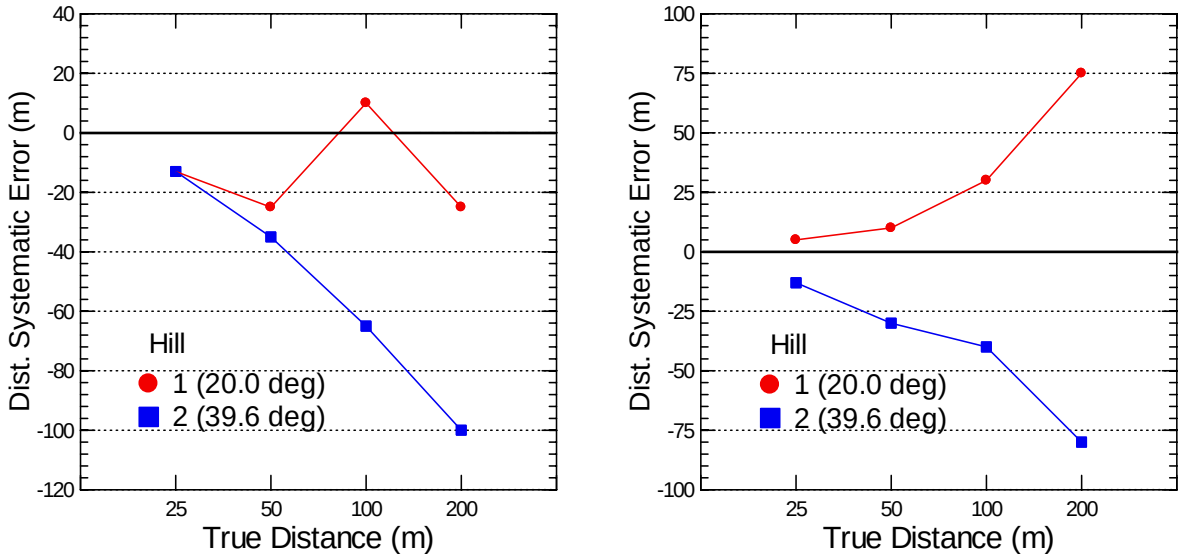

Figure 4.48 Distance errors of each hill for subjects #1 (left) and #2 (right) in DFS

Figure 4.48 indicates that distance was underestimated by Subject #1 for both hills and all true distances, with exception to the 100 meter distance for the 20° hill. Interestingly, Subject #1's distance estimates for the 39.6° slope were less than half the true distance in all cases. The distance method he indicated in the post-experiment feedback was a comparison to the calibration distances. Since the largest calibration distance was 110 meters (length of a football field, including end zones), it seems likely this subject was able to mentally compress the 200 m distance into this reference without the presence of familiar cues. This subject did, however, estimate the 200 m distance of the 20° hill to be 175 meters; however, this hill had a smaller height, which likely made it seem further away than the 110 meter reference. These results expose the vulnerability humans can make by wrongly assuming a distance reference frame between them and a hill without knowledge of the actual height of the hill.

Figure 4.48 indicates that Subject #2 both overestimated and underestimated distance, depending on the hill. He overestimated the 20° hill by 20 – 40% at each distance and underestimated the 39.6° hill by 40 – 60% at each distance. His post-experiment feedback indicated he used rocks of familiar size between him and base of the hill, previous knowledge of distances, and perspective to determine his estimates. A potential explanation for the difference in errors between the two hills includes either misinterpreting the height of the hills or the size of the rocks between him and the base. His results confirm our hypothesis that both underestimations and overestimations are likely to occur in a reduced cue environment and the distance estimates will be more variable without familiar objects of known size.

Figure 4.48 also shows that for 3/4 subject and hill combinations, the distance estimates at all four true distance locations were either all overestimations or all underestimations. Furthermore, Table 5.54 shows that that the correlation coefficient for these three combinations was either between -0.9 and -1.0 (underestimations) or 0.9 and 1.0 (overestimations). This result suggest that when a subject established a reference frame for any particular hill, regardless of its accuracy, this reference frame was continuously used for estimates at all true distance locations. Therefore, it is critical that astronauts can develop an accurate reference frame of their landing site and areas for lunar excursions with knowledge of the true heights of the surrounding landmarks using a VR training tool to avoid making repeated distance errors.

Table 5.54 Correlation coefficients between estimated distance and true distance for each subject in DFS

Subject	Hill	Slope (deg)	N	Correlation
1	1	20.0	4	-0.158
	2	39.6	4	**-0.982**
2	1	20.0	4	**0.996**
	2	39.6	4	**-0.991**

The Devon Island Field Study did not analyze the effects of sun elevation and the appearance of shadows on slope and distance estimates. Subject #2 did not identify the presence of any shadows from the overcast weather conditions; however, he believed that their presence may have made the slopes appear steeper, supporting Hypothesis #1. The lunar-like environment of Devon Island and low sun elevation during the summer months make it an ideal location for future field studies that analyze the effect of sun elevation. Many thanks are due to Dr. Marcelo Vasquez for making the DFS a success and Subject #1 stated “Marcelo did a great job of administering the experiment under adverse conditions.”

CHAPTER 5

CONCLUSIONS AND RECOMMENDATIONS

This study tested the hypotheses stated in Chapter 1, providing a foundation of knowledge on the perception of slope, distance, and height under lunar conditions. It also presents areas of future research that will increase our understanding of perception in a lunar environment while proposing tools that will aid astronauts prior to and during lunar missions. This chapter will provide a summary of the critical results obtained in this study and recommendations for future research. Section 5.1 summarizes the unique properties of the lunar environment that may pose difficulties and potential safety risks for astronauts. Section 5.2 summarizes the important results of this study, including the factors affecting slope, distance, and height estimates, the most common and accurate estimation methods used, and the systematic and random errors across all experiments. Section 5.3 presents rationale and support for developing a VR Training Tool that will provide astronauts with prior knowledge of the terrain characteristics near their landing sites/lunar bases and calibrate their slope, distance, and height estimates. Section 5.4 proposes the integration of human perception with lunar navigational instruments that will warn astronauts when environmental factors exist that may distort one's perception. Section 5.5 concludes by providing recommendations for future research.

5.1 The Challenging Lunar Environment

The lunar environment presents unique and unfamiliar conditions that caused difficulties for the Apollo astronauts and pose risks to both safety and efficiency during future lunar excursions. Without an atmosphere, the lack of aerial perspective (haze) eliminates a common cue that makes distant objects appear fainter and further away. Apollo 14 Astronaut Al Shepard remarked: "It's crystal clear up there – there's no closeness that you try to associate with it in Earth terms – it just looks a lot closer than it is" [44]. The non-Lambertian reflectance properties of the lunar regolith preferentially reflect light directly back to its source, known as backscatter. Backscatter causes a spike of brightness intensity when viewing terrain directly away from the sun's azimuth, washing out surface texture and causing Apollo 16 Astronaut John Young to temporarily lose visibility of the craters lying before him [44]. The lack of an atmosphere also prevents the scattering of light, allowing the formation of deep shadows, especially at low sun elevations that distorted Apollo 12 Astronaut Al Bean's slope perception, causing him to overestimate the 11 degree side of the Surveyor Crater by almost 30 degrees when partially concealed by

a shadow [44]. The lack of familiar, recognizable objects on the lunar surface inhibits one's ability to use the relationship between size and distance of an object to scale one's reference frame correctly. Apollo 12 Astronaut Pete Conrad mistakenly judged a 500 m diameter crater that was 4500 m from his position as only 35 m in diameter and 300 m away [44]. Future errors such as this could cause astronauts to become spatially disorientated (i.e. lost) and make flawed and even life-threatening decisions. Finally, the reduced gravity of the lunar environment may also distort visual perception by inhibiting one's ability to judge the down vector, the depth of objects, or even the use of size-constancy. These challenges necessitate an understanding of visual perception in a lunar environment, methods that may be employed to make accurate judgments, and development of training protocols and instruments that will help overcome future navigational difficulties.

5.2 Summary of Important Results

The present study analyzed the effects of true slope, true distance, sun elevation, and body position on slope, distance, and height estimates in lunar-like and lunar environments. The systematic and random errors of each type of estimate were calculated and the most common estimation methods were determined and used to explain these errors. This section summarizes the most important results found.

5.2.1 Effects, Methods, and Errors of Slope Estimation

The effects of true slope, true distance to the base of the hills, sun elevation, and body position were analyzed in the Lunar-like Field Study (MFS), Lunar-like VR Study (MVS), and the Lunar VR Study (LVS). All three experiments found a significant effect of the hills used as stimuli and indicate that slopes were overestimated, and these overestimates increased with the true slope of the hill. Mixed regressions found slope estimates were significantly greater at closer distances to the base of the hills in the LVS and MVS. Post-experiment feedback indicated that 60% of MVS subjects and 64% of LVS subjects confirmed this conclusion, commenting that closer distances offered more visual cues, occupied a greater Field-of-View (FOV), and seemed taller, impressive, and intimidating. Twenty-five percent of MVS subjects and 12% of LVS subjects opposed this conclusion commenting that far away hills appeared like walls. Slope estimates were also significantly greater at a lower sun elevation in the MVS using mixed regressions and confirmed using individual paired t-tests and subject feedback, where 35% and 25% of subjects reported using texture and shadows, respectively, to judge slope. Slope estimates were significantly greater from the supine, lunar G_z, body position in both the MVS and LVS. Surprisingly, the majority of subjects in both studies reported no noticeable effect of body position, though comments

supporting an effect agreed that slopes appeared steeper or one's physical potential was less from the supine position. These results support Hypothesis #1, and suggest potential interactions between both distance and texture on slope estimates (closer distance makes texture more visible), as well as sun elevation and texture (lower sun elevations increase the contrast of texture). The MFS failed to find significant effects of distance and sun elevation on slope estimates, though this was likely caused by the psychological effect of viewing the same hills under different conditions with knowledge that the hill slope is constant. The interpolation of the side of the hills was the most commonly reported slope estimation method in both the MVS and LVS (80% of subjects in each). This method was likely the cause of Subject #1's gross slope *underestimations* in the Lunar-like Field Study #2 (DFS) of a 39.6^{o} hill. Future research should investigate the accuracy of this method. Table 5.1 shows the estimated slope systematic errors (mean bias) and random errors (standard deviation) for the MFS, MVS, and LVS experiments.

Table 5.1 Overall estimated slope systematic and random errors for each experiment

Experiment	Mean Bias (deg)	Stand. Dev (deg)	Stand. Err (deg)
Lunar-like Field Study (MFS)	13.0 **to** 22.9	8.3 **to** 12.8	1.2 **to** 1.9
Lunar-like VR Study (MVS)	4.9 **to** 15.7	7.7 **to** 17.3	1.2 **to** 2.8
Lunar VR Stuyd (LVS)	2.7 **to** 14.0	8.7 **to** 15.2	1.4 **to** 3.2

The systematic bias found in the MFS is consistent with Proffitt's prior research [60]. The standard deviations in Table 5.1 illustrate the large between-subject differences in estimates and support the need for training and calibration of slope estimation methods for astronauts prior to lunar missions.

5.2.2 Effects, Methods, and Errors of Distance Estimation

The effects of hill shape, true distance, sun elevation, and body position on distance estimates to the base of the hills were analyzed in the MVS and LVS experiments. Mixed regressions showed that the estimates between the hills were significantly different ($p < 0.05$) in both studies due to numerous cues, including the hill height and the presence of familiar objects. The shortest hills in both studies received significantly greater distance estimates than all other hills ($p < 0.01$), suggesting that subjects used the size-distance relationship and misinterpreted the smaller FOV subtended by these hills when compared to other hills. The true distance also possessed a significant effect on the distance estimates in both the MVS and LVS ($p < 0.001$). The visual angle subtended by the MVS hills from 25 meters was over 9

degrees greater than the angle subtended at 75 meters. The increased visual angle and the presence of surrounding objects were likely causes of this effect. Distance estimates at low sun elevations (10^o) were significantly greater ($p < 0.001$) than at higher elevations (33^o) in the MVS and likely caused by the greater textural contrast of the ground plane and hills. Sun elevation could not be analyzed in the LVS due to its collinearity with the distance variable (The limited number of Apollo images used were either from a near distance with a low sun elevation or a far distance with high sun elevation). The supine, lunar G_z, body position caused significantly greater distance estimates in the MVS ($p < 0.01$), potentially due to a subject's decreased physical potential, but not in the LVS (hills: $p = 0.931$, craters: $p = 0.360$), where vast distances may have minimized this effect. These results support Hypothesis #2. The most common distance estimation methods in both studies were the use of surrounding objects (MVS: 55% of subjects, LVS: 68% of subjects), followed by the standard reference presented at the start of the experiments (MVS: 50% of subjects, LVS: 28% of subjects). Table 5.2 shows the estimated distance systematic errors (mean bias) and random errors (standard deviation) for the hills in the MFS and LVS experiments.

Table 5.2 Overall estimated distance systematic and random errors for each experiment

Experiment	Mean Bias (m)	Mean Bias (%)	Stand. Dev (m)	Stand. Dev (%)
Lunar-like VR Study (MVS)	(-16.3) **to** 21.1	(-21.8) **to** 84.6	14.0 **to** 21.3	22.7 **to** 79.5
Lunar VR Study (LVS)	(-4512) **to** 4696	(-33.2) **to** 117.4	2372 **to** 5217	24.7 **to** 103.5

Although the mean bias and standard deviations increase greatly between the near distances of the MVS (25 – 75 meters) and the far distances of the LVS (4000 – 13900 meters), these errors appear quite similar as a percent of the actual distance. Future studies should seek to determine whether these percentages remain consistent between these two ranges in both field and VR environments.

5.2.3 Effects, Methods, and Errors of Height Estimation

The effects of hill, true distance, and body position on height estimates were analyzed for the LVS. A mixed regression found a significant effect between hills, with coefficients that indicate the height estimates increased with true height ($p < 0.001$). No significant effect of distances for each hill was observed ($p = 0.191$), despite the increased visual angle subtended by the hills at closer distances. The supine, lunar G_z, body position did not significantly affect height estimates ($p = 0.625$), though the vast distances may have again minimized this effect. The most commonly used height estimation methods included the influence of the standard reference (40% of subjects), the use of surrounding objects (32% of subjects), and the influence from their distance estimates (28% of subjects). The systematic errors of the height estimates ranged from -568 meters to 688 meters (-27.2% to 249.3%) with random errors (standard

deviations) ranging between 548 – 844 meters. The heights of the three shortest hills were significantly overestimated at all distances ($p < 0.01$), though these hills all had true heights below the standard reference, which likely influenced the overestimations. The random errors were also greater than the systematic errors, indicating the need for a training tool that can calibrate estimates.

5.2.4 Contrasting Slope Perception Between Lunar Hills and Craters

A personal interview with Apollo 16 Astronaut Charles Duke motivated Hypothesis #5 that lunar craters appeared steeper than lunar hills. The difference between the overall mean systematic bias for lunar hills and for lunar craters was calculated for each subject and compared to zero using a one-sample t-test. In all cases, the estimates were made of an "up-slope," either of the hill or of the far side of the crater. The estimated slope bias of lunar craters was found to be significantly greater than lunar hills by 5.3 degrees on average ($p < 0.001$). Post-experiment feedback confirmed this result with 60% of subjects indicating that craters appeared steeper because they possessed greater texture, lacked a horizon for comparison, and possessed more indications of rock slide. This error is suspected to be even greater in lunar gravity, with the uncertainty of the down vector and the greater safety risk of being trapped within a crater.

5.3 Development of a VR Training Tool

Apollo astronauts have consistently agreed upon the difficulty of making accurate size, distance, and slope estimates on the lunar surface. After misjudging the distance to a boulder, Apollo 11 Astronauts Armstrong and Aldrin commented on size and distance estimation, insisting "these skills may require refinement in the lunar environment" [44]. The perceptual challenges of the lunar environment has not changed since Astronaut Cernan left the Moon in 1972 and will likely hinder navigation for the future astronauts who walk upon the lunar surface. Following Apollo 14, Astronaut Al Shepard stated: "Until we really get a feel for navigation on the surface, there should be some strong [that is, well-defined] checkpoints to follow" [44]. Checkpoints can only become "well-defined" when the astronaut knows what to expect and has seen the checkpoint before leaving Earth. The current VR technology provides a capable platform to train and calibrate astronauts for future lunar missions. The development of a VR training tool would be an invaluable asset to ensure the safety and efficiency of lunar missions.

A VR training tool for lunar missions would serve several important purposes, including the familiarization of landmarks and terrain surrounding the landing sites, lunar bases, and excursions areas, as well as the calibration of slope, distance, and size estimation techniques. A VR training tool would first provide astronauts with the appearance of hills, craters, and navigational landmarks from the surface

perspective and knowledge of their size and heights. Results from the present study indicate a 0.590 correlation between distance and height errors, suggesting that with knowledge of the heights of surrounding terrain features, astronauts can use the size-distance relationship and the visual angle subtended by a feature to deduce the distance. The clarity of distant objects and lack of salient surface texture provide unreliable distance cues, thus making the proper use of the size-distance relationship more important. Previous knowledge and appearance of terrain slopes will allow astronauts to make more prudent decisions, potentially saving time and energy during lunar excursions. A VR training tool would also allow astronauts to practice slope, distance, and size estimation to avoid the large systematic and random errors found in Tables 5.1 and 5.2. Calibration would increase confidence in navigational instruments and may be necessary for emergencies if these instruments are not available or not operable. By exposing astronauts to the types of estimation error they should anticipate, one should reduce the negative consequences of these estimates when they occur on the surface of the Moon.

This study also shows that a VR training environment using realistic images of terrain can produce consistent estimation errors as the actual field environment. Two-sample t-tests comparing the mean slope biases of the lunar-like field and VR environments showed a non-significant difference for all hill/distance/sun elevation combinations of conditions, except for the steepest hill, at the lowest sun elevation and closest distance. Figures 4.17 and 4.18 illustrate the differences between the two studies and suggest that slope estimates may be slightly larger in a field environment from the unlimited resolution, the affordance one experiences of being actually present, and any fatiguing effects of the spacesuits. Although this study used photographic images, high-resolution LIDAR and RADAR data of future landing sites and realistic sun-models of the lunar environment are becoming available and would be necessary to develop the terrain and atmospheric conditions in a realistic VR training tool. Future research toward the development of this tool should investigate the capabilities of this data.

5.4 Integration of Human Perception with Navigational Instruments

Even with training of visual slope, distance, and size perception prior to lunar missions, astronauts will encounter unfamiliar terrain with unknown sizes and slopes and can make false judgments or become disoriented under certain environmental conditions. Apollo 12 Astronaut Al Bean overestimated the slope of the Surveyor Crater by almost 30 degrees because of a shadow causing the slope to appear much steeper than under normal lighting conditions [44]. Integrating navigational instruments with a mathematical model that predicts estimation errors from the factors distorting human perception can increase awareness when illusions may exist. This can be accomplished using feedback in a Heads-Up-

Display (HUD) that informs an astronaut when they shouldn't trust their perception and only their instruments. The proposed model design includes sun elevation, distance to the target terrain, sun azimuth, presence of shadows, textural contrast, surface slipperiness, and other factors as input variables and computes the estimated slope errors and estimate distance errors. If these errors breach specific thresholds, salient warnings should be displayed to the astronaut, warning him/her of the potential illusions. The MVS has identified that both distance and sun elevation have significant effects on slope and distance estimates, though only two conditions for each variable were tested. Future experiments should seek to identify the interaction these variables have with shadows, texture, height, and surface slipperiness and the regression coefficients for each of these continuous variables. Besides feedback of the likelihood of perceptual errors, the HUD would be an advantageous location for rangefinding data of both distances and slopes. The use of inclinometers for measuring slopes may be ineffective if an astronaut is at a distance from the base of the sloped terrain; therefore, the slope measurement method using the laser rangefinder output and the Laws of Sines and Cosines in Section 3.4.1.1 of this report should be considered for future HUD designs. The availability of actual slope and distance information, as well as perceptual error warnings would ultimately provide future lunar astronauts with confidence in their instruments and their decisions.

5.5 Future Research

Many new areas of future research to further understanding of visual perception in the lunar environment still exist. The MVS and the LVS should also be conducted again, though with the height given for each hill to determine if the subject's slope or distance systematic and random errors would significantly change. Slope and distance estimation training methods should be investigated and tested to determine how trained subjects and untrained subjects perform on new and unfamiliar hills. The effects of hill shadows, textural contrast, and surface slipperiness should be investigated in realistic lunar-like field environments, such as Devon Island, or in locations with large sand dunes. Interpolation of the side of the hills to judge the slope head-on was the most frequently used method in all the current studies; therefore, future studies should determine the effect of hill shape. The effect of lunar gravity on slope and distance estimates should be further investigated in parabolic flight. Development of a VR training tool for lunar missions should begin with investigating the use of available LIDAR data and sun models in constructing a 3-D VR terrain model. Integrating human perception and navigational instruments should begin with determining what other factors may significantly affect slope and distance estimates and form continuous variable mixed regressions modeling the errors created by these factors. Apollo astronauts have

consistently expressed the difficulties with visual perception in the lunar environment; **NOW** is the time to face these challenges and develop innovative designs that ensure the safety of future astronauts.

REFERENCES

[1] "Apollo Lunar Surface Journal." E.M. Jones, K. Glover (Eds.), 25 Nov. 2008 <http://history.nasa.gov/alsj/>.

[2] Baird, J.C. (1970). Psychophysical analysis of visual space. New York: Pergamon.

[3] Baird, J.C. & Biersdorf, W.R. (1967). Quantitative functions for size and distance judgments. *Perception & Psychophysics*, 2, 161 – 166.

[4] Beall, A.C. & Loomis, J.M. (1995). Absolute motion parallax weakly determines visual scale in real and virtual environments. *Proceedings of SPIE, 2411,* 288 – 297.

[5] Bee, L. (1991). Effect of Magnification on Distance Estimation. Army Personnel Research Establishment, Ministry of Defense: Farnborough Hampshire.

[6] Berkeley, G. (1709). *An Essay Towards a New Theory of Vision*. In A. A. Luce and T. E. Jessop (ed.), *The works of George Berkeley bishop of Cloyne*, Vol. 1, pp. 143 – 239. London: T. Nelson and Sons, 1948. In H. Ross (Ed.), *The Mystery of the Moon Illusion* (pp. 154 - 155). Oxford, UK: Oxford University Press.

[7] Bhalla, M. & Proffitt, D.R. (1999). Visual – Motor Recalibration in Geographical Slant Perception, *Journal of Experimental Psychology: Human Perception and Performance*, 25(4), 1076 – 1096.

[8] Bingham, G.P., Bradley, A., Bailey, M., & Vinner, R. (2001). Accommodation, occlusion, and disparity matching are used to guide reaching: A comparison of actual versus virtual environments. *Journal of Experimental Psychology: Human Perception and Performance*, 24, 145 – 168.

[9] Bingham, G.P., Pangano, C.C. (1998). The necessity of a perception-action approach to definite distance perception: Monocular distance perception to guide reaching. *Journal of Experimental Psychology: Human Perception and Performance,* 24, 145 – 168.

[10] Braunstein, M.L. (1968). Motion and texture as sources of slant information. *Journal of Experimental Psychology*, 78, 247 – 253.

[11] Bruce, Vicki, and Patrick R. Green. Visual Perception: Physiology, Psychology and Ecology. 2nd Ed. London: Lawrence Erlbaum Associates Ltd., 1990.

[12] Buratti, B.J., Gibson, J., & Mosher, J. (1992). CCD observations of the uranian satellites. *Astronomical Journal*, 104, 1618 – 1622.

[13] Buratti, B.J., Hillier, J.K., & Wang, M. (1996). The lunar opposition surge: observations by Clementine. *Icarus*, 124, 490 – 499.

[14] Carlson, V.R. (1977). Instructions and perceptual constancy judgments. In W. Epstein (Ed.), Stability and constancy in visual perception: Mechanisms and processes. New York: Wiley.

[15] Carr, C.E., Newman D.J., & Hodges K.V. (2003) Geologic Traverse Planning for Planetary EVA. *SAE International, 33rd International Conference on Environmental Systems (ICES).*

[16] Carter, D. S. (1977). The Moon Illusion: A Test of the Vestibular Hypothesis under Monocular Viewing Conditions. *Perceptual and Motor Skills*, 45, 1127 – 1130.

[17] Clark, W.C., Smith, A.H., & Rabe, A. (1956). Retinal gradients of outline distortion and binocular disparity as stimuli for slant. *Canadian Journal of Psychology*, 10, 77 – 81.

[18] Clement, G. & Eckardt, J. (2005). Influence of the gravitational vertical on geometric visual illusions, *Acta Astronautica*, 56, 911 – 917.

[19] Clement, G., Lathan C., & Lockerd, A. (2008). Perception of depth in microgravity during parabolic flight. *Acta Astronautica*, 63, 828 – 832.

[20] Collins, J.R. (1976). Distance perception as a function of age. *Australian Journal of Psychology*, 28, 109 – 113.

[21] Coren, S. (1992). The Moon Illusion: A Different View through the Legs. *Perceptual and Motor Skills*, 75, 827-31. In H. Ross (Ed.), *The Mystery of the Moon Illusion* (p. 172). Oxford, UK: Oxford University Press.

[22] Creem, S.H., & Proffitt, D.R. (1998). Two memories for geographical slant: Separation and interdependence of action and awareness. *Psychonomic Bulletin & Review*, 5, 22 – 36.

[23] Da Silva, J.A., (1985). Scales for Perceived Egocentric Distance in a Large Open Field: Comparison of Three Psychophysical Methods. *The American Journal of Psychology*, 98(1), 119 – 144.

[24] Da Silva, J.A., & Rozestraten, R.J.A. (1979). Construcao de uma escala subjetiva de distancia pelo metodo de fracionamento. *Psicologia*, 5, 45 – 58.

[25] Daum, S.O. & Hecht, H. (2007). Distance Estimation in Vista Space, submitted to *Perception and Psychophysics*.

[26] De Weck, O. & Simchi-Levi, D. (2006). Haughton-Mars Project Expedition 2005: Interplanetary Supple Chain Management & Logistics Architectures. *Massachusetts Institute of Technology*

[27] Duke, Charles. Personal interview, 14 May 2008.

[28] Durgin, F.H., Fox, L.F., Lewis, J., & Walley, K. (2002, November). *Perceptuomotor adaptation: More than meets the eye*. Paper presented at the annual meeting of the Psychonomic Society, Kansas City, MO.

[29] Epstein, W. (1981). The relationship between texture gradient and perceived slant-in-depth: Direct or mediated? *Perception*, 10, 695 – 702.

[30] Eriksson, E.S. (1964). Monocular slant perception and the texture gradient concept. *Scandinavian Journal of Psychology*, 5, 123 – 128.

[31] "Exploration: NASA's Plans to Explore the Moon, Mars, and Beyond." nasa.gov. 25 Nov. 2008. <http://www.nasa.gov/directorates/esmd/home/whyweexplore/why_we_explore_main.html>

[32] Fine, B.J. & Kobrick, J.L. (1983). Individual differences in distance estimation: comparison of judgments in the field with those from projected slides of the same scenes. *Perceptual and Motor Skills*, 57, 3 – 14.

[33] Flock, H.R. (1964). Some conditions sufficient for accurate monocular perception of moving surface slants. *Journal of Experimental Psychology*, 67, 560 – 572.

[34] Flock, H.R., Graves, D., Tennet, J., & Stepehenson, B. (1967). Slant judgments of single rectangles at a slant. *Psychonomic Science*, 7, 57 – 58.

[35] Freeman, R.B. (1966). The effect of size on visual slant. *Journal of Experimental Psychology*, 71, 96 – 103.

[36] Friederici, A. & Levelt, W.J.M. (1990). Spatial reference in weightlessness: perceptual factors and mental representation, *Perception Psychophysics*, 47, 253 – 266.

[37] Fry, G.A., Bridgman, C.S., & Ellebrock, V.J. (1949). The effects of atmospheric scattering on binocular depth perception. *American Journal of Optometry & Archives of American Academy of Optometry*, 26, 9 – 15. In Ross, Helen E. Behaviour and Perception in Strange Environments. London: George Allen & Unwill Ltd., 1974.

[38] Foley, J.M. (1977). Effect of distance information and range on two indices of visually perceived distance. *Perception*, 6, 449 – 460.

[39] Gibson, E.J. & Bergman, R. (1954). The effect of training on absolute estimation of distance over the ground. *Journal of Experimental Psychology*, 48, 473 – 482.

[40] Gibson, J.J. (1950). The perception of visual surfaces. *American Journal of Psychology*, 63, 367 – 384.

[41] Gibson, J.J. (1979). The ecological approach to visual perception. Boston: Houghton Mifflin.

[42] Gibson, J.J. & Cornsweet, J. (1952). The perceived slant of visual surfaces – optical and geographical. *Journal of Experimental Psychology*, 44, 11 – 15.

[43] Gogel, W.C. (1961). Convergence as a cue to the perceived distance of objects in a binocular configuration. *Journal of Psychology*, 52, 303 – 315.

[44] Heiken, Grant and Eric Jones. On the Moon: the Apollo Journals. Chichester, UK: Praxis Publishing Ltd., 2007.

[45] Holway, A. H. and Boring E. G. (1940). The Moon Illusion and Angle of Regard. *The American Journal of Psychology*, 53 (1), 109 – 116.

[46] Horn, B. & Brooks, M.J. (1989). Shape from Shading. Boston: MIT Press.

[47] Kammann, R. (1967). The overestimation of vertical distance and slope and its role in the moon illusion. *Perception & Psychophysics*, 2, 585 – 589.

[48] King, W. L. and Gruber H. E. (1962) Moon Illusion and Emmert's Law. *Science*, 135 (3509), 1125 – 1126.

[49] Kinsella-Shaw, J.M., Shaw, B., & Turvey, M.T. (1992). Perceiving walk-on-able slopes. *Ecological Psychology*, 4, 223 – 239.

[50] Kline, P.B. & Witmer, B.G. (1996). Distance perception in virtual environments: Effects of field of view and surface texture at near distances. *Proceedings of the HFES 40th annual meeting*, Philadelphia, 112 – 116.

[51] Knapp, J.M. (1999). *The visual perception of egocentric distance in virtual environments*. Unpublished doctoral dissertation, University of California, Santa Barbara.

[52] Knapp, J.M. & Loomis, J.M. (2004). Limited field of view of head-mounted display is not the cause of distance underestimation in virtual environments. *Presence*, 13, 572 – 577.

[53] Kraft, A.L. & Winnick, W.A. (1967). The effect of pattern and texture gradient on slant and shape judgments. *Perception & Psychophysics*, 2, 141 – 147.

[54] "Lewis and Clark's Historic Trail." 25 Nov. 2008. <http://www.lewisclark.net/index.html/>

[55] Meili, R. (1960). Ueberlegungen zur Mondtauschung. *Psychologische Beitrage*, 5, 154-66. In H. Ross (Ed.), *The Mystery of the Moon Illusion* (p. 171). Oxford, UK: Oxford University Press

[56] Mingolla, E. & Todd, JT. (1986). Perception of solid shape from shading. *Biological Cybernetics*, 53, 137 – 151.

[57] Miskie, D., Dainoff, M., Sherman, R., & Johnston, L. (1975). Does distance perception change as the degree of enclosure changes? Some psychophysical studies under real and simulated conditions. *Man-Environment Systems*, 5, 317 – 320.

[58] Nefs, H.T., Koenderink, J.J., & Kappers, A.M.L. (2006). Shape-from-shading for matte and glossy objects. *Acta Psychologica* 121, 297 – 316.

[59] Ooi, T.L., Wu, B., & He, Z.J. (2001). Distance determined by the angular declination below the horizon. *Nature*, 414, 197 – 200.

[60] Proffitt, D. R. P., Bhalla, M., Gossweiler, R. & Midgett, J. (1995). Perceiving geographical slant. *Psychonomic Bulletin & Review*, 2, 409 – 428.

[61] Proffitt, D.R., Creem, S.H., & Zosh W.D. (2001). Seeing mountains in mole hills: Geographical-Slant Perception. *Psychonomic Science*, 5, 418 – 423.

[62] Proffitt, D.R., Stefanucci, J., Banton, T., & Epstein W. (2003). The role of effort in perceiving distance. *Psychological Science*, 14(2), 106 – 112.

[63] Purdy, J. & Gibson, E.J. (1955). Distance judgment by the method of fractionation. *Journal of Experimental Psychology*, 50, 374 – 380.

[64] Ramachandran, V.S. (1988). Perceiving shape from shading. *Scientific America*, 256(8), 76 – 83.

[65] Reynolds H.N. (1969). Visual perception beyond the atmosphere. *Aerospace Medicine*, 40 (6), 615-621.

[66] Robinett, W., & Rolland, J.P, (1992). A computational model for the stereoscopic optics of a head-mounted display. *Presence: Teleoperators and Virtual Environments*, 1, 45 – 62.

[67] Ross, Helen E. Behaviour and Perception in Strange Environments. London: George Allen & Unwill Ltd., 1974.

[68] Ross, Helen and Cornelis Plug. The Mystery of the Moon Illusion. Oxford, UK: Oxford University Press, 2002.

[69] Schmitt, Jack. Personal interview, 5 November 2007.

[70] Sedgwick, H.A. (1973). The visible horizon: A potential source of visual information for the perception of size and distance. *Dissertation Abstracts International*, 34, 1301B-1302B. (University Microfilms No. 73-22530).

[71] Seminara, J.L. & Kincaid, W.K. (1969). Control Task Performance in the Lunar Visual Environment. *Aerospace Medicine*, 40(4), 397 – 402.

[72] Smith, A.H. (1967). Perceived slant as a function of stimulus contour and vertical dimension. *Perceptual & Motor Skills*, 24, 167 – 173.

[73] Stefanucci, J.K., Proffitt, D.R., Banton, T., & Epstein, W. (2005). Distances appear different on hills. *Perception and Psychophysics*, 67, 1052 – 1060.

[74] Teghtsoonian, R. & Teghtsoonian, M. (1969). Scaling apparent distance in natural indoor settings. *Psychonomic Science*, 16, 281 – 283.

[75] Teghtsoonian, R. & Teghtsoonian, M. (1978). Range and regression effects in magnitude scaling. *Perception & Psychophysics*, 24, 305 – 314.

[76] Thompson, W.B., Willemsen, P., Gooch, A.A., Creem-Regehr, S.H., Loomis, J.M., & Beall, A.C. (2004). Does the quality of the computer graphics matter when judging distance in visually immersive environments? *Presence: Teleoperators and Virtual Environments*, 13, 560 – 571.

[77] Watt, S.J., Bradshaw, M.F., & Rushton, S.K. (2000). Field of view affects reaching, not grasping. *Experimental Brain Research*, 135, 411 – 416.

[78] Willemsen, P., Gooch, A.A., Thompson, W.B., Cream-Regehr, S.H. (2008). Effects of Stereo Viewing Conditions on Distance Perception in Virtual Environments. *Presence*, 17, 91 – 101.

[79] Willey, R., & Gyr. J.W. (1969). Motion parallax and projective similarity as factors in slant perception. *Journal of Experimental Psychology*, 79, 525 – 532.

[80] Witmer, B.G. & Kline, P.B. (1998). Judging perceived and traversed distance in virtual environments. *Presence: Teleoperators and Virtual Environments*, 7, 144 – 167.

[81] Witmer, B.G. & Sadowski, W.J., Jr. (1998). Nonvisually guided locomotion to a previously viewed target in real and virtual environments. *Human Factors*, 40, 478 – 488.

[82] Wu, B., Ooi, T.L., & Zijiang, J.H. (2004). Perceiving distance accurately by a directional process of integrating ground information, *Nature*, 428.

[83] Young, L.R. (2007). Proposal for Research on Astronaut Slope and Surface Estimation for Lunar Exploration, Submitted to National Biomedical Research Institute.

[84] Zinkus, P. W. and Mountjoy, P. T. (1969). The Effect of Head Position on Size Discrimination. *Psychonomic Science*, 14, 80. In H. Ross (Ed.), *The Mystery of the Moon Illusion* (pp. 174 - 175). Oxford, UK: Oxford University Press.

APPENDIX

A

SUBJECT CONSENT FORM

CONSENT TO PARTICIPATE IN
NON-BIOMEDICAL RESE 3bARCH

Lunar Slope Estimation

You are asked to participate in a research study conducted by Laurence R. Young, Sc.D., from the Department of Aeronautics and Astronautics and HST at the Massachusetts Institute of Technology (M.I.T.). You were selected as a possible participant in this study because NASA and the National Space Biomedical Research Institute are interested in understanding how well humans estimate slope and surface characteristics, in order to better plan lunar surface activities. You should read the information below, and ask questions about anything you do not understand, before deciding whether or not to participate.

- **PARTICIPATION AND WITHDRAWAL**

Your participation in this study is completely voluntary. If you choose to be in this study, you may subsequently withdraw from it at any time without penalty or consequences of any kind. If you choose not to participate, this decision will not affect your relationship with M.I.T. or your right to health care or other services to which you are otherwise entitled.

- **PURPOSE OF THE STUDY**

Slope estimation for mission planning and route implementation will be critical in the planning of astronaut excursions during lunar (and later Martian) exploration. Judging the slope, height, distance and surface characteristics of a distant hill or valley will be essential in determining, for example, whether a planned route is safe, efficient, and can be performed in an allotted time within the constraints of available oxygen and energy and return capabilities. The purpose of this study is to understand the types of errors that occur in the estimation of surface slope and other surface characteristics under different lighting and viewing conditions and with different measures.

- **PROCEDURES**

If you volunteer to participate in this study, we would ask you to do the following things:

You will be asked to complete three separate sessions of this study consisting of a field survey and two Virtual Reality surveys. Before the initial stage, you will be asked to answer several questions concerning personal mountaineering experience and biographical information. You will also receive training in the slope magnitude estimation procedure, which will involve using both a subjective scale of steepness, and a "palm board" which you will align to appear parallel to the slope you see.
The first test session of this study will be a field survey conducted at an off-campus site. You may need to obtain transportation to and from the field survey sites; however, costs will be reimbursed as stated below. You will be asked to estimate the slope, distance, height, and surface slipperiness of the terrain of certain pre-selected hills from a fixed vantage point. Your estimations will include a visual estimation of the slope using reference plywood ramps and a haptic (motor skill) estimation by adjusting a palm tilt-board to the slope indicated by the perceived hill. All estimates will be made from both an upright, standing position and a prone, lying condition. This test session will last no more than 2 – 3 hours, not including the driving time to and from the test location.

The second test session will be conducted using a Virtual Reality display at the Man Vehicle Laboratory at MIT. This session will last no more than one hour, including a scheduled break. You will be asked again to estimate the slope, distance, height, and surface slipperiness of the terrain of hills viewed through a stereoscopic head mounted display. Your estimations will include the visual placement of a computer generated push-pin in an orientation such that the flat head appears tangent to the slope and a haptic estimate by adjusting a palm tilt-board to the slope indicated by the perceived hill. Again, all estimates will be made from an upright, standing position and a prone, lying condition.

The third stage of this study will be identical to the second stage; however photographs of the lunar surface will be substituted for the hills shown in the second stage.

Each experiment test session will take place on separate days and will take place between October 2007 and June 2008. There may be significant durations of time between each stage; however, there are no obligations to this study between the stages. Following the third stage, you will be debriefed on the study and allowed to ask questions and offer feedback about the experiment to the investigator.

- **POTENTIAL RISKS AND DISCOMFORTS**

1. Possible eye fatigue from fusing stereoscopic images during the VR tests
2. Fatigue or headache from weight of the HMD in the VR tests.

In the event of eye fatigue or headache during the laboratory session, the VR head mounted display may be removed at any time if desired.

- **POTENTIAL BENEFITS**

No direct benfits except learning about your own perceptual biases in estimating slopes.

The knowledge from this study may save lunar astronauts from unanticipated dangers resulting from misperceived estimates of terrain characteristics.

- **PAYMENT FOR PARTICIPATION**

$10.00 per hour payment plus mileage for driving to field sites will be reimbursed at standard MIT Travel Policy rates.

- **CONFIDENTIALITY**

Any information that is obtained in connection with this study and that can be identified with you will remain confidential and will be disclosed only with your permission or as required by law. All data will be coded to remove any personal information from being associated with you and kept at the Man Vehicle Laboratory in electronic format but not available to the general public. The data will only be reported as part of a group analysis.

- **IDENTIFICATION OF INVESTIGATORS**

If you have any questions or concerns about the research, please feel free to contact:

Principal Investigator: Prof. Laurence Young, 617-253-7759, lry@mit.edu

- **EMERGENCY CARE AND COMPENSATION FOR INJURY**

In the unlikely event of physical injury resulting from participation in this research you may receive medical treatment from the M.I.T. Medical Department, including emergency treatment and follow-up care as needed. Your insurance carrier may be billed for the cost of such treatment. M.I.T. does not provide any other form of compensation for injury. Moreover, neither the offer to provide medical assistance nor the actual provision of medical services shall be construed as an admission of negligence or acceptance of liability. Questions regarding this policy may be directed to M.I.T's Insurance Office, (617) 253-2823.

- **RIGHTS OF RESEARCH SUBJECTS**

You are not waiving any legal claims, rights or remedies because of your participation in this research study. If you feel you have been treated unfairly, or you have questions regarding your rights as a research subject, you may contact the Chairman of the Committee on the Use of Humans as Experimental Subjects, M.I.T., Room E25-143B, 77 Massachusetts Ave, Cambridge, MA 02139, phone 1-617-253 6787.

SIGNATURE OF RESEARCH SUBJECT OR LEGAL REPRESENTATIVE

I understand the procedures described above. My questions have been answered to my satisfaction, and I agree to participate in this study. I have been given a copy of this form.

_____
Name of Subject

_____
Name of Legal Representative (if applicable)

_____ _____
Signature of Subject or Legal Representative Date

SIGNATURE OF INVESTIGATOR

In my judgment the subject is voluntarily and knowingly giving informed consent and possesses the legal capacity to give informed consent to participate in this research study.

_____ _____
Signature of Investigator Date

APPENDIX

B

SUBJECT INFORMATION FORM

Subject #:_____

Age:_____ **Height:**_____

Gender: Male Female

Educational Background: Undergraduate Graduate Faculty/Staff
Year: 1 2 3 4 5+ _____ _____

Previous knowledge/experience with estimating slopes:

Corrected Vision:_____

Difficulties with depth perception? Yes No

Pilot
Rating:_____ Cockpit Hours:_____

Simulator
Airframe:_____ Hours:_____

Sports

Baseball	Years: _____	Beginner	Intermediate	Advanced
Basketball	Years: _____	Beginner	Intermediate	Advanced
Tennis	Years: _____	Beginner	Intermediate	Advanced
Golf	Years: _____	Beginner	Intermediate	Advanced
Skiing	Years: _____	Beginner	Intermediate	Advanced
Running	Years: _____	Beginner	Intermediate	Advanced
Cycling	Years: _____	Beginner	Intermediate	Advanced

Hobbies

R/C Airplane	Years: _____	Beginner	Intermediate	Advanced
Hiking	Years: _____	Beginner	Intermediate	Advanced
Rock Climbing	Years: _____	Beginner	Intermediate	Advanced
Archery	Years: _____	Beginner	Intermediate	Advanced
Rifle	Years: _____	Beginner	Intermediate	Advanced
Video Games	Years: _____	Beginner	Intermediate	Advanced

APPENDIX C

EXPERIMENT ADVERTISEMENT

Advertisement for Subjects in Lunar Slope Estimation

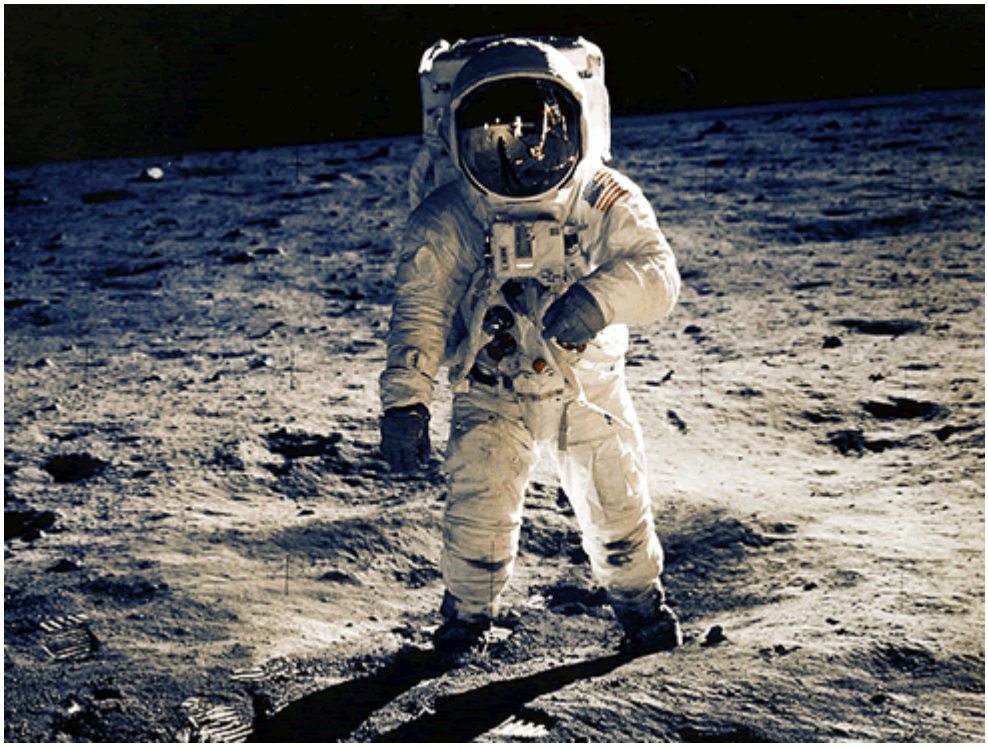

Help the lunar astronauts in planning their excursions when we return to the moon!

We need healthy subjects to participate in tests of subjective distance, slope and surface of real scenes. The field studies will be conducted at nearby hills. The laboratory studies will be conducted at MIT with virtual reality images of earth and moon.

Test sessions last approximately one hour.
Subjects will be paid $10/hour for their participation.

If interested, contact Chris Oravetz (3-5487, coravetz@mit.edu) to arrange an appointment

APPENDIX D

TEST STIMULI

D.1 Mars Desert Research Station Field/VR Study

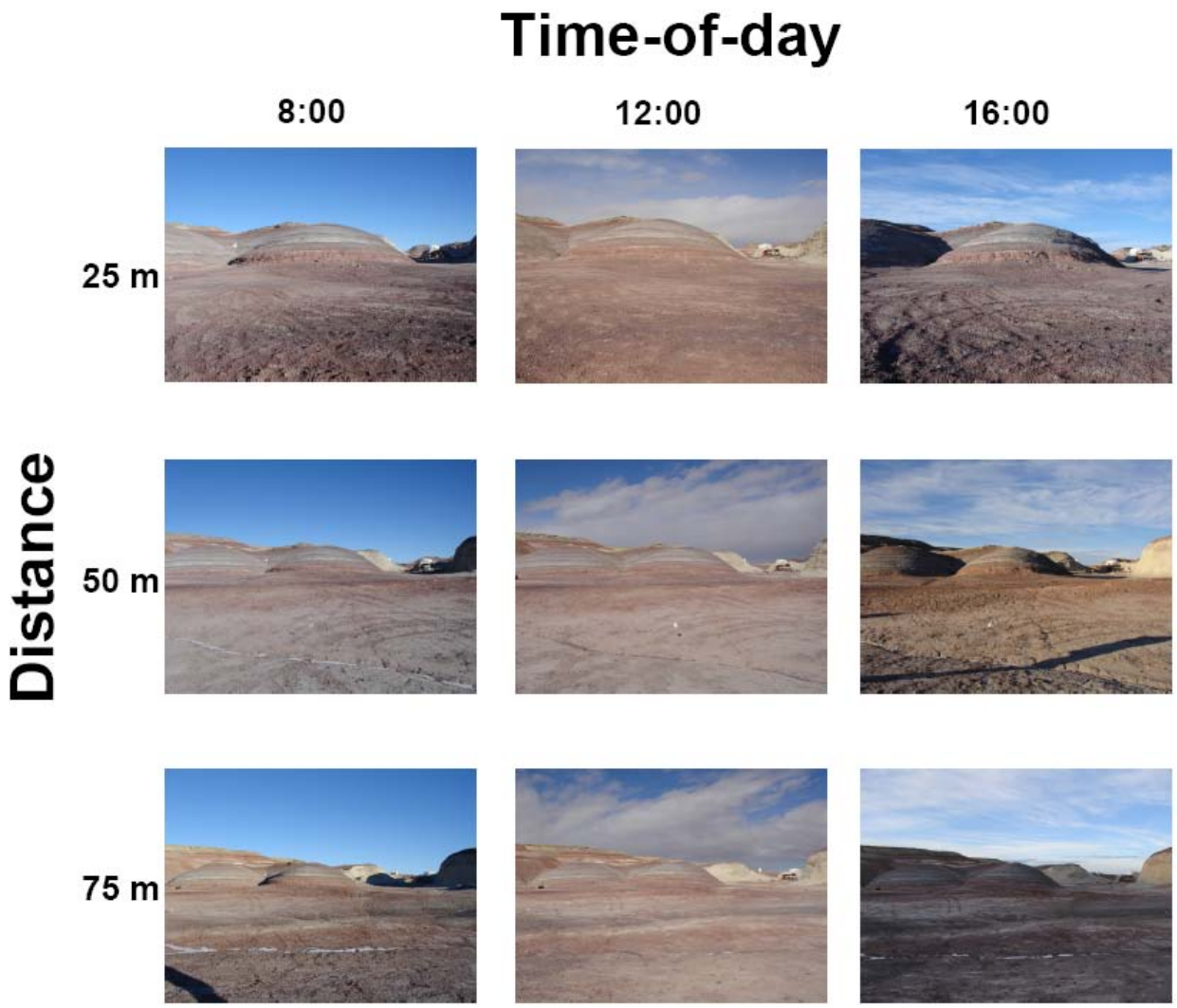

18.1° Hill

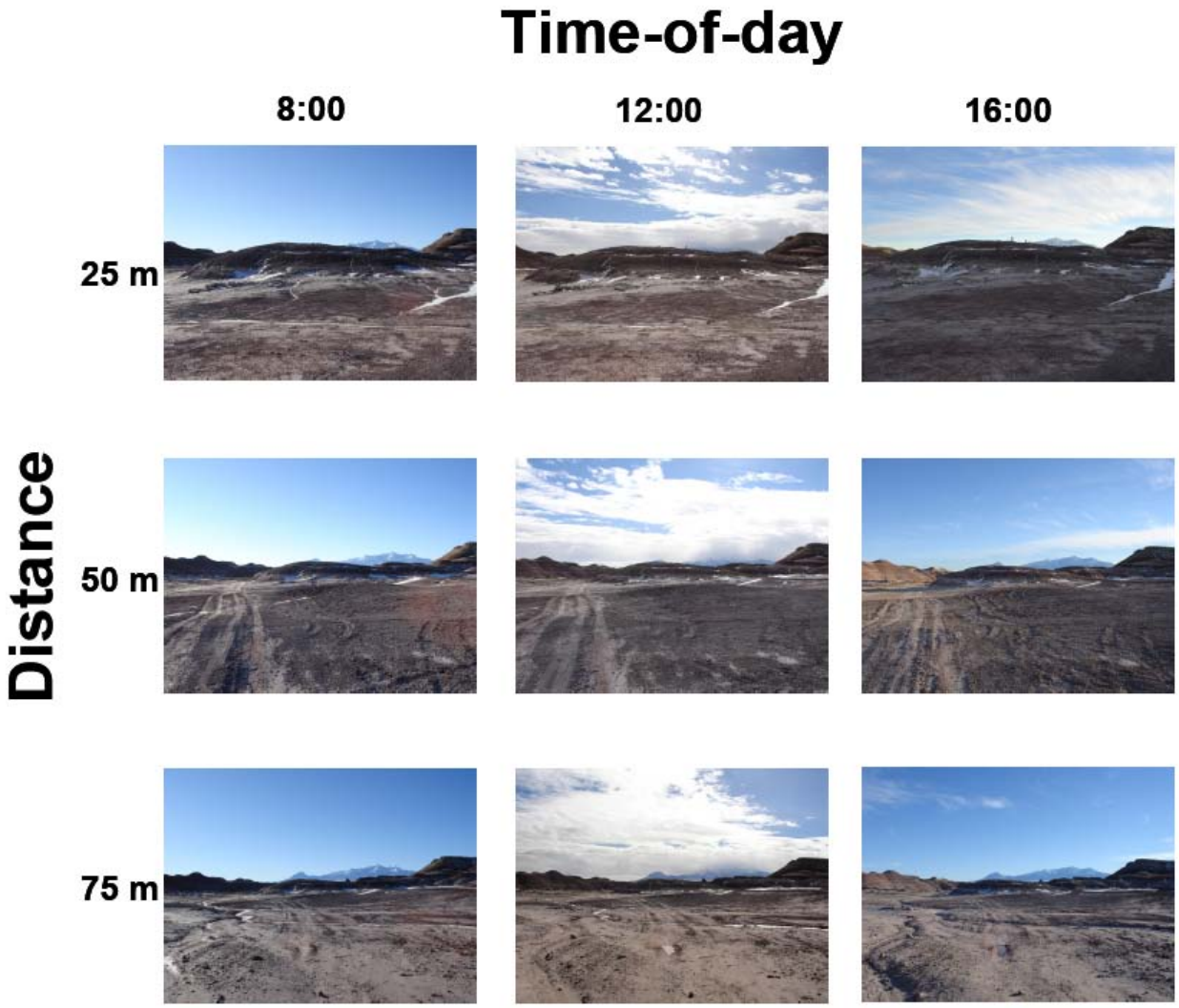

19.2° Hill

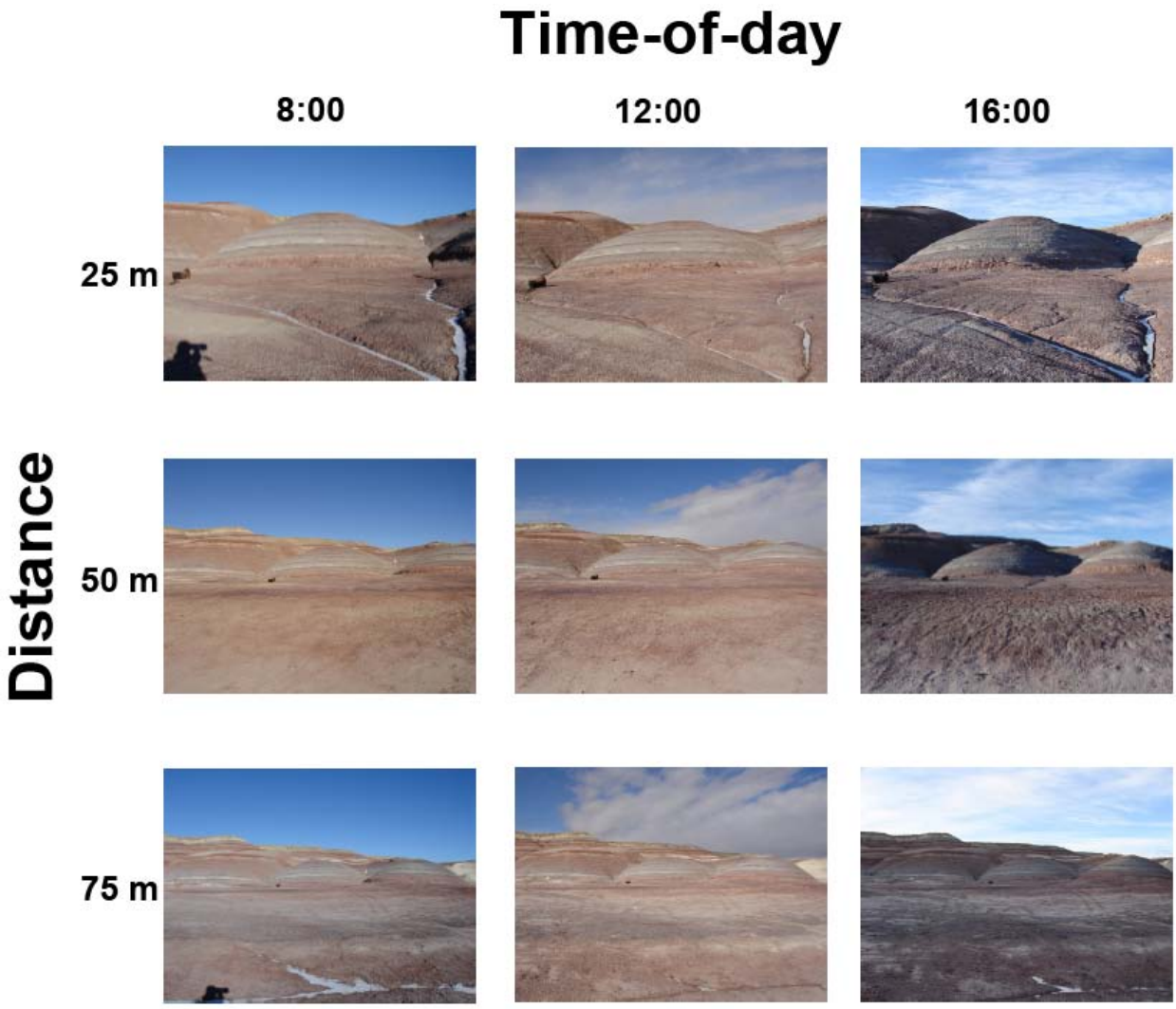

22.8° Hill

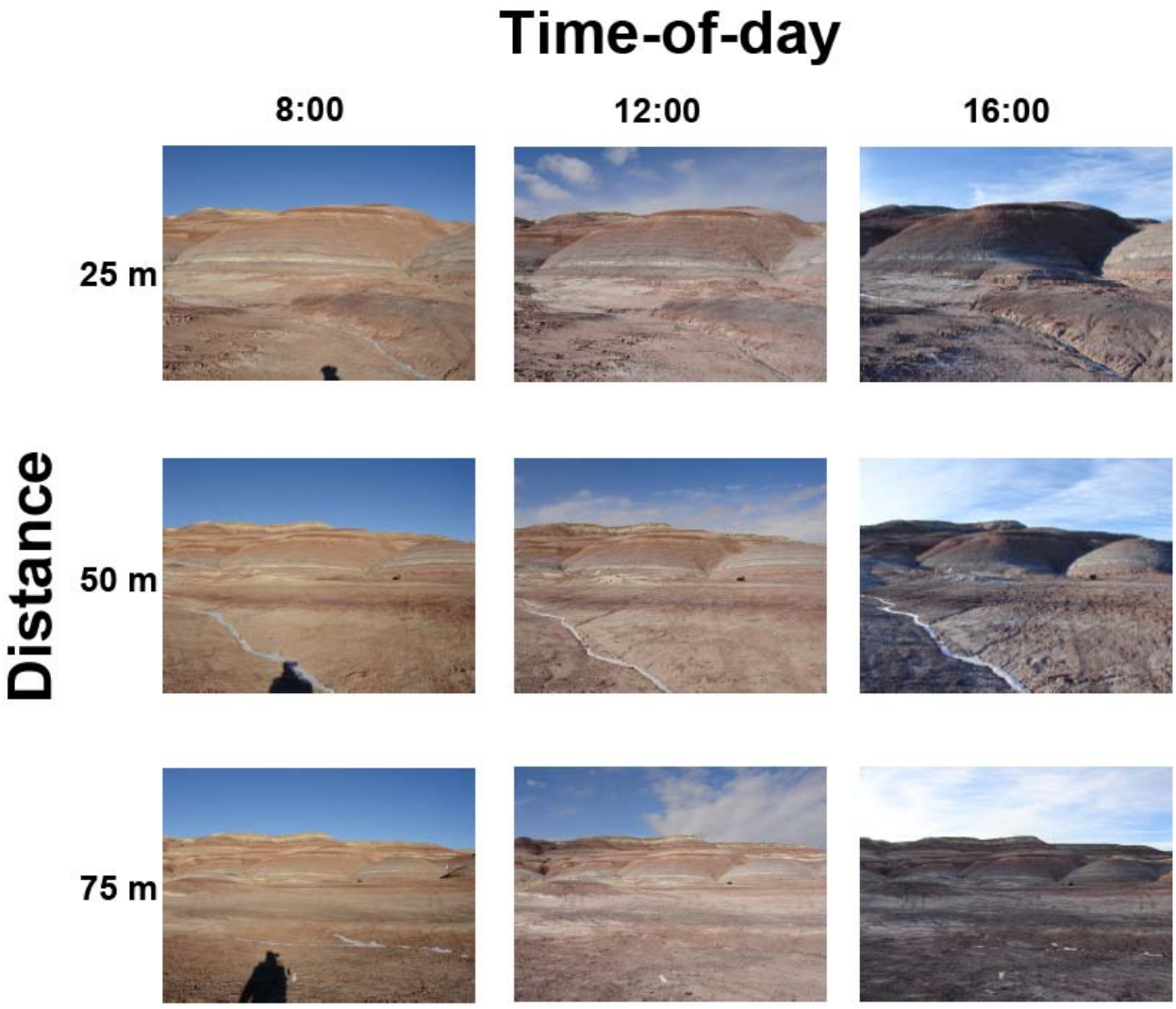

23.3° Hill

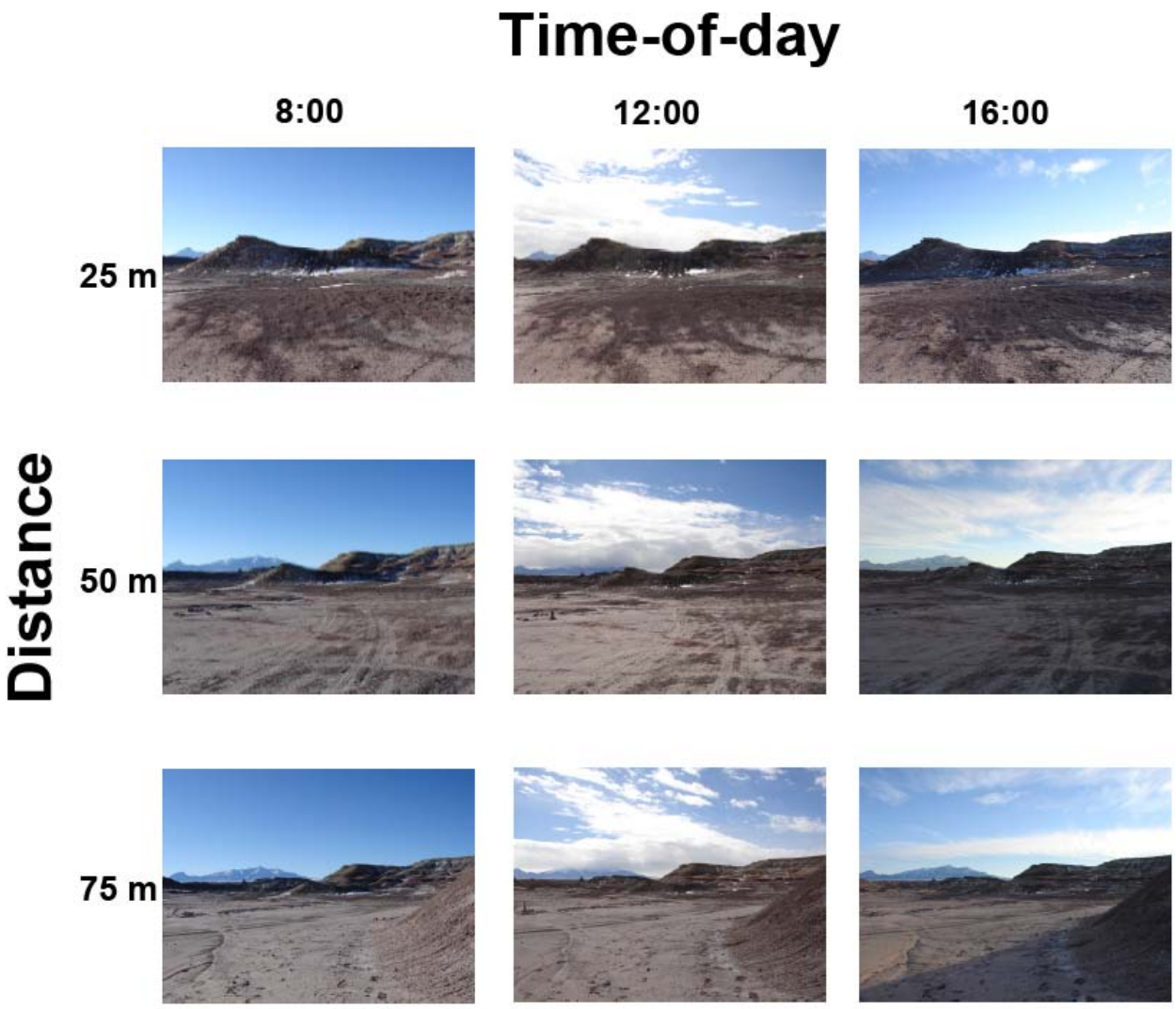

D.2 Lunar VR Study

Wessex Cleft (Apollo 17)
Slope: 14.7°
Height: 700 m

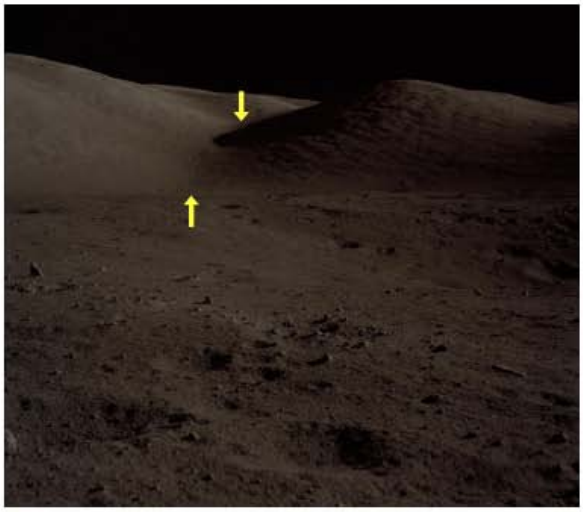

Distance: 5200 m (Station 1)
Sun Elevation: 16°

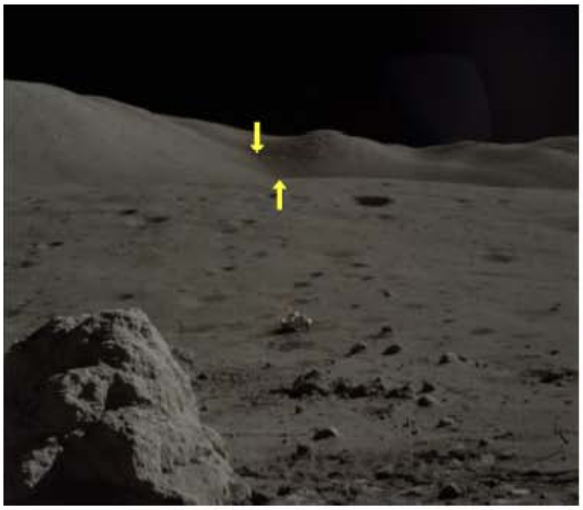

Distance: 11400 m (Station 2)
Sun Elevation: 26°

Bear Mountain (Apollo 17)
Slope: 15.1°
Height: 276 m

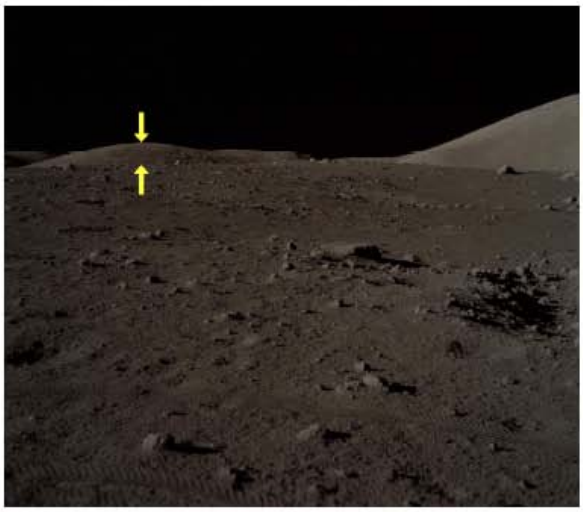

Distance: 4000 m (Station 1)
Sun Elevation: 16°

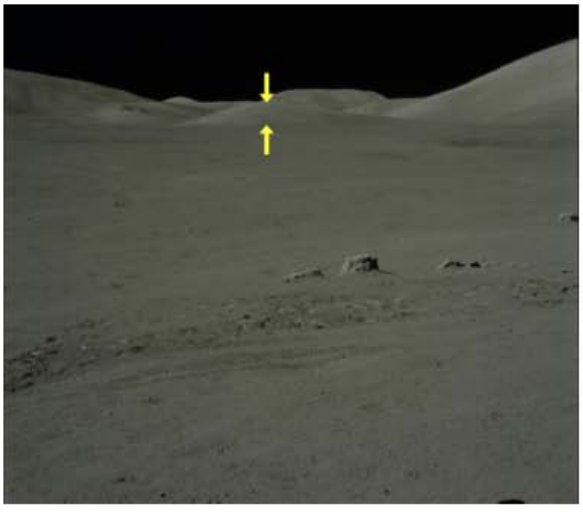

Distance: 8400 m (Station 7)
Sun Elevation: 37°

Sculptured Hills (Apollo 17)

Slope: 22.2°
Height: 1100 m

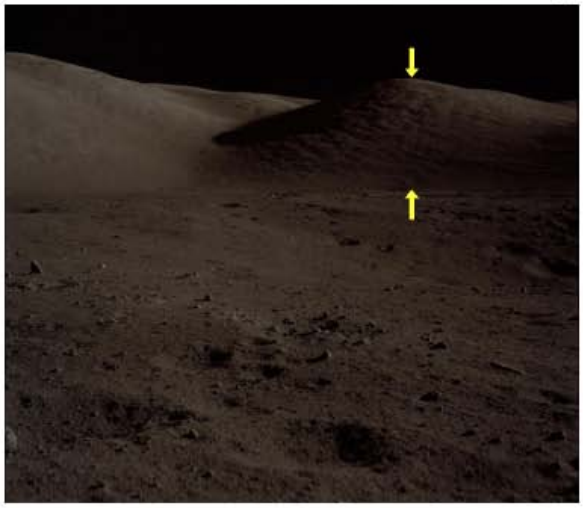

Distance: 5000 m (Station 1)
Sun Elevation: 16°

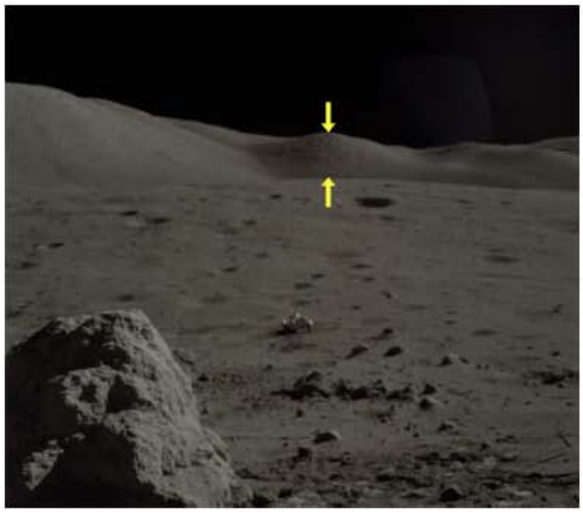

Distance: 11500 m (Station 2)
Sun Elevation: 26°

Mons Vitruvius (Apollo 17)

Slope: 24.1°
Height: 2091 m

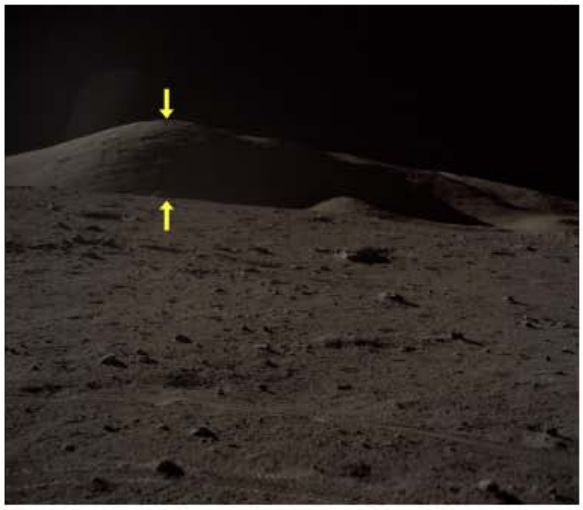

Distance: 10900 m (Station 1)
Sun Elevation: 16°

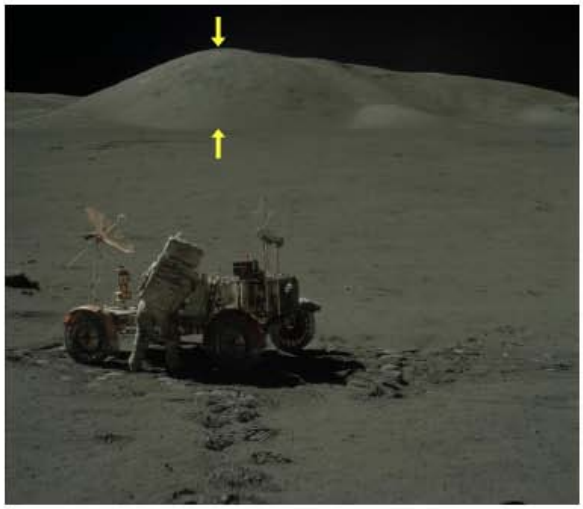

Distance: 13900 m (Station 7)
Sun Elevation: 37°

North Massif (Apollo 17)

Slope: 25.6°
Height: 1551 m

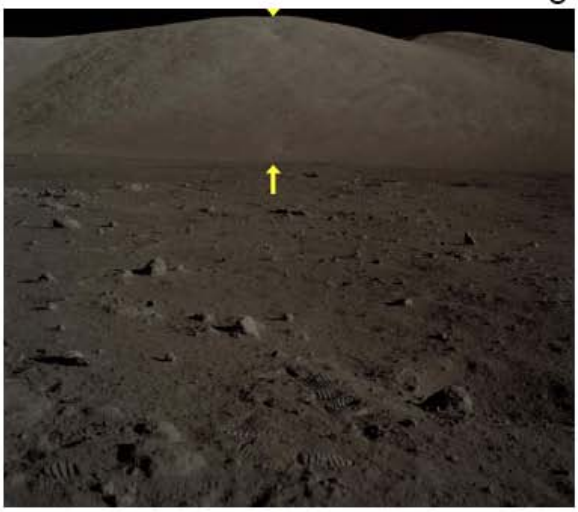

Distance: 4300 m (Station 1)
Sun Elevation: 16°

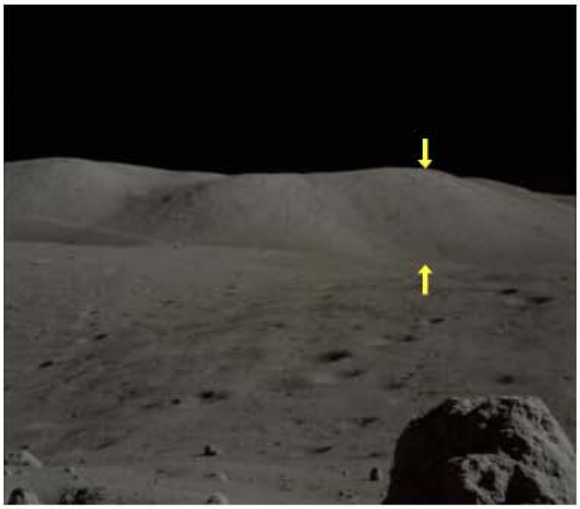

Distance: 8800 m (Station 2)
Sun Elevation: 26°

South Massif (Apollo 17)

Slope: 25.6°
Height: 2341 m

Distance: 6500 m (Station 1)
Sun Elevation: 16°

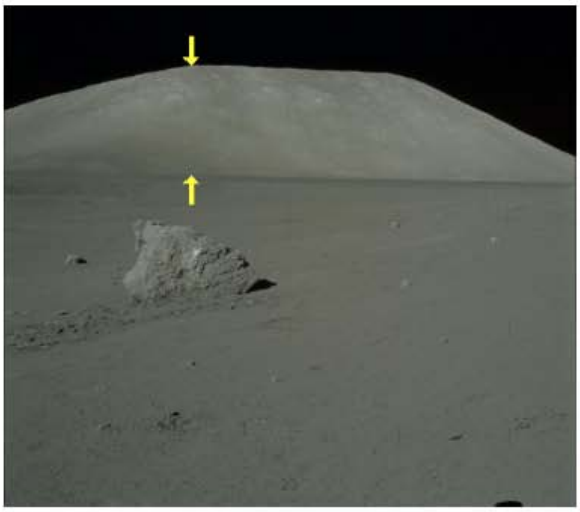

Distance: 9800 m (Station 7)
Sun Elevation: 37°

North Massif-Center (Apollo 17)

Slope: 24°
Height: 1200 m

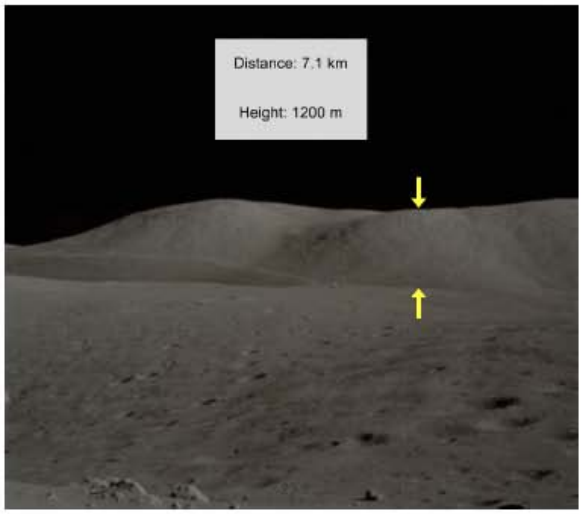

Distance: 7100 m (Station 2)
Sun Elevation: 26°

St. George (Apollo 15)

Slope: 20°
Height: 2600 m

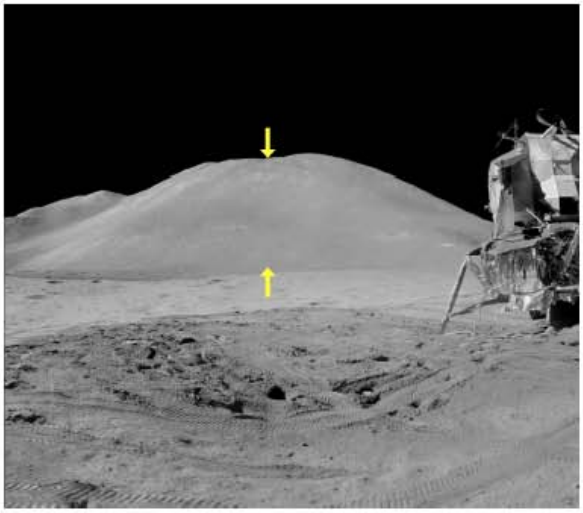

Distance: 3900 m (Lunar Module)
Sun Elevation: 24°

Dune Crater (Apollo 15)

Slope: 17°

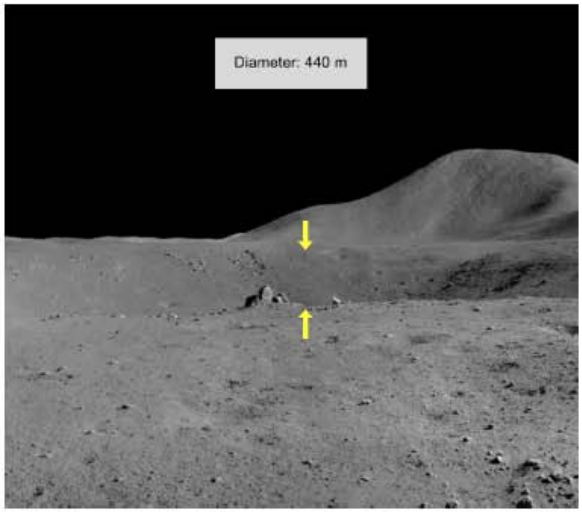

Distance: 440 m (Station 4)
Sun Elevation: 31°

Rille Valley (Apollo 15)

Slope: 31°

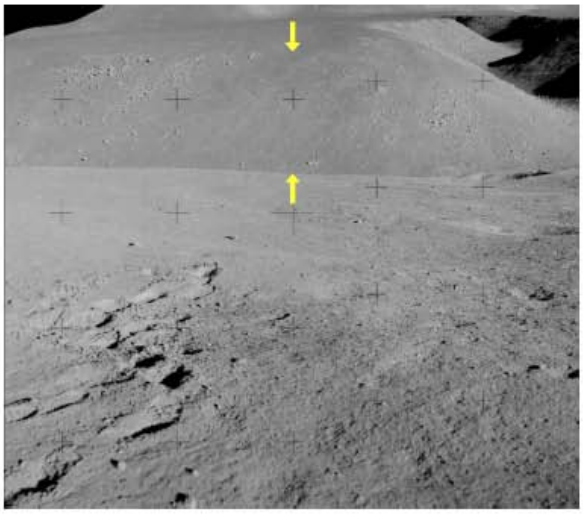

Distance: 1440 m (Station 2)
Sun Elevation: 31°

Surveyor Crater (Apollo 12)
Slope: 7°

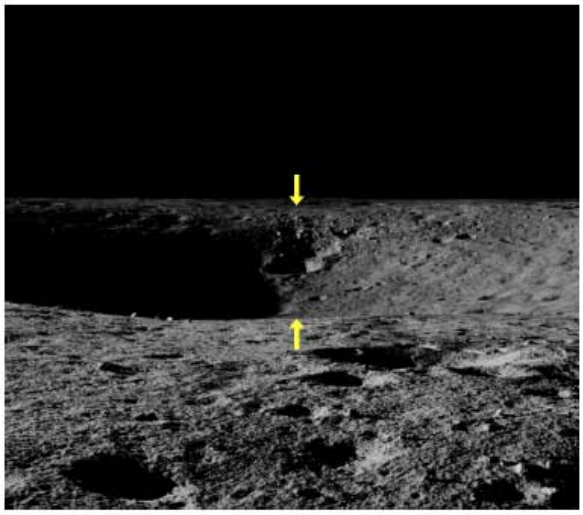

Distance: 180 m (Lunar Module)

Camelot Crater (Apollo 17)
Slope: 16°

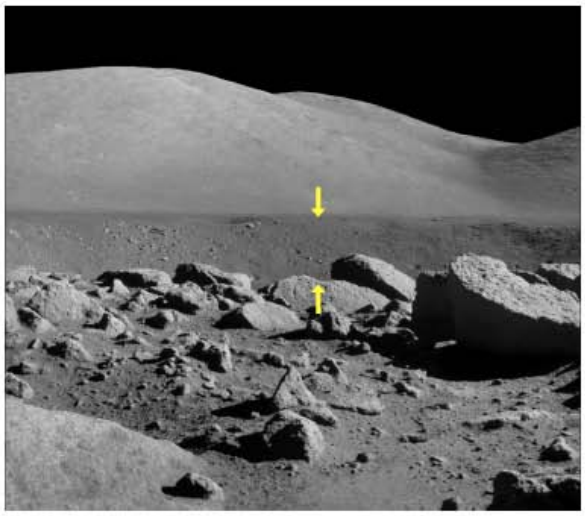

Distance: 550 m (Station 5)
Sun Elevation: 28°

Spook Crater (Apollo 16)
Slope: 17°

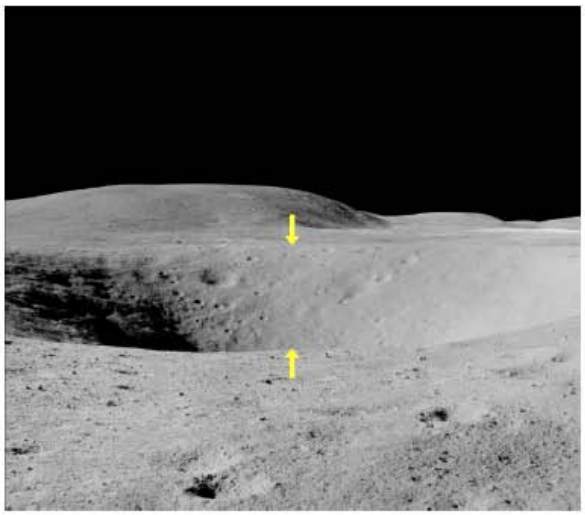

Distance: 250 m (Station 2)
Sun Elevation: 25°

Shorty Crater (Apollo 17)
Slope: 20°

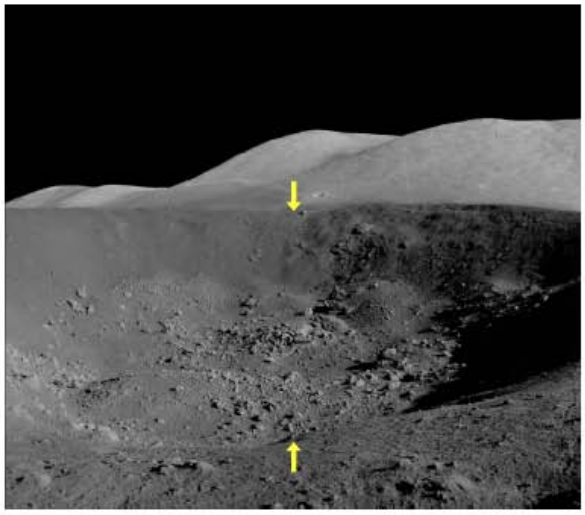

Distance: 123 m (Station 4)
Sun Elevation: 27°

North Ray Crater (Apollo 16)
Slope: 30°

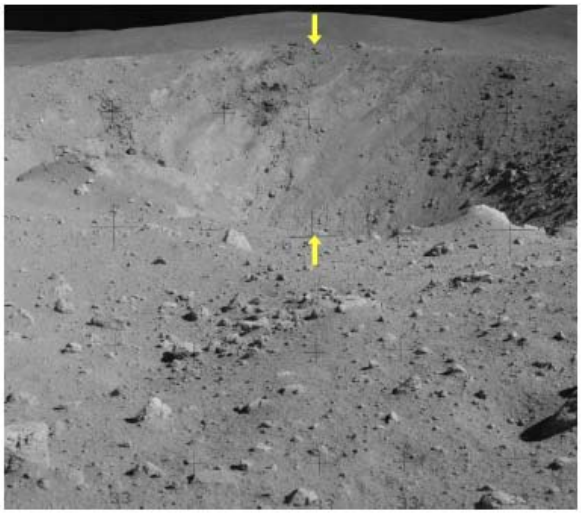

Distance: 877 m (Station 11)
Sun Elevation: 46°

Flag Crater (Apollo 16)
Slope: 30°

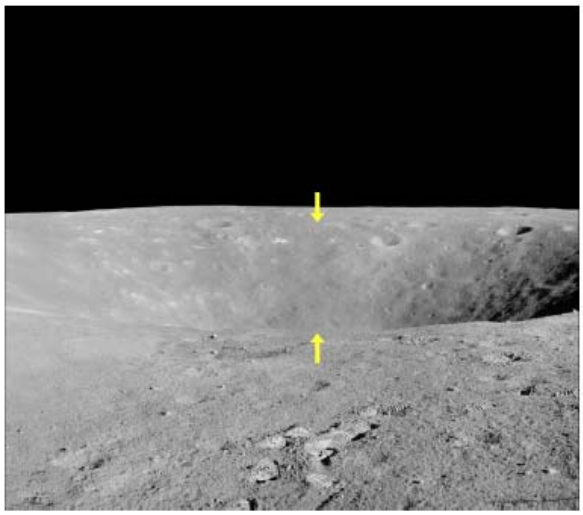

Distance: 209 m (Station 1)
Sun Elevation: 24°

D.3 Devon Island Field Study

20.0^{o} Hill

39.6^{o} Hill

APPENDIX

E

VIZARD SCRIPTS

Two asterisks (**) indicate the line of code is a continuation of the previous line

E.1 MDRS PILOT VR Study (MPVS)

```
#Human Slope and Distance Estimation of MDRS Terrain - PILOT Study

#Christopher Oravetz
#Man Vehicle Lab - MIT
#4 April 2008

import viz
import vizinfo
viz.go(viz.STEREO | viz.FULLSCREEN)

#Input Session Number (Training = 0, Standing = 1,4, Supine = 2,3) and Subject Number
session = viz.input('Session')
subject = viz.input('What is your subject number?')
estimation_data = open('Subject #'+str(subject), 'a')

#Initialize photograph arrays
left0 = []
right0 = []
left1 = []
right1 = []
left2 = []
right2 = []
left3 = []
right3 = []
left4 = []
right4 = []

#Append photograph arrays with all photographs
#EndSession photographs is only a white background
#All photographs were previously scaled to 2048x1024 to be quickly uploaded by Vizard
left0.append('EndSession.jpg')
left0.append('MDRS_Left_062_scaled2.jpg')
left0.append('MDRS_Left_063_scaled2.jpg')
left0.append('MDRS_Left_110_scaled2.jpg')
left0.append('MDRS_Left_111_scaled2.jpg')

right0.append('EndSession.jpg')
right0.append('MDRS_Right_062_scaled2.jpg')
right0.append('MDRS_Right_063_scaled2.jpg')
right0.append('MDRS_Right_110_scaled2.jpg')
right0.append('MDRS_Right_111_scaled2.jpg')

left1.append('EndSession.jpg')
left1.append('MDRS_Left_102_scaled2.jpg')
left1.append('MDRS_Left_112_scaled2.jpg')
left1.append('MDRS_Left_060_scaled2.jpg')
left1.append('MDRS_Left_113_scaled2.jpg')
left1.append('MDRS_Left_061_scaled2.jpg')
left1.append('MDRS_Left_104_scaled2.jpg')
left1.append('MDRS_Left_114_scaled2.jpg')
```

```
left1.append('MDRS_Left_051_scaled2.jpg')
left1.append('MDRS_Left_055_scaled2.jpg')
left1.append('MDRS_Left_054_scaled2.jpg')
left1.append('MDRS_Left_058_scaled2.jpg')
left1.append('MDRS_Left_103_scaled2.jpg')

left2.append('EndSession.jpg')
left2.append('MDRS_Left_061_scaled2.jpg')
left2.append('MDRS_Left_112_scaled2.jpg')
left2.append('MDRS_Left_055_scaled2.jpg')
left2.append('MDRS_Left_058_scaled2.jpg')
left2.append('MDRS_Left_104_scaled2.jpg')
left2.append('MDRS_Left_054_scaled2.jpg')
left2.append('MDRS_Left_060_scaled2.jpg')
left2.append('MDRS_Left_102_scaled2.jpg')
left2.append('MDRS_Left_113_scaled2.jpg')
left2.append('MDRS_Left_114_scaled2.jpg')
left2.append('MDRS_Left_051_scaled2.jpg')
left2.append('MDRS_Left_103_scaled2.jpg')

left3.append('EndSession.jpg')
left3.append('MDRS_Left_103_scaled2.jpg')
left3.append('MDRS_Left_051_scaled2.jpg')
left3.append('MDRS_Left_114_scaled2.jpg')
left3.append('MDRS_Left_113_scaled2.jpg')
left3.append('MDRS_Left_102_scaled2.jpg')
left3.append('MDRS_Left_060_scaled2.jpg')
left3.append('MDRS_Left_054_scaled2.jpg')
left3.append('MDRS_Left_104_scaled2.jpg')
left3.append('MDRS_Left_058_scaled2.jpg')
left3.append('MDRS_Left_055_scaled2.jpg')
left3.append('MDRS_Left_112_scaled2.jpg')
left3.append('MDRS_Left_061_scaled2.jpg')

left4.append('EndSession.jpg')
left4.append('MDRS_Left_103_scaled2.jpg')
left4.append('MDRS_Left_058_scaled2.jpg')
left4.append('MDRS_Left_054_scaled2.jpg')
left4.append('MDRS_Left_055_scaled2.jpg')
left4.append('MDRS_Left_051_scaled2.jpg')
left4.append('MDRS_Left_114_scaled2.jpg')
left4.append('MDRS_Left_104_scaled2.jpg')
left4.append('MDRS_Left_061_scaled2.jpg')
left4.append('MDRS_Left_113_scaled2.jpg')
left4.append('MDRS_Left_060_scaled2.jpg')
left4.append('MDRS_Left_112_scaled2.jpg')
left4.append('MDRS_Left_102_scaled2.jpg')

#Right eye is presented a synoptic image in session 1 and 3 and a stereo images in sessions 2 and 4
right1.append('EndSession.jpg')
right1.append('MDRS_Left_102_scaled2.jpg')
right1.append('MDRS_Left_112_scaled2.jpg')
right1.append('MDRS_Left_060_scaled2.jpg')
right1.append('MDRS_Left_113_scaled2.jpg')
right1.append('MDRS_Left_061_scaled2.jpg')
right1.append('MDRS_Left_104_scaled2.jpg')
right1.append('MDRS_Left_114_scaled2.jpg')
right1.append('MDRS_Left_051_scaled2.jpg')
right1.append('MDRS_Left_055_scaled2.jpg')
right1.append('MDRS_Left_054_scaled2.jpg')
right1.append('MDRS_Left_058_scaled2.jpg')
right1.append('MDRS_Left_103_scaled2.jpg')

right2.append('EndSession.jpg')
right2.append('MDRS_Right_061_scaled2.jpg')
right2.append('MDRS_Right_112_scaled2.jpg')
right2.append('MDRS_Right_055_scaled2.jpg')
right2.append('MDRS_Right_058_scaled2.jpg')
right2.append('MDRS_Right_104_scaled2.jpg')
```

```
right2.append('MDRS_Right_054_scaled2.jpg')
right2.append('MDRS_Right_060_scaled2.jpg')
right2.append('MDRS_Right_102_scaled2.jpg')
right2.append('MDRS_Right_113_scaled2.jpg')
right2.append('MDRS_Right_114_scaled2.jpg')
right2.append('MDRS_Right_051_scaled2.jpg')
right2.append('MDRS_Right_103_scaled2.jpg')

right3.append('EndSession.jpg')
right3.append('MDRS_Left_103_scaled2.jpg')
right3.append('MDRS_Left_051_scaled2.jpg')
right3.append('MDRS_Left_114_scaled2.jpg')
right3.append('MDRS_Left_113_scaled2.jpg')
right3.append('MDRS_Left_102_scaled2.jpg')
right3.append('MDRS_Left_060_scaled2.jpg')
right3.append('MDRS_Left_054_scaled2.jpg')
right3.append('MDRS_Left_104_scaled2.jpg')
right3.append('MDRS_Left_058_scaled2.jpg')
right3.append('MDRS_Left_055_scaled2.jpg')
right3.append('MDRS_Left_112_scaled2.jpg')
right3.append('MDRS_Left_061_scaled2.jpg')

right4.append('EndSession.jpg')
right4.append('MDRS_Right_103_scaled2.jpg')
right4.append('MDRS_Right_058_scaled2.jpg')
right4.append('MDRS_Right_054_scaled2.jpg')
right4.append('MDRS_Right_055_scaled2.jpg')
right4.append('MDRS_Right_051_scaled2.jpg')
right4.append('MDRS_Right_114_scaled2.jpg')
right4.append('MDRS_Right_104_scaled2.jpg')
right4.append('MDRS_Right_061_scaled2.jpg')
right4.append('MDRS_Right_113_scaled2.jpg')
right4.append('MDRS_Right_060_scaled2.jpg')
right4.append('MDRS_Right_112_scaled2.jpg')
right4.append('MDRS_Right_102_scaled2.jpg')

#Turn Off mouse navigation and visibility of the mouse
viz.mouse(viz.OFF)
viz.mouse.setVisible(viz.OFF)

#Create two rectangles to map images on as textures
quad1 = viz.add(viz.TEXQUAD)
quad2 = viz.add(viz.TEXQUAD,viz.WORLD,2)
quad1.setScale(1.3333333333333333333333333333333333333333333333333333333,1,1)
quad2.setScale(1.3333333333333333333333333333333333333333333333333333333,1,1)

#Instructions upon start of each session
#infoBoxLeftTitle displays the Session Number to the left eye
infoBoxLeftTitle = viz.add(viz.TEXT3D,'',viz.WORLD,1)
infoBoxLeftTitle.message('Session #'+ str(session))
infoBoxLeftTitle.setPosition([0,2.0,1.3])
infoBoxLeftTitle.setScale([.05,.05,1])
infoBoxLeftTitle.resolution(1)
infoBoxLeftTitle.alignment(viz.TEXT_CENTER_CENTER)
infoBoxLeftTitle.color(viz.BLACK)

#infoBoxLeft diplays the body position instructions to the left eye
#infoBoxLeftTrain displays the distance instructions for the training session to the left eye
infoBoxLeft = viz.add(viz.TEXT3D,'',viz.WORLD,1)
infoBoxTrainLeft = viz.add(viz.TEXT3D,'',viz.WORLD,1)
if session == 0:
        infoBoxLeft.message('Estimate the following slopes in the Standing Position')
        infoBoxTrainLeft.message('For TRAINING purposes the distance to the base of each hill is diplayed at the top of the
**screen')
elif session == 1 or session == 4:
        infoBoxLeft.message('Estimate the following slopes in the Standing Position')
elif session == 2 or session == 3:
        infoBoxLeft.message('Estimate the following slopes in the Supine Position')
infoBoxLeft.setPosition([0,1.92,1.379])
infoBoxLeft.setScale([.03,.03,1])
```

```
infoBoxLeft.resolution(1)
infoBoxLeft.alignment(viz.TEXT_CENTER_CENTER)
infoBoxLeft.color(viz.BLACK)
infoBoxTrainLeft.setPosition([0,1.84,1.379])
infoBoxTrainLeft.setScale([.02,.02,1])
infoBoxTrainLeft.resolution(1)
infoBoxTrainLeft.alignment(viz.TEXT_CENTER_CENTER)
infoBoxTrainLeft.color(viz.RED)

#infoBoxRightTitle displays the Session Number to the right eye
infoBoxRightTitle = viz.add(viz.TEXT3D,'',viz.WORLD,2)
infoBoxRightTitle.message('Session #' + str(session))
infoBoxRightTitle.setPosition([0,2.0,1.3])
infoBoxRightTitle.setScale([.05,.05,1.3])
infoBoxRightTitle.resolution(1)
infoBoxRightTitle.alignment(viz.TEXT_CENTER_CENTER)
infoBoxRightTitle.color(viz.BLACK)

#infoBoxRight diplays the body position instructions to the right eye
#infoBoxRightTrain displays the distance instructions for the training session to the right eye
infoBoxRight = viz.add(viz.TEXT3D,'',viz.WORLD,2)
infoBoxTrainRight = viz.add(viz.TEXT3D,'',viz.WORLD,2)
if session == 0:
	infoBoxRight.message('Estimate the following slopes in the Standing Position')
	infoBoxTrainRight.message('For TRAINING purposes the distance to the base of each hill is diplayed at the top of the
**screen')
elif session == 1 or session == 4:
	infoBoxRight.message('Estimate the following slopes in the Standing Position')
elif session == 2 or session == 3:
	infoBoxRight.message('Estimate the following slopes in the Supine Position')
infoBoxRight.setPosition([0,1.92,1.379])
infoBoxRight.setScale([.03,.03,1])
infoBoxRight.resolution(1)
infoBoxRight.alignment(viz.TEXT_CENTER_CENTER)
infoBoxRight.color(viz.BLACK)
infoBoxTrainRight.setPosition([0,1.84,1.379])
infoBoxTrainRight.setScale([.02,.02,1])
infoBoxTrainRight.resolution(1)
infoBoxTrainRight.alignment(viz.TEXT_CENTER_CENTER)
infoBoxTrainRight.color(viz.RED)

#infoBoxEndSessionLeft notifies the subject of the end of the session and is displayed in the left eye
infoBoxEndSessionLeft = viz.add(viz.TEXT3D,'',viz.WORLD,1)
infoBoxEndSessionLeft.message('End of Session')
if session == 1 or session == 3:
	infoBoxEndSessionLeft.setPosition([0,1.9,1.379])
	infoBoxEndSessionLeft.setScale([.1,.1,1])
else:
	infoBoxEndSessionLeft.setPosition([0,1.9,1.35])
	infoBoxEndSessionLeft.setScale([.1,.1,1])
infoBoxEndSessionLeft.resolution(1)
infoBoxEndSessionLeft.alignment(viz.TEXT_CENTER_CENTER)
infoBoxEndSessionLeft.color(viz.BLACK)
infoBoxEndSessionLeft.visible(viz.OFF)

#infoBoxEndSessionRight notifies the subject of the end of the session and is displayed in the right eye
infoBoxEndSessionRight = viz.add(viz.TEXT3D,'',viz.WORLD,2)
infoBoxEndSessionRight.message('End of Session')
if session == 1 or session == 3:
	infoBoxEndSessionRight.setPosition([0,1.9,1.379])
	infoBoxEndSessionRight.setScale([.1,.1,1])
else:
	infoBoxEndSessionRight.setPosition([-.003,1.925,1.35])
	infoBoxEndSessionRight.setScale([.1,.1,1])
infoBoxEndSessionRight.resolution(1)
infoBoxEndSessionRight.alignment(viz.TEXT_CENTER_CENTER)
infoBoxEndSessionRight.color(viz.BLACK)
infoBoxEndSessionRight.visible(viz.OFF)

#Distance output for training session
```

```
#A rectangular box and the distance output is displayed in the center of the screen above each hill
#Distance refers to the length between the observer and the base of each hill
#All the distances are stored in arrays for each eye
if session == 0:
	infoBoxDistanceLeft = viz.add(viz.TEXT3D,'',viz.WORLD,1)
	infoBoxDistanceRight = viz.add(viz.TEXT3D,'',viz.WORLD,2)
	infoBoxDistanceLeft.setPosition([0,2.15,1.35])
	infoBoxDistanceLeft.setScale([.03,.03,1])
	infoBoxDistanceLeft.resolution(1)
	infoBoxDistanceLeft.alignment(viz.TEXT_CENTER_CENTER)
	infoBoxDistanceLeft.color(viz.RED)
	infoBoxDistanceRight.setPosition([-.016,2.174,1.35])
	infoBoxDistanceRight.setScale([.03,.03,1])
	infoBoxDistanceRight.resolution(1)
	infoBoxDistanceRight.alignment(viz.TEXT_CENTER_CENTER)
	infoBoxDistanceRight.color(viz.RED)
	DistanceLeftArray = ['Nice Job!','25 meters','75 meters', '25 meters', '75 meters']
	DistanceRightArray = ['Nice Job!','25 meters','75 meters', '25 meters', '75 meters']
	infoQuadDistanceLeft = viz.add(viz.TEXQUAD,viz.WORLD,1)
	infoQuadDistanceLeft.setScale([.3,.1,1])
	infoQuadDistanceLeft.setPosition([0,2.15,1.36])
	infoQuadDistanceLeft.color(viz.WHITE)
	infoQuadDistanceRight = viz.add(viz.TEXQUAD,viz.WORLD,2)
	infoQuadDistanceRight.setScale([.3,.1,1])
	infoQuadDistanceRight.setPosition([-.016,2.174,1.36])
	infoQuadDistanceRight.color(viz.WHITE)

#Set the position of the Quads containing the photographs so they are in the center of each eye and they take of the entire screen
quad1.setPosition([0,1.82,1.38])
quad2.setPosition([0,1.82,1.38])

#Visual estimation device - semicircular wedge - for the left eye
wedgeLeft = viz.add('wedge2.ac',viz.WORLD,1)
wedgeLeft.setPosition(.4,1.5,1.34998)
wedgeLeft.color(viz.BLACK)
wedgeLeft.center([-.5,0,0])
wedgeLeft.setScale([.2,.2,.2])
wedgeLeft.visible(viz.OFF)

#Visual estimation device - semicircular wedge - for the right eye
wedgeRight = viz.add('wedge2.ac',viz.WORLD,2)
if session == 1 or session == 3:
	wedgeRight.setPosition(.4,1.5,1.34998)
	wedgeRight.setScale([.2,.2,.2])
else:
	wedgeRight.setPosition(.357,1.527,1.34998)
	wedgeRight.setScale([.2,.2,.2])
wedgeRight.color(viz.BLACK)
wedgeRight.center([-.5,0,0])
wedgeRight.visible(viz.OFF)

#Ground reference within the visual estimation device for the left eye
greenLeft = viz.add(viz.TEXQUAD,viz.WORLD,1)
greenLeft.setScale([.3,.11,1])
greenLeft.setPosition([0,1,1.34999])
greenLeft.center([0,.5,0])
greenLeft.color(viz.GREEN)
greenLeft.visible(viz.OFF)

#Sky reference within the visual estimation device for the left eye
whiteLeft = viz.add(viz.TEXQUAD,viz.WORLD,1)
whiteLeft.setScale([.3,.31,1])
whiteLeft.setPosition([0,1.2,1.35])
whiteLeft.center([0,.5,0])
whiteLeft.color(viz.WHITE)
whiteLeft.visible(viz.OFF)

#Ground reference within the visual estimation device for the right eye
greenRight = viz.add(viz.TEXQUAD,viz.WORLD,2)
if session == 1 or session == 3:
```

```
		greenRight.setScale([.3,.11,1])
		greenRight.setPosition([0,1,1.34999])
else:
		greenRight.setScale([.3,.11,1])
		greenRight.setPosition([-.043,1.027,1.34999])
greenRight.center([0,.5,0])
greenRight.color(viz.GREEN)
greenRight.visible(viz.OFF)

#Sky reference within the visual estimation device for the right eye
whiteRight = viz.add(viz.TEXQUAD,viz.WORLD,2)
if session == 1 or session == 3:
		whiteRight.setScale([.3,.31,1])
		whiteRight.setPosition([0,1.2,1.35])
else:
		whiteRight.setScale([.3,.31,1])
		whiteRight.setPosition([-.043,1.227,1.35])
whiteRight.center([0,.5,0])
whiteRight.color(viz.WHITE)
whiteRight.visible(viz.OFF)

#Create scenes for each eye
viz.scene(1,viz.LEFT_EYE)
viz.scene(2,viz.RIGHT_EYE)

#Define rotation actions of the visual estimation wedge
rotateCounter = vizact.spin(0,0,1,50,.01)
rotateClock = vizact.spin(0,0,1,-50,.01)

#Add rotation actions to the wedges in the left and right scenes
wedgeLeft.addAction(rotateCounter)
wedgeLeft.addAction(rotateClock)
wedgeRight.addAction(rotateCounter)
wedgeRight.addAction(rotateClock)

#Position varibles for the rectangular reticle that identifies the area of the hill to estimate
#Each variable contains the location of the reticle for each photograph

#Position variables for the left eye
Position_102_Left = [.03,1.899,1.35]
Position_112_Left = [-.032,1.983,1.35]
Position_060_Left = [-.012,1.892,1.35]
Position_113_Left = [.015,1.95,1.35]
Position_061_Left = [-.019,1.927,1.35]
Position_104_Left = [-.015,1.90,1.35]
Position_114_Left = [.04,1.927,1.35]
Position_051_Left = [-0.025,1.888,1.35]
Position_055_Left = [.007,1.97,1.35]
Position_054_Left = [-0.025,1.915,1.35]
Position_058_Left = [.04,1.96,1.35]
Position_103_Left = [.065,1.895,1.35]

#Position variables for the right eye
Position_102_Right = [.015,1.923,1.35]
Position_112_Right = [-.050,2.005,1.35]
Position_060_Right = [-.010,1.914,1.35]
Position_113_Right = [.000,1.973,1.35]
Position_061_Right = [-.022,1.951,1.35]
Position_104_Right = [-.028,1.924,1.35]
Position_114_Right = [.02,1.952,1.35]
Position_051_Right = [-0.025,1.915,1.35]
Position_055_Right = [.007,1.993,1.35]
Position_054_Right = [-.023,1.94,1.35]
Position_058_Right = [.038,1.983,1.35]
Position_103_Right = [.05,1.92,1.35]

#Scale varibles for the rectangular reticle that identifies the area of the hill to estimate
#Each variable contains the scale of the reticle for each photograph

#Scale variables for the left eye
```

```
Scale_102_Left = [0.08,0.06,1]
Scale_112_Left = [0.1,0.09,1]
Scale_060_Left = [0.1,0.07,1]
Scale_113_Left = [0.1,0.15,1]
Scale_061_Left = [0.15,0.22,1]
Scale_104_Left = [0.1,0.07,1]
Scale_114_Left = [0.15,0.22,1]
Scale_051_Left = [0.08,0.06,1]
Scale_055_Left = [0.1,0.15,1]
Scale_054_Left = [0.07,0.1,1]
Scale_058_Left = [0.1,0.09,1]
Scale_103_Left = [0.07,0.1,1]

#Scale variables for the right eye
Scale_102_Right = [0.08,0.06,1]
Scale_112_Right = [0.1,0.09,1]
Scale_060_Right = [0.1,0.07,1]
Scale_113_Right = [0.1,0.15,1]
Scale_061_Right = [0.15,0.22,1]
Scale_104_Right = [0.1,0.07,1]
Scale_114_Right = [0.15,0.22,1]
Scale_051_Right = [0.08,0.06,1]
Scale_055_Right = [0.1,0.15,1]
Scale_054_Right = [0.07,0.1,1]
Scale_058_Right = [0.1,0.09,1]
Scale_103_Right = [0.07,0.1,1]

#Create the reticle object for the left eye
reticleLeft = viz.add('reticle2.wrl',viz.WORLD,1)
#Add the position variables to an array for each session (left eye)
reticleLeftPositionArray0 = [[0,0,0],[.017,1.83,1.35],[.098,1.80,1.35],[.025,1.83,1.35],[.005,1.818,1.35]]
reticleLeftPositionArray1 = [[0,0,0],Position_102_Left, Position_112_Left, Position_060_Left, Position_113_Left, Position_061_Left,
**Position_104_Left, Position_114_Left, Position_051_Left, Position_055_Left, Position_054_Left, Position_058_Left,
**Position_103_Left]
reticleLeftPositionArray2 = [[0,0,0],Position_061_Left, Position_112_Left, Position_055_Left, Position_058_Left, Position_104_Left,
**Position_054_Left, Position_060_Left, Position_102_Left, Position_113_Left, Position_114_Left, Position_051_Left,
**Position_103_Left]
reticleLeftPositionArray3 = [[0,0,0],Position_103_Left, Position_051_Left, Position_114_Left, Position_113_Left, Position_102_Left,
**Position_060_Left, Position_054_Left, Position_104_Left, Position_058_Left, Position_055_Left, Position_112_Left,
**Position_061_Left]
reticleLeftPositionArray4 = [[0,0,0],Position_103_Left, Position_058_Left, Position_054_Left, Position_055_Left, Position_051_Left,
**Position_114_Left, Position_104_Left, Position_061_Left, Position_113_Left, Position_060_Left, Position_112_Left,
**Position_102_Left]
#Add the scale variables to an array for each session (left eye)
reticleLeftScaleArray0 = [[0.25,0.25,1],[0.1,0.07,1],[0.03,0.04,1],[0.08,0.10,1],[0.05,0.03,1]]
reticleLeftScaleArray1 = [[0.25,0.25,1],Scale_102_Left, Scale_112_Left, Scale_060_Left, Scale_113_Left, Scale_061_Left,
**Scale_104_Left, Scale_114_Left, Scale_051_Left, Scale_055_Left, Scale_054_Left, Scale_058_Left, Scale_103_Left]
reticleLeftScaleArray2 = [[0.25,0.25,1],Scale_061_Left, Scale_112_Left, Scale_055_Left, Scale_058_Left, Scale_104_Left,
**Scale_054_Left, Scale_060_Left, Scale_102_Left, Scale_113_Left, Scale_114_Left, Scale_051_Left, Scale_103_Left]
reticleLeftScaleArray3 = [[0.25,0.25,1],Scale_103_Left, Scale_051_Left, Scale_114_Left, Scale_113_Left, Scale_102_Left,
**Scale_060_Left, Scale_054_Left, Scale_104_Left, Scale_058_Left, Scale_055_Left, Scale_102_Left, Scale_061_Left]
reticleLeftScaleArray4 = [[0.25,0.25,1],Scale_103_Left, Scale_058_Left, Scale_054_Left, Scale_055_Left, Scale_051_Left,
**Scale_114_Left, Scale_104_Left, Scale_061_Left, Scale_113_Left, Scale_060_Left, Scale_112_Left, Scale_102_Left]

#Create the reticle object for the right eye
reticleRight = viz.add('reticle2.wrl',viz.WORLD,2)
#Add the position variables to an array for each session (right eye)
reticleRightPositionArray0 = [[0,0,0],[.015,1.855,1.35],[.1,1.824,1.35],[.005,1.855,1.35],[-.01,1.842,1.35]]
reticleRightPositionArray1 = [[0,0,0],Position_102_Left, Position_112_Left, Position_060_Left, Position_113_Left,
**Position_061_Left, Position_104_Left, Position_114_Left, Position_051_Left, Position_055_Left, Position_054_Left,
**Position_058_Left, Position_103_Left]
reticleRightPositionArray2 = [[0,0,0],Position_061_Right, Position_112_Right, Position_055_Right, Position_058_Right,
**Position_104_Right, Position_054_Right, Position_060_Right, Position_102_Right, Position_113_Right, Position_114_Right,
**Position_051_Right, Position_103_Right]
reticleRightPositionArray3 = [[0,0,0],Position_103_Left, Position_051_Left, Position_114_Left, Position_113_Left,
**Position_102_Left, Position_060_Left, Position_054_Left, Position_104_Left, Position_058_Left, Position_055_Left,
**Position_112_Left, Position_061_Left]
reticleRightPositionArray4 = [[0,0,0],Position_103_Right, Position_058_Right, Position_054_Right, Position_055_Right,
**Position_051_Right, Position_114_Right, Position_104_Right, Position_061_Right, Position_113_Right, Position_060_Right,
**Position_112_Right, Position_102_Right]
```

```
#Add the scale variables to an array for each session (right eye)
reticleRightScaleArray0 = [[0.25,0.25,1],[0.1,0.07,1],[0.03,0.04,1],[0.08,0.10,1],[0.05,0.03,1]]
reticleRightScaleArray1 = [[0.25,0.25,1],Scale_102_Left, Scale_112_Left, Scale_060_Left, Scale_113_Left, Scale_061_Left,
**Scale_104_Left, Scale_114_Left, Scale_051_Left, Scale_055_Left, Scale_054_Left, Scale_058_Left, Scale_103_Left]
reticleRightScaleArray2 = [[0.25,0.25,1],Scale_061_Right, Scale_112_Right, Scale_055_Right, Scale_058_Right, Scale_104_Right,
**Scale_054_Right, Scale_060_Right, Scale_102_Right, Scale_113_Right, Scale_114_Right, Scale_051_Right, Scale_103_Right]
reticleRightScaleArray3 = [[0.25,0.25,1],Scale_103_Left, Scale_051_Left, Scale_114_Left, Scale_113_Left, Scale_102_Left,
**Scale_060_Left, Scale_054_Left, Scale_104_Left, Scale_058_Left, Scale_055_Left, Scale_102_Left, Scale_061_Left]
reticleRightScaleArray4 = [[0.25,0.25,1],Scale_103_Right, Scale_058_Right, Scale_054_Right, Scale_055_Right, Scale_051_Right,
**Scale_114_Right, Scale_104_Right, Scale_061_Right, Scale_113_Right, Scale_060_Right, Scale_112_Right, Scale_102_Right]

#Create a beep sound to be used when the reticle is displayed
beep = viz.addAudio('BUZZER.wav')
beep.volume(.5)
beep.setTime(3)

#Create a sound to advise the subject when each session is complete
JFK = viz.addAudio('jfk.wav')
beep.volume(.5)
beep.setTime(3)

#Slider and labels for adjusting distance - set visible ON if using slider
sliderLeft = viz.add(viz.SLIDER,1)
sliderLeft.horizontal()
sliderLeft.setPosition(.49,.2)
sliderLeft.setScale(1,1)
sliderLeft.visible(viz.OFF)
sliderRight = viz.add(viz.SLIDER,2)
sliderRight.horizontal()
sliderRight.setPosition(.472,.229)
sliderRight.setScale(1,1)
sliderRight.visible(viz.OFF)
distanceTitleLeft = viz.add(viz.TEXT3D,'',viz.WORLD,1)
distanceTitleLeft.message('Distance')
distanceTitleLeft.setPosition([0,1.65,1.34])
distanceTitleLeft.setScale([.03,.03,1])
distanceTitleLeft.resolution(1)
distanceTitleLeft.alignment(viz.TEXT_CENTER_CENTER)
distanceTitleLeft.color(viz.BLACK)
distanceTitleLeft.visible(viz.OFF)
distanceTitleRight = viz.add(viz.TEXT3D,'',viz.WORLD,2)
distanceTitleRight.message('Distance')
distanceTitleRight.setPosition([-.043,1.677,1.34])
distanceTitleRight.setScale([.03,.03,1])
distanceTitleRight.resolution(1)
distanceTitleRight.alignment(viz.TEXT_CENTER_CENTER)
distanceTitleRight.color(viz.BLACK)
distanceTitleRight.visible(viz.OFF)
distanceBoxLeft = viz.add(viz.TEXT3D,'',viz.WORLD,1)
distanceBoxLeft.setPosition([0,1.6,1.34])
distanceBoxLeft.setScale([.03,.03,1])
distanceBoxLeft.resolution(1)
distanceBoxLeft.alignment(viz.TEXT_CENTER_CENTER)
distanceBoxLeft.color(viz.BLACK)
distanceBoxLeft.visible(viz.OFF)
distanceBoxRight = viz.add(viz.TEXT3D,'',viz.WORLD,2)
distanceBoxRight.setPosition([-.043,1.627,1.34])
distanceBoxRight.setScale([.03,.03,1])
distanceBoxRight.resolution(1)
distanceBoxRight.alignment(viz.TEXT_CENTER_CENTER)
distanceBoxRight.color(viz.BLACK)
distanceBoxRight.visible(viz.OFF)



#Create a timer function that will define when to make the reticle visible and when to play the beep
def onTimer(num):
        #Set the position and scales of the reticle in the Training Sequence
        if num == 0 and session == 0:
                CurrentLeftPosition = reticleLeftPositionArray0.pop()
```

```
		reticleLeft.setPosition(CurrentLeftPosition)
		reticleLeft.setScale(reticleLeftScaleArray0.pop())
		if CurrentLeftPosition == [0,0,0]:
			JFK.play()
		else:
			beep.play()
		reticleLeft.visible(viz.ON)
		reticleRight.setPosition(reticleRightPositionArray0.pop())
		reticleRight.setScale(reticleRightScaleArray0.pop())
		reticleRight.visible(viz.ON)
		viz.starttimer(1,2)
#Set the position and scales of the reticle in Session 1
elif num == 0 and session == 1:
		beep.play()
		reticleLeft.setPosition(reticleLeftPositionArray1.pop())
		reticleLeft.setScale(reticleLeftScaleArray1.pop())
		reticleLeft.visible(viz.ON)
		reticleRight.setPosition(reticleRightPositionArray1.pop())
		reticleRight.setScale(reticleRightScaleArray1.pop())
		reticleRight.visible(viz.ON)
		viz.starttimer(1,2)
#Set the position and scales of the reticle in Session 2
elif num == 0 and session == 2:
		beep.play()
		reticleLeft.setPosition(reticleLeftPositionArray2.pop())
		reticleLeft.setScale(reticleLeftScaleArray2.pop())
		reticleLeft.visible(viz.ON)
		reticleRight.setPosition(reticleRightPositionArray2.pop())
		reticleRight.setScale(reticleRightScaleArray2.pop())
		reticleRight.visible(viz.ON)
		viz.starttimer(1,2)
#Set the position and scales of the reticle in Session 3
elif num == 0 and session == 3:
		beep.play()
		reticleLeft.setPosition(reticleLeftPositionArray3.pop())
		reticleLeft.setScale(reticleLeftScaleArray3.pop())
		reticleLeft.visible(viz.ON)
		reticleRight.setPosition(reticleRightPositionArray3.pop())
		reticleRight.setScale(reticleRightScaleArray3.pop())
		reticleRight.visible(viz.ON)
		viz.starttimer(1,2)
#Set the position and scales of the reticle in Session 4
elif num == 0 and session == 4:
		beep.play()
		reticleLeft.setPosition(reticleLeftPositionArray4.pop())
		reticleLeft.setScale(reticleLeftScaleArray4.pop())
		reticleLeft.visible(viz.ON)
		reticleRight.setPosition(reticleRightPositionArray4.pop())
		reticleRight.setScale(reticleRightScaleArray4.pop())
		reticleRight.visible(viz.ON)
		viz.starttimer(1,2)
#Turn off the visibility of the reticle after 2 seconds
elif num == 1:
		reticleLeft.visible(viz.OFF)
		reticleRight.visible(viz.OFF)
		greenLeft.visible(viz.ON)
		whiteLeft.visible(viz.ON)
		wedgeLeft.visible(viz.ON)
		greenRight.visible(viz.ON)
		whiteRight.visible(viz.ON)
		wedgeRight.visible(viz.ON)
elif num == 2:
		reticleLeft.visible(viz.ON)
		reticleRight.visible(viz.ON)
		beep.play()
		viz.starttimer(3,2)
elif num == 3:
		reticleLeft.visible(viz.OFF)
		reticleRight.visible(viz.OFF)
```

```
#Create mouse function that manipulates the visibility of the visual estimation device
def onMouseDown(button):
	#Turn on the visibility of the device if the left mouse buttom is pressed
	if button == viz.MOUSEBUTTON_LEFT:
		greenLeft.visible(viz.ON)
		whiteLeft.visible(viz.ON)
		wedgeLeft.visible(viz.ON)
		greenRight.visible(viz.ON)
		whiteRight.visible(viz.ON)
		wedgeRight.visible(viz.ON)
	#Turn off the visibility of the device if the right mouse buttom is pressed
	if button == viz.MOUSEBUTTON_RIGHT:
		greenLeft.visible(viz.OFF)
		whiteLeft.visible(viz.OFF)
		wedgeLeft.visible(viz.OFF)
		greenRight.visible(viz.OFF)
		whiteRight.visible(viz.OFF)
		wedgeRight.visible(viz.OFF)

#Defines wedge rotation using the slider
def myslider(obj, pos):
	print pos

#Create key function to adjust the visual estimation device, record th and progress through the p
def onkeydown(key):
	#Obtain the current slope of the wedge in the visual estimation device
	current_slope = wedgeLeft.getAxisAngle(viz.ABS_PARENT)
	current_distance = sliderLeft.get()
	#If the Up arrow is pressed, increase the slope of the wedge by 0.5 degrees
	if key == viz.KEY_UP and current_slope[3] < 90:
		wedgeLeft.addAction(rotateCounter)
		wedgeRight.addAction(rotateCounter)
	#If the Down arrow is pressed, decrease the slope of the wedge by 0.5 degrees
	elif key == viz.KEY_DOWN and current_slope[3] > 0 and current_slope[2] == 1 and current_slope[3] >= 0.0001:
		wedgeLeft.addAction(rotateClock)
		wedgeRight.addAction(rotateClock)
	elif key == viz.KEY_RIGHT:
		sliderLeft.set(current_distance + .01)
		sliderRight.set(current_distance + .01)
		distanceBoxLeft.message(str(int(current_distance*100)) + ' m')
		distanceBoxRight.message(str(int(current_distance*100)) + ' m')
	elif key == viz.KEY_LEFT:
		sliderLeft.set(current_distance - .01)
		sliderRight.set(current_distance - .01)
		distanceBoxLeft.message(str(int(current_distance*100)) + ' m')
		distanceBoxRight.message(str(int(current_distance*100)) + ' m')
	elif key == viz.KEY_ALT_L:
		viz.starttimer(2,1)
	elif key == ' ':
			infoBoxLeftTitle.visible(viz.OFF)
			infoBoxRightTitle.visible(viz.OFF)
			infoBoxLeft.visible(viz.OFF)
			infoBoxRight.visible(viz.OFF)
			#If TRAINING, display the distance to the base of the slope
			if greenLeft.getVisible() == True:
				#Turn off the visibility of the visual estimation device
				greenLeft.visible(viz.OFF)
				wedgeLeft.visible(viz.OFF)
				greenRight.visible(viz.OFF)
				wedgeRight.visible(viz.OFF)
				#Turn on the visibility of the distance estimation device
				sliderLeft.visible(viz.ON)
				sliderRight.visible(viz.ON)
				distanceTitleLeft.visible(viz.ON)
				distanceTitleRight.visible(viz.ON)
				distanceBoxLeft.visible(viz.ON)
				distanceBoxRight.visible(viz.ON)
				#Record the slope of the wedge into a data file
				estimation_data.write(str(int(current_slope[3]))+' ')
				#Reset the distance to zero
```

```
                sliderLeft.set(0)
                sliderRight.set(0)
                distanceBoxLeft.message('0 m')
                distanceBoxRight.message('0 m')

        else:
                #Start the timer for the reticle appearance
                viz.starttimer(0,3)
                #Turn off the visibility of the distance estimation device
                sliderLeft.visible(viz.OFF)
                sliderRight.visible(viz.OFF)
                distanceTitleLeft.visible(viz.OFF)
                distanceTitleRight.visible(viz.OFF)
                distanceBoxLeft.visible(viz.OFF)
                distanceBoxRight.visible(viz.OFF)
                whiteLeft.visible(viz.OFF)
                whiteRight.visible(viz.OFF)
                #Record the distance into the data file
                estimation_data.write(str(int(current_distance*100))+'\n')
                #Reset the slope of the wedge to zero
                wedgeLeft.setAxisAngle([0.0,0.0,1.0,0.0], viz.ABS_PARENT)
                wedgeRight.setAxisAngle([0.0,0.0,1.0,0.0], viz.ABS_PARENT)
                #Remove the next scene from the photograph arrays
                if session == 0:
                        infoBoxDistanceLeft.message(DistanceLeftArray.pop())
                        infoBoxDistanceRight.message(DistanceRightArray.pop())
                        textureLeft = left0.pop()
                        textureRight = right0.pop()
                if session == 1:
                        textureLeft = left1.pop()
                        textureRight = right1.pop()
                elif session == 2:
                        textureLeft = left2.pop()
                        textureRight = right2.pop()
                elif session == 3:
                        textureLeft = left3.pop()
                        textureRight = right3.pop()
                elif session == 4:
                        textureLeft = left4.pop()
                        textureRight = right4.pop()
                #Attach the scene as a texture to the rectangles
                quad1.texture(viz.add(textureLeft))
                quad2.texture(viz.add(textureRight))
                #Display text indicating when the session is complete
                if textureLeft == 'EndSession.jpg':
                        infoBoxEndSessionLeft.visible(viz.ON)
                        infoBoxEndSessionRight.visible(viz.ON)

#Action callback code for mouse/keyboard/timer events
viz.callback(viz.MOUSEDOWN_EVENT, onMouseDown)
viz.callback(viz.KEYDOWN_EVENT,onkeydown)
viz.callback(viz.TIMER_EVENT, onTimer)
viz.callback(viz.SLIDER_EVENT,myslider)
```

E.2 MDRS VR Study (MVS)

```
#Human Slope and Distance Estimation of MDRS Terrain

#Christopher Oravetz
#Man Vehicle Lab - MIT
#16 June 2008

import viz
import vizinfo

viz.go(viz.STEREO | viz.FULLSCREEN)
viz.ipd(0.13)

#Input Session Number (Training = 0, Standing = 1,4, Supine = 2,3) and Subject Number
session = viz.input('Session')
subject = viz.input('What is your subject number?')
estimation_data = open('Subject #'+str(subject), 'a')

#Initialize photograph arrays
left0 = []
right0 = []
left1 = []
right1 = []
left2 = []
right2 = []
left3 = []
right3 = []
left4 = []
right4 = []

#Append photograph arrays with all photographs
#EndSession photographs is only a white background
#All photographs were previously scaled to 2048x1024 to be quickly uploaded by Vizard
left0.append('EndSession.jpg')
left0.append('MDRS_Left_062_scaled2.jpg')
left0.append('MDRS_Left_063_scaled2.jpg')
left0.append('MDRS_Left_110_scaled2.jpg')
left0.append('MDRS_Left_111_scaled2.jpg')
left0.append('MDRS_Left_106_scaled2.jpg')

right0.append('EndSession.jpg')
right0.append('MDRS_Left_062_scaled2.jpg')
right0.append('MDRS_Left_063_scaled2.jpg')
right0.append('MDRS_Left_110_scaled2.jpg')
right0.append('MDRS_Left_111_scaled2.jpg')
right0.append('MDRS_Left_106_scaled2.jpg')

left1.append('EndSession.jpg')
left1.append('MDRS_Left_102_scaled2.jpg')
left1.append('MDRS_Left_112_scaled2.jpg')
left1.append('MDRS_Left_060_scaled2.jpg')
left1.append('MDRS_Left_113_scaled2.jpg')
left1.append('MDRS_Left_061_scaled2.jpg')
left1.append('MDRS_Left_104_scaled2.jpg')
left1.append('MDRS_Left_114_scaled2.jpg')
left1.append('MDRS_Left_051_scaled2.jpg')
left1.append('MDRS_Left_055_scaled2.jpg')
left1.append('MDRS_Left_054_scaled2.jpg')
left1.append('MDRS_Left_058_scaled2.jpg')
left1.append('MDRS_Left_103_scaled2.jpg')

left2.append('EndSession.jpg')
left2.append('MDRS_Left_061_scaled2.jpg')
left2.append('MDRS_Left_112_scaled2.jpg')
left2.append('MDRS_Left_055_scaled2.jpg')
left2.append('MDRS_Left_058_scaled2.jpg')
left2.append('MDRS_Left_104_scaled2.jpg')
left2.append('MDRS_Left_054_scaled2.jpg')
```

```
left2.append('MDRS_Left_060_scaled2.jpg')
left2.append('MDRS_Left_102_scaled2.jpg')
left2.append('MDRS_Left_113_scaled2.jpg')
left2.append('MDRS_Left_114_scaled2.jpg')
left2.append('MDRS_Left_051_scaled2.jpg')
left2.append('MDRS_Left_103_scaled2.jpg')

left3.append('EndSession.jpg')
left3.append('MDRS_Left_103_scaled2.jpg')
left3.append('MDRS_Left_051_scaled2.jpg')
left3.append('MDRS_Left_114_scaled2.jpg')
left3.append('MDRS_Left_113_scaled2.jpg')
left3.append('MDRS_Left_102_scaled2.jpg')
left3.append('MDRS_Left_060_scaled2.jpg')
left3.append('MDRS_Left_054_scaled2.jpg')
left3.append('MDRS_Left_104_scaled2.jpg')
left3.append('MDRS_Left_058_scaled2.jpg')
left3.append('MDRS_Left_055_scaled2.jpg')
left3.append('MDRS_Left_112_scaled2.jpg')
left3.append('MDRS_Left_061_scaled2.jpg')

left4.append('EndSession.jpg')
left4.append('MDRS_Left_103_scaled2.jpg')
left4.append('MDRS_Left_058_scaled2.jpg')
left4.append('MDRS_Left_054_scaled2.jpg')
left4.append('MDRS_Left_055_scaled2.jpg')
left4.append('MDRS_Left_051_scaled2.jpg')
left4.append('MDRS_Left_114_scaled2.jpg')
left4.append('MDRS_Left_104_scaled2.jpg')
left4.append('MDRS_Left_061_scaled2.jpg')
left4.append('MDRS_Left_113_scaled2.jpg')
left4.append('MDRS_Left_060_scaled2.jpg')
left4.append('MDRS_Left_112_scaled2.jpg')
left4.append('MDRS_Left_102_scaled2.jpg')

#Right eye is presented the same images as the left eye in a synoptic configuration
right1.append('EndSession.jpg')
right1.append('MDRS_Left_102_scaled2.jpg')
right1.append('MDRS_Left_112_scaled2.jpg')
right1.append('MDRS_Left_060_scaled2.jpg')
right1.append('MDRS_Left_113_scaled2.jpg')
right1.append('MDRS_Left_061_scaled2.jpg')
right1.append('MDRS_Left_104_scaled2.jpg')
right1.append('MDRS_Left_114_scaled2.jpg')
right1.append('MDRS_Left_051_scaled2.jpg')
right1.append('MDRS_Left_055_scaled2.jpg')
right1.append('MDRS_Left_054_scaled2.jpg')
right1.append('MDRS_Left_058_scaled2.jpg')
right1.append('MDRS_Left_103_scaled2.jpg')

right2.append('EndSession.jpg')
right2.append('MDRS_Left_061_scaled2.jpg')
right2.append('MDRS_Left_112_scaled2.jpg')
right2.append('MDRS_Left_055_scaled2.jpg')
right2.append('MDRS_Left_058_scaled2.jpg')
right2.append('MDRS_Left_104_scaled2.jpg')
right2.append('MDRS_Left_054_scaled2.jpg')
right2.append('MDRS_Left_060_scaled2.jpg')
right2.append('MDRS_Left_102_scaled2.jpg')
right2.append('MDRS_Left_113_scaled2.jpg')
right2.append('MDRS_Left_114_scaled2.jpg')
right2.append('MDRS_Left_051_scaled2.jpg')
right2.append('MDRS_Left_103_scaled2.jpg')

right3.append('EndSession.jpg')
right3.append('MDRS_Left_103_scaled2.jpg')
right3.append('MDRS_Left_051_scaled2.jpg')
right3.append('MDRS_Left_114_scaled2.jpg')
right3.append('MDRS_Left_113_scaled2.jpg')
right3.append('MDRS_Left_102_scaled2.jpg')
```

```
right3.append('MDRS_Left_060_scaled2.jpg')
right3.append('MDRS_Left_054_scaled2.jpg')
right3.append('MDRS_Left_104_scaled2.jpg')
right3.append('MDRS_Left_058_scaled2.jpg')
right3.append('MDRS_Left_055_scaled2.jpg')
right3.append('MDRS_Left_112_scaled2.jpg')
right3.append('MDRS_Left_061_scaled2.jpg')

right4.append('EndSession.jpg')
right4.append('MDRS_Left_103_scaled2.jpg')
right4.append('MDRS_Left_058_scaled2.jpg')
right4.append('MDRS_Left_054_scaled2.jpg')
right4.append('MDRS_Left_055_scaled2.jpg')
right4.append('MDRS_Left_051_scaled2.jpg')
right4.append('MDRS_Left_114_scaled2.jpg')
right4.append('MDRS_Left_104_scaled2.jpg')
right4.append('MDRS_Left_061_scaled2.jpg')
right4.append('MDRS_Left_113_scaled2.jpg')
right4.append('MDRS_Left_060_scaled2.jpg')
right4.append('MDRS_Left_112_scaled2.jpg')
right4.append('MDRS_Left_102_scaled2.jpg')

#Turn Off mouse navigation and visibility of the mouse
viz.mouse(viz.OFF)
viz.mouse.setVisible(viz.OFF)

#Create two rectangles to map images on as textures
quad1 = viz.add(viz.TEXQUAD)
quad2 = viz.add(viz.TEXQUAD,viz.WORLD,2)
quad1.setScale(1.3333333333333333333333333333333333333333333333333333,1,1)
quad2.setScale(1.3333333333333333333333333333333333333333333333333333,1,1)

#Instructions upon start of each session
#infoBoxLeftTitle displays the Session Number to the left eye
infoBoxLeftTitle = viz.add(viz.TEXT3D,'',viz.WORLD,1)
infoBoxLeftTitle.message('Session #'+ str(session))
infoBoxLeftTitle.setPosition([0,1.92,1.3])
infoBoxLeftTitle.setScale([.05,.05,1])
infoBoxLeftTitle.resolution(1)
infoBoxLeftTitle.alignment(viz.TEXT_CENTER_CENTER)
infoBoxLeftTitle.color(viz.BLACK)

#infoBoxLeft diplays the body position instructions to the left eye
#infoBoxTrain Left displays the word "Training"
infoBoxLeft = viz.add(viz.TEXT3D,'',viz.WORLD,1)
infoBoxTrainLeft = viz.add(viz.TEXT3D,'',viz.WORLD,1)
if session == 0:
        infoBoxLeft.message('Estimate the following slopes in the Standing Position')
        infoBoxTrainLeft.message('TRAINING')
elif session == 1 or session == 4:
        infoBoxLeft.message('Estimate the following slopes in the Standing Position')
elif session == 2 or session == 3:
        infoBoxLeft.message('Estimate the following slopes in the Supine Position')
infoBoxLeft.setPosition([0,1.84,1.379])
infoBoxLeft.setScale([.03,.03,1])
infoBoxLeft.resolution(1)
infoBoxLeft.alignment(viz.TEXT_CENTER_CENTER)
infoBoxLeft.color(viz.BLACK)
infoBoxTrainLeft.setPosition([0,2.0,1.379])
infoBoxTrainLeft.setScale([.05,.05,1])
infoBoxTrainLeft.resolution(1)
infoBoxTrainLeft.alignment(viz.TEXT_CENTER_CENTER)
infoBoxTrainLeft.color(viz.RED)

#infoBoxRightTitle displays the Session Number to the right eye
infoBoxRightTitle = viz.add(viz.TEXT3D,'',viz.WORLD,2)
infoBoxRightTitle.message('Session #' + str(session))
infoBoxRightTitle.setPosition([0,1.92,1.3])
infoBoxRightTitle.setScale([.05,.05,1.3])
infoBoxRightTitle.resolution(1)
```

```
infoBoxRightTitle.alignment(viz.TEXT_CENTER_CENTER)
infoBoxRightTitle.color(viz.BLACK)

#infoBoxRight diplays the body position instructions to the right eye
#infoBoxTrainRight displays the word "Training"
infoBoxRight = viz.add(viz.TEXT3D,'',viz.WORLD,2)
infoBoxTrainRight = viz.add(viz.TEXT3D,'',viz.WORLD,2)
if session == 0:
	infoBoxRight.message('Estimate the following slopes in the Standing Position')
	infoBoxTrainRight.message('TRAINING')
elif session == 1 or session == 4:
	infoBoxRight.message('Estimate the following slopes in the Standing Position')
elif session == 2 or session == 3:
	infoBoxRight.message('Estimate the following slopes in the Supine Position')
infoBoxRight.setPosition([0,1.84,1.379])
infoBoxRight.setScale([.03,.03,1])
infoBoxRight.resolution(1)
infoBoxRight.alignment(viz.TEXT_CENTER_CENTER)
infoBoxRight.color(viz.BLACK)
infoBoxTrainRight.setPosition([0,2.0,1.379])
infoBoxTrainRight.setScale([.05,.05,1])
infoBoxTrainRight.resolution(1)
infoBoxTrainRight.alignment(viz.TEXT_CENTER_CENTER)
infoBoxTrainRight.color(viz.RED)

#infoBoxEndSessionLeft notifies the subject of the end of the session and is displayed in the left eye
infoBoxEndSessionLeft = viz.add(viz.TEXT3D,'',viz.WORLD,1)
infoBoxEndSessionLeft.message('End of Session')
infoBoxEndSessionLeft.setPosition([0,1.9,1.35])
infoBoxEndSessionLeft.setScale([.1,.1,1])
infoBoxEndSessionLeft.resolution(1)
infoBoxEndSessionLeft.alignment(viz.TEXT_CENTER_CENTER)
infoBoxEndSessionLeft.color(viz.BLACK)
infoBoxEndSessionLeft.visible(viz.OFF)

#infoBoxEndSessionRight notifies the subject of the end of the session and is displayed in the right eye
infoBoxEndSessionRight = viz.add(viz.TEXT3D,'',viz.WORLD,2)
infoBoxEndSessionRight.message('End of Session')
infoBoxEndSessionRight.setPosition([-.003,1.9,1.35])
infoBoxEndSessionRight.setScale([.1,.1,1])
infoBoxEndSessionRight.resolution(1)
infoBoxEndSessionRight.alignment(viz.TEXT_CENTER_CENTER)
infoBoxEndSessionRight.color(viz.BLACK)
infoBoxEndSessionRight.visible(viz.OFF)

#Set the position of the Quads containing the photographs so they are in the center of each eye and they take of the entire screen
quad1.setPosition([0,1.82,1.38])
quad2.setPosition([0,1.82,1.38])

#Visual estimation device - semicircular wedge - for the left eye
wedgeLeft = viz.add('wedge2.ac',viz.WORLD,1)
wedgeLeft.setPosition(.4,1.5,1.34998)
wedgeLeft.color(viz.BLACK)
wedgeLeft.center([-.5,0,0])
wedgeLeft.setScale([.2,.2,.2])
wedgeLeft.visible(viz.OFF)

#Visual estimation device - semicircular wedge - for the right eye
wedgeRight = viz.add('wedge2.ac',viz.WORLD,2)
wedgeRight.setPosition(.357,1.5,1.34998)
wedgeRight.setScale([.2,.2,.2])
wedgeRight.color(viz.BLACK)
wedgeRight.center([-.5,0,0])
wedgeRight.visible(viz.OFF)

#Ground reference within the visual estimation device for the left eye
greenLeft = viz.add(viz.TEXQUAD,viz.WORLD,1)
greenLeft.setScale([.3,.11,1])
greenLeft.setPosition([0,1,1.34999])
greenLeft.center([0,.5,0])
```

```
greenLeft.color(viz.GREEN)
greenLeft.visible(viz.OFF)

#Sky reference within the visual estimation device for the left eye
whiteLeft = viz.add(viz.TEXQUAD,viz.WORLD,1)
whiteLeft.setScale([.3,.31,1])
whiteLeft.setPosition([0,1.2,1.35])
whiteLeft.center([0,.5,0])
whiteLeft.color(viz.WHITE)
whiteLeft.visible(viz.OFF)

#Ground reference within the visual estimation device for the right eye
greenRight = viz.add(viz.TEXQUAD,viz.WORLD,2)
greenRight.setScale([.3,.11,1])
greenRight.setPosition([-.043,1.0,1.34999])
greenRight.center([0,.5,0])
greenRight.color(viz.GREEN)
greenRight.visible(viz.OFF)

#Sky reference within the visual estimation device for the right eye
whiteRight = viz.add(viz.TEXQUAD,viz.WORLD,2)
whiteRight.setScale([.3,.31,1])
whiteRight.setPosition([-.043,1.2,1.35])
whiteRight.center([0,.5,0])
whiteRight.color(viz.WHITE)
whiteRight.visible(viz.OFF)

#Create scenes for each eye
viz.scene(1,viz.LEFT_EYE)
viz.scene(2,viz.RIGHT_EYE)

#Define rotation actions of the visual estimation wedge
rotateCounter = vizact.spin(0,0,1,50,.01)
rotateClock = vizact.spin(0,0,1,-50,.01)

#Add rotation actions to the wedges in the left and right scenes
wedgeLeft.addAction(rotateCounter)
wedgeLeft.addAction(rotateClock)
wedgeRight.addAction(rotateCounter)
wedgeRight.addAction(rotateClock)

#Position varibles for the rectangular reticle that identifies the area of the hill to estimate
#Each variable contains the location of the reticle for each photograph

#Position variables for the left eye
Position_102 = [.03,1.899,1.35]
Position_112 =        [-.032,1.983,1.35]
Position_060 = [-.012,1.892,1.35]
Position_113 =        [.015,1.95,1.35]
Position_061 = [-.019,1.927,1.35]
Position_104 = [-.015,1.90,1.35]
Position_114 = [.04,1.927,1.35]
Position_051 = [-0.025,1.888,1.35]
Position_055 = [.007,1.97,1.35]
Position_054 = [-0.025,1.915,1.35]
Position_058 = [.04,1.96,1.35]
Position_103 = [.065,1.895,1.35]

#Scale varibles for the rectangular reticle that identifies the area of the hill to estimate
#Each variable contains the scale of the reticle for each photograph

#Scale variables for the left eye
Scale_102 = [0.08,0.06,1]
Scale_112 = [0.1,0.09,1]
Scale_060 = [0.1,0.07,1]
Scale_113 = [0.1,0.15,1]
Scale_061 = [0.15,0.22,1]
Scale_104 = [0.1,0.07,1]
Scale_114 = [0.15,0.22,1]
Scale_051 = [0.08,0.06,1]
```

```
Scale_055 = [0.1,0.15,1]
Scale_054 = [0.07,0.1,1]
Scale_058 = [0.1,0.09,1]
Scale_103 = [0.07,0.1,1]

#Create the reticle object for the left eye
reticleLeft = viz.add('reticle2.wrl',viz.WORLD,1)
#Add the position variables to an array for each session (left eye)
reticleLeftPositionArray0 = [[0,0,0],[.017,1.83,1.35],[.098,1.80,1.35],[.025,1.83,1.35],[.005,1.818,1.35],[0,1.832,1.35]]
reticleLeftPositionArray1 = [[0,0,0],Position_102, Position_112, Position_060, Position_113, Position_061, Position_104,
**Position_114, Position_051, Position_055, Position_054, Position_058, Position_103]
reticleLeftPositionArray2 = [[0,0,0],Position_061, Position_112, Position_055, Position_058, Position_104, Position_054,
**Position_060, Position_102, Position_113, Position_114, Position_051, Position_103]
reticleLeftPositionArray3 = [[0,0,0],Position_103, Position_051, Position_114, Position_113, Position_102, Position_060,
**Position_054, Position_104, Position_058, Position_055, Position_112, Position_061]
reticleLeftPositionArray4 = [[0,0,0],Position_103, Position_058, Position_054, Position_055, Position_051, Position_114,
**Position_104, Position_061, Position_113, Position_060, Position_112, Position_102]
#Add the scale variables to an array for each session (left eye)
reticleLeftScaleArray0 = [[0.25,0.25,1],[0.1,0.07,1],[0.03,0.04,1],[0.08,0.10,1],[0.05,0.03,1],[0.09,0.04,1]]
reticleLeftScaleArray1 = [[0.25,0.25,1],Scale_102, Scale_112, Scale_060, Scale_113, Scale_061, Scale_104, Scale_114,
**Scale_051, Scale_055, Scale_054, Scale_058, Scale_103]
reticleLeftScaleArray2 = [[0.25,0.25,1],Scale_061, Scale_112, Scale_055, Scale_058, Scale_104, Scale_054, Scale_060,
**Scale_102, Scale_113, Scale_114, Scale_051, Scale_103]
reticleLeftScaleArray3 = [[0.25,0.25,1],Scale_103, Scale_051, Scale_114, Scale_113, Scale_102, Scale_060, Scale_054,
**Scale_104, Scale_058, Scale_055, Scale_102, Scale_061]
reticleLeftScaleArray4 = [[0.25,0.25,1],Scale_103, Scale_058, Scale_054, Scale_055, Scale_051, Scale_114, Scale_104,
**Scale_061, Scale_113, Scale_060, Scale_112, Scale_102]

#Create the reticle object for the right eye
reticleRight = viz.add('reticle2.wrl',viz.WORLD,2)
#Add the position variables to an array for each session (right eye)
reticleRightPositionArray0 = [[0,0,0],[.017,1.83,1.35],[.098,1.80,1.35],[.025,1.83,1.35],[.005,1.818,1.35],[0,1.832,1.35]]
reticleRightPositionArray1 = [[0,0,0],Position_102, Position_112, Position_060, Position_113, Position_061, Position_104,
**Position_114, Position_051, Position_055, Position_054, Position_058, Position_103]
reticleRightPositionArray2 = [[0,0,0],Position_061, Position_112, Position_055, Position_058, Position_104, Position_054,
**Position_060, Position_102, Position_113, Position_114, Position_051, Position_103]
reticleRightPositionArray3 = [[0,0,0],Position_103, Position_051, Position_114, Position_113, Position_102, Position_060,
**Position_054, Position_104, Position_058, Position_055, Position_112, Position_061]
reticleRightPositionArray4 = [[0,0,0],Position_103, Position_058, Position_054, Position_055, Position_051, Position_114,
**Position_104, Position_061, Position_113, Position_060, Position_112, Position_102]
#Add the scale variables to an array for each session (right eye)
reticleRightScaleArray0 = [[0.25,0.25,1],[0.1,0.07,1],[0.03,0.04,1],[0.08,0.10,1],[0.05,0.03,1],[0.09,0.04,1]]
reticleRightScaleArray1 = [[0.25,0.25,1],Scale_102, Scale_112, Scale_060, Scale_113, Scale_061, Scale_104, Scale_114,
**Scale_051, Scale_055, Scale_054, Scale_058, Scale_103]
reticleRightScaleArray2 = [[0.25,0.25,1],Scale_061, Scale_112, Scale_055, Scale_058, Scale_104, Scale_054, Scale_060,
**Scale_102, Scale_113, Scale_114, Scale_051, Scale_103]
reticleRightScaleArray3 = [[0.25,0.25,1],Scale_103, Scale_051, Scale_114, Scale_113, Scale_102, Scale_060, Scale_054,
**Scale_104, Scale_058, Scale_055, Scale_102, Scale_061]
reticleRightScaleArray4 = [[0.25,0.25,1],Scale_103, Scale_058, Scale_054, Scale_055, Scale_051, Scale_114, Scale_104,
**Scale_061, Scale_113, Scale_060, Scale_112, Scale_102]

#Create a beep sound to be used when the reticle is displayed
beep = viz.addAudio('BUZZER.wav')
beep.volume(.5)
beep.setTime(3)

#Slider for adjusting distance - set visible ON if using slider
sliderLeft = viz.add(viz.SLIDER,1)
sliderLeft.horizontal()
sliderLeft.setPosition(.48,.215)
sliderLeft.setScale(1,1)
sliderLeft.visible(viz.OFF)
sliderRight = viz.add(viz.SLIDER,2)
sliderRight.horizontal()
sliderRight.setPosition(.482,.215       )
sliderRight.setScale(1,1)
sliderRight.visible(viz.OFF)

#Title within distance estimation device
distanceTitleLeft = viz.add(viz.TEXT3D,'',viz.WORLD,1)
```

```
distanceTitleLeft.message('Distance')
distanceTitleLeft.setPosition([0,1.65,1.34])
distanceTitleLeft.setScale([.03,.03,1])
distanceTitleLeft.resolution(1)
distanceTitleLeft.alignment(viz.TEXT_CENTER_CENTER)
distanceTitleLeft.color(viz.BLACK)
distanceTitleLeft.visible(viz.OFF)
distanceTitleRight = viz.add(viz.TEXT3D,'',viz.WORLD,2)
distanceTitleRight.message('Distance')
distanceTitleRight.setPosition([-.043,1.65,1.34])
distanceTitleRight.setScale([.03,.03,1])
distanceTitleRight.resolution(1)
distanceTitleRight.alignment(viz.TEXT_CENTER_CENTER)
distanceTitleRight.color(viz.BLACK)
distanceTitleRight.visible(viz.OFF)

#Display upper bound of distance estimation (100 meters)
upperLimitLeft = viz.add(viz.TEXT3D,'',viz.WORLD,1)
upperLimitLeft.setPosition([.128,1.49,1.34])
upperLimitLeft.setScale([.02,.02,1])
upperLimitLeft.message('100')
upperLimitLeft.resolution(1)
upperLimitLeft.alignment(viz.TEXT_CENTER_CENTER)
upperLimitLeft.color(viz.BLACK)
upperLimitLeft.visible(viz.OFF)
upperLimitRight = viz.add(viz.TEXT3D,'',viz.WORLD,2)
upperLimitRight.setPosition([.085,1.49,1.34])
upperLimitRight.setScale([.02,.02,1])
upperLimitRight.message('100')
upperLimitRight.resolution(1)
upperLimitRight.alignment(viz.TEXT_CENTER_CENTER)
upperLimitRight.color(viz.BLACK)
upperLimitRight.visible(viz.OFF)

#Display lower bound of distance estimation (0 meters)
lowerLimitLeft = viz.add(viz.TEXT3D,'',viz.WORLD,1)
lowerLimitLeft.setPosition([-.13,1.49,1.34])
lowerLimitLeft.setScale([.02,.02,1])
lowerLimitLeft.message('0')
lowerLimitLeft.resolution(1)
lowerLimitLeft.alignment(viz.TEXT_CENTER_CENTER)
lowerLimitLeft.color(viz.BLACK)
lowerLimitLeft.visible(viz.OFF)
lowerLimitRight = viz.add(viz.TEXT3D,'',viz.WORLD,2)
lowerLimitRight.setPosition([-.173,1.49,1.34])
lowerLimitRight.setScale([.02,.02,1])
lowerLimitRight.message('0')
lowerLimitRight.resolution(1)
lowerLimitRight.alignment(viz.TEXT_CENTER_CENTER)
lowerLimitRight.color(viz.BLACK)
lowerLimitRight.visible(viz.OFF)

#Display rectangle at lower bound of distance estimation slider
lowerSliderBoundaryLeft = viz.add(viz.TEXQUAD,viz.WORLD,1)
lowerSliderBoundaryLeft.setScale([.015,.04,1])
lowerSliderBoundaryLeft.setPosition([-.132,1.538,1.349])
lowerSliderBoundaryLeft.color(viz.BLUE)
lowerSliderBoundaryLeft.visible(viz.OFF)
lowerSliderBoundaryRight = viz.add(viz.TEXQUAD,viz.WORLD,2)
lowerSliderBoundaryRight.setScale([.015,.04,1])
lowerSliderBoundaryRight.setPosition([-.175,1.538,1.349])
lowerSliderBoundaryRight.color(viz.BLUE)
lowerSliderBoundaryRight.visible(viz.OFF)
upperSliderBoundaryLeft = viz.add(viz.TEXQUAD,viz.WORLD,1)

#Display rectangle at upper bound of distance estimation slider
upperSliderBoundaryLeft.setScale([.015,.04,1])
upperSliderBoundaryLeft.setPosition([.127,1.538,1.349])
upperSliderBoundaryLeft.color(viz.BLUE)
upperSliderBoundaryLeft.visible(viz.OFF)
```

```
upperSliderBoundaryRight = viz.add(viz.TEXQUAD,viz.WORLD,2)
upperSliderBoundaryRight.setScale([.015,.04,1])
upperSliderBoundaryRight.setPosition([.08114,1.538,1.349])
upperSliderBoundaryRight.color(viz.BLUE)
upperSliderBoundaryRight.visible(viz.OFF)

#Display distance for first hill in Training session to use as reference for experiment
distanceBoxLeft = viz.add(viz.TEXT3D,'',viz.WORLD,1)
distanceBoxLeft.message('50 m')
distanceBoxLeft.setPosition([0,2.15,1.35])
distanceBoxLeft.setScale([.03,.03,1])
distanceBoxLeft.resolution(1)
distanceBoxLeft.alignment(viz.TEXT_CENTER_CENTER)
distanceBoxLeft.color(viz.BLACK)
distanceBoxLeft.visible(viz.OFF)
distanceBoxRight = viz.add(viz.TEXT3D,'',viz.WORLD,2)
distanceBoxRight.message('50 m')
distanceBoxRight.setPosition([0,2.15,1.35])
distanceBoxRight.setScale([.03,.03,1])
distanceBoxRight.resolution(1)
distanceBoxRight.alignment(viz.TEXT_CENTER_CENTER)
distanceBoxRight.color(viz.BLACK)
distanceBoxRight.visible(viz.OFF)
infoQuadDistanceLeft = viz.add(viz.TEXQUAD,viz.WORLD,1)
infoQuadDistanceLeft.setScale([.3,.1,1])
infoQuadDistanceLeft.setPosition([0,2.15,1.36])
infoQuadDistanceLeft.color(viz.WHITE)
infoQuadDistanceLeft.visible(viz.OFF)
infoQuadDistanceRight = viz.add(viz.TEXQUAD,viz.WORLD,2)
infoQuadDistanceRight.setScale([.3,.1,1])
infoQuadDistanceRight.setPosition([0,2.15,1.36])
infoQuadDistanceRight.color(viz.WHITE)
infoQuadDistanceRight.visible(viz.OFF)

#Create a timer function that will define when to make the reticle (red box) visible and when to play the beep
def onTimer(num):
	#Set the position and scales of the reticle in the Training Sequence
	if num == 0 and session == 0:
		CurrentLeftPosition = reticleLeftPositionArray0.pop()
		reticleLeft.setPosition(CurrentLeftPosition)
		reticleLeft.setScale(reticleLeftScaleArray0.pop())
		beep.play()
		reticleLeft.visible(viz.ON)
		reticleRight.setPosition(reticleRightPositionArray0.pop())
		reticleRight.setScale(reticleRightScaleArray0.pop())
		reticleRight.visible(viz.ON)
		viz.starttimer(1,2)
	#Set the position and scales of the reticle in the Session A
	elif num == 0 and session == 1:
		beep.play()
		reticleLeft.setPosition(reticleLeftPositionArray1.pop())
		reticleLeft.setScale(reticleLeftScaleArray1.pop())
		reticleLeft.visible(viz.ON)
		reticleRight.setPosition(reticleRightPositionArray1.pop())
		reticleRight.setScale(reticleRightScaleArray1.pop())
		reticleRight.visible(viz.ON)
		viz.starttimer(1,2)
	#Set the position and scales of the reticle in the Session B
	elif num == 0 and session == 2:
		beep.play()
		reticleLeft.setPosition(reticleLeftPositionArray2.pop())
		reticleLeft.setScale(reticleLeftScaleArray2.pop())
		reticleLeft.visible(viz.ON)
		reticleRight.setPosition(reticleRightPositionArray2.pop())
		reticleRight.setScale(reticleRightScaleArray2.pop())
		reticleRight.visible(viz.ON)
		viz.starttimer(1,2)
	#Set the position and scales of the reticle in the Session C
	elif num == 0 and session == 3:
		beep.play()
```

```
                reticleLeft.setPosition(reticleLeftPositionArray3.pop())
                reticleLeft.setScale(reticleLeftScaleArray3.pop())
                reticleLeft.visible(viz.ON)
                reticleRight.setPosition(reticleRightPositionArray3.pop())
                reticleRight.setScale(reticleRightScaleArray3.pop())
                reticleRight.visible(viz.ON)
                viz.starttimer(1,2)
        #Set the position and scales of the reticle in the Session D
        elif num == 0 and session == 4:
                beep.play()
                reticleLeft.setPosition(reticleLeftPositionArray4.pop())
                reticleLeft.setScale(reticleLeftScaleArray4.pop())
                reticleLeft.visible(viz.ON)
                reticleRight.setPosition(reticleRightPositionArray4.pop())
                reticleRight.setScale(reticleRightScaleArray4.pop())
                reticleRight.visible(viz.ON)
                viz.starttimer(1,2)
        #Turn off the visibility of the reticle after 2 seconds
        elif num == 1:
                reticleLeft.visible(viz.OFF)
                reticleRight.visible(viz.OFF)
                if distanceBoxLeft.getVisible() == False:
                        greenLeft.visible(viz.ON)
                        whiteLeft.visible(viz.ON)
                        wedgeLeft.visible(viz.ON)
                        greenRight.visible(viz.ON)
                        whiteRight.visible(viz.ON)
                        wedgeRight.visible(viz.ON)
        #Rediplay reticle when left mouse button is pressed
        elif num == 2:
                reticleLeft.visible(viz.ON)
                reticleRight.visible(viz.ON)
                beep.play()
                viz.starttimer(3,2)
        #Turn off visibility of reticle after 2 seconds
        elif num == 3:
                reticleLeft.visible(viz.OFF)
                reticleRight.visible(viz.OFF)

#Create mouse function that manipulates the visibility of the reticle
def onMouseDown(button):
        #Redisplay the reticle if the left mouse button is pressed
        if button == viz.MOUSEBUTTON_LEFT:
                viz.starttimer(2,1)

#Create mouse wheel function to adjust the visual estimation device and distance estimation device
def onMouseWheel(dir):
        #Obtain the current slope of the wedge and distance of the slider
        current_slope = wedgeLeft.getAxisAngle(viz.ABS_PARENT)
        current_distance = sliderLeft.get()
        #Increase the slope of the wedge if wheel is moved away from subject
        if dir > 0 and current_slope[3] < 90 and greenLeft.getVisible() == True:
                wedgeLeft.addAction(rotateCounter)
                wedgeRight.addAction(rotateCounter)
        #Decrease the slope of the wedge if wheel is moved toward subject
        elif dir < 0 and current_slope[3] > 0 and current_slope[2] == 1 and current_slope[3] >= 0.0001 and greenLeft.getVisible()
**== True:
                wedgeLeft.addAction(rotateClock)
                wedgeRight.addAction(rotateClock)
        #Increase the position of slider if wheel is moved away from subject
        elif dir > 0 and current_distance < 1.0 and greenLeft.getVisible() == False:
                sliderLeft.set(current_distance + .01)
                sliderRight.set(current_distance + .01)
        #Decrease the position of slider if wheel is moved toward the subject
        elif dir < 0 and current_distance > 0.0 and greenLeft.getVisible() == False:
                new_distance = sliderLeft.set(current_distance - .01)
                sliderRight.set(current_distance - .01)

#Create key function to record the measurements and progress through the photographs
def onkeydown(key):
```

```
#Obtain the current slope of the wedge and distance of the slider
current_slope = wedgeLeft.getAxisAngle(viz.ABS_PARENT)
current_distance = sliderLeft.get()
#If space bar is pressed...
if key == ' ':
		#Ensure the visibility of the initial instructions is turned off
		infoBoxLeftTitle.visible(viz.OFF)
		infoBoxRightTitle.visible(viz.OFF)
		infoBoxLeft.visible(viz.OFF)
		infoBoxRight.visible(viz.OFF)
		infoBoxTrainRight.visible(viz.OFF)
		infoBoxTrainLeft.visible(viz.OFF)
		#If the slope estimation is currently visible
		if greenLeft.getVisible() == True:
			#Turn off the visibility of the visual estimation device
			greenLeft.visible(viz.OFF)
			wedgeLeft.visible(viz.OFF)
			greenRight.visible(viz.OFF)
			wedgeRight.visible(viz.OFF)
			#Turn on the visibility of the distance estimation device
			sliderLeft.visible(viz.ON)
			sliderRight.visible(viz.ON)
			lowerSliderBoundaryLeft.visible(viz.ON)
			lowerSliderBoundaryRight.visible(viz.ON)
			upperSliderBoundaryLeft.visible(viz.ON)
			upperSliderBoundaryRight.visible(viz.ON)
			distanceTitleLeft.visible(viz.ON)
			distanceTitleRight.visible(viz.ON)
			upperLimitLeft.visible(viz.ON)
			upperLimitRight.visible(viz.ON)
			lowerLimitLeft.visible(viz.ON)
			lowerLimitRight.visible(viz.ON)
			#Record the slope of the wedge into a data file
			estimation_data.write(str(int(current_slope[3]))+' ')
			#Reset the distance to zero
			sliderLeft.set(.5)
			sliderRight.set(.5)

		#Else (distance estimation is currently displayed)
		else:
			#Turn off the visibility of the distance estimation device
			sliderLeft.visible(viz.OFF)
			sliderRight.visible(viz.OFF)
			lowerSliderBoundaryLeft.visible(viz.OFF)
			lowerSliderBoundaryRight.visible(viz.OFF)
			upperSliderBoundaryLeft.visible(viz.OFF)
			upperSliderBoundaryRight.visible(viz.OFF)
			distanceTitleLeft.visible(viz.OFF)
			distanceTitleRight.visible(viz.OFF)
			upperLimitLeft.visible(viz.OFF)
			upperLimitRight.visible(viz.OFF)
			lowerLimitLeft.visible(viz.OFF)
			lowerLimitRight.visible(viz.OFF)
			whiteLeft.visible(viz.OFF)
			whiteRight.visible(viz.OFF)
			#Record the distance into the data file
			estimation_data.write(str(int(current_distance*100))+'\n')
			#Reset the slope of the wedge to zero
			wedgeLeft.setAxisAngle([0.0,0.0,1.0,0.0], viz.ABS_PARENT)
			wedgeRight.setAxisAngle([0.0,0.0,1.0,0.0], viz.ABS_PARENT)
			#Remove the next scene from the photograph arrays
			if session == 0:
				textureLeft = left0.pop()
				textureRight = right0.pop()
			elif session == 1:
				textureLeft = left1.pop()
				textureRight = right1.pop()
			elif session == 2:
				textureLeft = left2.pop()
				textureRight = right2.pop()
```

```
                                        elif session == 3:
                                                textureLeft = left3.pop()
                                                textureRight = right3.pop()
                                        elif session == 4:
                                                textureLeft = left4.pop()
                                                textureRight = right4.pop()
                                        #If first hill in Training session is displayed, also display the distance to that hill as a
**reference
                                        if textureLeft == 'MDRS_Left_106_scaled2.jpg':
                                                distanceBoxLeft.visible(viz.ON)
                                                distanceBoxRight.visible(viz.ON)
                                                infoQuadDistanceLeft.visible(viz.ON)
                                                infoQuadDistanceRight.visible(viz.ON)
                                                #Start the timer for the reticle appearance
                                                viz.starttimer(0,3)
                                        else:
                                                distanceBoxLeft.visible(viz.OFF)
                                                distanceBoxRight.visible(viz.OFF)
                                                infoQuadDistanceLeft.visible(viz.OFF)
                                                infoQuadDistanceRight.visible(viz.OFF)
                                                #Start the timer for the reticle appearance
                                                viz.starttimer(0,3)
                                        #Attach the scene as a texture to the rectangles
                                        quad1.texture(viz.add(textureLeft))
                                        quad2.texture(viz.add(textureRight))
                                        #Display text indicating when the session is complete
                                        if textureLeft == 'EndSession.jpg':
                                                infoBoxEndSessionLeft.visible(viz.ON)
                                                infoBoxEndSessionRight.visible(viz.ON)

#Action callback code for mouse/keyboard/timer events
viz.callback(viz.MOUSEDOWN_EVENT, onMouseDown)
viz.callback(viz.MOUSEWHEEL_EVENT, onMouseWheel)
viz.callback(viz.KEYDOWN_EVENT,onkeydown)
viz.callback(viz.TIMER_EVENT, onTimer)
```

E.3 Lunar VR Study (LVS)

```
#Human Slope, Distance, and Height Estimation of LUNAR Terrain

#Christopher Oravetz
#Man Vehicle Lab - MIT
#25 July 2008

import viz
import vizinfo

viz.go(viz.STEREO | viz.FULLSCREEN)
viz.ipd(0.13)

#Input Session Number (Training = 0, Standing = 1,2,5 Supine = 3,4) and Subject Number
session = viz.input('Session')
subject = viz.input('What is your subject number?')
estimation_data = open('Subject #'+str(subject), 'a')
count = 0

#Initialize photograph arrays
left0 = []
right0 = []
left1 = []
right1 = []
left2 = []
right2 = []
left3 = []
right3 = []
left4 = []
right4 = []
left5 = []
right5 = []

#Append photograph arrays with all photographs
#EndSession photographs is only a white background
#All photographs were previously scaled to 2048x1024 to be quickly uploaded by Vizard
left0.append('EndSession.jpg')
left0.append('RilleTraining.jpg')
left0.append('DuneTraining.jpg')
left0.append('StGeorgeTraining.jpg')
left0.append('NorthMassifTraining.jpg')

right0.append('EndSession.jpg')
right0.append('RilleTraining.jpg')
right0.append('DuneTraining.jpg')
right0.append('StGeorgeTraining.jpg')
right0.append('NorthMassifTraining.jpg')

left1.append('EndSession.jpg')
left1.append('NorthMassif_far_2048.jpg')
left1.append('Mons_far_2048.jpg')
left1.append('Cleft&Sculptured_near_2048.jpg')
left1.append('SouthMassif_near_2048.jpg')
left1.append('Bear_near_2048.jpg')
left1.append('Cleft&Sculptured_far_2048.jpg')
left1.append('Bear_far_2048.jpg')
left1.append('SouthMassif_far_2048.jpg')
left1.append('Cleft&Sculptured_near_2048.jpg')
left1.append('NorthMassif_near_2048.jpg')
left1.append('Cleft&Sculptured_far_2048.jpg')
left1.append('Mons_near_2048.jpg')

left2.append('EndSession.jpg')
left2.append('NorthRay_2048.jpg')
left2.append('Surveyor_2048.jpg')
left2.append('Spook_2048.jpg')
left2.append('Shorty_2048.jpg')
left2.append('Camelot_2048.jpg')
```

```
left2.append('Flag_2048.jpg')

left3.append('EndSession.jpg')
left3.append('NorthMassif_far_2048.jpg')
left3.append('Mons_far_2048.jpg')
left3.append('Cleft&Sculptured_near_2048.jpg')
left3.append('SouthMassif_near_2048.jpg')
left3.append('Bear_near_2048.jpg')
left3.append('Cleft&Sculptured_far_2048.jpg')
left3.append('Bear_far_2048.jpg')
left3.append('SouthMassif_far_2048.jpg')
left3.append('Cleft&Sculptured_near_2048.jpg')
left3.append('NorthMassif_near_2048.jpg')
left3.append('Cleft&Sculptured_far_2048.jpg')
left3.append('Mons_near_2048.jpg')

left4.append('EndSession.jpg')
left4.append('NorthRay_2048.jpg')
left4.append('Surveyor_2048.jpg')
left4.append('Spook_2048.jpg')
left4.append('Shorty_2048.jpg')
left4.append('Camelot_2048.jpg')
left4.append('Flag_2048.jpg')

left5.append('EndSession.jpg')
left5.append('Shorty_2048.jpg')
left5.append('Flag_2048.jpg')
left5.append('Camelot_2048.jpg')
left5.append('Surveyor_2048.jpg')
left5.append('NorthRay_2048.jpg')
left5.append('Spook_2048.jpg')
left5.append('NorthMassif_near_2048.jpg')
left5.append('Cleft&Sculptured_far_2048.jpg')
left5.append('Bear_far_2048.jpg')
left5.append('Mons_near_2048.jpg')
left5.append('Cleft&Sculptured_near_2048.jpg')
left5.append('SouthMassif_far_2048.jpg')

#Right eye is presented the same images as the left eye in a synoptic configuration
right1.append('EndSession.jpg')
right1.append('NorthMassif_far_2048.jpg')
right1.append('Mons_far_2048.jpg')
right1.append('Cleft&Sculptured_near_2048.jpg')
right1.append('SouthMassif_near_2048.jpg')
right1.append('Bear_near_2048.jpg')
right1.append('Cleft&Sculptured_far_2048.jpg')
right1.append('Bear_far_2048.jpg')
right1.append('SouthMassif_far_2048.jpg')
right1.append('Cleft&Sculptured_near_2048.jpg')
right1.append('NorthMassif_near_2048.jpg')
right1.append('Cleft&Sculptured_far_2048.jpg')
right1.append('Mons_near_2048.jpg')

right2.append('EndSession.jpg')
right2.append('NorthRay_2048.jpg')
right2.append('Surveyor_2048.jpg')
right2.append('Spook_2048.jpg')
right2.append('Shorty_2048.jpg')
right2.append('Camelot_2048.jpg')
right2.append('Flag_2048.jpg')

right3.append('EndSession.jpg')
right3.append('NorthMassif_far_2048.jpg')
right3.append('Mons_far_2048.jpg')
right3.append('Cleft&Sculptured_near_2048.jpg')
right3.append('SouthMassif_near_2048.jpg')
right3.append('Bear_near_2048.jpg')
right3.append('Cleft&Sculptured_far_2048.jpg')
right3.append('Bear_far_2048.jpg')
right3.append('SouthMassif_far_2048.jpg')
```

```
right3.append('Cleft&Sculptured_near_2048.jpg')
right3.append('NorthMassif_near_2048.jpg')
right3.append('Cleft&Sculptured_far_2048.jpg')
right3.append('Mons_near_2048.jpg')

right4.append('EndSession.jpg')
right4.append('NorthRay_2048.jpg')
right4.append('Surveyor_2048.jpg')
right4.append('Spook_2048.jpg')
right4.append('Shorty_2048.jpg')
right4.append('Camelot_2048.jpg')
right4.append('Flag_2048.jpg')

right5.append('EndSession.jpg')
right5.append('Shorty_2048.jpg')
right5.append('Flag_2048.jpg')
right5.append('Camelot_2048.jpg')
right5.append('Surveyor_2048.jpg')
right5.append('NorthRay_2048.jpg')
right5.append('Spook_2048.jpg')
right5.append('NorthMassif_near_2048.jpg')
right5.append('Cleft&Sculptured_far_2048.jpg')
right5.append('Bear_far_2048.jpg')
right5.append('Mons_near_2048.jpg')
right5.append('Cleft&Sculptured_near_2048.jpg')
right5.append('SouthMassif_far_2048.jpg')

#Turn Off mouse navigation and visibility of the mouse
viz.mouse(viz.OFF)
viz.mouse.setVisible(viz.OFF)

#Create two rectangles to map images on as textures
quad1 = viz.add(viz.TEXQUAD)
quad2 = viz.add(viz.TEXQUAD,viz.WORLD,2)
quad1.setScale(1.15,1.15,1)
quad2.setScale(1.15,1.15,1)

#Set the position of the Quads containing the photographs so they are in the center of each eye and take up the entire screen
quad1.setPosition([0,1.89,1.38])
quad2.setPosition([0,1.89,1.38])

#Instructions upon start of each session
#infoBoxLeftTitle displays the Session Number to the left eye
infoBoxLeftTitle = viz.add(viz.TEXT3D,'',viz.WORLD,1)
infoBoxLeftTitle.message('Session #'+ str(session))
infoBoxLeftTitle.setPosition([0,1.92,1.3])
infoBoxLeftTitle.setScale([.05,.05,1])
infoBoxLeftTitle.resolution(1)
infoBoxLeftTitle.alignment(viz.TEXT_CENTER_CENTER)
infoBoxLeftTitle.color(viz.BLACK)

#infoBoxLeft diplays the body position instructions to the left eye
#infoBoxTrain Left displays the word "Training"
infoBoxLeft = viz.add(viz.TEXT3D,'',viz.WORLD,1)
infoBoxTrainLeft = viz.add(viz.TEXT3D,'',viz.WORLD,1)
if session == 0:
        infoBoxLeft.message('Estimate the following slopes in the Standing Position')
        infoBoxTrainLeft.message('TRAINING')
elif session == 1 or session == 2 or session == 5:
        infoBoxLeft.message('Estimate the following slopes in the Standing Position')
elif session == 3 or session == 4:
        infoBoxLeft.message('Estimate the following slopes in the Supine Position')
infoBoxLeft.setPosition([0,1.84,1.379])
infoBoxLeft.setScale([.03,.03,1])
infoBoxLeft.resolution(1)
infoBoxLeft.alignment(viz.TEXT_CENTER_CENTER)
infoBoxLeft.color(viz.BLACK)
infoBoxTrainLeft.setPosition([0,2.0,1.379])
infoBoxTrainLeft.setScale([.05,.05,1])
infoBoxTrainLeft.resolution(1)
```

```
infoBoxTrainLeft.alignment(viz.TEXT_CENTER_CENTER)
infoBoxTrainLeft.color(viz.RED)

#infoBoxRightTitle displays the Session Number to the right eye
infoBoxRightTitle = viz.add(viz.TEXT3D,'',viz.WORLD,2)
infoBoxRightTitle.message('Session #' + str(session))
infoBoxRightTitle.setPosition([0,1.92,1.3])
infoBoxRightTitle.setScale([.05,.05,1.3])
infoBoxRightTitle.resolution(1)
infoBoxRightTitle.alignment(viz.TEXT_CENTER_CENTER)
infoBoxRightTitle.color(viz.BLACK)

#infoBoxRight diplays the body position instructions to the right eye
#infoBoxTrainRight displays the word "Training"
infoBoxRight = viz.add(viz.TEXT3D,'',viz.WORLD,2)
infoBoxTrainRight = viz.add(viz.TEXT3D,'',viz.WORLD,2)
if session == 0:
	infoBoxRight.message('Estimate the following slopes in the Standing Position')
	infoBoxTrainRight.message('TRAINING')
elif session == 1 or session == 2 or session == 5:
	infoBoxRight.message('Estimate the following slopes in the Standing Position')
elif session == 3 or session == 4:
	infoBoxRight.message('Estimate the following slopes in the Supine Position')
infoBoxRight.setPosition([0,1.84,1.379])
infoBoxRight.setScale([.03,.03,1])
infoBoxRight.resolution(1)
infoBoxRight.alignment(viz.TEXT_CENTER_CENTER)
infoBoxRight.color(viz.BLACK)
infoBoxTrainRight.setPosition([0,2.0,1.379])
infoBoxTrainRight.setScale([.05,.05,1])
infoBoxTrainRight.resolution(1)
infoBoxTrainRight.alignment(viz.TEXT_CENTER_CENTER)
infoBoxTrainRight.color(viz.RED)

#infoBoxEndSessionLeft notifies the subject of the end of the session and is displayed in the left eye
infoBoxEndSessionLeft = viz.add(viz.TEXT3D,'',viz.WORLD,1)
infoBoxEndSessionLeft.message('End of Session')
infoBoxEndSessionLeft.setPosition([0,1.9,1.35])
infoBoxEndSessionLeft.setScale([.1,.1,1])
infoBoxEndSessionLeft.resolution(1)
infoBoxEndSessionLeft.alignment(viz.TEXT_CENTER_CENTER)
infoBoxEndSessionLeft.color(viz.BLACK)
infoBoxEndSessionLeft.visible(viz.OFF)

#infoBoxEndSessionRight notifies the subject of the end of the session and is displayed in the right eye
infoBoxEndSessionRight = viz.add(viz.TEXT3D,'',viz.WORLD,2)
infoBoxEndSessionRight.message('End of Session')
infoBoxEndSessionRight.setPosition([-.003,1.9,1.35])
infoBoxEndSessionRight.setScale([.1,.1,1])
infoBoxEndSessionRight.resolution(1)
infoBoxEndSessionRight.alignment(viz.TEXT_CENTER_CENTER)
infoBoxEndSessionRight.color(viz.BLACK)
infoBoxEndSessionRight.visible(viz.OFF)

#Visual estimation device - semicircular wedge - for the left eye
wedgeLeft = viz.add('wedge2.ac',viz.WORLD,1)
wedgeLeft.setPosition(.4,1.5,1.37898)
wedgeLeft.color(viz.BLACK)
wedgeLeft.center([-.5,0,0])
wedgeLeft.setScale([.2,.2,.2])
wedgeLeft.visible(viz.OFF)

#Visual estimation device - semicircular wedge - for the right eye
wedgeRight = viz.add('wedge2.ac',viz.WORLD,2)
wedgeRight.setPosition(.357,1.5,1.37898)
wedgeRight.setScale([.2,.2,.2])
wedgeRight.color(viz.BLACK)
wedgeRight.center([-.5,0,0])
wedgeRight.visible(viz.OFF)
```

```
#Ground reference within the visual estimation device for the left eye
greenLeft = viz.add(viz.TEXQUAD,viz.WORLD,1)
greenLeft.setScale([.3,.11,1])
greenLeft.setPosition([0,1,1.37899])
greenLeft.center([0,.5,0])
greenLeft.color(viz.GREEN)
greenLeft.visible(viz.OFF)

#Sky reference within the visual estimation device for the left eye
whiteLeft = viz.add(viz.TEXQUAD,viz.WORLD,1)
whiteLeft.setScale([.3,.31,1])
whiteLeft.setPosition([0,1.2,1.379])
whiteLeft.center([0,.5,0])
whiteLeft.color(viz.WHITE)
whiteLeft.visible(viz.OFF)

#Ground reference within the visual estimation device for the right eye
greenRight = viz.add(viz.TEXQUAD,viz.WORLD,2)
greenRight.setScale([.3,.11,1])
greenRight.setPosition([-.043,1.0,1.37899])
greenRight.center([0,.5,0])
greenRight.color(viz.GREEN)
greenRight.visible(viz.OFF)

#Sky reference within the visual estimation device for the right eye
whiteRight = viz.add(viz.TEXQUAD,viz.WORLD,2)
whiteRight.setScale([.3,.31,1])
whiteRight.setPosition([-.043,1.2,1.379])
whiteRight.center([0,.5,0])
whiteRight.color(viz.WHITE)
whiteRight.visible(viz.OFF)

#Create scenes for each eye
viz.scene(1,viz.LEFT_EYE)
viz.scene(2,viz.RIGHT_EYE)

#Define rotation actions of the visual estimation wedge
rotateCounter = vizact.spin(0,0,1,50,.01)
rotateClock = vizact.spin(0,0,1,-50,.01)

#Add rotation actions to the wedges in the left and right scenes
wedgeLeft.addAction(rotateCounter)
wedgeLeft.addAction(rotateClock)
wedgeRight.addAction(rotateCounter)
wedgeRight.addAction(rotateClock)

#Position varibles for the arrows that identify the area of the hill to estimate
#Each variable contains the location of the arrow for each photograph

#Position variables for the left eye
Position_NorthMassif_Bottom_near =      [-.03,1.98,1.379]
Position_NorthMassif_Top_near =         [-.03,2.335,1.379]
Position_NorthMassif_Bottom_far =       [.27,1.77,1.379]
Position_NorthMassif_Top_far =          [.27,2.023,1.379]
Position_SouthMassif_Bottom_near =      [-.29,2.037,1.379]
Position_SouthMassif_Top_near =         [-.29,2.345,1.379]
Position_SouthMassif_Bottom_far =       [-.2,1.955,1.379]
Position_SouthMassif_Top_far =          [-.2,2.232,1.379]
Position_Mons_Bottom_near =             [-.25,1.9,1.379]
Position_Mons_Top_near =                [-.25,2.125,1.379]
Position_Mons_Bottom_far =              [-.15,2.045,1.379]
Position_Mons_Top_far =                 [-.15,2.27,1.379]
Position_Sculptured_Bottom_near =       [.24,1.92,1.379]
Position_Sculptured_Top_near =          [.24,2.205,1.379]
Position_Sculptured_Bottom_far =        [0.07,1.95,1.379]
Position_Sculptured_Top_far =           [0.07,2.1,1.379]
Position_Cleft_Bottom_near =            [-.2,1.91,1.379]
Position_Cleft_Top_near =               [-.1,2.12,1.379]
Position_Cleft_Bottom_far =             [-.025,1.942,1.379]
Position_Cleft_Top_far =                [-.070,2.055,1.379]
```

```
Position_Bear_Bottom_near =                [-.3,1.975,1.379]
Position_Bear_Top_near =                   [-.3,2.08,1.379]
Position_Bear_Bottom_far=                  [-0.05,2.048,1.379]
Position_Bear_Top_far=                     [-0.05,2.152,1.379]
Position_Shorty_Bottom =                   [0,1.42,1.379]
Position_Shorty_Top =                      [0,1.94,1.379]
Position_Camelot_Bottom =                  [.05,1.74,1.379]
Position_Camelot_Top =                     [.05,1.93,1.379]
Position_Flag_Bottom =                     [.05,1.64,1.379]
Position_Flag_Top =                        [.05,1.92,1.379]
Position_Spook_Bottom =                    [0,1.61,1.379]
Position_Spook_Top =                       [0,1.875,1.379]
Position_NorthRay_Bottom =                 [.05,1.835,1.379]
Position_NorthRay_Top =                    [.05,2.275,1.379]
Position_Dune_Bottom =                     [.03,1.685,1.379]
Position_Dune_Top =                        [.03,1.86,1.379]
Position_Rille1_Bottom =                   [.065,1.88,1.379]
Position_Rille1_Top =                      [.065,2.07,1.379]
Position_Rille2_Bottom =                   [.0,1.955,1.379]
Position_Rille2_Top =                      [.0,2.26,1.379]
Position_Rille9_Bottom =                   [.065,1.35,1.35]
Position_Rille9_Top =                      [.065,2.03,1.35]
Position_Surveyor_Bottom =                 [.01,1.67,1.35]
Position_Surveyor_Top =                    [.01,1.95,1.35]
Position_DuneTraining_Bottom =             [.03,1.685,1.379]
Position_DuneTraining_Top =                [.03,1.86,1.379]
Position_RilleTraining_Bottom =            [.0,1.955,1.379]
Position_RilleTraining_Top =               [.0,2.26,1.379]
Position_StGeorgeTraining_Bottom =         [-.05,1.77,1.35]
Position_StGeorgeTraining_Top =            [-.05,2.04,1.35]
Position_NorthMassifTraining_Bottom =      [.25,1.73,1.35]
Position_NorthMassifTraining_Top =         [.25,1.945,1.35]

#Create the arrow objects for the left eye
arrowLeftBottom = viz.add('arrow2_gold.ac',viz.WORLD,1)
arrowLeftBottom.setScale(0.1,0.1,1)
arrowLeftTop= viz.add('arrow2_gold.ac',viz.WORLD,1)
arrowLeftTop.setAxisAngle([0.0,0.0,1.0,180.0], viz.ABS_PARENT)
arrowLeftTop.setScale(0.1,0.1,1)

#Add the bottom arrow position variables to an array for each session (left eye)
**arrowLeftBottomPositionArray0 = [[0,0,0],Position_RilleTraining_Bottom,Position_DuneTraining_Bottom,
**Position_StGeorgeTraining_Bottom, Position_NorthMassifTraining_Bottom]
arrowLeftBottomPositionArray1 = [[0,0,0],Position_NorthMassif_Bottom_far, Position_Mons_Bottom_far,
**Position_Cleft_Bottom_near, Position_SouthMassif_Bottom_near, Position_Bear_Bottom_near, Position_Sculptured_Bottom_far,
**Position_Bear_Bottom_far, Position_SouthMassif_Bottom_far, Position_Sculptured_Bottom_near,
**Position_NorthMassif_Bottom_near, Position_Cleft_Bottom_far,Position_Mons_Bottom_near]
arrowLeftBottomPositionArray2 = [[0,0,0],Position_NorthRay_Bottom, Position_Surveyor_Bottom,Position_Spook_Bottom,
**Position_Shorty_Bottom, Position_Camelot_Bottom, Position_Flag_Bottom]
arrowLeftBottomPositionArray3 = [[0,0,0],Position_NorthMassif_Bottom_far, Position_Mons_Bottom_far,
**Position_Cleft_Bottom_near, Position_SouthMassif_Bottom_near, Position_Bear_Bottom_near, Position_Sculptured_Bottom_far,
**Position_Bear_Bottom_far, Position_SouthMassif_Bottom_far, Position_Sculptured_Bottom_near,
**Position_NorthMassif_Bottom_near, Position_Cleft_Bottom_far,Position_Mons_Bottom_near]
arrowLeftBottomPositionArray4 = [[0,0,0],Position_NorthRay_Bottom, Position_Surveyor_Bottom,Position_Spook_Bottom,
**Position_Shorty_Bottom, Position_Camelot_Bottom, Position_Flag_Bottom]
arrowLeftBottomPositionArray5 = [[0,0,0],Position_Shorty_Bottom, Position_Flag_Bottom, Position_Camelot_Bottom,
**Position_Surveyor_Bottom, Position_NorthRay_Bottom, Position_Spook_Bottom, Position_NorthMassif_Bottom_near,
**Position_Sculptured_Bottom_far,Position_Bear_Bottom_far, Position_Mons_Bottom_near, Position_Cleft_Bottom_near,
**Position_SouthMassif_Bottom_far]

#Add the top arrow position variables to an array for each session (left eye)
arrowLeftTopPositionArray0 = [[0,0,0],Position_RilleTraining_Top,Position_DuneTraining_Top, Position_StGeorgeTraining_Top,
**Position_NorthMassifTraining_Top]
arrowLeftTopPositionArray1 = [[0,0,0],Position_NorthMassif_Top_far, Position_Mons_Top_far, Position_Cleft_Top_near,
**Position_SouthMassif_Top_near, Position_Bear_Top_near, Position_Sculptured_Top_far, Position_Bear_Top_far,
**Position_SouthMassif_Top_far, Position_Sculptured_Top_near, Position_NorthMassif_Top_near,
**Position_Cleft_Top_far,Position_Mons_Top_near]
arrowLeftTopPositionArray2 = [[0,0,0],Position_NorthRay_Top, Position_Surveyor_Top,Position_Spook_Top, Position_Shorty_Top,
**Position_Camelot_Top, Position_Flag_Top]
arrowLeftTopPositionArray3 = [[0,0,0],Position_NorthMassif_Top_far, Position_Mons_Top_far, Position_Cleft_Top_near,
```

```
**Position_SouthMassif_Top_near, Position_Bear_Top_near, Position_Sculptured_Top_far, Position_Bear_Top_far,
**Position_SouthMassif_Top_far, Position_Sculptured_Top_near, Position_NorthMassif_Top_near,
**Position_Cleft_Top_far,Position_Mons_Top_near]
arrowLeftTopPositionArray4 = [[0,0,0],Position_NorthRay_Top, Position_Surveyor_Top,Position_Spook_Top, Position_Shorty_Top,
**Position_Camelot_Top, Position_Flag_Top]
arrowLeftTopPositionArray5 = [[0,0,0],Position_Shorty_Top, Position_Flag_Top, Position_Camelot_Top, Position_Surveyor_Top,
**Position_NorthRay_Top, Position_Spook_Top, Position_NorthMassif_Top_near,
**Position_Sculptured_Top_far,Position_Bear_Top_far, Position_Mons_Top_near, Position_Cleft_Top_near,
**Position_SouthMassif_Top_far]

#Create the arrow object for the right eye
arrowRightBottom = viz.add('arrow2_gold.ac',viz.WORLD,2)
arrowRightBottom.setScale(0.1,0.1,1)
arrowRightTop = viz.add('arrow2_gold.ac',viz.WORLD,2)
arrowRightTop.setAxisAngle([0.0,0.0,1.0,180.0], viz.ABS_PARENT)
arrowRightTop.setScale(0.1,0.1,1)

#Add the bottom arrow position variables to an array for each session (right eye)
arrowRightBottomPositionArray0 = [[0,0,0],Position_RilleTraining_Bottom,Position_DuneTraining_Bottom,
**Position_StGeorgeTraining_Bottom, Position_NorthMassifTraining_Bottom]
arrowRightBottomPositionArray1 = [[0,0,0],Position_NorthMassif_Bottom_far, Position_Mons_Bottom_far,
**Position_Cleft_Bottom_near, Position_SouthMassif_Bottom_near, Position_Bear_Bottom_near, Position_Sculptured_Bottom_far,
**Position_Bear_Bottom_far, Position_SouthMassif_Bottom_far, Position_Sculptured_Bottom_near,
**Position_NorthMassif_Bottom_near, Position_Cleft_Bottom_far,Position_Mons_Bottom_near]
arrowRightBottomPositionArray2 = [[0,0,0],Position_NorthRay_Bottom, Position_Surveyor_Bottom,Position_Spook_Bottom,
**Position_Shorty_Bottom, Position_Camelot_Bottom, Position_Flag_Bottom]
arrowRightBottomPositionArray3 = [[0,0,0],Position_NorthMassif_Bottom_far, Position_Mons_Bottom_far,
**Position_Cleft_Bottom_near, Position_SouthMassif_Bottom_near, Position_Bear_Bottom_near, Position_Sculptured_Bottom_far,
**Position_Bear_Bottom_far, Position_SouthMassif_Bottom_far, Position_Sculptured_Bottom_near,
**Position_NorthMassif_Bottom_near, Position_Cleft_Bottom_far,Position_Mons_Bottom_near]
arrowRightBottomPositionArray4 = [[0,0,0],Position_NorthRay_Bottom, Position_Surveyor_Bottom,Position_Spook_Bottom,
**Position_Shorty_Bottom, Position_Camelot_Bottom, Position_Flag_Bottom]
arrowRightBottomPositionArray5 = [[0,0,0],Position_Shorty_Bottom, Position_Flag_Bottom, Position_Camelot_Bottom,
**Position_Surveyor_Bottom, Position_NorthRay_Bottom, Position_Spook_Bottom, Position_NorthMassif_Bottom_near,
**Position_Sculptured_Bottom_far,Position_Bear_Bottom_far, Position_Mons_Bottom_near, Position_Cleft_Bottom_near,
**Position_SouthMassif_Bottom_far]

#Add the top arrow position variables to an array for each session (right eye)
arrowRightTopPositionArray0 = [[0,0,0],Position_RilleTraining_Top,Position_DuneTraining_Top, Position_StGeorgeTraining_Top,
**Position_NorthMassifTraining_Top]
arrowRightTopPositionArray1 = [[0,0,0],Position_NorthMassif_Top_far, Position_Mons_Top_far, Position_Cleft_Top_near,
**Position_SouthMassif_Top_near, Position_Bear_Top_near, Position_Sculptured_Top_far, Position_Bear_Top_far,
**Position_SouthMassif_Top_far, Position_Sculptured_Top_near, Position_NorthMassif_Top_near,
**Position_Cleft_Top_far,Position_Mons_Top_near]
arrowRightTopPositionArray2 = [[0,0,0],Position_NorthRay_Top, Position_Surveyor_Top,Position_Spook_Top,
**Position_Shorty_Top, Position_Camelot_Top, Position_Flag_Top]
arrowRightTopPositionArray3 = [[0,0,0],Position_NorthMassif_Top_far, Position_Mons_Top_far, Position_Cleft_Top_near,
**Position_SouthMassif_Top_near, Position_Bear_Top_near, Position_Sculptured_Top_far, Position_Bear_Top_far,
**Position_SouthMassif_Top_far, Position_Sculptured_Top_near, Position_NorthMassif_Top_near,
**Position_Cleft_Top_far,Position_Mons_Top_near]
arrowRightTopPositionArray4 = [[0,0,0],Position_NorthRay_Top, Position_Surveyor_Top,Position_Spook_Top,
**Position_Shorty_Top, Position_Camelot_Top, Position_Flag_Top]
arrowRightTopPositionArray5 = [[0,0,0],Position_Shorty_Top, Position_Flag_Top, Position_Camelot_Top, Position_Surveyor_Top,
**Position_NorthRay_Top, Position_Spook_Top, Position_NorthMassif_Top_near,
**Position_Sculptured_Top_far,Position_Bear_Top_far, Position_Mons_Top_near, Position_Cleft_Top_near,
**Position_SouthMassif_Top_far]

#Create a beep sound to be used when the arrow is displayed
beep = viz.addAudio('BUZZER.wav')
beep.volume(.5)
beep.setTime(3)

#Slider for adjusting distance - set visible ON if using slider
distSliderLeft = viz.add(viz.SLIDER,1)
distSliderLeft.horizontal()
distSliderLeft.setPosition(.48,.215)
distSliderLeft.setScale(1,1)
distSliderLeft.visible(viz.OFF)
distSliderRight = viz.add(viz.SLIDER,2)
distSliderRight.horizontal()
```

```
distSliderRight.setPosition(.485,.215)
distSliderRight.setScale(1,1)
distSliderRight.visible(viz.OFF)
#Slider for adjusting height - set visible ON if using slider
heightSliderLeft = viz.add(viz.SLIDER,1)
heightSliderLeft.vertical()
heightSliderLeft.setPosition(.55,.225)
heightSliderLeft.setScale(1,1)
heightSliderLeft.visible(viz.OFF)
heightSliderRight = viz.add(viz.SLIDER,2)
heightSliderRight.vertical()
heightSliderRight.setPosition(.555,.225)
heightSliderRight.setScale(1,1)
heightSliderRight.visible(viz.OFF)

#Title within distance estimation device
distTitleLeft = viz.add(viz.TEXT3D,'',viz.WORLD,1)
if session == 0 or session == 1 or session == 3 or session == 5:
	distTitleLeft.message('Distance')
else:
	distTitleLeft.message('Diameter')
distTitleLeft.setPosition([0,1.65,1.378])
distTitleLeft.setScale([.04,.04,1])
distTitleLeft.resolution(1)
distTitleLeft.alignment(viz.TEXT_CENTER_CENTER)
distTitleLeft.color(viz.BLACK)
distTitleLeft.visible(viz.OFF)
distTitleRight = viz.add(viz.TEXT3D,'',viz.WORLD,2)
if session == 0 or session == 1 or session == 3 or session == 5:
	distTitleRight.message('Distance')
else:
	distTitleRight.message('Diameter')
distTitleRight.setPosition([-.043,1.65,1.378])
distTitleRight.setScale([.04,.04,1])
distTitleRight.resolution(1)
distTitleRight.alignment(viz.TEXT_CENTER_CENTER)
distTitleRight.color(viz.BLACK)
distTitleRight.visible(viz.OFF)

#Title within height estimation device
heightTitleLeft = viz.add(viz.TEXT3D,'',viz.WORLD,1)
heightTitleLeft.message('Height')
heightTitleLeft.setPosition([-.05,1.60,1.378])
heightTitleLeft.setScale([.04,.04,1])
heightTitleLeft.resolution(1)
heightTitleLeft.alignment(viz.TEXT_CENTER_CENTER)
heightTitleLeft.color(viz.BLACK)
heightTitleLeft.visible(viz.OFF)
heightTitleRight = viz.add(viz.TEXT3D,'',viz.WORLD,2)
heightTitleRight.message('Height')
heightTitleRight.setPosition([-.093,1.60,1.378])
heightTitleRight.setScale([.04,.04,1])
heightTitleRight.resolution(1)
heightTitleRight.alignment(viz.TEXT_CENTER_CENTER)
heightTitleRight.color(viz.BLACK)
heightTitleRight.visible(viz.OFF)

#Display upper bound of distance estimation (20 km for hills and 1500 m for craters)
distUpperLimitLeft = viz.add(viz.TEXT3D,'',viz.WORLD,1)
distUpperLimitLeft.setScale([.02,.02,1])
if session == 0 or session == 1 or session == 3 or session == 5:
	distUpperLimitLeft.message('20')
	distUpperLimitLeft.setPosition([.131,1.5,1.378])
else:
	distUpperLimitLeft.message('1500')
	distUpperLimitLeft.setPosition([.128,1.5,1.378])
distUpperLimitLeft.resolution(1)
distUpperLimitLeft.alignment(viz.TEXT_CENTER_CENTER)
distUpperLimitLeft.color(viz.BLACK)
distUpperLimitLeft.visible(viz.OFF)
```

```
distUpperLimitRight = viz.add(viz.TEXT3D,'',viz.WORLD,2)
distUpperLimitRight.setScale([.02,.02,1])
if session == 0 or session == 1 or session == 3 or session == 5:
	distUpperLimitRight.message('20')
	distUpperLimitRight.setPosition([.088,1.5,1.378])
else:
	distUpperLimitRight.message('1500')
	distUpperLimitRight.setPosition([.085,1.5,1.378])
distUpperLimitRight.resolution(1)
distUpperLimitRight.alignment(viz.TEXT_CENTER_CENTER)
distUpperLimitRight.color(viz.BLACK)
distUpperLimitRight.visible(viz.OFF)

#Display upper bound of height estimation (4000 meters)
heightUpperLimitLeft = viz.add(viz.TEXT3D,'',viz.WORLD,1)
heightUpperLimitLeft.setPosition([.040,1.676,1.378])
heightUpperLimitLeft.setScale([.02,.02,1])
heightUpperLimitLeft.message('4000')
heightUpperLimitLeft.resolution(1)
heightUpperLimitLeft.alignment(viz.TEXT_CENTER_CENTER)
heightUpperLimitLeft.color(viz.BLACK)
heightUpperLimitLeft.visible(viz.OFF)
heightUpperLimitRight = viz.add(viz.TEXT3D,'',viz.WORLD,2)
heightUpperLimitRight.setPosition([-.002,1.676,1.378])
heightUpperLimitRight.setScale([.02,.02,1])
heightUpperLimitRight.message('4000')
heightUpperLimitRight.resolution(1)
heightUpperLimitRight.alignment(viz.TEXT_CENTER_CENTER)
heightUpperLimitRight.color(viz.BLACK)
heightUpperLimitRight.visible(viz.OFF)

#Display lower bound of distance estimation (0 meters)
distLowerLimitLeft = viz.add(viz.TEXT3D,'',viz.WORLD,1)
distLowerLimitLeft.setPosition([-.133,1.5,1.378])
distLowerLimitLeft.setScale([.02,.02,1])
distLowerLimitLeft.message('0')
distLowerLimitLeft.resolution(1)
distLowerLimitLeft.alignment(viz.TEXT_CENTER_CENTER)
distLowerLimitLeft.color(viz.BLACK)
distLowerLimitLeft.visible(viz.OFF)
distLowerLimitRight = viz.add(viz.TEXT3D,'',viz.WORLD,2)
distLowerLimitRight.setPosition([-.176,1.5,1.378])
distLowerLimitRight.setScale([.02,.02,1])
distLowerLimitRight.message('0')
distLowerLimitRight.resolution(1)
distLowerLimitRight.alignment(viz.TEXT_CENTER_CENTER)
distLowerLimitRight.color(viz.BLACK)
distLowerLimitRight.visible(viz.OFF)

#Display lower bound of height estimation (0 meters)
heightLowerLimitLeft = viz.add(viz.TEXT3D,'',viz.WORLD,1)
heightLowerLimitLeft.setPosition([.053,1.413,1.378])
heightLowerLimitLeft.setScale([.02,.02,1])
heightLowerLimitLeft.message('0')
heightLowerLimitLeft.resolution(1)
heightLowerLimitLeft.alignment(viz.TEXT_CENTER_CENTER)
heightLowerLimitLeft.color(viz.BLACK)
heightLowerLimitLeft.visible(viz.OFF)
heightLowerLimitRight = viz.add(viz.TEXT3D,'',viz.WORLD,2)
heightLowerLimitRight.setPosition([.011,1.413,1.378])
heightLowerLimitRight.setScale([.02,.02,1])
heightLowerLimitRight.message('0')
heightLowerLimitRight.resolution(1)
heightLowerLimitRight.alignment(viz.TEXT_CENTER_CENTER)
heightLowerLimitRight.color(viz.BLACK)
heightLowerLimitRight.visible(viz.OFF)

#Display rectangle at lower bound of distance estimation slider
distLowerSliderBoundaryLeft = viz.add(viz.TEXQUAD,viz.WORLD,1)
distLowerSliderBoundaryLeft.setScale([.015,.04,1])
```

```
distLowerSliderBoundaryLeft.setPosition([-.133,1.534,1.378])
distLowerSliderBoundaryLeft.color(viz.BLUE)
distLowerSliderBoundaryLeft.visible(viz.OFF)
distLowerSliderBoundaryRight = viz.add(viz.TEXQUAD,viz.WORLD,2)
distLowerSliderBoundaryRight.setScale([.015,.04,1])
distLowerSliderBoundaryRight.setPosition([-.176,1.534,1.378])
distLowerSliderBoundaryRight.color(viz.BLUE)
distLowerSliderBoundaryRight.visible(viz.OFF)

#Display rectangle at lower bound of height estimation slider
heightLowerSliderBoundaryLeft = viz.add(viz.TEXQUAD,viz.WORLD,1)
heightLowerSliderBoundaryLeft.setScale([.04,.015,1])
heightLowerSliderBoundaryLeft.setPosition([.086,1.412,1.378])
heightLowerSliderBoundaryLeft.color(viz.BLUE)
heightLowerSliderBoundaryLeft.visible(viz.OFF)
heightLowerSliderBoundaryRight = viz.add(viz.TEXQUAD,viz.WORLD,2)
heightLowerSliderBoundaryRight.setScale([.04,.015,1])
heightLowerSliderBoundaryRight.setPosition([.043,1.412,1.378])
heightLowerSliderBoundaryRight.color(viz.BLUE)
heightLowerSliderBoundaryRight.visible(viz.OFF)

#Display rectangle at upper bound of distance estimation slider
distUpperSliderBoundaryLeft = viz.add(viz.TEXQUAD,viz.WORLD,1)
distUpperSliderBoundaryLeft.setScale([.015,.04,1])
distUpperSliderBoundaryLeft.setPosition([.13,1.534,1.378])
distUpperSliderBoundaryLeft.color(viz.BLUE)
distUpperSliderBoundaryLeft.visible(viz.OFF)
distUpperSliderBoundaryRight = viz.add(viz.TEXQUAD,viz.WORLD,2)
distUpperSliderBoundaryRight.setScale([.015,.04,1])
distUpperSliderBoundaryRight.setPosition([.087,1.534,1.378])
distUpperSliderBoundaryRight.color(viz.BLUE)
distUpperSliderBoundaryRight.visible(viz.OFF)

#Display rectangle at upper bound of height estimation slider
heightUpperSliderBoundaryLeft = viz.add(viz.TEXQUAD,viz.WORLD,1)
heightUpperSliderBoundaryLeft.setScale([.04,.015,1])
heightUpperSliderBoundaryLeft.setPosition([.086,1.676,1.378])
heightUpperSliderBoundaryLeft.color(viz.BLUE)
heightUpperSliderBoundaryLeft.visible(viz.OFF)
heightUpperSliderBoundaryRight = viz.add(viz.TEXQUAD,viz.WORLD,2)
heightUpperSliderBoundaryRight.setScale([.04,.015,1])
heightUpperSliderBoundaryRight.setPosition([.043,1.676,1.378])
heightUpperSliderBoundaryRight.color(viz.BLUE)
heightUpperSliderBoundaryRight.visible(viz.OFF)

#Display distance of current position of distance estimation slider
distBoxLeft = viz.add(viz.TEXT3D,'',viz.WORLD,1)
if session == 0 or session == 1 or session == 3 or session == 5:
	distBoxLeft.message('10.0 km')
else:
	distBoxLeft.message('750 m')
distBoxLeft.setPosition([0,1.60,1.378])
distBoxLeft.setScale([.03,.03,1])
distBoxLeft.resolution(1)
distBoxLeft.alignment(viz.TEXT_CENTER_CENTER)
distBoxLeft.color(viz.BLACK)
distBoxLeft.visible(viz.OFF)
distBoxRight = viz.add(viz.TEXT3D,'',viz.WORLD,2)
if session == 0 or session == 1 or session == 3 or session == 5:
	distBoxRight.message('10.0 km')
else:
	distBoxRight.message('750 m')
distBoxRight.setPosition([-.043,1.60,1.378])
distBoxRight.setScale([.03,.03,1])
distBoxRight.resolution(1)
distBoxRight.alignment(viz.TEXT_CENTER_CENTER)
distBoxRight.color(viz.BLACK)
distBoxRight.visible(viz.OFF)

#Display height of current position of height estimation slider
```

```
heightBoxLeft = viz.add(viz.TEXT3D,'',viz.WORLD,1)
heightBoxLeft.message('2000 m')
heightBoxLeft.setPosition([-.05,1.55,1.378])
heightBoxLeft.setScale([.03,.03,1])
heightBoxLeft.resolution(1)
heightBoxLeft.alignment(viz.TEXT_CENTER_CENTER)
heightBoxLeft.color(viz.BLACK)
heightBoxLeft.visible(viz.OFF)
heightBoxRight = viz.add(viz.TEXT3D,'',viz.WORLD,2)
heightBoxRight.message('2000 m')
heightBoxRight.setPosition([-.093,1.55,1.378])
heightBoxRight.setScale([.03,.03,1])
heightBoxRight.resolution(1)
heightBoxRight.alignment(viz.TEXT_CENTER_CENTER)
heightBoxRight.color(viz.BLACK)
heightBoxRight.visible(viz.OFF)

#Display distance for first hill in Training session to use as reference for experiment
HillDistanceBoxLeft = viz.add(viz.TEXT3D,'',viz.WORLD,1)
HillDistanceBoxLeft.message('Distance: 7.1 km')
HillDistanceBoxLeft.setPosition([0,2.20,1.35])
HillDistanceBoxLeft.setScale([.03,.03,1])
HillDistanceBoxLeft.resolution(1)
HillDistanceBoxLeft.alignment(viz.TEXT_CENTER_CENTER)
HillDistanceBoxLeft.color(viz.BLACK)
HillDistanceBoxLeft.visible(viz.OFF)
HillDistanceBoxRight = viz.add(viz.TEXT3D,'',viz.WORLD,2)
HillDistanceBoxRight.message('Distance: 7.1 km')
HillDistanceBoxRight.setPosition([0,2.20,1.35])
HillDistanceBoxRight.setScale([.03,.03,1])
HillDistanceBoxRight.resolution(1)
HillDistanceBoxRight.alignment(viz.TEXT_CENTER_CENTER)
HillDistanceBoxRight.color(viz.BLACK)
HillDistanceBoxRight.visible(viz.OFF)
HillHeightBoxLeft = viz.add(viz.TEXT3D,'',viz.WORLD,1)
HillHeightBoxLeft.message('Height: 1200 m')
HillHeightBoxLeft.setPosition([0,2.10,1.35])
HillHeightBoxLeft.setScale([.03,.03,1])
HillHeightBoxLeft.resolution(1)
HillHeightBoxLeft.alignment(viz.TEXT_CENTER_CENTER)
HillHeightBoxLeft.color(viz.BLACK)
HillHeightBoxLeft.visible(viz.OFF)
HillHeightBoxRight = viz.add(viz.TEXT3D,'',viz.WORLD,2)
HillHeightBoxRight.message('Height: 1200 m')
HillHeightBoxRight.setPosition([0,2.10,1.35])
HillHeightBoxRight.setScale([.03,.03,1])
HillHeightBoxRight.resolution(1)
HillHeightBoxRight.alignment(viz.TEXT_CENTER_CENTER)
HillHeightBoxRight.color(viz.BLACK)
HillHeightBoxRight.visible(viz.OFF)
HillInfoQuadDistanceLeft = viz.add(viz.TEXQUAD,viz.WORLD,1)
HillInfoQuadDistanceLeft.setScale([.3,.2,1])
HillInfoQuadDistanceLeft.setPosition([0,2.15,1.36])
HillInfoQuadDistanceLeft.color(viz.WHITE)
HillInfoQuadDistanceLeft.visible(viz.OFF)
HillInfoQuadDistanceRight = viz.add(viz.TEXQUAD,viz.WORLD,2)
HillInfoQuadDistanceRight.setScale([.3,.2,1])
HillInfoQuadDistanceRight.setPosition([0,2.15,1.36])
HillInfoQuadDistanceRight.color(viz.WHITE)
HillInfoQuadDistanceRight.visible(viz.OFF)

#Display distance for first crater in Training session to use as reference for experiment
CraterDistanceBoxLeft = viz.add(viz.TEXT3D,'',viz.WORLD,1)
CraterDistanceBoxLeft.message('Diameter: 440 m')
CraterDistanceBoxLeft.setPosition([0,2.20,1.35])
CraterDistanceBoxLeft.setScale([.03,.03,1])
CraterDistanceBoxLeft.resolution(1)
CraterDistanceBoxLeft.alignment(viz.TEXT_CENTER_CENTER)
CraterDistanceBoxLeft.color(viz.BLACK)
CraterDistanceBoxLeft.visible(viz.OFF)
```

```
CraterDistanceBoxRight = viz.add(viz.TEXT3D,'',viz.WORLD,2)
CraterDistanceBoxRight.message('Diameter: 440 m')
CraterDistanceBoxRight.setPosition([0,2.20,1.35])
CraterDistanceBoxRight.setScale([.03,.03,1])
CraterDistanceBoxRight.resolution(1)
CraterDistanceBoxRight.alignment(viz.TEXT_CENTER_CENTER)
CraterDistanceBoxRight.color(viz.BLACK)
CraterDistanceBoxRight.visible(viz.OFF)
CraterInfoQuadDistanceLeft = viz.add(viz.TEXQUAD,viz.WORLD,1)
CraterInfoQuadDistanceLeft.setScale([.3,.1,1])
CraterInfoQuadDistanceLeft.setPosition([0,2.20,1.36])
CraterInfoQuadDistanceLeft.color(viz.WHITE)
CraterInfoQuadDistanceLeft.visible(viz.OFF)
CraterInfoQuadDistanceRight = viz.add(viz.TEXQUAD,viz.WORLD,2)
CraterInfoQuadDistanceRight.setScale([.3,.1,1])
CraterInfoQuadDistanceRight.setPosition([0,2.20,1.36])
CraterInfoQuadDistanceRight.color(viz.WHITE)
CraterInfoQuadDistanceRight.visible(viz.OFF)

#Create a timer function that will define when to make the arrow (red box) visible and when to play the beep
def onTimer(num):

	#Set the position and scales of the arrows in the Training Sequence
	if num == 0 and session == 0:
		global count
		count = count+1
		arrowLeftBottom.setPosition(arrowLeftBottomPositionArray0.pop())
		arrowLeftTop.setPosition(arrowLeftTopPositionArray0.pop())
		beep.play()
		arrowLeftBottom.visible(viz.ON)
		arrowLeftTop.visible(viz.ON)
		arrowRightBottom.setPosition(arrowRightBottomPositionArray0.pop())
		arrowRightTop.setPosition(arrowRightTopPositionArray0.pop())
		arrowRightBottom.visible(viz.ON)
		arrowRightTop.visible(viz.ON)
		viz.starttimer(1,2)

	#Set the position and scales of the arrows in the Session 1
	elif num == 0 and session == 1:
		beep.play()
		arrowLeftBottom.setPosition(arrowLeftBottomPositionArray1.pop())
		arrowLeftBottom.visible(viz.ON)
		arrowRightBottom.setPosition(arrowRightBottomPositionArray1.pop())
		arrowRightBottom.visible(viz.ON)
		arrowLeftTop.setPosition(arrowLeftTopPositionArray1.pop())
		arrowLeftTop.visible(viz.ON)
		arrowRightTop.setPosition(arrowRightTopPositionArray1.pop())
		arrowRightTop.visible(viz.ON)
		viz.starttimer(1,2)

	#Set the position and scales of the arrows in the Session 2
	elif num == 0 and session == 2:
		beep.play()
		arrowLeftBottom.setPosition(arrowLeftBottomPositionArray2.pop())
		arrowLeftBottom.visible(viz.ON)
		arrowRightBottom.setPosition(arrowRightBottomPositionArray2.pop())
		arrowRightBottom.visible(viz.ON)
		arrowLeftTop.setPosition(arrowLeftTopPositionArray2.pop())
		arrowLeftTop.visible(viz.ON)
		arrowRightTop.setPosition(arrowRightTopPositionArray2.pop())
		arrowRightTop.visible(viz.ON)
		viz.starttimer(1,2)

	#Set the position and scales of the arrows in the Session 3
	elif num == 0 and session == 3:
		beep.play()
		arrowLeftBottom.setPosition(arrowLeftBottomPositionArray3.pop())
		arrowLeftBottom.visible(viz.ON)
		arrowRightBottom.setPosition(arrowRightBottomPositionArray3.pop())
		arrowRightBottom.visible(viz.ON)
```

```
		arrowLeftTop.setPosition(arrowLeftTopPositionArray3.pop())
		arrowLeftTop.visible(viz.ON)
		arrowRightTop.setPosition(arrowRightTopPositionArray3.pop())
		arrowRightTop.visible(viz.ON)
		viz.starttimer(1,2)

	#Set the position and scales of the arrows in the Session 4
	elif num == 0 and session == 4:
		beep.play()
		arrowLeftBottom.setPosition(arrowLeftBottomPositionArray4.pop())
		arrowLeftBottom.visible(viz.ON)
		arrowRightBottom.setPosition(arrowRightBottomPositionArray4.pop())
		arrowRightBottom.visible(viz.ON)
		arrowLeftTop.setPosition(arrowLeftTopPositionArray4.pop())
		arrowLeftTop.visible(viz.ON)
		arrowRightTop.setPosition(arrowRightTopPositionArray4.pop())
		arrowRightTop.visible(viz.ON)
		viz.starttimer(1,2)

	#Set the position and scales of the arrows in the Session 5
	elif num == 0 and session == 5:
		global count
		count = count+1
		beep.play()
		arrowLeftBottom.setPosition(arrowLeftBottomPositionArray5.pop())
		arrowLeftBottom.visible(viz.ON)
		arrowRightBottom.setPosition(arrowRightBottomPositionArray5.pop())
		arrowRightBottom.visible(viz.ON)
		arrowLeftTop.setPosition(arrowLeftTopPositionArray5.pop())
		arrowLeftTop.visible(viz.ON)
		arrowRightTop.setPosition(arrowRightTopPositionArray5.pop())
		arrowRightTop.visible(viz.ON)
		viz.starttimer(1,2)

	#Turn off the visibility of the arrows after 2 seconds
	elif num == 1:
		arrowLeftBottom.visible(viz.OFF)
		arrowRightBottom.visible(viz.OFF)
		arrowLeftTop.visible(viz.OFF)
		arrowRightTop.visible(viz.OFF)
		greenLeft.visible(viz.ON)
		whiteLeft.visible(viz.ON)
		wedgeLeft.visible(viz.ON)
		greenRight.visible(viz.ON)
		whiteRight.visible(viz.ON)
		wedgeRight.visible(viz.ON)

	#Rediplay arrows when left mouse button is pressed
	elif num == 2:
		arrowLeftBottom.visible(viz.ON)
		arrowRightBottom.visible(viz.ON)
		arrowLeftTop.visible(viz.ON)
		arrowRightTop.visible(viz.ON)
		beep.play()
		viz.starttimer(3,2)

	#Turn off visibility of arrows after 2 seconds
	elif num == 3:
		arrowLeftBottom.visible(viz.OFF)
		arrowRightBottom.visible(viz.OFF)
		arrowLeftTop.visible(viz.OFF)
		arrowRightTop.visible(viz.OFF)

#Create mouse function that manipulates the visibility of the arrow
def onMouseDown(button):

	#Redisplay the arrows if the left mouse button is pressed
	if button == viz.MOUSEBUTTON_LEFT:
		viz.starttimer(2,1)
```

```
#Turn off visibility of estimation devices
elif button == viz.MOUSEBUTTON_RIGHT and whiteRight.getVisible() == True:
	whiteRight.visible(viz.OFF)
	whiteLeft.visible(viz.OFF)
	if measurement == 1:
		greenLeft.visible(viz.OFF)
		wedgeLeft.visible(viz.OFF)
		greenRight.visible(viz.OFF)
		wedgeRight.visible(viz.OFF)
	elif measurement == 2:
		distSliderLeft.visible(viz.OFF)
		distSliderRight.visible(viz.OFF)
		distLowerSliderBoundaryLeft.visible(viz.OFF)
		distLowerSliderBoundaryRight.visible(viz.OFF)
		distUpperSliderBoundaryLeft.visible(viz.OFF)
		distUpperSliderBoundaryRight.visible(viz.OFF)
		distTitleLeft.visible(viz.OFF)
		distTitleRight.visible(viz.OFF)
		distUpperLimitLeft.visible(viz.OFF)
		distUpperLimitRight.visible(viz.OFF)
		distLowerLimitLeft.visible(viz.OFF)
		distLowerLimitRight.visible(viz.OFF)
		distBoxLeft.visible(viz.OFF)
		distBoxRight.visible(viz.OFF)
	elif measurement == 3:
		heightSliderLeft.visible(viz.OFF)
		heightSliderRight.visible(viz.OFF)
		heightLowerSliderBoundaryLeft.visible(viz.OFF)
		heightLowerSliderBoundaryRight.visible(viz.OFF)
		heightUpperSliderBoundaryLeft.visible(viz.OFF)
		heightUpperSliderBoundaryRight.visible(viz.OFF)
		heightTitleLeft.visible(viz.OFF)
		heightTitleRight.visible(viz.OFF)
		heightUpperLimitLeft.visible(viz.OFF)
		heightUpperLimitRight.visible(viz.OFF)
		heightLowerLimitLeft.visible(viz.OFF)
		heightLowerLimitRight.visible(viz.OFF)
		heightBoxLeft.visible(viz.OFF)
		heightBoxRight.visible(viz.OFF)

#Turn on visibility of estimation devices
elif button == viz.MOUSEBUTTON_RIGHT and whiteRight.getVisible() == False:
	whiteRight.visible(viz.ON)
	whiteLeft.visible(viz.ON)
	if measurement == 1:
		greenLeft.visible(viz.ON)
		wedgeLeft.visible(viz.ON)
		greenRight.visible(viz.ON)
		wedgeRight.visible(viz.ON)
	if measurement == 2:
		distSliderLeft.visible(viz.ON)
		distSliderRight.visible(viz.ON)
		distLowerSliderBoundaryLeft.visible(viz.ON)
		distLowerSliderBoundaryRight.visible(viz.ON)
		distUpperSliderBoundaryLeft.visible(viz.ON)
		distUpperSliderBoundaryRight.visible(viz.ON)
		distTitleLeft.visible(viz.ON)
		distTitleRight.visible(viz.ON)
		distUpperLimitLeft.visible(viz.ON)
		distUpperLimitRight.visible(viz.ON)
		distLowerLimitLeft.visible(viz.ON)
		distLowerLimitRight.visible(viz.ON)
		distBoxLeft.visible(viz.ON)
		distBoxRight.visible(viz.ON)
	if measurement == 3:
		heightSliderLeft.visible(viz.ON)
		heightSliderRight.visible(viz.ON)
		heightLowerSliderBoundaryLeft.visible(viz.ON)
		heightLowerSliderBoundaryRight.visible(viz.ON)
		heightUpperSliderBoundaryLeft.visible(viz.ON)
```

```
                heightUpperSliderBoundaryRight.visible(viz.ON)
                heightTitleLeft.visible(viz.ON)
                heightTitleRight.visible(viz.ON)
                heightUpperLimitLeft.visible(viz.ON)
                heightUpperLimitRight.visible(viz.ON)
                heightLowerLimitLeft.visible(viz.ON)
                heightLowerLimitRight.visible(viz.ON)
                heightBoxLeft.visible(viz.ON)
                heightBoxRight.visible(viz.ON)

#Create mouse wheel function to adjust the visual estimation device and distance estimation device
def onMouseWheel(dir):

        #Obtain the current slope of the wedge and distance of the slider
        current_slope = wedgeLeft.getAxisAngle(viz.ABS_PARENT)
        current_distance = distSliderLeft.get()
        current_height = heightSliderLeft.get()
        global count

        #Increase the slope of the wedge if wheel is moved away from subject
        if dir > 0 and current_slope[3] < 90 and greenLeft.getVisible() == True:
                wedgeLeft.addAction(rotateCounter)
                wedgeRight.addAction(rotateCounter)

        #Decrease the slope of the wedge if wheel is moved toward subject
        elif dir < 0 and current_slope[3] > 0 and current_slope[2] == 1 and current_slope[3] >= 0.0001 and greenLeft.getVisible()
**== True:
                wedgeLeft.addAction(rotateClock)
                wedgeRight.addAction(rotateClock)

        #Increase the position of distance slider if wheel is moved away from subject
        elif dir > 0 and current_distance < 0.995 and distSliderLeft.getVisible() == True:
                if (session == 0 and count <= 2) or session == 1 or session == 3 or (session == 5 and count <= 6):
                        distSliderLeft.set(current_distance + .005)
                        distSliderRight.set(current_distance + .005)
                        distBoxLeft.message(str(round((current_distance + .005)*20,1)) + ' km')
                        distBoxRight.message(str(round((current_distance + .005)*20,1)) + ' km')
                else:
                        distSliderLeft.set(current_distance + .006666666667)
                        distSliderRight.set(current_distance + .006666666667)
                        distBoxLeft.message(str(int(round((current_distance + .006666666667)*1500,1))) + ' m')
                        distBoxRight.message(str(int(round((current_distance + .006666666667)*1500,1))) + ' m')

        #Decrease the position of distance slider if wheel is moved toward the subject
        elif dir < 0 and current_distance > 0.005 and distSliderLeft.getVisible() == True:
                if (session == 0 and count <= 2) or session == 1 or session == 3 or (session == 5 and count <= 6):
                        new_distance = distSliderLeft.set(current_distance - .005)
                        distSliderRight.set(current_distance - .005)
                        distBoxLeft.message(str(round((current_distance - .005)*20,1)) + ' km')
                        distBoxRight.message(str(round((current_distance - .005)*20,1)) + ' km')
                else:
                        new_distance = distSliderLeft.set(current_distance - .006666666667)
                        distSliderRight.set(current_distance - .006666666667)
                        distBoxLeft.message(str(int(round((current_distance - .006666666667)*1500,1))) + ' m')
                        distBoxRight.message(str(int(round((current_distance - .006666666667)*1500,1))) + ' m')

        #Increase the height position of slider if wheel is moved away from subject
        elif dir > 0 and current_height < 0.999 and heightSliderLeft.getVisible() == True:
                heightSliderLeft.set(current_height + .00625)
                heightSliderRight.set(current_height + .00625)
                heightBoxLeft.message(str(int(round((current_height + .00625)*4000,0))) + ' m')
                heightBoxRight.message(str(int(round((current_height + .00625)*4000,0))) + ' m')

        #Decrease the position of height slider if wheel is moved toward the subject
        elif dir < 0 and current_height > 0.001 and heightSliderLeft.getVisible() == True:
                new_height = heightSliderLeft.set(current_height - .00625)
                heightSliderRight.set(current_height - .00625)
                heightBoxLeft.message(str(int(round((current_height - .00625)*4000,0))) + ' m')
                heightBoxRight.message(str(int(round((current_height - .00625)*4000,0))) + ' m')
```

```
#Create key function to record the measurements and progress through the photographs
def onkeydown(key):

	#Obtain the current slope of the wedge and distance of the slider
	current_slope = wedgeLeft.getAxisAngle(viz.ABS_PARENT)
	current_distance = distSliderLeft.get()
	current_height = heightSliderLeft.get()
	global measurement
	global count

	#If space bar is pressed...
	if key == ' ':
		#Ensure the visibility of the initial instructions is turned off
		infoBoxLeftTitle.visible(viz.OFF)
		infoBoxRightTitle.visible(viz.OFF)
		infoBoxLeft.visible(viz.OFF)
		infoBoxRight.visible(viz.OFF)
		infoBoxTrainRight.visible(viz.OFF)
		infoBoxTrainLeft.visible(viz.OFF)

		#If the slope estimation is currently visible
		if greenLeft.getVisible() == True:

			#Turn off the visibility of the slope estimation device
			greenLeft.visible(viz.OFF)
			wedgeLeft.visible(viz.OFF)
			greenRight.visible(viz.OFF)
			wedgeRight.visible(viz.OFF)

			#Turn on the visibility of the distance estimation device
			distSliderLeft.visible(viz.ON)
			distSliderRight.visible(viz.ON)
			distLowerSliderBoundaryLeft.visible(viz.ON)
			distLowerSliderBoundaryRight.visible(viz.ON)
			distUpperSliderBoundaryLeft.visible(viz.ON)
			distUpperSliderBoundaryRight.visible(viz.ON)
			distTitleLeft.visible(viz.ON)
			distTitleRight.visible(viz.ON)
			distUpperLimitLeft.visible(viz.ON)
			distUpperLimitRight.visible(viz.ON)
			distLowerLimitLeft.visible(viz.ON)
			distLowerLimitRight.visible(viz.ON)
			distBoxLeft.visible(viz.ON)
			distBoxRight.visible(viz.ON)
			if (session == 0 and count > 2) or (session == 5 and count > 6):
				distUpperLimitLeft.message('1500')
				distUpperLimitRight.message('1500')
				distLowerLimitLeft.message('0')
				distLowerLimitRight.message('0')
				distBoxLeft.message('750 m')
				distBoxRight.message('750 m')
				distTitleLeft.message('Diameter')
				distTitleRight.message('Diameter')
			measurement = 2

			#Record the slope of the wedge into a data file
			estimation_data.write(str(int(round(current_slope[3])))+' ')

			#Reset the distance to zero
			distSliderLeft.set(.5)
			distSliderRight.set(.5)
			if (session == 0 and count <= 2) or session == 1 or session == 3 or (session == 5 and count <= 6):
				distBoxLeft.message('10.0 km')
				distBoxRight.message('10.0 km')
			else:
				distBoxLeft.message('750 m')
				distBoxRight.message('750 m')

		#Else if distance estimation is currently displayed
		elif distSliderLeft.getVisible() == True:
```

```
#Record the slope of the wedge into a data file
if session == 1 or session == 3 or (session == 0 and count <= 2) or (session == 5 and count <= 6):
	estimation_data.write(str(int(round(current_distance*20000)))+' ')
else:
	estimation_data.write(str(int(round(current_distance*1500)))+'\n')

#Turn off the visibility of the distance estimation device
distSliderLeft.visible(viz.OFF)
distSliderRight.visible(viz.OFF)
distLowerSliderBoundaryLeft.visible(viz.OFF)
distLowerSliderBoundaryRight.visible(viz.OFF)
distUpperSliderBoundaryLeft.visible(viz.OFF)
distUpperSliderBoundaryRight.visible(viz.OFF)
distTitleLeft.visible(viz.OFF)
distTitleRight.visible(viz.OFF)
distUpperLimitLeft.visible(viz.OFF)
distUpperLimitRight.visible(viz.OFF)
distLowerLimitLeft.visible(viz.OFF)
distLowerLimitRight.visible(viz.OFF)
distBoxLeft.visible(viz.OFF)
distBoxRight.visible(viz.OFF)

#If a hill is currently being displayed
if session == 1 or session == 3 or (session == 0 and count <= 2) or (session == 5 and count <= 6):
	#Turn on the visibility of the height estimation device
	heightSliderLeft.visible(viz.ON)
	heightSliderRight.visible(viz.ON)
	heightLowerSliderBoundaryLeft.visible(viz.ON)
	heightLowerSliderBoundaryRight.visible(viz.ON)
	heightUpperSliderBoundaryLeft.visible(viz.ON)
	heightUpperSliderBoundaryRight.visible(viz.ON)
	heightTitleLeft.visible(viz.ON)
	heightTitleRight.visible(viz.ON)
	heightUpperLimitLeft.visible(viz.ON)
	heightUpperLimitRight.visible(viz.ON)
	heightLowerLimitLeft.visible(viz.ON)
	heightLowerLimitRight.visible(viz.ON)
	heightBoxLeft.visible(viz.ON)
	heightBoxRight.visible(viz.ON)
	measurement = 3

	#Reset the height to zero
	heightSliderLeft.set(.5)
	heightSliderRight.set(.5)
	heightBoxLeft.message('2000 m')
	heightBoxRight.message('2000 m')

#If a crater is currently being displayed
elif session == 2 or session == 4 or (session == 0 and count > 2) or (session == 5 and count > 6):
	measurement = 1
	whiteRight.visible(viz.OFF)
	whiteLeft.visible(viz.OFF)

	#Reset the slope of the wedge to zero
	wedgeLeft.setAxisAngle([0.0,0.0,1.0,0.0], viz.ABS_PARENT)
	wedgeRight.setAxisAngle([0.0,0.0,1.0,0.0], viz.ABS_PARENT)

	#Remove the next scene from the photograph arrays
	if session == 0:
		textureLeft = left0.pop()
		textureRight = right0.pop()
	elif session == 2:
		textureLeft = left2.pop()
		textureRight = right2.pop()
	elif session == 4:
		textureLeft = left4.pop()
		textureRight = right4.pop()
	elif session == 5:
		textureLeft = left5.pop()
```

```
                                        textureRight = right5.pop()
                                HillDistanceBoxLeft.visible(viz.OFF)
                                HillDistanceBoxRight.visible(viz.OFF)
                                HillHeightBoxLeft.visible(viz.OFF)
                                HillHeightBoxRight.visible(viz.OFF)
                                HillInfoQuadDistanceLeft.visible(viz.OFF)
                                HillInfoQuadDistanceRight.visible(viz.OFF)
                                CraterDistanceBoxLeft.visible(viz.OFF)
                                CraterDistanceBoxRight.visible(viz.OFF)
                                CraterInfoQuadDistanceLeft.visible(viz.OFF)
                                CraterInfoQuadDistanceRight.visible(viz.OFF)

                                #Start the timer for the arrow appearance
                                viz.starttimer(0,3)

                                #Attach the scene as a texture to the rectangles
                                quad1.texture(viz.add(textureLeft))
                                quad2.texture(viz.add(textureRight))
                                if textureLeft == 'EndSession.jpg':
                                        infoBoxEndSessionLeft.visible(viz.ON)
                                        infoBoxEndSessionRight.visible(viz.ON)

        #Else if height estimation is currently displayed
        else:
                measurement = 1

                #Turn off the visibility of the distance estimation device
                heightSliderLeft.visible(viz.OFF)
                heightSliderRight.visible(viz.OFF)
                heightLowerSliderBoundaryLeft.visible(viz.OFF)
                heightLowerSliderBoundaryRight.visible(viz.OFF)
                heightUpperSliderBoundaryLeft.visible(viz.OFF)
                heightUpperSliderBoundaryRight.visible(viz.OFF)
                heightTitleLeft.visible(viz.OFF)
                heightTitleRight.visible(viz.OFF)
                heightUpperLimitLeft.visible(viz.OFF)
                heightUpperLimitRight.visible(viz.OFF)
                heightLowerLimitLeft.visible(viz.OFF)
                heightLowerLimitRight.visible(viz.OFF)
                heightBoxLeft.visible(viz.OFF)
                heightBoxRight.visible(viz.OFF)
                whiteRight.visible(viz.OFF)
                whiteLeft.visible(viz.OFF)

                #Record the distance into the data file
                estimation_data.write(str(int(round(current_height*4000)))+'\n')

                #Reset the slope of the wedge to zero
                wedgeLeft.setAxisAngle([0.0,0.0,1.0,0.0], viz.ABS_PARENT)
                wedgeRight.setAxisAngle([0.0,0.0,1.0,0.0], viz.ABS_PARENT)

                #Remove the next scene from the photograph arrays
                if session == 0:
                        textureLeft = left0.pop()
                        textureRight = right0.pop()
                elif session == 1:
                        textureLeft = left1.pop()
                        textureRight = right1.pop()
                elif session == 2:
                        textureLeft = left2.pop()
                        textureRight = right2.pop()
                elif session == 3:
                        textureLeft = left3.pop()
                        textureRight = right3.pop()
                elif session == 4:
                        textureLeft = left4.pop()
                        textureRight = right4.pop()
                elif session == 5:
                        textureLeft = left5.pop()
                        textureRight = right5.pop()
```

```
                #If first hill in Training session is displayed, also display the distance to that hill as a reference
                if textureLeft == 'NorthMassifTraining.jpg':
                        HillDistanceBoxLeft.visible(viz.ON)
                        HillDistanceBoxRight.visible(viz.ON)
                        HillHeightBoxLeft.visible(viz.ON)
                        HillHeightBoxRight.visible(viz.ON)
                        HillInfoQuadDistanceLeft.visible(viz.ON)
                        HillInfoQuadDistanceRight.visible(viz.ON)
                        #Start the timer for the arrow appearance
                        viz.starttimer(0,3)

                #If first crater in Training session is displayed, display the distance across that crater as a reference
                elif textureLeft == 'DuneTraining.jpg':
                        CraterDistanceBoxLeft.visible(viz.ON)
                        CraterDistanceBoxRight.visible(viz.ON)
                        CraterInfoQuadDistanceLeft.visible(viz.ON)
                        CraterInfoQuadDistanceRight.visible(viz.ON)

                        #Start the timer for the arrow appearance
                        viz.starttimer(0,3)
                else:
                        HillDistanceBoxLeft.visible(viz.OFF)
                        HillDistanceBoxRight.visible(viz.OFF)
                        HillHeightBoxLeft.visible(viz.OFF)
                        HillHeightBoxRight.visible(viz.OFF)
                        HillInfoQuadDistanceLeft.visible(viz.OFF)
                        HillInfoQuadDistanceRight.visible(viz.OFF)
                        CraterDistanceBoxLeft.visible(viz.OFF)
                        CraterDistanceBoxRight.visible(viz.OFF)
                        CraterInfoQuadDistanceLeft.visible(viz.OFF)
                        CraterInfoQuadDistanceRight.visible(viz.OFF)

                        #Start the timer for the arrow appearance
                        viz.starttimer(0,3)

                #Attach the scene as a texture to the rectangles
                quad1.texture(viz.add(textureLeft))
                quad2.texture(viz.add(textureRight))

                #Display text indicating when the session is complete
                if textureLeft == 'EndSession.jpg':
                        infoBoxEndSessionLeft.visible(viz.ON)
                        infoBoxEndSessionRight.visible(viz.ON)

#Action callback code for mouse/keyboard/timer events
viz.callback(viz.MOUSEDOWN_EVENT, onMouseDown)
viz.callback(viz.MOUSEWHEEL_EVENT, onMouseWheel)
viz.callback(viz.KEYDOWN_EVENT,onkeydown)
viz.callback(viz.TIMER_EVENT, onTimer)
```

APPENDIX

F

VR TRAINING PRESENTATIONS

F.1 MDRS Pilot VR Study (MPVS)

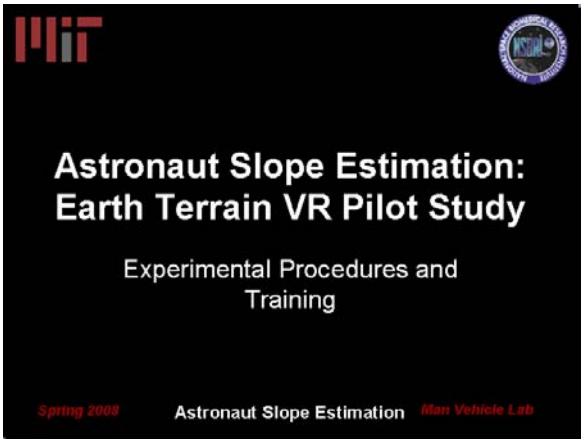

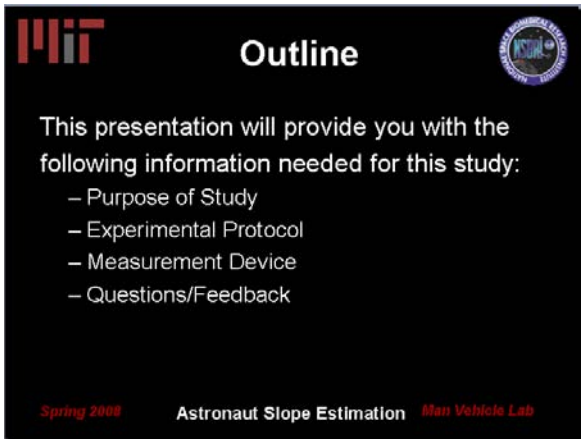

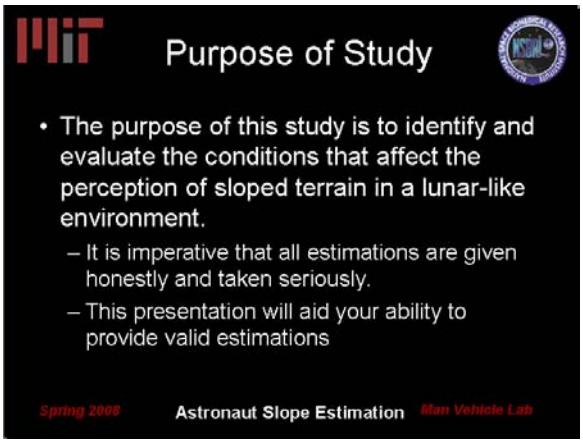

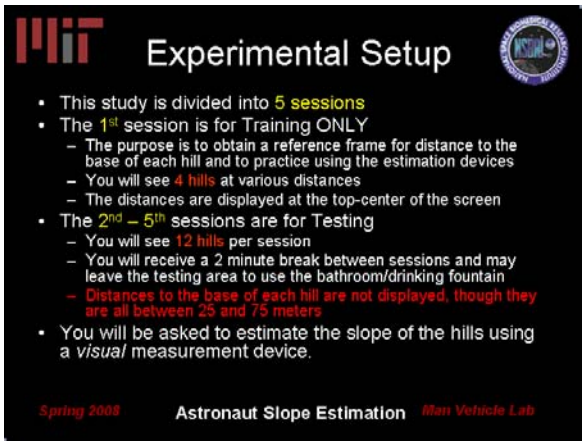

Experimental Setup

- The 1st, 2nd, and 5th sessions will be conducted from a *standing position* with the feet spread about shoulder's width apart.

- The 3rd and 4th sessions will be conducted from a *supine position*. You will be asked to lie against the padded board with your neck supported by the foam

Spring 2008 Astronaut Slope Estimation Man Vehicle Lab

Experimental Setup

- After each image is displayed, a highlighted box will be displayed for 3.0 second and will indicate the region of interest for slope estimation.

- After the box vanishes, you will proceed to the *visual* estimation
- If you need the highlighted box to be displayed again, press the left arrow (←) key

Spring 2008 Astronaut Slope Estimation Man Vehicle Lab

Estimation Methods

- Visual Estimation
  - Use the up arrow (↑) and the down arrow (↓) to adjust the slope of the wedge located below the picture to the cross-sectional view of the tangent surface of the highlighted slope.
    - This entails cognitively rotating the hill along its vertical axis

Spring 2008 Astronaut Slope Estimation Man Vehicle Lab

Estimation Methods (Visual)

– After completing your adjustment, press the space bar to advance the scene to the next hill

Spring 2008 Astronaut Slope Estimation Man Vehicle Lab

Questions/Comments?

Good Luck!

Spring 2008 Astronaut Slope Estimation Man Vehicle Lab

F.2 MDRS VR Study (MVS)

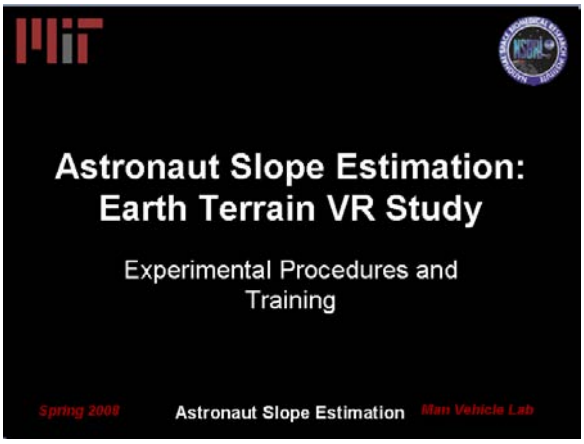

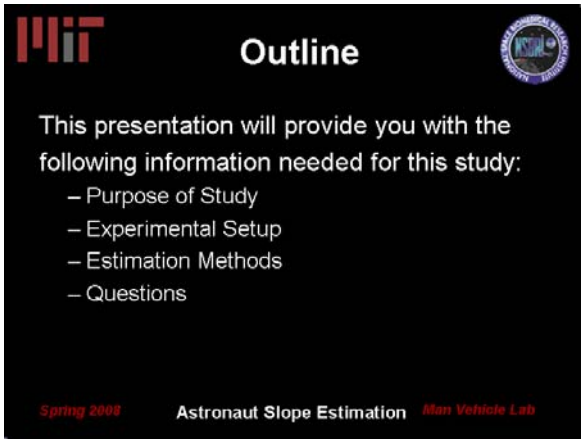

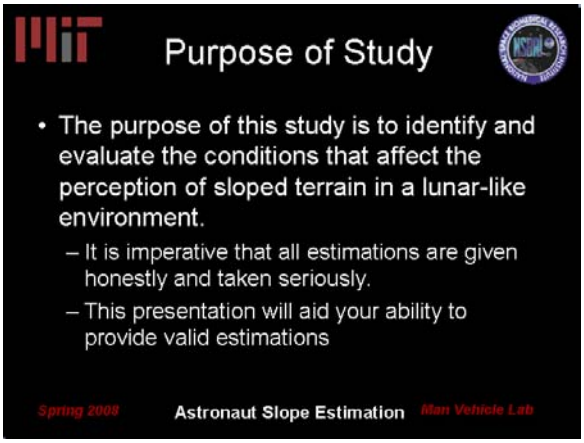

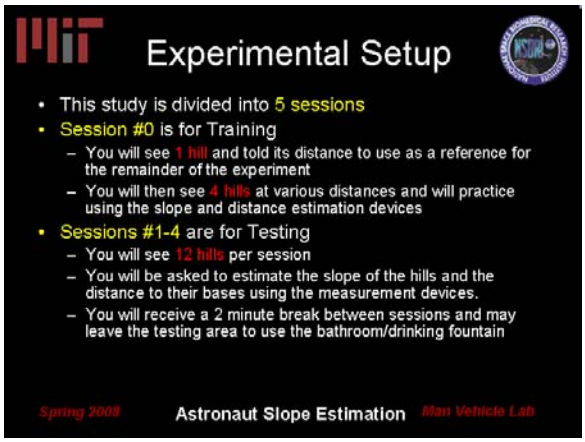

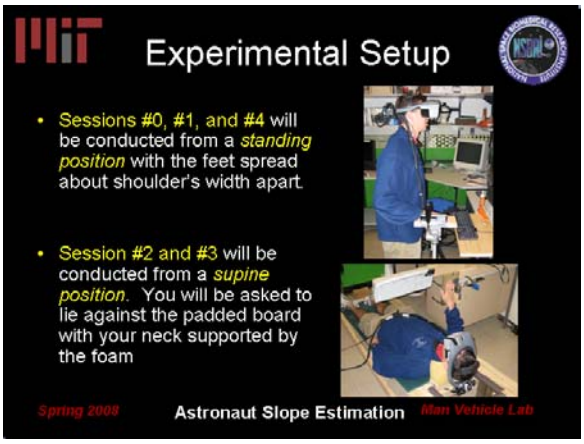

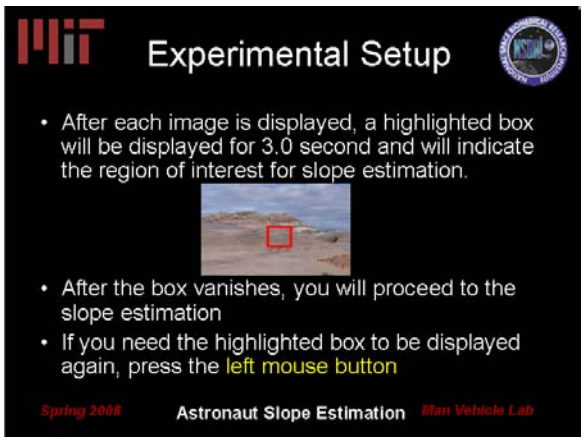

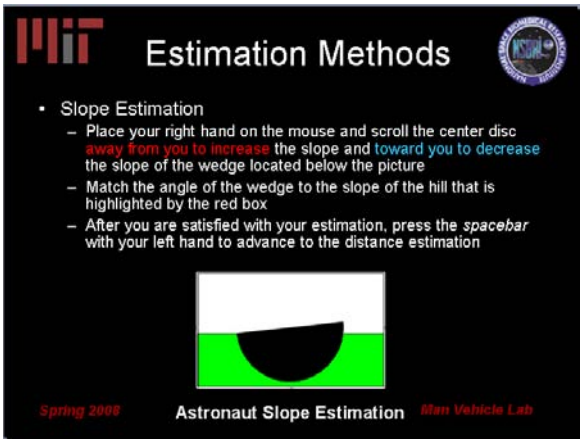
Estimation Methods
• Slope Estimation
– Place your right hand on the mouse and scroll the center disc away from you to increase the slope and toward you to decrease the slope of the wedge located below the picture
– Match the angle of the wedge to the slope of the hill that is highlighted by the red box
– After you are satisfied with your estimation, press the spacebar with your left hand to advance to the distance estimation
Spring 2008
Astronaut Slope Estimation
Man Vehicle Lab

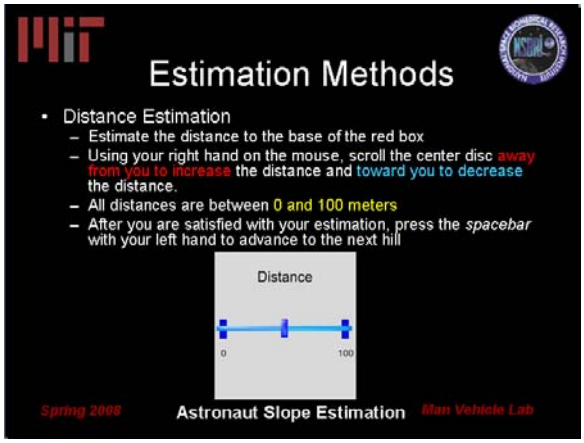
Estimation Methods
• Distance Estimation
– Estimate the distance to the base of the red box
– Using your right hand on the mouse, scroll the center disc away from you to increase the distance and toward you to decrease the distance.
– All distances are between 0 and 100 meters
– After you are satisfied with your estimation, press the spacebar with your left hand to advance to the next hill
Distance
0
100
Spring 2008
Astronaut Slope Estimation
Man Vehicle Lab


Questions/Comments?
Good Luck!
Spring 2008
Astronaut Slope Estimation
Man Vehicle Lab

F.3 Lunar VR Study (LVS)

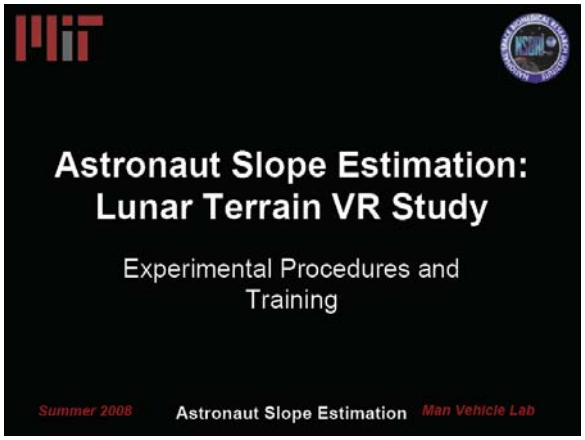

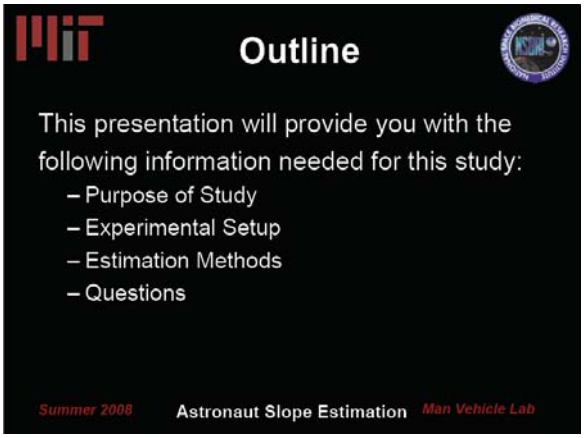

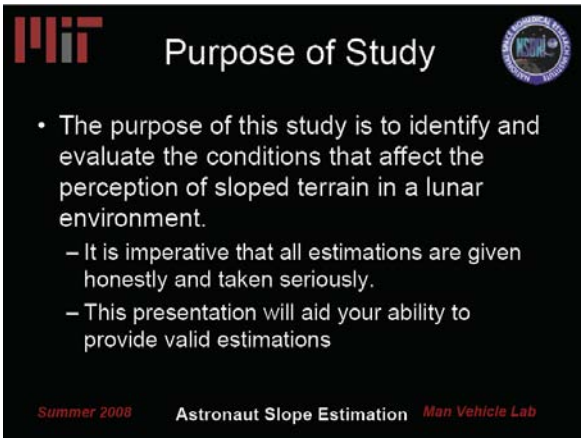

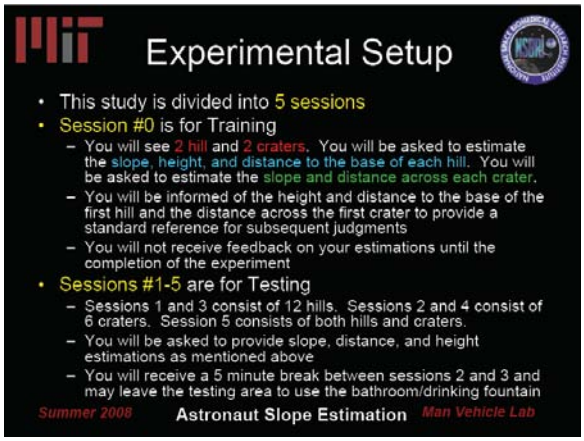

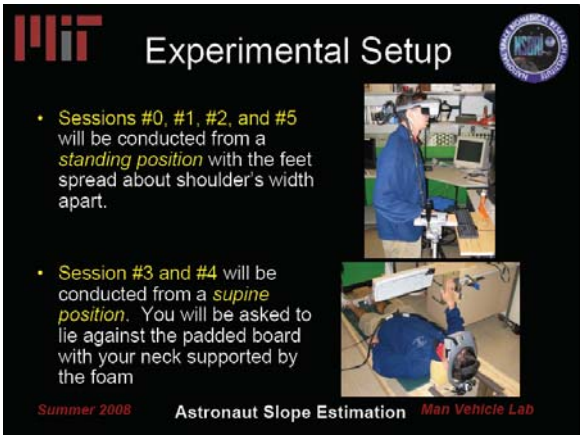

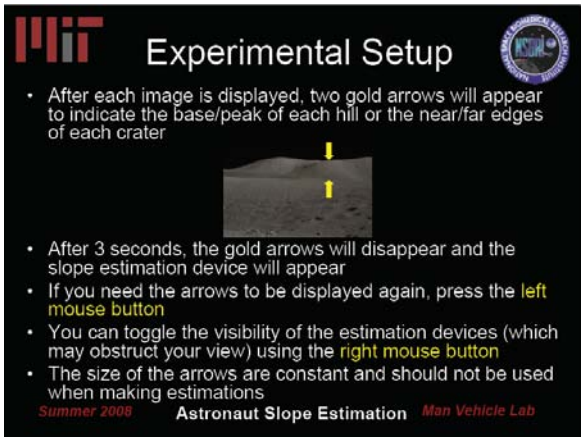

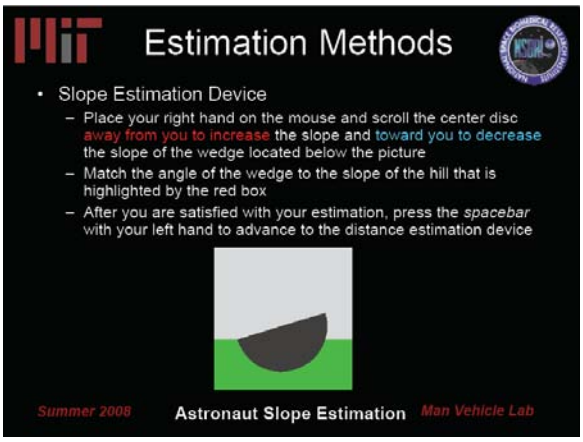
Estimation Methods
• Slope Estimation Device
– Place your right hand on the mouse and scroll the center disc away from you to increase the slope and toward you to decrease the slope of the wedge located below the picture
– Match the angle of the wedge to the slope of the hill that is highlighted by the red box
– After you are satisfied with your estimation, press the spacebar with your left hand to advance to the distance estimation device
Summer 2008
Astronaut Slope Estimation
Man Vehicle Lab

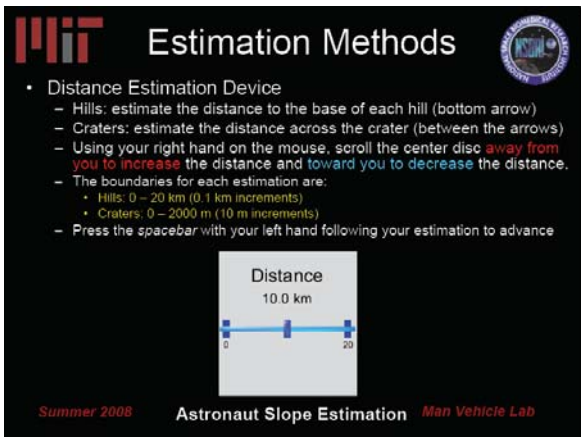
Estimation Methods
• Distance Estimation Device
– Hills: estimate the distance to the base of each hill (bottom arrow)
– Craters: estimate the distance across the crater (between the arrows)
– Using your right hand on the mouse, scroll the center disc away from you to increase the distance and toward you to decrease the distance.
– The boundaries for each estimation are:
• Hills: 0 – 20 km (0.1 km increments)
• Craters: 0 – 2000 m (10 m increments)
– Press the spacebar with your left hand following your estimation to advance
Distance
10.0 km
0
20
Summer 2008
Astronaut Slope Estimation
Man Vehicle Lab

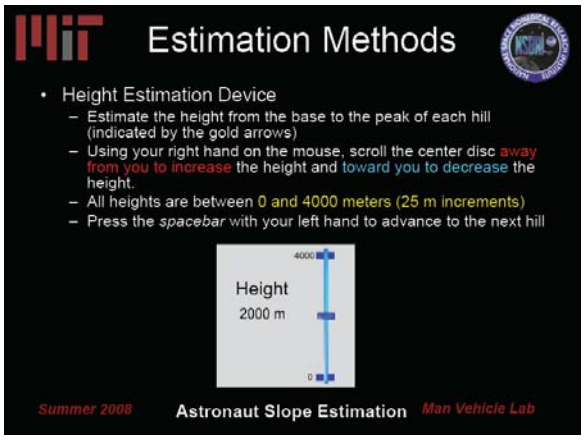
Estimation Methods
• Height Estimation Device
– Estimate the height from the base to the peak of each hill (indicated by the gold arrows)
– Using your right hand on the mouse, scroll the center disc away from you to increase the height and toward you to decrease the height.
– All heights are between 0 and 4000 meters (25 m increments)
– Press the spacebar with your left hand to advance to the next hill
4000
Height
2000 m
0
Summer 2008
Astronaut Slope Estimation
Man Vehicle Lab


Review
1 km = 1000 m
1 mile = 1600 m
1 mile = 1.6 km
Increase/Decrease Estimation
Toggle visibility of measurement devices
Redisplay arrows
Advance to next measurement/scene
Summer 2008
Astronaut Slope Estimation
Man Vehicle Lab


Questions/Comments?
Good Luck!
Summer 2008
Astronaut Slope Estimation
Man Vehicle Lab

APPENDIX G

SUBJECT FEEDBACK FORMS

G.1 MDRS VR Study

1. What methods did you use to estimate the slopes of the hills?

2. Were there any specific cues that biased your judgment of slope?

3. Did the hills appear steeper up close or far away? Why?

4. What methods did you use to estimate the distance to the hills?

5. Were there any specific cues that biased your judgment of distance?

6. Did you use a relative frame of reference for your distance estimation (football field, track length)?

7. How did the limits of the distance estimation affect your judgment (i.e. if the limits were 0 – 200 m, would you have increased your estimations?)

8. Did you experience boredom or fatigue at any point during the experiment? When? Did it affect your estimations?

9. What is the maximum slope you can climb without slipping and without using your arms or support devices (hiking poles)?

10. Do you feel your body position affected your estimation? If so, how?

G.2 Lunar VR Study

1. What methods did you use to estimate the slopes of the hills?

2. Did the hills appear steeper up close or far away? Why?

3. Did either the hills or the craters appear steeper than the other? Why?

4. What methods did you use to estimate the distance to the hills?

5. What methods did you use to estimate the height of the hills?

6. Rate your physical fitness on a scale from 1 (poor) to 10 (excellent):

   1 2 3 4 5 6 7 8 9 10

7. Did your ability to climb the hills affect your slope or distance estimates? How?

8. Did you experience boredom or fatigue at any point during the experiment? When? Did it affect your estimations?

9. What is the maximum slope you can walk up without slipping and without using your arms or support devices (hiking poles)?

10. Did the position of the sun or presence of shadows affect your estimations?

11. Did the position of your body affect your estimation? If so, how?

12. Other comments:

G.1 Devon Island Field Study

1. What methods did you use to estimate the slopes of the hills?

2. Did the hills appear steeper up close or far away? Why?

3. What methods did you use to estimate the distance to the hills?

4. Rate your physical fitness on a scale from 1 (poor) to 10 (excellent):

   1 2 3 4 5 6 7 8 9 10

5. Did your ability to climb the hills affect your slope or distance estimates? How?

6. Did you experience boredom or fatigue at any point during the experiment? When? Did it affect your estimations?

7. What is the maximum slope you can walk up without slipping and without using your arms or support devices (hiking poles)?

8. Did the position of the sun or presence of shadows affect your estimations?

9. Other comments:

APPENDIX

H

LUNAR TOPOGRAPHIC MAPS

Apollo 12 Surveyor Crater Topographic Map

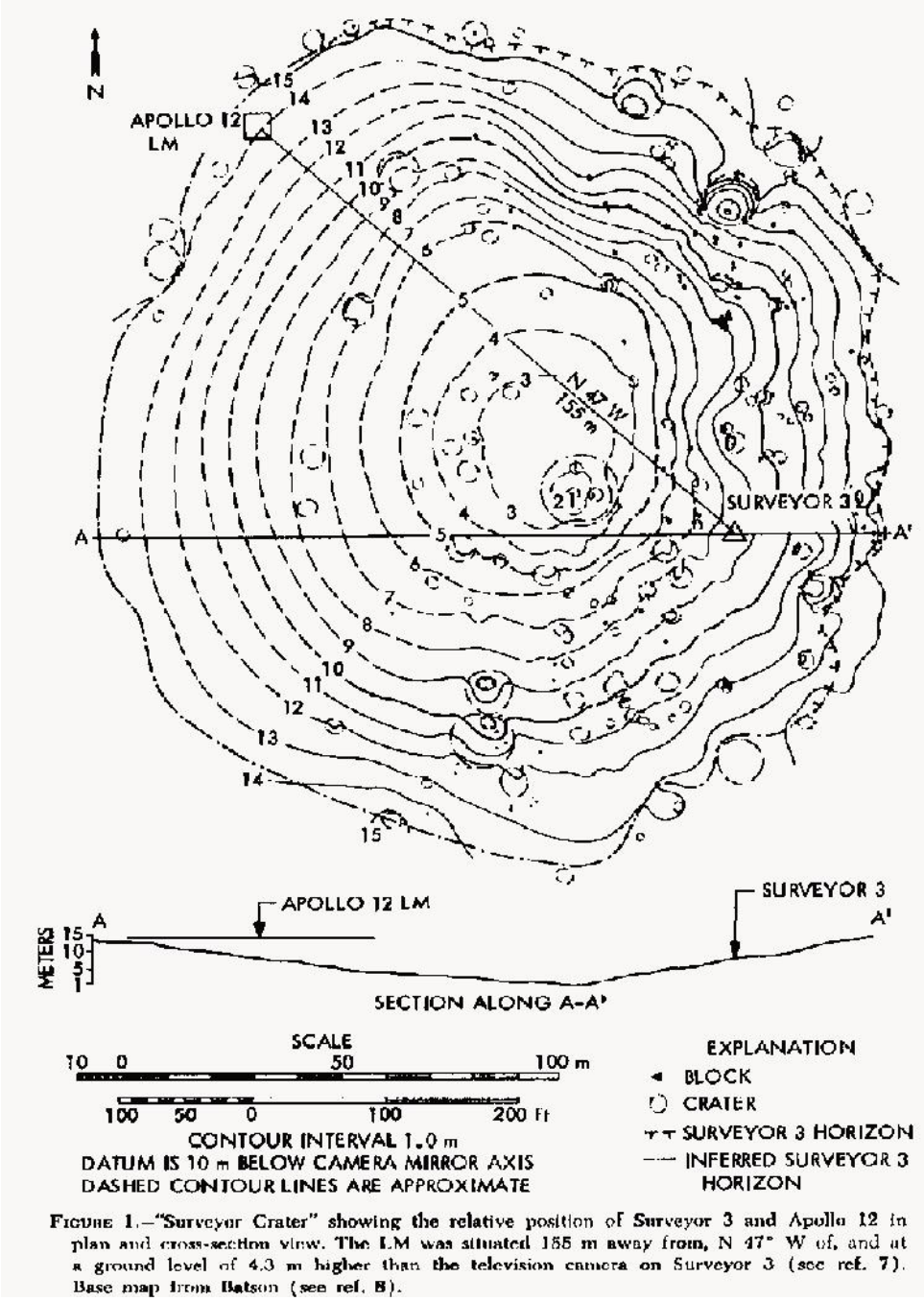

FIGURE 1.—"Surveyor Crater" showing the relative position of Surveyor 3 and Apollo 12 in plan and cross-section view. The LM was situated 155 m away from, N 47° W of, and at a ground level of 4.3 m higher than the television camera on Surveyor 3 (see ref. 7). Base map from Batson (see ref. 8).

Apollo 15 EVA 1 Topographic Map (Rille Valley)

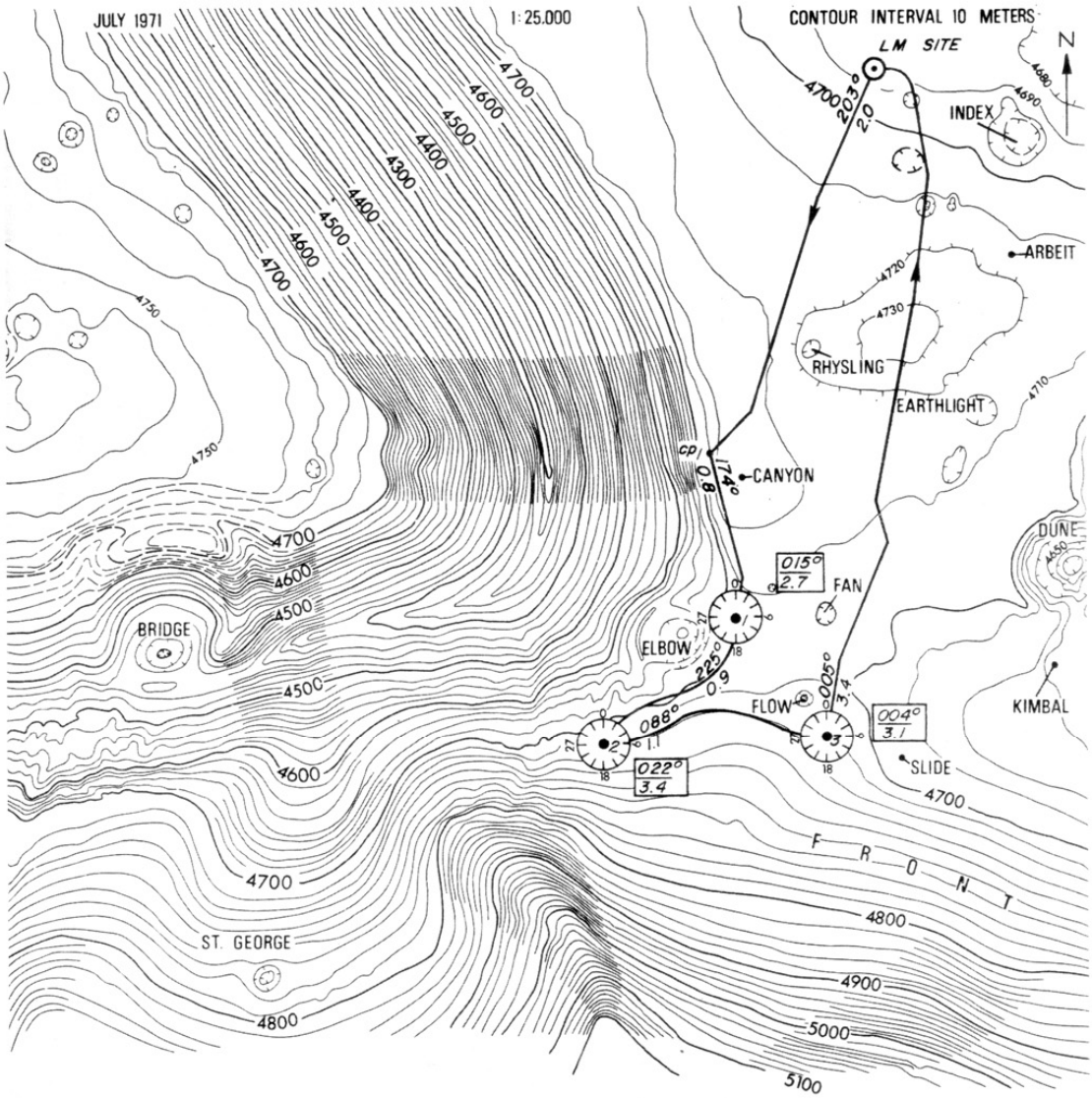

Figure 3.6-6a EVA-1 1:25,000 Contour Map

HADLEY RILLE
EVA-1

230

Apollo 15 EVA 2 Topographic Map (Dune Crater)

Figure 3.6-7a EVA-2 1:25,000 Contour Map

Apollo 15 Topographic Map (St. George Mountain)

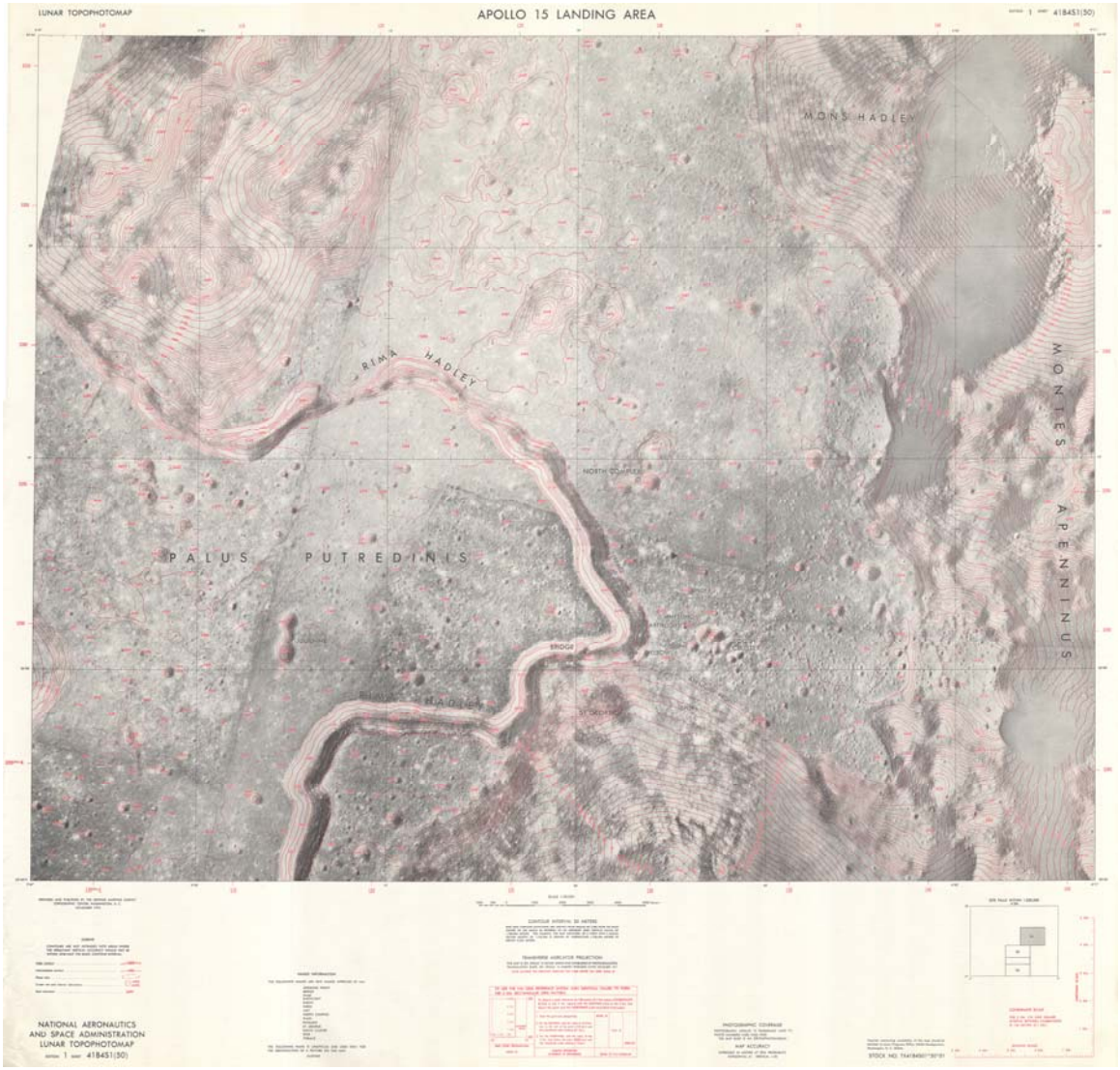

Apollo 16 EVA 3 Photographic Map

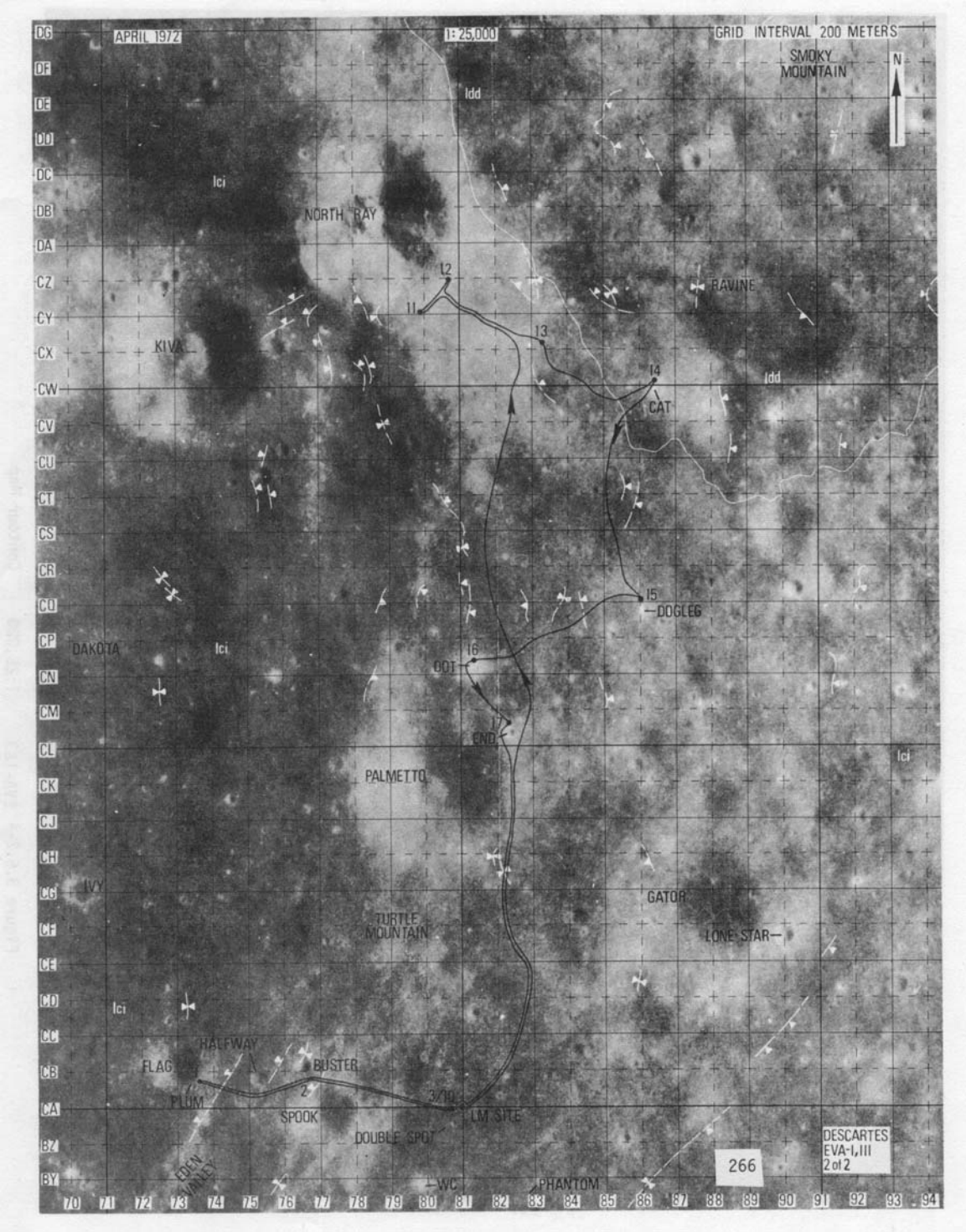

Apollo 16 EVA 3 Topographic Map

Figure 3.6.2-4 EVA-1&3 1:25,000 Contour Map

Apollo 17 Topographic Map (Lower Region)

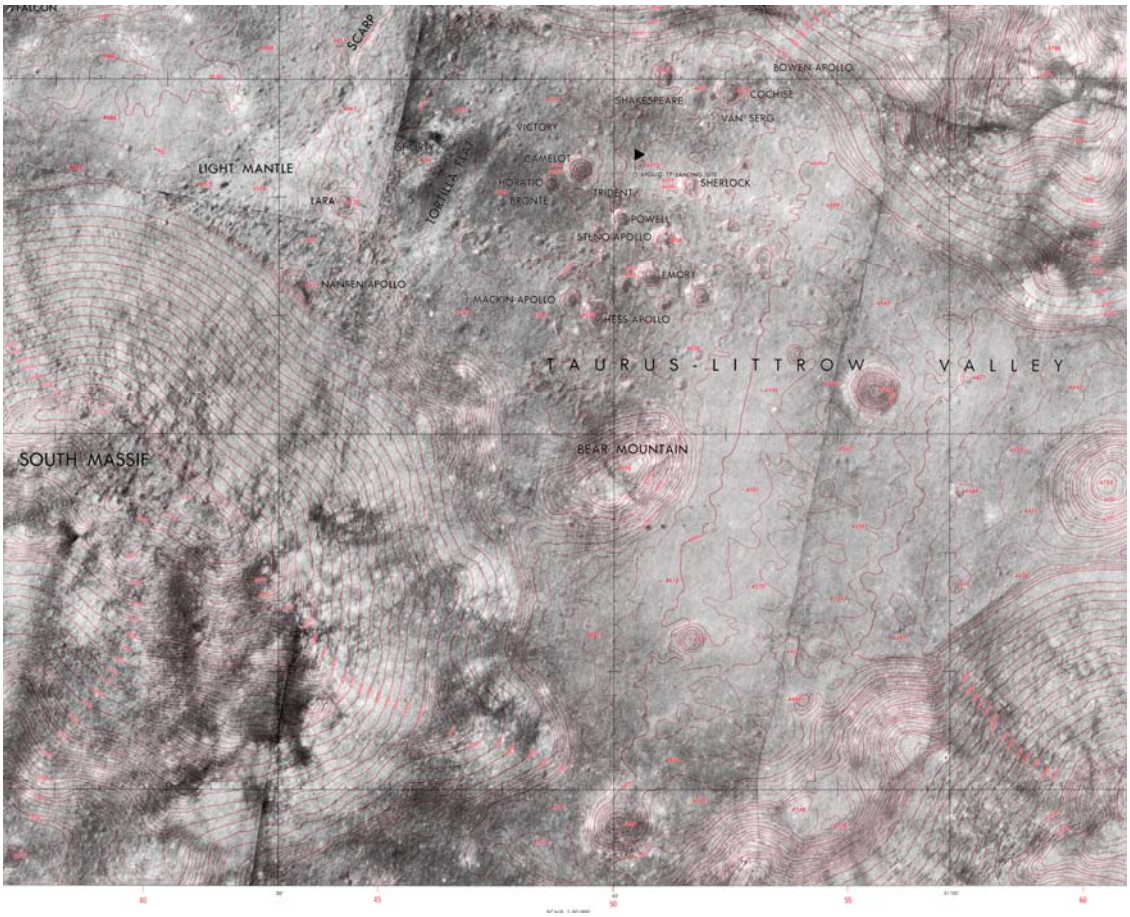

Apollo 17 Topographic Map (Upper Region)

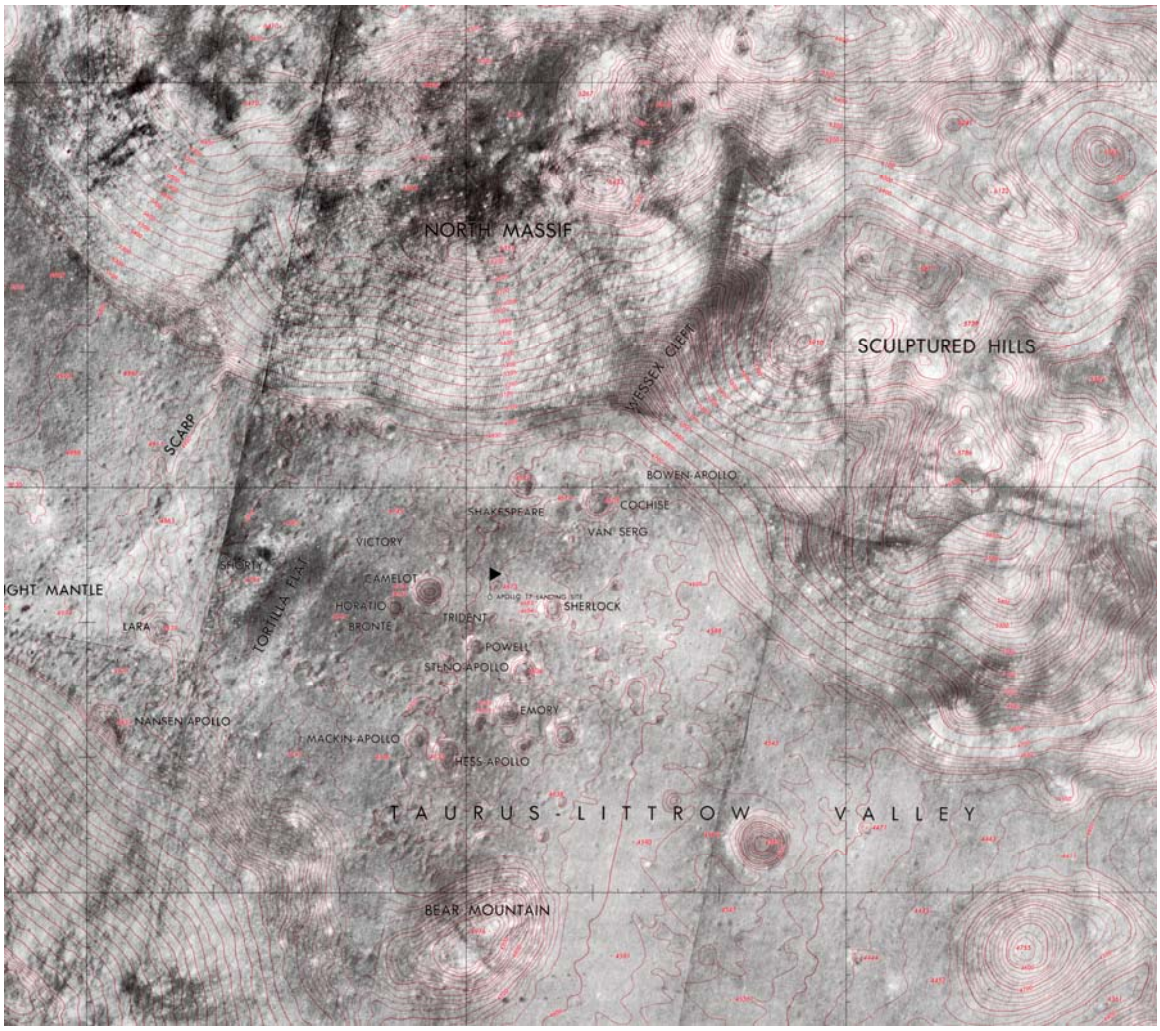

APPENDIX

I

DEVON ISLAND INSTRUCTIONS

Lunar Slope Estimation Study Instructions

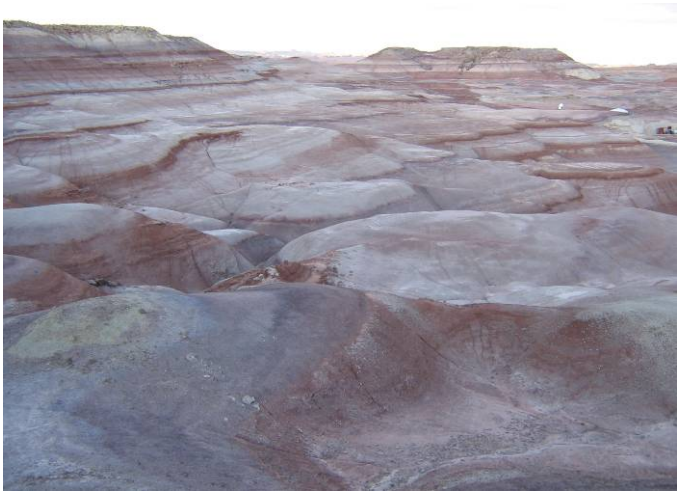

This document explains the procedures for both the investigator and the subjects in the Lunar Slope Estimation Study. It explains the measurement devices and data collection techniques in detail. Address any questions or issues to Chris Oravetz, coravetz@mit.edu.

Electronic Documents

- Lunar Slope Instructions.doc
  - Outlines the instructions for executing the experiment
- Informed Conset.doc
  - Subject consent form to conduct experimental research.
- Subject Information.doc
  - Background information form that needs to be competed by all subjects prior to participating in the study
- Subject Information (example).doc
  - Example of the Subject Information Form
- Post-Experiment Feedback.doc
  - Feedback information form that needs to be completed by all subjects following all sessions of the experiment
- Devon_Island_Datasheet.xls
  - Spreadsheet where all the data collected will be input
- Laser Rangefinder Datasheet.doc
  - Data collection tables for laser rangefinder data

- Slope Datasheet.doc
  - Data collection tables for slope estimation data
- Photography Datasheet.doc
  - Data collection tables for photography data
- Consistency Check Datasheet.doc
  - Data collection tables for Internal Consistency Check data
- V3 Users Manual.pdf
  - Informational manual for the Sony digital cameras

Equipment

The following equipment will be sent to you and the pictures show how the equipment looks dissembled and how it will appear when it first arrives.

1. Sony DSC-V3 Digital Cameras

2. LANC Controller

3. Tripod

4. Palmboard

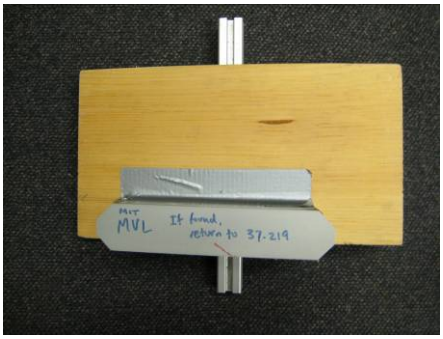

5. Laser Rangefinder

6. Flashcards

7. Camera Charger

Equipment Preparation

The following steps will aid you in putting the equipment together to prepare for data collection

1. Fully expand the three legs of the tripod. Loosen the knobs and turn the hand crank (highlighted in yellow below) to extend the upper portion of the tripod to its highest position and tighten the knobs to lock it into place. Loosen the black handle (highlighted in red) and position the platform at the top to be parallel to the ground. The full expansion of the tripod is shown below.

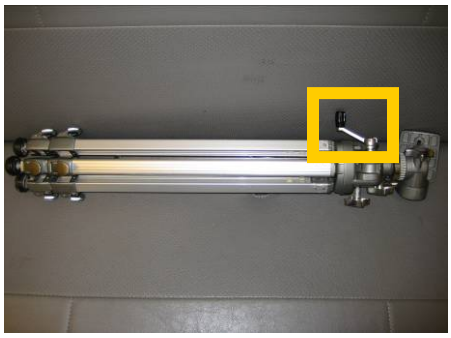

Hand crank (highlighted in yellow)

Fully-expanded tripod (black handle highlighted in red)

2. Place the end of the metal beam supporting the palmboard that is closest to the digital slope gauge against the tripod screw highlighted in the picture below. Finger-tighten the screw until the palmboard is secure. You may want to turn on the digital slope gauge while tightening the screw to ensure the palmboard is level.

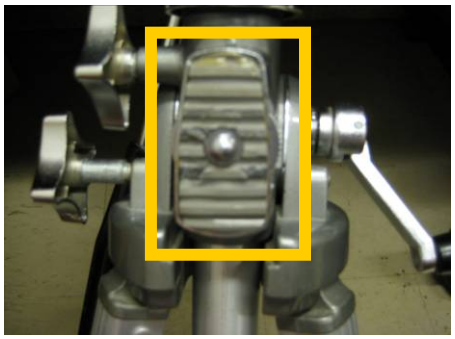

Tripod screw for attaching palmboard gauge highlighted in red)

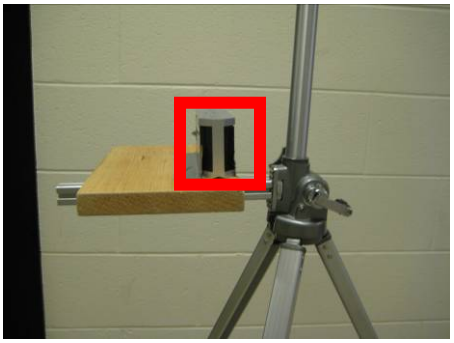

Attached palmboard (digital slope

3. Ensure the cameras batteries are fully charged. Do this by turning each camera on and within 5 seconds, a battery symbol will appear in the upper left corner of the LCD with the amount of time the batteries have left. If you experience low battery while using the cameras, a battery symbol with a "slash" through it will flash in the middle of the LCD screen. To charge the batteries, plug the battery charger into the camera as shown in the picture below. NOTE: Charging time for a dead camera battery is 180 minutes.

Camera battery charging (indicated by flashing yellow light next to viewfinder)

4. Insert the LANC Controller into the left sides of each camera as shown in the picture below. Insert the "Master" cord into the right camera and the "Slave" cord into the left camera. Ensure the controller is working properly by pressing the "on" button and ensuring both cameras turn on and the synchronization time (in milliseconds) appears in the LCD screen of the LANC Controller.

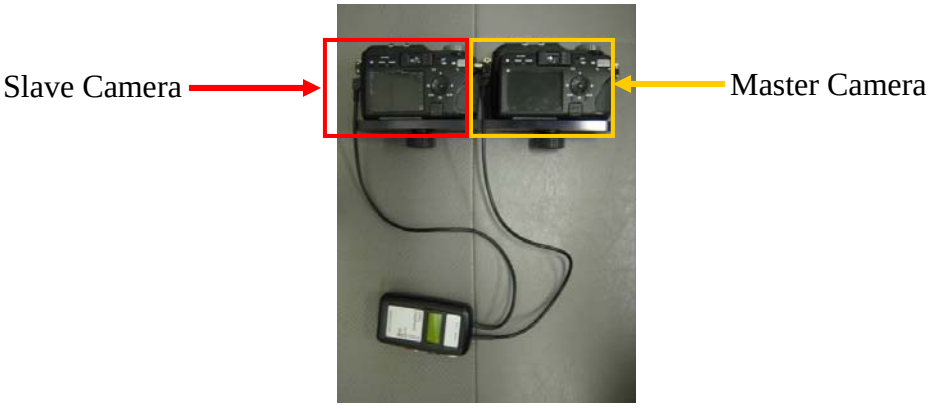

5. Align the cameras on the stereo mount and tighten them in place by turning the black knobs on the bottom. Align the "Master" camera first by placing the red line on the bottom surface of the camera in the center of the mount gap (see picture below). Secure it into place by turning the knob. Next, slide the "Slave" camera as close to the "Master" camera as possible, to minimize the inter-ocular distance, and align its red line to the center of the mount gap. Tighten the knob of the "Slave" camera.

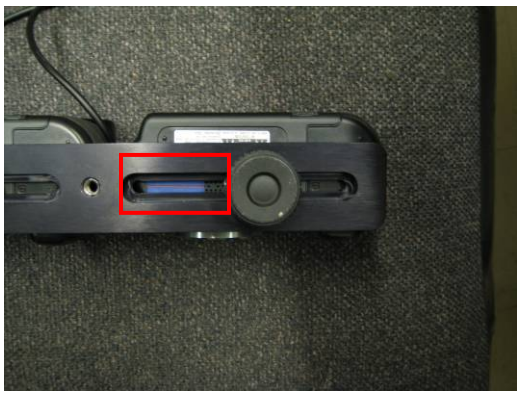

Master Camera with red line highlighted

Both cameras aligned and secured

6. Place the stereo mount on the platform of the tripod. Place the platform screw into the center of the mount and position the stereo mount as far forward as possible (see the pictures below). Tighten screw #1 first, followed by screw #2. Velcro the LANC Controller to the tripod behind the cameras.

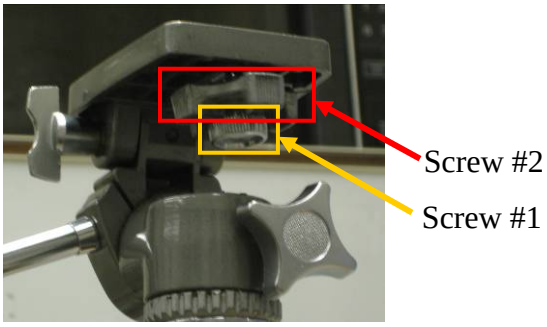

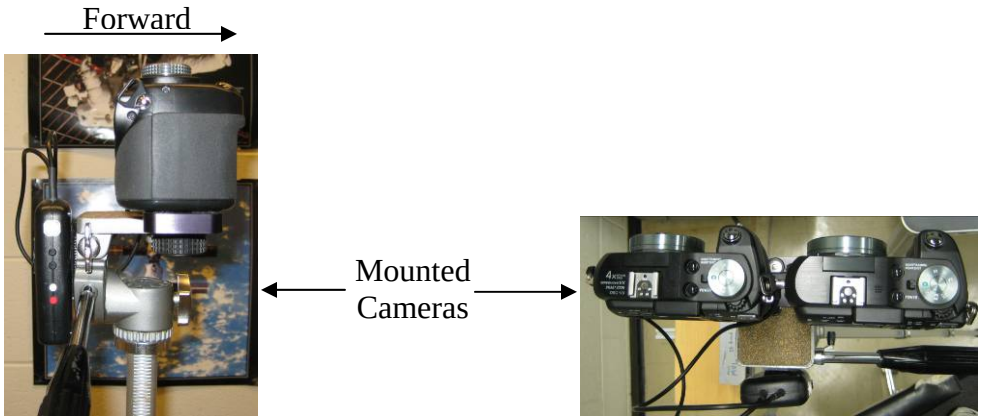

7. The tripod setup with the palmboard and cameras are all set to use. It is important to remember bringing both the tripod and the flashcards out during the experiment. It is also helpful to bring the Laser rangefinder along during the experiment in case any hill needs to be re-measured. It is recommended to recharge the battery after each day. If the cameras are removed to recharge the batteries, follow steps 3 – 6 after charging is complete.

Slope/Distance Measurement Procedures

1. Select 3 – 5 hills that have slopes between 10 and 30 degrees. **Best case scenario is to use 5 slopes (10^o, 15^o, 20^o, 25^o, 30^o).** Worse case scenario is to use 3 slopes (15^o, 20^o, 25^o). The height of the selected hills should be no less than the height of the observers. Best case scenario is for the hills to have similar textural/color characteristics without familiar objects within the observers' field of view. The ground from the estimation location to the base of the hill should be mostly level.

2. Measure the slopes of the selected hills using the following steps.

    a. Stand 10 – 15 meters from the base of the hill. Aim the Laser Rangefinder (LRF) at the base of the *region of interest* (region of the hill that is being estimated – may not be the base of the hill) and measure both the distance to that point and the angle of the LRF. Repeat 14 more times, aiming at the same point for each repetition and recording the measurements into the Laser Rangefinder Datasheet.

    b. Enter this information into "Devon_Island_Datasheet.xls" under the "Hill Information" tab in the "Lower" area of the spreadsheet (shaded yellow). For each hill, enter the distance to the left of the angle.

    c. While standing from the same location, measure the distance and the LRF angle to the top of the *region of interest*. Repeat 14 more times, aiming at the same point for each repetition and recording the measurements into the Laser Rangefinder Datasheet.

    d. Enter this information into the same spreadsheet under the "Upper" area (shaded red).

    e. The Law of Sines/Cosines is programmed into this spreadsheet and the computed slope will appear in row 2 for each hill.

3. Measure the distances for each of the selected hills
    a. **Best case scenario is to test at 3 distances (25 m, 50 m, and 75 m).** Locate the point 25 meters from the bottom of the *region of interest* and mark the point so it can be easy to find in the future. Repeat this step for 50 meters and 75 meters (worst case scenario – 2 distances: 25 and 75 meters). All three estimation locations should be in line with each other (The compass heading from the estimation locations to the hill should be the same for all 3 distances)

   b. Measure the compass heading from the 75 m distance location to the *region of interest* for each hill. Record this information into the "Devon_Island_Datasheet" under the "Data" tab and the "Heading" column.

4. Select the time of day to conduct the experiments. **Best case scenario is to have 3 time-of-day conditions, each separated by 6 hours.** The sun elevation and sun azimuth data for the first and last day of your deployment is shown in the "Devon_Island_Datasheet" under the "Sun Data" tab. Because the sun elevation is symmetrical between its angles in the morning and the afternoon, best case is to test at one of the following sets of time conditions: **(noon, 6 pm, midnight)** OR **(midnight, 6 am, noon)**. If only two time-of-day conditions are possible, best case scenario is to test at noon and midnight. Avoid testing at both 6 am and 6 pm because the sun elevation is about the same for both. If only 2 time-of-day conditions are possible, I recommend testing at noon and as late in the afternoon as possible. Please email me with your selected time-of-day conditions prior to starting tests.

5. Randomize the order of the estimation locations for each session. **Best case scenario is to avoid having subjects estimate the same hill consecutively from different distances.** If only 2 time-of-day conditions are selected, then try to run the second session in the reverse order as the first session. Have all the subjects go through the same order for a particular time-of-day condition to eliminate learning advantages.

6. **All tests should be conducted with minimum days between sessions.** The sun azimuth remains fairly constant between the start and end of the deployment; however, the peak sun elevation is higher at the beginning of the deployment than the end. Therefore, to maximize the range of sun elevations tested, it would be favorable to complete the experiments as early as possible.

7. After marking the locations for all estimations and creating a randomized order for each session, it is helpful to dry-run the experiment by yourself and travel from location to location ensuring you can find all locations.

Pre-Experiment Procedures

1. Although the subject pool may be limited, it is favorable to have an equal number of male and female subjects participate in this experiment.

2. Have all subjects read and complete the form entitled "Consent to Participate in Non-Biomedical Research: Lunar Slope Estimation." Clarify that they are only being asked to participate in the field study experiment and will not be required to complete the Virtual Reality tests.

3. Have all subjects complete the form entitled "Subject Information." You can choose your own convention for the "subject #" field to keep their identity anonymous.

a. Subjects should be naïve in their knowledge of slope estimation; however, if they are familiar with the work done by Dennis Proffitt or other slope researchers, this information should be noted.

b. Subject should have vision that is correctable to 20/20. If they wear glasses, they should wear them throughout the experiment.

4. Show all subjects a demonstration of both the flashcard estimation and a palm-board estimation

a. **Flashcard Demonstration:** The subjects will be given the flashcards with a random card on top. The angle between the flat surface of the semicircle and the green horizon is the "slope" of that card. All flashcards are in increasing order. When subjects are first given the flashcards, they should look at the hill they are judging and envision the view of the hill from the side. Next, they should flip through all the cards and select the card that has a slope that matches the slope of the hill that they envision from the side view. There is unlimited time to select a card, so subjects should take their time when selecting a card. Subjects should avoid looking at the back of the cards, which contain letters that correspond to a code that tells the investigator the actual slope. After the subject has selected their card, they should give the stack of cards back to the investigator with the selected card on top.

b. **Palmboard Demonstration:** After handing the flashcards to the investigator, subjects should place the palm of their right hand on the surface of the palmboard. They should be standing with the board to their right and in front of their body so their right elbow makes a 90 degree angle. Without looking at the board, they should be instructed to match the angle of the board to the slope of the hill they are judging. They have unlimited time and may move the board up and down before stopping at their final position. When they are in their final position, they should notify the investigator who will look at the digital slope gauge and record their measurement.

Flashcard Estimation

Palmboard Estimation

Experimental Procedures

1. Instruct the subjects to refrain from talking to each other about the slopes of the hills surrounding them during the duration of the experiment. Additionally, tell them not to obtain a cross-sectional view of the hills.

2. The subjects are to follow the investigator to the first test location. After arriving, the investigator will spread the legs of the tripod and level the camera mount by using both the black handle and the "pitch" knob at the end of the platform on the top of the tripod. The bubble level on the camera mount should be used to verify its level.

3. The investigator should next record the time on the Photography and Slope datasheets.

4. The investigator should turn on the LANC controller and watch the initial synchronization time displayed on the LANC LCD. If the synchronization time is less than 0.5 ms, the cameras should be powered off and powered back on using the LANC controller. Repeat until the synchronization time is below 0.5 ms. (NOTE: the synchronization time will change slightly over time).

5. The zoom option should NOT be used (the zoom should be at 1.0) and the investigator should verify both cameras are on the Automatic Setting. The investigator should then aim the cameras at the hill of estimation and place the hill in the center of the viewfinders.

6. The investigator should verify that the flash is turned OFF by observing a "lightning bolt with a slash through it" near the battery level indicator in the upper left corner of the LCD screen for each camera.

7. The investigator should then press the large button on the LANC halfway down and watch the bottom of the LCD's of the digital cameras to see the shutter speed and aperture values for each camera appear. The investigator should ensure the shutter speed and aperture values correspond between cameras. If they do, the large button on the LANC should continued to be pressed the full way down until the picture is taken. If the values do not correspond, the investigator should release the large button on the LANC and then press it halfway again to see if they correspond again. After several tries without consistency between cameras, the investigator should then set one or both camera dials to "M" to manually set the aperture and shutter speed values before pressing the large button on the LANC to take the picture.

8. After the picture is taken, the "off" button on the LANC should be pressed to preserve the camera batteries. The investigator should also record the synchronization, shutter speed, and aperture values onto the Photography datasheet.

9. The investigator should next have each subject step forward, one after another, and take the flashcards and following the directions outlined in the Pre-Experiment Procedures, estimate the slope of the hill and hand the cards back to the investigator. The investigator should record the letter code from the selected card onto the Slope datasheet.

10. While each subject selects a flashcard, the investigator should ensure the digital slope gauge on the palmboard reads 0 +/-0.5 degrees.

11. After selecting a flashcard, each subject should then place their right hand on the palmboard and estimate the slope using the directions outlined in the Pre-Experiment Procedures. The investigator should be prepared to record the estimated slope from the digital slope gauge onto the Slope datasheet.

12. After all subjects have estimated the hill, the investigator should lead them to the next estimation location and repeat steps 2 – 10. Complete this process for each estimation location in a particular session. NOTE: As you fill out multiple Slope datasheets, please indicate the order of your datasheets (1, 2, 3, …).

To be completed ONCE for each subject:

13. After all estimation locations have been visited, the investigator should execute an internal consistency check for each subject
    a. The investigator should ask the subject to position themselves to make palmboard estimations.
    b. The investigator should present the following flashcards in front of the subject in the order specified below and ask the subject to adjust the palmboard to the slope of the flashcard.
        i. 20 degrees – Flashcard U
        ii. 30 degrees – Flashcard AE
        iii. 10 degrees – Flashcard K
        iv. 5 degrees – Flashcard F
        v. 25 degrees – Flashcard Z
        vi. 15 degrees – Flashcard P
        vii. 50 degrees – Flashcard AY
        viii. 40 degrees – Flashcard AO
    c. The investigator should record the palmboard measurement for each slope into the Consistency Check datasheet.

Post-Experiment Procedures

1. Have all subjects complete the form entitled “Slope Estimation Feedback”

2. Dissemble the tripod in the opposite order as it was assembled.

3. The data on the Photography and Slope datasheets does not need to be input into the “Devon_Island_Datasheet” excel spreadsheet; however, inputting data will allow the investigator to see if there were any conditions that were missed.

Christopher Oravetz
coravetz@mit.edu OR ctoravetz@gmail.com
Work: 617-253-5487 Cell: 617-462-9643

APPENDIX

J

DEVON ISLAND DISTANCE REFERENCE

Distance References

NBA Basketball Court *Width*
15 meters
50 feet

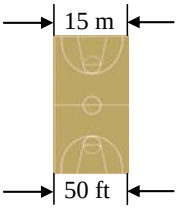

Tennis Court *Length*
24 meters
78 feet

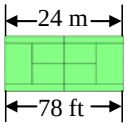

OLYMPIC-sized Swimming Pool *Length*
50 meters
164 feet

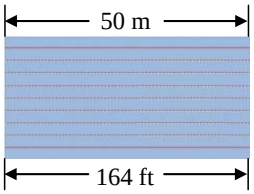

NHL Hockey Rink *Length*
61 meters
200 feet

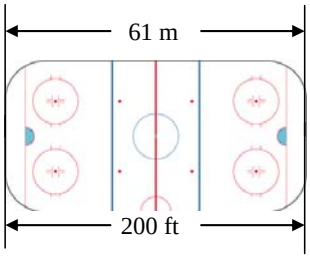

NFL Football Field *Length*
(Including End zones)
110 meters
360 feet